

CHROMATIN STRUCTURE OF THE INTEGRATED VIRAL
SEQUENCES IN ADENOVIRUS-TRANSFORMED CELLS

CENTRE FOR NEWFOUNDLAND STUDIES

**TOTAL OF 10 PAGES ONLY
MAY BE XEROXED**

(Without Author's Permission)

FRASER AIRD, B.Sc.(Honours)



CHROMATIN STRUCTURE OF THE
INTEGRATED VIRAL SEQUENCES IN
ADENOVIRUS-TRANSFORMED CELLS

BY

Copyright © Fraser Aird, B.Sc.(Honours)

A thesis submitted to the School of Graduate

Studies in partial fulfillment of the

requirements of the degree of

Doctor of Philosophy

Faculty of Medicine

Memorial University of Newfoundland

March, 1989

St. John's

Newfoundland

Abstract

In the eukaryotic cell nucleus, chromatin is organized into higher-order structures through hierarchical levels of folding and coiling. Active genes are contained in chromatin domains with a more "open" conformation that is preferentially sensitive to DNase I digestion compared to inactive chromatin. The spatial organization of chromatin is maintained by the nuclear matrix, the major structural component of the nucleus. Chromosomal DNA is organized into supercoiled loops anchored at their bases to the nuclear matrix, and in most cases examined, active genes are located at or near the base of the loops.

I have examined the DNase I sensitivity of the integrated viral sequences of four adenovirus type 5-transformed cell lines, and the organization of these sequences relative to the nuclear matrix. DNase I sensitivity was analysed by digesting nuclei with DNase I and monitoring the disappearance of virus-specific restriction fragments by Southern blotting and hybridization. In each cell line, the integrated viral sequences were in a conformation typical of active chromatin, *i.e.* they were preferentially sensitive to DNase I compared to inactive chromatin. The DNase I sensitive region included not only the active transforming (E1) genes, but extended into the adjacent inactive viral sequences. Thus, the integrated viral sequences were contained within active chromatin domains.

In addition to these extended domains, DNase I hypersensitive sites were detected in the E1A 5'-flanking sequences. These sites were mapped to sequences previously shown to contain the E1A transcriptional enhancers and binding sites for cellular transcription factors. Therefore, the DNase I hypersensitive sites likely reflect alterations in local chromatin structure associated with regulation of transcription of the integrated E1A genes.

The organization of the integrated viral sequences relative to the nuclear matrix was analysed by assessing the matrix associated and non-associated DNA fractions for their content of viral sequences by Southern blotting and hybridization. There

was no enrichment or depletion of the viral sequences in either of these fractions relative to total unfractionated DNA, consistent with a random organization relative to the nuclear matrix. However, control studies indicated that these results may be due to the conditions used to isolate the nuclear matrix DNA fractions.

(Keywords: adenovirus type 5; chromatin domain; DNase I sensitivity; hypersensitive sites; nuclear matrix.)

Aknowledgements

To Dr H. Banfield Younghusband, I express my sincere thanks for his supervision, help and guidance. I am grateful to him for the opportunity to work in his laboratory, and for his sound advice and encouragement. I also thank Drs Alfred Burness and Roger Green for reading the drafts of this manuscript and for their helpful suggestions. I am deeply indebted to Shahid Hameed for his invaluable assistance with the word processing programme used to compile this manuscript, and to Pah Baldeh for his assistance with the graphics programme. I gratefully acknowledge the financial support provided by the Faculty of Medicine and School of Graduate Studies, MUN, and the Cancer Research Society, Inc., Montreal, Quebec.

Finally, I thank Sheila for her love, support and understanding during this work.

Publications

Part of the work presented here has been published in abstract form or is in preparation. These papers are:

Aird, F. & Younghusband, H.B. (1986). Chromatin structure of integrated adenovirus sequences and organization relative to the nuclear matrix in adenovirus-transformed cells. *Proceedings of the Canadian Federation of Biological Societies* **29**, 157.

Aird, F. & Younghusband, H.B. (1989). Chromatin structure of the integrated viral sequences in adenovirus-transformed cells. *Manuscript in preparation.*

Table of Contents

Abstract	ii
Aknowledgements	iv
Publications	v
Table of Contents	vi
List of Figures	ix
List of Abbreviations	xi
1. Introduction	1
1.1. Active chromatin structure	1
1.1.1. Introduction	1
1.1.2. Hierarchies of chromatin structure	3
1.1.3. Morphology of active chromatin	8
1.1.4. Nuclease sensitivity of active chromatin	17
1.1.5. Active chromatin domains	25
1.1.6. DNase I hypersensitive sites	35
1.2. The nuclear matrix	40
1.2.1. Introduction	40
1.2.2. Structure and composition	41
1.2.3. Organization of DNA relative to the nuclear matrix	53
1.3. Adenovirus transformation	66
1.3.1. Introduction	66
1.3.2. Integration of viral DNA	70
1.3.3. The transforming region	72
1.3.4. The E1 proteins	76
1.3.5. The E1A and E1B regions in transformation	80
1.3.6. The E1A proteins and transformation	83
1.3.7. The E1A enhancers	95
1.4. Summary and statement of objectives	99
2. Materials and Methods (General)	102
2.1. Cells	102
2.2. Plasmids	103
2.3. Purification of DNA	103
2.4. Analysis of DNA	104
2.5. Isolation of RNA	105
2.6. Analysis of RNA	107

3. Viral DNA and RNA in transformed cells	108
3.1. Introduction	108
3.2. Results and Discussion	112
3.2.1. Viral DNA in adenovirus-transformed cells	112
3.2.2. Viral RNA in adenovirus-transformed cells	129
3.2.3. Conclusions	134
4. Chromatin Structure	137
4.1. Introduction	137
4.2. Materials and Methods	138
4.2.1. Preparation of DNase I digested chromatin	138
4.2.2. DNase I digestion of DNA	139
4.2.3. Determination of extent of DNase I digestion	139
4.2.4. Quantitation of DNase I sensitivity	140
4.3. Results	145
4.3.1. Rationale of the experiment	145
4.3.2. DNase I sensitivity of naked DNA	147
4.3.3. DNase I sensitivity of chromatin	147
4.3.3.1. 293 cells	147
4.3.3.2. 14b cells	162
4.3.3.3. 637-4 cells	170
4.3.3.4. 945-C1 cells	182
4.3.4. DNase I hypersensitive sites	187
4.3.4.1. Rationale of the experiment	187
4.3.4.2. 293 cells	190
4.3.4.3. 637-4 cells	195
4.3.4.4. 14b cells	199
4.3.4.5. 945-C1 cells	202
4.4. Discussion	202
4.4.1. General level of DNase I sensitivity	202
4.4.2. DNase I hypersensitive sites	213
5. Nuclear Matrix	220
5.1. Introduction	220
5.2. Materials and Methods	221
5.2.1. Heat shock	221
5.2.2. Preparation of nuclear matrix DNA fractions	221
5.2.2.1. Method 1	224
5.2.2.2. Method 2a	225
5.2.2.3. Method 2b	226
5.2.3. Analysis of nuclear matrix DNA	227
5.3. Results	227
5.3.1. Rationale of the experiment	227
5.3.2. Nuclear matrix DNA fractions	228
5.3.2.1. Method 1	228
5.3.2.2. Method 2	230

5.3.3. Viral sequences in Ad5-transformed cells	234
5.3.3.1. Method 1	234
5.3.3.2. Method 2	239
5.3.4. <i>HSP70</i> sequences in heat shocked cells	252
5.4. Discussion	253
References	261

List of Figures

Figure 1-1:	Ad5 early transcription units	60
Figure 1-2:	E1A and E1B transcription units and gene products	75
Figure 1-3:	E1A protein conserved regions	93
Figure 1-4:	E1A enhancers	97
Figure 3-1:	Ad5 restriction maps and DNA probes	114
Figure 3-2:	Analysis of Ad5 DNA in 637-4, 14b, and 293 cells	116
Figure 3-3:	Analysis of Ad5 DNA in 945-C1 cells	121
Figure 3-4:	Analysis of Ad5 DNA in <i>Sma</i> I-digested 945-C1 cell DNA	124
Figure 3-5:	Integrated Ad5 sequences in 945-C1 cell DNA	127
Figure 3-6:	Analysis of viral RNA in Ad5-transformed cells	132
Figure 3-7:	Viral sequences present in Ad5-transformed cells	136
Figure 4-1:	DNase I digested chromatin	142
Figure 4-2:	Quantitation of DNase I sensitivity	144
Figure 4-3:	DNase I digested 14b cell DNA	149
Figure 4-4:	DNase I sensitivity of Ad5 sequences in 14b cell DNA	151
Figure 4-5:	DNase I sensitivity of different length DNA fragments	154
Figure 4-6:	DNase I digested 293 chromatin	157
Figure 4-7:	DNase I sensitivity of Ad5 E1 sequences in 293 chromatin	159
Figure 4-8:	DNase I sensitivity of the IgH gene J region in 293 chromatin	161
Figure 4-9:	DNase I digested 14b chromatin	165
Figure 4-10:	DNase I sensitivity of Ad5 sequences in 14b chromatin	167
Figure 4-11:	DNase I sensitivity of Ad5 E1 sequences in 14b chromatin	169
Figure 4-12:	DNase I digested 637-4 chromatin (<i>Hind</i> III)	172
Figure 4-13:	DNase I sensitivity of Ad5 sequences in 637-4 chromatin	174
Figure 4-14:	DNase I digested 637-4 chromatin (<i>Sac</i> I)	178
Figure 4-15:	DNase I sensitivity of Ad5 E1 sequences in 637-4 chromatin	180
Figure 4-16:	DNase I digested 945-C1 chromatin	184
Figure 4-17:	DNase I sensitivity of Ad5 sequences in 945-C1 chromatin	186
Figure 4-18:	DNase I sensitivity of the integrated viral sequences in Ad5-transformed cell lines	189
Figure 4-19:	DNase I HS sites in 293 E1A 5' region	193

Figure 4-20:	DNase I HS sites in 637-4 E1A 5' region	198
Figure 4-21:	DNase I HS sites in 14b E1A 5' region	201
Figure 4-22:	DNase I HS sites in 945-C1 Ad5 sequences	204
Figure 4-23:	DNase I HS sites in the 5' region of integrated E1A genes in Ad5-transformed cells	206
Figure 5-1:	<i>HSP70</i> RNA in Ad5-transformed cells and HeLa cells	223
Figure 5-2:	Nuclear matrix DNA fractions	232
Figure 5-3:	Ad5 sequences in nuclear matrix DNA fractions from 14b and 637-4 cells	236
Figure 5-4:	Ad5 and <i>HSP70</i> sequences in nuclear matrix DNA fractions from 945-C1 cells	238
Figure 5-5:	Ad5 and <i>HSP70</i> sequences in nuclear matrix DNA fractions from 945-C1 cells	241
Figure 5-6:	DNase I digested 945-C1 and 637-4 chromatin	244
Figure 5-7:	Ad5 and <i>HSP70</i> sequences in nuclear matrix DNA fractions from 14b cells	247
Figure 5-8:	Ad5 and <i>HSP70</i> sequences in nuclear matrix DNA fractions from 293 cells	249
Figure 5-9:	Ad5 and <i>HSP70</i> sequences in nuclear matrix DNA fractions from 293 cells	251
Figure 5-10:	<i>HSP70</i> sequences in nuclear matrix DNA fractions from heat shocked and non-heat shocked cells	255

List of Abbreviations

289R/243R	E1A 289/243 amino acid residue gene products
5-mC	5-methylcytosine
Ad5	adenovirus type 5
ATF	activating transcription factor
BHK	baby hamster kidney
BRK	baby rat kidney
bp	base pairs
BR	Balbiansi ring
cDNA	complementary DNA
cpm	counts per minute
CR	conserved region
DBP	DNA binding protein
DNase I	deoxyribonuclease I
E1A	early region 1A
EDTA	ethylenediaminetetra-acetic acid
EM	electron microscope
Exo III	exonuclease III
GRE	glucocorticoid responsive element
HEF	hamster embryo fibroblast
HEK	human embryonic kidney
HMG	high mobility group
hnRNA	heterogeneous nuclear RNA
HPV	human papilloma virus
HS	hypersensitive
HSE	heat shock control element
HSP70	70K heat shock protein
HSV tk	herpes simplex virus thymidine kinase gene
I	intensity of hybridization
IAA	iodoacetamide

IF	intermediate filament
IgH	immunoglobulin heavy chain
IgL	immunoglobulin light chain
kb	kilobase pairs
LIS	lithium diiodosalicylate
LMW	low molecular weight
<i>MAR (SAR)</i>	matrix (scaffold) attached region
MEM	minimal essential medium
<i>MLP</i>	major late promoter
MNase	micrococcal nuclease
MOPS	3-(N-morpholino)propane-sulphonic acid
<i>Mr</i>	relative molecular mass
<i>Mw</i>	mass average molecular weight
mRNA	messenger RNA
mu	map units
NaTT	sodium tetrathionate
NEM	<i>N</i> -ethylmaleimide
NP-40	Nonidet P-40
PBS	phosphate-buffered saline
PCNA	proliferating cell nuclear antigen
p.i.	post-infection
PMSF	phenylmethylsulphonylfluoride
<i>Rb</i>	<i>retinoblastoma</i> gene
RNase	ribonuclease
RNP	ribonucleoprotein
rRNA	ribosomal RNA
RSB	reticulocyte standard buffer
RSBs	RSB containing 0.25 M sucrose
RSV	Rous sarcoma virus
SDS	sodium dodecyl sulphate
S phase	DNA synthetic phase

SSC	saline sodium citrate
SSPE	saline sodium phosphate-EDTA
SV40	simian virus 40
T antigen	tumour antigen
TAE	Tris-acetate-EDTA
TE	Tris-EDTA
topo I/II	DNA topoisomerase I/II
uH2A	ubiquitinated histone H2A
<i>uv</i>	ultra-violet

Chapter 1

Introduction

1.1. Active chromatin structure

1.1.1. Introduction

The eukaryotic cell contains an enormous length of DNA which must be packaged into the relatively small volume of the nucleus. To achieve this, the DNA molecule of each chromosome is condensed in a series of hierarchical levels of folding into a compact and highly-ordered structure. At the first level of folding, the DNA is complexed with histone proteins to form chromatin, which is further condensed by higher-order levels of coiling and folding. In addition to being highly condensed, chromatin is also a dynamic structure, capable of rapid decondensation to allow access to the enzymes and factors involved in the various aspects of DNA metabolism such as replication, repair, recombination and transcription.

It has become apparent that chromatin structure is related to transcriptional activity, and that the small fraction of the genome which is transcribed (7-10%) has an altered chromatin structure from the inactive bulk chromatin. Studies on polytene and lampbrush chromosomes have provided evidence that chromatin is organized into looped domains, with transcriptionally active domains in a less

condensed conformation than inactive domains. Evidence for a looped organization has also come from studies with histone-depleted nuclei, which reveal the DNA to be organized in large, supercoiled loops attached at their bases to a nuclear substructure or matrix. Each loop, therefore, appears to represent a separate chromatin domain, whose structure can be controlled as a unit independently from adjacent domains, in order to facilitate transcription. Studies with nucleases and cloned genes have confirmed that chromatin is organized into domains, and shown that the structure of active and potentially active domains is more "open" and sensitive to nucleases than inactive domains. The molecular basis for this altered structure is unknown, but may involve modified or variant histones, non-histone proteins, or modifications affecting DNA structure such as methylation or torsional stress. The nature of these structural changes and how they are regulated are important aspects of gene regulation, since the transition from a transcriptionally inactive to a transcriptionally competent chromatin structure is a precondition for gene expression, and represents the first step in gene activation.

The topics reviewed in this section include the association of DNA with histones to form chromatin, the organization of chromatin into higher-order structures, and the changes in chromatin structure associated with transcription. Nuclear architecture and the spatial organization of chromatin within the nucleus and relative to the nuclear matrix are discussed in more detail in section 1.2.

1.1.2. Hierarchies of chromatin structure

The first level of chromatin folding is the organization of DNA and histone proteins into tandemly repeating arrays of nucleosomes, as proposed by Kornberg (1974). The nucleosome core particle consists of 146 base pairs (bp) of DNA wrapped in 1.8 superhelical turns around the surface of an octamer of histone proteins - two each of histones H2A, H2B, H3 and H4 (Richmond, Finch, Rushton, Rhodes & Klug, 1984). One molecule of histone H1 binds to each core particle at the points where the DNA enters and exits the histone octamer, stabilizing 166 bp of DNA in two full superhelical turns (Simpson, 1978). Nucleosomes are connected by linker DNA, which may vary in length from 0-80 bp, depending on the species and tissue (Kornberg, 1977). Nucleosome core particles can be isolated by digestion of chromatin with micrococcal nuclease (MNase), which cleaves the linker DNA and releases histone H1. The core particle has been subjected to intensive analysis by a variety of physicochemical techniques, and its structure is now understood in some detail (reviewed in Pederson, Thoma & Simpson, 1986). It is a flattened disc 11 nm in diameter and 5.7 nm thick, with right-handed B-form DNA wound into two left-handed turns around the surface of the disc. Repeating nucleosomes are arranged in a linear nucleofilament of 10 nm diameter, the "beads-on-a-string" structure observed in the electron microscope (EM) (Olins & Olins, 1974; Oudet, Gross-Bellard & Chambon, 1975; Thoma, Koller & Klug, 1979), which represents a DNA packing ratio of 6-9:1 relative to extended B-form DNA (Suau, Bradbury & Baldwin, 1979).

In the interphase nucleus, the majority of chromatin is in the form of a

thick fibre of diameter 30 nm (Davies & Haynes, 1976; Olins & Olins, 1979; Langmore & Schutt, 1980; Langmore & Paulson, 1983). This structure represents the second level of chromatin condensation, and is formed by folding of the 10 nm nucleofilament. Chromatin isolated at low ionic strength (~ 1 mM NaCl and in the absence of divalent cations) unfolds reversibly into 10 nm nucleofilaments, and with increasing ionic strength (to ~ 60 mM NaCl or ~ 0.3 mM $MgCl_2$) refolds through a series of intermediates to form 30 nm fibres (Finch & Klug, 1976; Thoma *et al.* 1979). The DNA packing ratio of this structure is 40-50:1, similar to that of bulk interphase chromatin (Finch & Klug, 1976; Suau *et al.* 1979). Based on EM observations of the 10 nm to 30 nm fibre transition, Finch & Klug (1976) proposed a model for the structure of the 30 nm fibre, in which the 10 nm nucleofilament is wound into a solenoid (or contact helix) with six nucleosomes per turn, and a pitch of 11 nm (the diameter of a nucleosome). Variations on the solenoid model have been proposed (*e.g.* Thoma *et al.* 1979; McGhee, Rau, Charney & Felsenfeld, 1980; Worcel, Strogatz & Riley, 1981; McGhee, Nickol, Felsenfeld & Rau, 1983; Woodcock, Frado & Rattner, 1984; Williams, Athey, Muglia, Schappe, Gough & Langmore, 1986), but they all propose a continuous solenoidal structure formed by the superhelical coiling of the 10 nm nucleofilament, with the flat faces of the nucleosome discs arranged radially (reviewed in Felsenfeld & McGhee, 1986; Pedersen *et al.* 1986). The exact location of the linker DNA in the 30 nm fibre is not known, although it is thought to be on the inside of the fibre. Other features of the 30 nm fibre which have not been determined unequivocally include whether the linker DNA follows the superhelical path of the core particle DNA, and whether the fibre diameter varies with the length of linker DNA.

The linker histone H1 plays an important role in higher-order structure, since in its absence the 30 nm fibre does not form (Finch & Klug, 1976; Renz, Nehls & Hozier, 1977; Thoma *et al.* 1979). The exact location of histone H1 is not known, as for the linker DNA. However, the observations that anti-H1 antibodies bind histone H1 in unfolded chromatin, but not in the 30 nm fibre (Takahashi & Tashiro, 1979), and that histone H1 is digested by chymotrypsin in unfolded chromatin, but is resistant in the 30 nm fibre (Losa, Thoma & Koller, 1984), suggest that histone H1 is located on the inside of the fibre. In crosslinking studies, H1 homopolymers are crosslinked in a head-to-tail arrangement in both folded and unfolded chromatin (Lennard & Thomas, 1985). However, more H1 crosslinks are formed in the folded form than the unfolded form, suggesting greater H1-H1 interactions in the 30 nm fibre. These results support the hypothesis that histone H1 stabilizes the 30 nm fibre by forming a continuous solenoidal homopolymer on the inside of the fibre, as proposed by Thoma *et al.* (1979). The role of histone H1 in the structure of the 30 nm fibre has also been examined in relation to transcriptional regulation, since the formation of transcriptionally active chromatin appears to involve decondensation of the 30 nm fibre (see section 1.1.5).

At the third level of chromatin folding, the 30 nm fibres appear to be organized into a series of loops anchored at their bases to a nuclear substructure or matrix (see section 1.2.3). Evidence for a loop organization first came from observations of the lateral loops of lampbrush chromosomes. These greatly enlarged chromosomes are present at the diplotene stage of meiosis in the oocytes

of most animals (reviewed in Callan, 1982). They are visible in the light microscope, with lateral loops of DNA extending perpendicularly from the central chromosomal axis. A loop organization has also been demonstrated for chromosomal DNA in somatic cells. When cells are lysed in non-ionic detergent and extracted with 2 M NaCl to remove histones, the chromosomal DNA remains highly folded and constrained, and attached to a residual structure that resembles the original nucleus (Cook, Brazell & Jost, 1976; Vogelstein, Pardoll & Coffey, 1980). The rate of sedimentation in sucrose gradients of these histone-depleted nuclei, or "nucleoids", reflects the conformation of the DNA, and is modified by DNA-intercalating agents such as ethidium bromide and actinomycin D in a manner characteristic of supercoiled, circular DNA (Cook & Brazell, 1975, 1976; Ide, Nakane, Anzai & Andoh, 1975; Benyajati & Worcel, 1976). The linear DNA molecules, therefore, appear to be organized into topologically constrained, supercoiled loops by attachment to the residual nuclear matrix. The size of these loops has been estimated by a variety of techniques, including γ -irradiation and deoxyribonuclease I (DNase I) target size, the length of chromatin fragments released by DNase I digestion, the diameter of the fluorescent "halo" in ethidium bromide-stained nucleoids, and direct measurement in the EM, and ranges from 20-180 kilobases (kb), with most estimates between 50-85 kb (reviewed in Hancock, 1982; Nelson, Pienta, Barrack & Coffey, 1986b).

At mitosis, chromatin is further condensed to form the characteristic compact mitotic chromosomes visible in the light microscope. Mitotic chromosomes are on average $\sim 5 \mu\text{m}$ in length and $\sim 0.7 \mu\text{m}$ in diameter, and

represent a packing ratio of $\sim 10,000:1$. Laemmli and co-workers have presented evidence that the DNA loop organization seen in interphase nuclei is maintained during mitosis by attachment to a non-histone protein chromosome "scaffold". Treatment of HeLa cell metaphase chromosomes with the polyanions dextran sulphate and heparin, or with 2 M NaCl, removes all of the histones and most of the non-histone proteins, leaving a residual protein scaffold, which contains only a few non-histone proteins but retains many of the morphological features of metaphase chromosomes (Adolph, Cheng & Laemmli, 1977; Paulson & Laemmli, 1977). The DNA remains attached to the scaffold in a highly folded conformation, forming a "halo" of DNA around a central structure (Adolph *et al.* 1977). In the EM, the chromosome scaffold is surrounded by loops of DNA 30-90 kb in length (about the length of interphase DNA loops), anchored at their bases to the scaffold (Paulson & Laemmli, 1977). In cross-sections of unextracted metaphase chromosomes, the chromatin loops appear to be organized in a radial fashion, with their bases attached at the central axis of the chromatid (Marsden & Laemmli, 1979; Earnshaw & Laemmli, 1983).

The scaffold is composed predominantly of two proteins, Sc1 and Sc2, of relative molecular mass (*Mr*) 170,000 and 135,000, respectively (Lewis & Laemmli, 1982), and Sc1 has been identified as DNA topoisomerase II by the use of specific anti-Sc1 and anti-topoisomerase II antibodies (Earnshaw, Halligan, Cook, Heck & Liu, 1985). In intact metaphase chromosomes, topoisomerase II is localized to the central axial region of the chromatid, at the base of the radial chromatin loops (Earnshaw & Heck, 1985; Gasser, Laroche, Falquet, Boy de la Tour & Laemmli,

1986). This is the expected location for topoisomerase II if it were to play a role in the topological conformation of the DNA loops, as has been suggested (see sections 1.1.5 and 1.2.3.).

While these EM observations support the radial loop model for chromatin organization in metaphase chromosomes, other models have been proposed, including successive higher-order helical coiling (Sedat & Manuelidis, 1978). In the light and electron micrographs presented by Rattner & Lin (1985), there is evidence for both radial loops and helical coiling in metaphase chromosomes. They suggest a model in which the 30 nm chromatin fibres form radial loops attached to the central axial region, resulting in a fibre of diameter 200-300 nm. This fibre is then helically coiled about the central axis, resulting in a further compaction ratio of 9:1, to form the native chromatid of 700 nm diameter (Rattner & Lin, 1985).

1.1.3. Morphology of active chromatin

Although many studies have indicated that the structure of transcriptionally active chromatin differs both morphologically and biochemically from bulk inactive chromatin, a detailed structure for transcribing chromatin has not been determined. At the level of the light microscope, interphase chromosomes generally appear too diffuse and tangled to detect morphological changes associated with transcription. However, such changes can be detected at the level of the light microscope in the giant lampbrush and polytene chromosomes. Lampbrush chromosomes are present during meiosis in the oocytes of most animals, and have been studied mostly in Amphibians, as these contain some of

the largest lampbrush chromosomes (Callan, 1982). The lateral loops have been shown to be the sites of active transcription, and during oocyte development the loops are extended and retracted in a specific sequence, reflecting their order of transcription (Scheer, Spring & Trendelenburg, 1979b). The lateral loops are maximally extended in the developing oocyte, at sites where the rate of transcription is highest. As the transcription rate decreases, either due to oocyte maturation or the addition of actinomycin D, the loops retract and become condensed. The lateral loop, therefore, appears to define a chromatin domain, whose structure is regulated as a unit, either to facilitate transcription, or as a consequence of it.

Polytene chromosomes are present in many cell types, and have been studied mostly in the salivary gland cells of the larvae of dipteran insects such as *Drosophila* and *Chironomus* (reviewed in Korge, 1987). These giant chromosomes result from multiple cycles of DNA replication without cell division or separation of homologous chromatids. In the light microscope, stained polytene chromosomes have a species-specific pattern of alternating dark bands (chromomeres) and light interbands (interchromomeres), which reflect differences in DNA packing. During larval development, this banding pattern is altered by the appearance and disappearance of chromosome "puffs", or local regions of chromatin decondensation, in a stage- and tissue-specific pattern (Ashburner, 1972). The puffs have been shown by ^3H -uridine incorporation to be sites of active transcription (Pelling, 1964), and puffing has been interpreted as a local modification of chromatin structure associated with transcriptional activity (Beerman, 1952).

Studies with *Drosophila melanogaster* mutants have demonstrated that puffing and transcription can be uncoupled. For example, in the larval salivary gland, eight genes (*Sgs-1-8*) coding for secretion proteins are expressed at specific stages during larval development. Expression of the *Sgs* genes correlates with puffing at their corresponding gene loci (Korge, 1977). In a temperature sensitive mutant, the secretion proteins *sgs-3*, *-4*, *-7* and *-8* and their messenger RNAs (mRNAs) are not synthesized at the non-permissive temperature (30°C) (Hansson & Lambertsson, 1983). However, chromosome puffs form at the corresponding gene loci, despite the absence of transcription (Hansson, Lineruth & Lambertsson, 1981), suggesting that puff formation is not merely a consequence of transcription, but represents a modification of chromatin structure that precedes and facilitates transcription.

The morphology of active chromatin has been analysed at the ultrastructural level in the EM, and many workers have examined how the nucleosomal organization of active genes might be altered or disrupted during transcription. The nucleosome would appear to pose a steric barrier to the passage of an RNA polymerase molecule along the DNA axis, but it is still unclear how the structure of the nucleosome is altered to accommodate this. EM sections of nuclei fixed *in situ* reveal regions of condensed chromatin (heterochromatin) mostly associated with the nuclear membrane and around the nucleolus, and regions of more diffuse chromatin (euchromatin) dispersed throughout the remainder of the nucleoplasm (Heumann, 1974; Olins & Olins, 1979; Derenzini, Hernandez-Verdun & Bouteille, 1981). The euchromatin regions at the border

with heterochromatin have been shown to be the sites of active transcription by ^3H -uridine incorporation, whereas the heterochromatin is transcriptionally inactive (Fakan, 1978). Individual nucleosomes can be seen in the EM at higher magnifications, but detailed structural differences in the nucleosomal organization of active and inactive regions are difficult to detect due to the compactness of chromatin within the confines of the intact nucleus.

This problem was partially overcome with the development of the "Miller spreading" technique (Miller & Beatty, 1969; Hamkalo & Miller, 1973), in which nuclei are lysed in a low ionic strength buffer (0.5 mM Na-borate; pH 8-9), resulting in extensive chromatin unfolding. The spread chromatin is then prepared for EM observation by centrifugation through sucrose onto an EM grid. Chromatin prepared in this way is unravelled to the lowest level of chromatin organization, and bulk inactive chromatin from a wide variety of eukaryotic species displays the typical beaded morphology of repeating nucleosomes connected by linker DNA (Scheer, 1987). Also, ribonucleoprotein (RNP) fibrils, corresponding to nascent transcripts, remain associated with the extended nucleofilament, so that regions of chromatin in the process of active transcription can be identified. Although inactive chromatin has a beaded morphology when spread by the Miller technique, it commonly has a packing ratio of ~ 2 (Foe, Wilkinson & Laird, 1976; Lamb & Daneholt, 1979), whereas the native 10 nm filament has a packing ratio of ~ 6 . Thus it is obvious that this treatment not only unravels the higher-order levels of chromatin folding, but also disrupts to some degree the nucleosome structure of the native 10 nm filament. Since the

nucleosomal organization observed in Miller spreads does not necessarily reflect the situation *in vivo*, interpretations of their morphology must be made with caution. Nevertheless, this technique has revealed differences between active and inactive chromatin, and between ribosomal and non-ribosomal chromatin.

The ribosomal RNA (rRNA) genes of amphibian oocytes were the first genes to be seen in the act of transcription in the EM (Miller & Beatty, 1969), and these genes have subsequently been studied in Miller spreads of chromatin from a wide variety of organisms (Scheer, 1987). The rRNA genes are located in the nucleolus, and in most organisms are arranged in tandem repeats separated by non-transcribed spacers. Each active transcription unit has a series of RNP fibrils, corresponding to nascent pre-rRNA transcripts, extending laterally from the chromatin axis. The lateral fibrils increase in length in the direction of transcription, resulting in the characteristic "Christmas tree" appearance (Miller & Beatty, 1969). Highly transcribed rRNA genes are densely packed with RNP fibrils, obscuring the morphology of the underlying chromatin axis. However, the compaction ratio of the transcribed chromatin indicates that it is in the form of fully-extended B-form DNA, and so not organized into nucleosomes (Miller & Hamkalo, 1972; Foe *et al.* 1976). Under conditions of reduced transcriptional activity, the chromatin axis can be seen between the more sparsely distributed RNP fibrils, and exhibits a smooth, non-beaded morphology (Foe *et al.* 1976; Foe, 1978; Scheer, 1978) similar to that of pure DNA (Labhart & Koller, 1982; Labhart, Ness, Banz, Parish & Koller, 1983). The apparently non-transcribed spacers are also devoid of nucleosomes (Labhart & Koller, 1982; Labhart *et al.* 1983).

Foe (1978) examined the morphology of the ribosomal chromatin of the milkweed bug *Oncopeltus fasciatus* during embryonic development. The rRNA genes are not transcribed in the early embryonic stages (up to 32 h) and the ribosomal chromatin is in a beaded conformation indistinguishable from bulk inactive chromatin. At later stages, when the rRNA genes are highly transcribed, the ribosomal chromatin adopts a smooth, non-beaded morphology. However, in 38-44 h embryos, just before the onset of rRNA transcription, extended, non-beaded ribosomal chromatin can be seen with no associated lateral RNP fibrils. The absence of nucleosomes is therefore not merely a consequence of transcription, but appears to represent a conformational change in ribosomal chromatin structure that precedes rRNA transcription.

The fact that the Miller technique results in some degree of disruption of the nucleosomal organization of the native 10 nm nucleofilament raises the possibility that active rRNA genes are in fact associated with nucleosomes, but these are somehow altered from bulk inactive nucleosomes, and are preferentially extracted at low ionic strength. However, studies with *in situ*-fixed and *in vivo* chromatin support the idea that nucleosomes are absent from active rRNA genes. Antibodies against calf thymus histone H2B injected into *Pleurodeles waltii* oocyte nuclei cross-react with active non-ribosomal chromatin, but not with active ribosomal chromatin (Scheer, Sommerville & Bustin, 1979a). Also, anti-core histone antibodies fail to bind to ribosomal chromatin in *in situ*-fixed human lymphocytes, suggesting that histones are absent from the rRNA genes (Derenzini, Pession, Licastro & Novello, 1985). In EM sections of *in situ*-fixed rat and

human nuclei, the ribosomal chromatin appears to be non-nucleosomal, and in the form of fully-extended B-form DNA (Derenzini, Hernandez-Verdun & Bouteille, 1982; Derenzini, Hernandez-Verdun, Farabegoli, Pession & Novello, 1987). Although only a small proportion of the rRNA genes are transcriptionally active in human lymphocytes, all the ribosomal chromatin is in the extended, non-nucleosomal configuration (Derenzini *et al.* 1987). Thus, ribosomal chromatin, including both active and inactive rRNA genes, appears to form a chromatin domain which is devoid of nucleosomes.

In Miller spreads, highly transcribed non-ribosomal chromatin, like ribosomal chromatin, is densely covered with nascent RNP fibrils, with few, if any, nucleosome-sized particles associated with the chromatin axis (Franke, Scheer, Trendelenburg, Spring & Zentgraf, 1976; Scheer, 1978; Lamb & Daneholt, 1979). However, the majority of non-ribosomal genes are transcribed at a more moderate rate, and nucleosome-sized particles can be detected between the RNP fibrils of these genes (Foe *et al.* 1976; Laird, Wilkinson, Foe & Chooi, 1976; McKnight, Bustin & Miller, 1978; Scheer, 1978; Wurtz & Fakan, 1983), in contrast to the unbeaded morphology of sparsely transcribed ribosomal chromatin. Scheer (1978) examined nucleosomal organization in states of reduced transcriptional activity in the retracting loops of *Xenopus* oocyte lampbrush chromosomes. Highly transcribed loops have a fully-extended, non-beaded morphology, but as the rate of transcription decreases, nucleosome-sized particles appear between the more sparsely distributed RNP fibrils. Thus, in the case of non-ribosomal chromatin, but not ribosomal chromatin, nucleosomes appear to

reform immediately after the passage of an RNA polymerase complex, provided sufficient time elapses before the next transcription event. Evidence from immunological studies suggests that histones remain associated with even highly transcribed genes. Anti-histone H2B antibodies injected into the nuclei of *P. waltii* oocytes cross-react with the highly transcribed and extended lampbrush chromosome loops, demonstrating that histone H2B remains associated with highly transcribed chromatin *in vivo* (Scheer *et al.* 1979a).

The non-nucleosomal morphology of Miller spreads of highly active non-ribosomal chromatin may be an artifact of the spreading technique. Lamb & Daneholt (1979) examined the highly active Balbiani ring (BR) puffs in polytene chromosomes from the salivary gland cells of *Chironomus tentans*. In chromatin spreads, the active BR genes are sparsely beaded and have a packing ratio of 1.6, compared to the regularly beaded morphology and packing ratio of 1.9 for inactive chromatin. However, Olins and co-workers estimated the compaction ratio in the active BR region to be ~ 8 from three-dimensional reconstructions of EM sections of *in situ*-fixed nuclei (Olins, Olins, Levy, Durfee, Margle, Tinnel & Dover, 1983). This value is similar to the packing ratio of the 10 nm nucleofilament, implying that even these highly transcribed genes are organized into nucleosomes. These nucleosomes may be somewhat modified compared to inactive nucleosomes, since they appear to be preferentially susceptible to disruption by the Miller spreading technique.

The nucleosome structure of *in vivo*-transcribing chromatin has been examined in psoralin crosslinking studies in the DNA tumour virus simian virus 40

(SV40) (DeBernardin, Koller & Sogo, 1986). In infected cells, the circular, double-stranded DNA genome of SV40 is complexed with cellular histones and organized into a "minichromosome" of ~ 27 nucleosomes, and is transcribed by RNA polymerase II (Griffith, 1975; Gariglio, Llopis, Oudet & Chambon, 1979). Psoralin induces crosslinks between the strands of the DNA double helix. In chromatin, crosslinks are induced primarily in linker DNA, whereas nucleosomal DNA is protected. When transcribing SV40 minichromosomes are crosslinked and deproteinized, and the DNA denatured and viewed in the EM, single-stranded "bubbles" of length 135-140 bp corresponding to nucleosomal DNA can be seen, separated by crosslinked regions corresponding to linker DNA. Also, nascent RNA transcripts are crosslinked to the DNA at their points of attachment, identifying sites in the process of active transcription. DeBernardin *et al.* (1986) found that *in vivo*-transcribing and non-transcribing minichromosomes contain the same number of nucleosomal bubbles, indicating that transcription does not lead to a loss of nucleosomes. They also found nascent RNA transcripts crosslinked to both nucleosomal bubbles and linker DNA, suggesting that a transcribing RNA polymerase II molecule can form a complex with a nucleosome, or a nucleosome-sized particle. These particles contain histones, since the nucleosomal bubbles, both with and without crosslinked RNA, disappear if the histones are extracted with 1.2 M NaCl before crosslinking. These results suggest that RNA polymerase II can transcribe through a histone-containing nucleosome-sized particle, and that physical displacement of the nucleosome core from the DNA axis is not required.

1.1.4. Nuclease sensitivity of active chromatin

Chromatin structure has been analysed by its sensitivity to relatively non-specific nucleases such as pancreatic DNase I (deoxyribonuclease I) and MNase (micrococcal nuclease). Numerous studies have shown that transcriptionally active chromatin has an altered structure from bulk inactive chromatin, which renders the DNA preferentially sensitive to nuclease digestion (reviewed in Igo-Kemenes, Horz & Zachau, 1982; Weisbrod, 1982a; Reeves, 1984).

MNase digestion studies have analysed three properties of chromatin: *a*) accessibility to the enzyme, *b*) disruption of the nucleosomal repeat pattern, and *c*) solubility in Mg^{2+} - and EDTA-containing buffers. MNase preferentially cleaves the linker DNA between nucleosomes, while the intranucleosomal DNA remains protected. A light MNase digestion generates a series of nucleosomal particles corresponding to monomers, dimers, trimers and higher oligomers. The DNA fragments purified from these particles are multiples of ~ 200 bp in length, reflecting the nucleosomal repeat length. Initial studies demonstrated that MNase digestion does not result in preferential degradation of the transcriptionally active globin genes of avian erythrocytes (Lacy & Axel, 1975; Weintraub & Groudine, 1976) or ovalbumin genes of hen oviduct cells (Garel & Axel, 1976). This implies that active genes are packaged in nucleosomes, in agreement with the EM observations of other RNA polymeraseII-transcribed genes. However, analysis of the MNase digestion products suggests that MNase preferentially cleaves transcriptionally active sequences into mono- and dinucleosomes, rather than higher oligomers.

MNase digested chromatin can be fractionated by sucrose density sedimentation, and the DNA fragments extracted from the separated monomer- and higher oligomer-size particles. Alternatively, the DNA fragments can be purified from MNase digested but unfractionated chromatin, and separated by gel electrophoresis. The distribution of specific sequences between these fractions can then be assayed by hybridization. In hen oviduct cells, the chromatin fraction released as mono- and dinucleosomes is enriched in the active ovalbumin genes relative to the inactive globin genes and bulk DNA, whereas there is no enrichment in mature erythrocytes, where both genes are inactive (Bellard, Gannon & Chambon, 1978; Bloom & Anderson, 1978). Also, Bloom & Anderson (1979, 1982) showed that the enrichment of active genes in the monomer fraction is greatest at the early stages of MNase digestion (1-3% acid solubility), demonstrating that active chromatin is cleaved into monomers faster than bulk chromatin. It is important to note that in these studies active chromatin is not preferentially degraded, i.e. digested to non-hybridizable fragments, but is cleaved into nucleosome-size particles faster than inactive chromatin, and so is more accessible to the enzyme.

The increased accessibility of active chromatin to MNase is related to transcriptional activity, since the enrichment of ovalbumin genes in the monomer fraction of chromatin from estrogen-stimulated immature chick oviduct cells is progressively lost when the hormone is withdrawn and the ovalbumin gene becomes inactive (Bloom & Anderson, 1979). Also, the globin genes of chick immature erythrocytes are no longer selectively cleaved into nucleosomes in

transcriptionally inactive mature erythrocytes (Bloom & Anderson, 1979). MNase can also distinguish between genes transcribed at different rates, since the ovalbumin-related X and Y genes, which are transcribed at low rates compared to the ovalbumin gene, are not preferentially accessible to MNase (Anderson, Vanderbilt, Lawson, Tsai & O'Malley, 1983). The sequences flanking the 5' and 3' termini are also not enriched in the mono- and dinucleosome fraction, indicating that the region of chromatin that is preferentially accessible to MNase is restricted to the transcribed sequences (Anderson *et al.* 1983).

Several groups have reported that the nucleosomal repeat pattern of highly transcribed genes is smeared or blurred, reflecting a disruption of the nucleosomal organization of these genes. The typical nucleosomal repeat pattern of bulk chromatin is seen by gel electrophoresis of DNA purified from MNase digested nuclei. This DNA forms a ladder of discrete fragments in multiples of nucleosomal-length DNA (~200 bp). The nucleosomal organization of specific genes can be analysed by transfer of this DNA to filters by Southern (1975) blotting and hybridization with gene-specific probes. The coding region of the *Drosophila* 70K heat shock protein gene (*HSP70*), which is inactive in normal cells, has a discrete nucleosomal repeat pattern similar to that of bulk inactive chromatin. On heat shock, this pattern becomes increasingly blurred, suggesting that the nucleosomal organization is disrupted during transcription (Wu, Wong & Elgin, 1979b; Levy & Noll, 1981). The nucleosomal repeat pattern of the transcriptionally active ovalbumin genes of hen and estrogen-stimulated chick oviduct cells is smeared and less distinct than that of the inactive globin genes in

these cells, or the ovalbumin gene in erythrocytes (Bellard, Dretzen, Bellard, Oudet & Chambon, 1982; Bloom & Anderson, 1982). The discrete nucleosomal repeat pattern of the ovalbumin gene returns when estrogen is withdrawn from the chick oviduct cells and the gene becomes inactive (Bloom & Anderson, 1982).

The smearing of the MNase cleavage pattern of the active ovalbumin sequences is not due to the loss of nucleosomes, as discussed above, but could be due to increased MNase cleavage of either the nucleosomal or linker DNA. Bloom & Anderson (1982) analysed the MNase cleavage sites in the chromatin of transcriptionally active and inactive ovalbumin genes after extensive MNase digestion of hen oviduct and liver chromatin. The DNA was purified, denatured, and the resulting monomer (140-160 bp) and submonomer (<140 bp) fragments separated by electrophoresis. The concentration of ovalbumin sequences in each of these fractions was found to be the same in hen oviduct and liver chromatin, indicating that the active ovalbumin gene is not cleaved into submonomer fragments more often than the inactive gene. Also, the lengths of the single-stranded DNA fragments generated by MNase cleavage are the same in the active and inactive genes. These results suggest that the smearing of the nucleosomal repeat pattern is not due to an increase in the number of internal MNase cleavage sites in nucleosomal DNA, but rather to an expansion of the region of MNase cleavage in the linker DNA, and possibly reflects unfolding of the higher-order chromatin structure (Bloom & Anderson, 1982).

Chromatin structure has also been analysed using a fractionation procedure based on differential solubility of MNase digested chromatin in Mg^{2+} - and EDTA-

containing buffers (Rose & Garrard, 1984). After MNase digestion in 5 mM $MgCl_2$, nuclei are centrifuged to yield a Mg^{2+} -soluble supernatant fraction (S1). The pellet is resuspended in 2 mM EDTA, and centrifuged to yield an EDTA-soluble supernatant (S2) and an EDTA-insoluble pellet (P). The S1 fraction contains 5-8% of the total DNA - predominantly in the form of mononucleosomes, is depleted in histone H1, and is enriched in non-histone proteins, including the high mobility group (HMG) proteins (see section 1.1.5). The S2 and P fractions contain higher nucleosomal oligomers, with the bulk of the DNA (80-85%) in the histone H1-containing S2 fraction, and 10-15% of the DNA in the histone H1-depleted P fraction.

Rose & Garrard (1984) found that the active κ immunoglobulin light chain (κ IgL) genes in a murine plasmacytoma cell line are enriched in the S1 and P fractions and depleted in the S2 fraction, relative to total DNA and to the inactive β -globin genes. The enrichment in the P fraction is greatest at early times of MNase digestion, but with increasing digestion these sequences appear to be processed into the S1 fraction. The nucleosomal repeat pattern of the κ IgL sequences in the insoluble P fraction is highly disrupted, whereas in the S1 fraction these sequences are in the form of discrete monomers. Thus the disrupted P fraction κ IgL sequences appear to be processed by MNase cleavage into soluble mononucleosomes.

These workers also examined κ IgL chromatin structure in a cell line in which one of the κ IgL alleles is transcriptionally inactive due to a promoter deletion (Rose & Garrard, 1984). Both the inactive (κ^+) and active (κ) alleles are

enriched in the P fraction and depleted in the S2 fraction, and the nucleosomal repeat pattern of the P fraction sequences is disrupted for both alleles. Also, these two properties extend at least 6.5 kb downstream from the transcription termination region of the active κ IgL gene (Xu, Barnard, Rose, Cockerill, Huang & Garrard, 1986). Therefore, transcription *per se* is not responsible for the insolubility of this chromatin or the disruption of the nucleosomal repeat pattern. At the early stages of MNase digestion, the S1 fraction contains lower levels of the κ^+ sequences relative to κ_f sequences (Rose & Garrard, 1984). The κ^+ sequences are processed into the S1 fraction only after a longer MNase digestion, implying that the inactive allele is less accessible to the enzyme than the active allele. This suggests that accessibility of chromatin to MNase is directly related to transcription, in agreement with the studies of Bloom & Anderson (1979) and Anderson *et al.* (1983) discussed above.

Histone H1 is required for regular nucleosomal spacing in reconstituted chromatin *in vitro* (Stein & Kunzler, 1983). Therefore, the disruption of the nucleosomal repeat pattern in the histone H1-depleted P fraction may be due to irregular nucleosomal spacing. This would explain why active sequences initially form a smear, but are processed to discrete monomers. The insolubility of active chromatin in EDTA may be due to interactions with insoluble residual nuclear structures, as the method used to generate the insoluble P fraction is similar to that used by Long & Ochs (1983) to prepare nuclear matrix (see section 1.2).

Unlike MNase, DNase I cleaves intranucleosomal DNA as efficiently as linker DNA, resulting in a series of DNA fragments of length 20-160 bp in

multiples of 10 bp (Noll, 1974). The 10 bp repeat is thought to reflect the helical repeat due to cleavage at the exposed side of the DNA helix wrapped around the nucleosome core. In all cases studied, transcriptionally active genes have been found in an altered chromatin structure that renders the DNA preferentially susceptible to degradation by DNase I (reviewed in Igo-Kemenes *et al.* 1982; Weisbrod, 1982a; Reeves, 1984). The DNase I sensitive regions span many kilobases, and differ from the shorter (100-500 bp) DNase I hypersensitive sites detected at lower levels of DNase I digestion (section 1.1.6).

Weintraub & Groudine (1976) first showed that DNase I preferentially degrades the active globin genes of chicken erythrocytes, but not the inactive globin genes of fibroblasts, or the inactive ovalbumin genes of erythrocytes. Conversely, the ovalbumin genes are DNase I sensitive in hen oviduct cells, where they are expressed, but not in tissues where they are inactive (Garel & Axel, 1976). The DNase I sensitive regions are not confined to the transcribed sequences themselves, but extend well into the non-transcribed 5'- and 3'-flanking sequences. In hen oviduct cells, the DNase I sensitive domain surrounding the ovalbumin gene spans ~100 kb, and includes the ovalbumin-related X and Y genes (Lawson, Knoll, March, Woo, Tsai & O'Malley, 1982). The boundaries of the DNase I sensitive domains of two other cellular genes have been mapped. The chicken glyceraldehyde-3-phosphate dehydrogenase gene, a constitutively expressed "housekeeping" gene, is surrounded by a DNase I sensitive domain of ~12 kb, which includes ~4 kb of transcribed DNA, plus ~5 kb of 5'-flanking and ~3 kb of 3'-flanking non-transcribed sequences (Alvey, Tsai & O'Malley,

1984). In hen oviduct cells, the lysozyme gene is embedded in a DNase I sensitive domain of ~24 kb, comprising ~4 kb of transcribed DNA, plus ~14 kb of 5'-flanking and ~6 kb of 3'-flanking non-transcribed sequences (Jantzen, Fritton & Igo-Kemenes, 1986). In all three cases, the transition from the DNase I sensitive to the resistant conformation appears to occur gradually, over 5-10 kb.

The DNase I sensitive conformation of the chicken erythrocyte globin genes is retained in mature erythrocytes, even though these genes are inactive (Weintraub & Groudine, 1976; Bloom & Anderson, 1979). Similarly, the entire ~100 kb surrounding the ovalbumin genes of estrogen-stimulated chick oviduct cells remains DNase I sensitive when the hormone is withdrawn (Lawson *et al.* 1982). In contrast, these genes are no longer selectively cleaved or disrupted by MNase (Bloom & Anderson, 1979, 1982), indicating that different features of chromatin structure are recognized by DNase I and MNase. The DNase I sensitive conformation is acquired by newly replicated chromatin within 3 min of synthesis, and so precedes transcription (Weintraub, 1979). Also, in embryonic chicken erythroid cells, the adult β -globin genes are already in a DNase I sensitive conformation, even though they are not yet expressed (Stalder, Groudine, Dodgson, Engel & Weintraub, 1980a). Therefore, DNase I sensitivity appears to reflect a permanent change in chromatin structure which is necessary, but not sufficient, for transcription. This altered structure may be related to differentiation, signifying the commitment of a cell type to express a specific gene.

The question arises as to how this altered chromatin structure is propagated uniformly through a domain containing hundreds of nucleosomes. DNase I

sensitivity may be due to modifications of the individual nucleosomes themselves that result in enhanced digestion of the associated DNA, or due to unfolding of higher-order structures to form a more "open" fibre more accessible to the enzyme. These two possibilities are not mutually exclusive, and in fact either could induce the other. Bloom & Anderson (1982) compared the patterns of DNase I cleavage sites in active and inactive chromatin. Hen oviduct chromatin was digested with DNase I, and the purified DNA fragments denatured, fractionated by gel electrophoresis, and analysed by Southern blotting and hybridization. Similar 10 bp repeats were observed for the active ovalbumin and inactive globin genes, implying that although the active sequences are more sensitive to DNase I digestion, active and inactive nucleosomes are cleaved at the same sites. These results suggest that enhanced DNase I sensitivity is not due to modified nucleosome-DNA interactions, but due to unfolding of higher-order structures.

1.1.5. Active chromatin domains

The nuclease digestion studies indicate that active and potentially active genes lie in chromatin domains with an altered structure compared with bulk inactive chromatin. The biochemical composition of active chromatin has been analysed in order to identify the component(s) responsible for this altered structure. Most procedures for generating active and inactive chromatin fractions involve MNase digestion followed by fractionation on the basis of differential solubility in mono- and divalent cations (*e.g.* Sanders, 1978; Levy-Wilson, Connor & Dixon, 1979; Davie & Saunders, 1981; Rose & Garrard, 1984). Generally, these

studies have shown that active chromatin is depleted in histone H1, has an altered distribution of H1 variants, is enriched in ubiquitinated and acetylated core histones, and enriched in non-histone chromosomal proteins, including the HMG (high mobility group) proteins, although contrary results have also been reported (reviewed in Igo-Kemenes *et al.* 1982; Weisbrod, 1982a; Reeves, 1984). However, these features merely correlate with active chromatin, and the actual cause of the conformational change remains to be identified.

A role for the linker histone in regulation of active chromatin structure is suggested by the occurrence of tissue- and stage-specific H1 variants, such as histone H5 in the transcriptionally silent mature avian erythrocyte (Weintraub, 1978), and histone H1⁰ in non-dividing cells (Pehrson & Cole, 1980), where it is preferentially associated with inactive genes (Roche, Gorka, Goeltz & Lawrence, 1985). Also, many chromatin fractionation studies have shown that the active fraction is depleted in histone H1 (Sanders, 1978; Levy-Wilson *et al.* 1979; Davie & Saunders, 1981; Rocha, Davie, van Holde & Weintraub, 1984; Rose & Garrard, 1984; Huang, Barnard, Xu, Matsui, Rose & Garrard, 1986). Together with the observations that histone H1 is required for the higher-order folding of the 10 nm filament into the 30 nm fibre *in vitro* (section 1.1.2), and that the compaction ratio of the active regions of *in situ*-fixed chromatin is similar to that of the 10 nm filament (section 1.1.3), these results suggest that the less condensed structure of active chromatin may be maintained by reduced binding of histone H1. However, the fractionation studies do not establish whether the depletion of histone H1 in the active fraction necessarily reflects the composition of active

nucleosomes *in vivo*, and other studies suggest that histone H1 is in fact present in active chromatin.

Weintraub (1984) used mild MNase digestion of chicken erythrocyte chromatin to generate supranucleosomal fragments, which migrate as discrete nucleoprotein particles in agarose gels. The particles containing inactive sequences remain intact with increasing MNase digestion, indicating that adjacent nucleosomes are held together despite extensive cleavage of the linker DNA. Histone H1/H5 is required for this crosslinking, since in its absence the supranucleosomal particles do not remain intact. Nucleoprotein particles containing the β -globin gene, which although not transcribed in mature erythrocytes is maintained in a DNase I sensitive conformation (Weintraub & Groudine, 1976), also contain histone H1/H5, and in similar amounts to the inactive particles. However, these particles do not remain intact with increasing MNase digestion. These results suggest that histone H1/H5 is present in active chromatin, but its binding is somehow altered so that it does not crosslink adjacent nucleosomes.

In another study, the sedimentation rate of an *Eco*RI chromatin fragment containing the β -globin gene from chicken erythrocytes was compared with that of the same size fragment from bulk inactive chromatin (Caplan, Kimura, Gould & Allan, 1987). The fragment containing the β -globin gene sediments more slowly than the inactive fragments, indicating a more open structure. The protein:DNA ratios as measured by buoyant density in CsCl gradients suggest that this altered structure is not due to a reduced amount of histone H1 in the active fragment.

The evidence to date, therefore, is unclear as to whether histone H1 is depleted in active chromatin, or whether the amount of histone H1 is unaltered, but its binding properties are modified.

The HMG proteins 14 and 17 are small acid-soluble non-histone chromosomal proteins of $M_r \sim 10,000-12,000$. Active chromatin fractions have been shown to be enriched in HMG 14 and 17, and HMG 14- and 17-containing nucleosomes have been shown to be enriched in active sequences, although evidence to the contrary has also been presented (reviewed in Reeves, 1984). Even in cases where HMG 14 and 17 have been found to be preferentially associated with active chromatin, a significant proportion of the total HMG 14 and 17 content ($\sim 50-65\%$) remains associated with inactive chromatin (Davie & Saunders, 1981; Levinger, Barsoum & Varshavsky, 1981; Rocha *et al.* 1984; Brotherton & Ginder, 1986).

All nucleosomes can bind HMG 14 and 17 at two sites, at the DNA entry and exit points on the nucleosome (Sandeen, Wood & Felsenfeld, 1980). As these correspond to the histone H1 binding sites, it was suggested that HMG 14 and 17 binding may displace histone H1 in active chromatin. However, nucleosome cores can simultaneously bind one molecule of histone H1 and two molecules of HMG 14/17 *in vitro* (Albright, Wiseman, Lange & Garrard, 1980), and chemical crosslinking of chromatin produces H1-HMG 14/17 crosslinks (Ring & Cole, 1979), again implying that nucleosomes can simultaneously bind histone H1 and HMG 14/17.

HMG 14 and 17 have been shown to confer the property of DNase I sensitivity on active genes. When chicken erythrocyte chromatin is eluted with 0.35 M NaCl, which removes almost all of the non-histone chromosomal proteins, including HMG 14 and 17, the active β -globin gene is no longer preferentially sensitive to DNase I digestion. DNase I sensitivity is restored by adding back either the 0.35 M NaCl wash, or purified HMG 14 or 17 (Weisbrod & Weintraub, 1979; Gazit, Panet & Cedar, 1980; Weisbrod, Groudine & Weintraub, 1980). However, others have reported that HMG 14 and 17 do not restore DNase I sensitivity to the active β -globin gene in chicken erythrocytes (Nicolas, Wright, Cockerill, Wyke & Goodwin, 1983) or in mouse erythroleukaemia cells (Reeves & Chang, 1983).

HMG 14 and 17 have been shown to bind preferentially to active nucleosomes in HMG-depleted chromatin (Sandeel *et al.* 1980; Brotherton & Ginder, 1986). Weisbrod & Weintraub (1981) used this property to isolate active nucleosomes on an "HMG-affinity" column, consisting of immobilized HMG 14 and 17 and HMG-depleted chicken erythrocyte chromatin. The bound nucleosomes were enriched in active β -globin sequences, whereas the unbound fraction was enriched in inactive ovalbumin sequences. These results imply that the HMG-depleted active nucleosome cores retain the ability to bind preferentially to the exogenous HMG 14 and 17 proteins. Analysis of the composition of the bound and unbound nucleosomes, however, failed to identify differences which could account for this (Weisbrod & Weintraub, 1981; Weisbrod, 1982b).

There is some evidence that post-translational modifications of core histones,

such as ubiquitination or acetylation, may be associated with transcriptionally active nucleosomes. In chromatin the small polypeptide ubiquitin (*Mr* 8,500) is conjugated with 5-15% of histone H2A and minor amounts of histone H2B (Wu, Kohn & Bonner, 1981). Nucleosomes containing ubiquitinated H2A (uH2A) have been shown to be preferentially associated with the transcribed *Drosophila HSP70* and *copia* genes, but absent from non-transcribed satellite DNA sequences (Levinger & Varshavsky, 1982), and preferentially associated with the 5' end of the transcribed mouse dihydrofolate reductase gene (Barsoum & Varshavsky, 1985). However, chromatin fractionation studies have provided evidence both for (Davie & Nickel, 1987) and against (Huang *et al.* 1986) enrichment of uH2A and uH2B in active chromatin.

Acetylated core histones may also be associated with transcriptionally active chromatin. Fractionation studies based on preferential solubilization of active nucleosomes in mono- and divalent cations have shown that the active fraction is enriched in hyperacetylated core histones (Davie & Candido, 1978; Perry & Chalkley, 1982; Nelson, Ferris, Zhang & Ferenz, 1986a). The Mg^{2+} -soluble polynucleosomes of chicken erythrocyte chromatin are enriched in β -globin gene sequences and hyperacetylated core histones (Nelson *et al.* 1986a). Deacetylation of these polynucleosomes *in vitro* renders them as insoluble as bulk inactive polynucleosomes, implying that the preferential solubility of active nucleosomes in Mg^{2+} -containing buffers is due to hyperacetylation of their core histones (Alonso, Ferris, Zhang & Nelson, 1987).

The effect of histone hyperacetylation can be studied by treating cells with

n-butyrate, an inhibitor of histone deacetylase, which results in accumulation of hyperacetylated forms of histones H3 and H4 (Vidali, Boffa, Bradbury & Allfrey, 1978). This is accompanied by an increase in chromatin DNase I sensitivity, suggesting that preferential DNase I sensitivity of active chromatin may be the result of core histone hyperacetylation. Furthermore, hyperacetylation does not result in unfolding of the structure of individual nucleosome cores (Vidali *et al.* 1978; Imai, Yan, Baldwin, Ibel, May & Bradbury, 1986), in accordance with the studies of Bloom & Anderson (1982), which suggest that DNase I sensitivity reflects changes in the higher-order folding of chromatin, rather than changes in the structure of individual nucleosomes.

The structural changes associated with active chromatin domains may reflect modifications to the structure of the underlying DNA chain itself, rather than the protein component of chromatin. The modified base 5-methylcytosine (5-mC) occurs in the DNA of higher eukaryotes, predominantly at the sequence 5'-CpG-3'. Hypomethylation at these sites usually, but not always, correlates with gene activity (reviewed in Doerfler, 1983; Reeves, 1984). In various animal cells, the content of 5-mC is reduced 2- to 3-fold in the DNase I sensitive active chromatin regions compared with that in total chromatin (Naveh-Mani & Cedar, 1981), and 5-mC has been shown to be preferentially associated with histone H1-containing nucleosomes in the inactive fraction of chromatin (Ball, Gross & Garrard, 1983). However, in human placenta and the tumour-derived KB and HeLa cell lines, which do not express the β -globin gene locus, these sequences are hypomethylated (van der Ploeg & Flavell, 1980), and many highly methylated

genes are actively transcribed, *e.g.* the chicken $\alpha 2$ (type I) collagen gene (McKeon, Ohkubo, Pastan & deCrombrugge, 1982). Therefore, although DNA methylation may be important in the regulation of expression of certain genes, hypomethylation does not appear to be a general signal for the formation of active chromatin.

The structure of active chromatin may be related to supercoiling in the underlying DNA chain. The degree of supercoiling, or superhelical density, is determined by the number of times the two strands of the DNA helix are intertwined, and in topologically closed DNA molecules, the introduction or removal of supercoils induces torsional stress. The intracellular level of supercoiling is regulated by the balancing effects of two types of enzymes, DNA topoisomerase type I (topo I), which introduces transient single-strand breaks into DNA and relaxes supercoils, and DNA topoisomerase type II (topo II), which makes transient double-strand breaks, and can both introduce and remove supercoils (reviewed in Vosberg, 1985; Wang, 1985).

In prokaryotes, the chromosomal DNA is organized into negatively supercoiled loops, and it has been shown that negative supercoiling is required for transcription of some genes (Smith, 1981). In eukaryotes, removal of the histones reveals the chromosomal DNA to be organized into negatively supercoiled loops topologically constrained by attachment to a residual nuclear matrix (Cook & Brazell, 1975, 1976; Benyajati & Worcel, 1976). No significant torsional stress has been detected in the eukaryotic genome *in vivo* (Sinden, Carlson & Pettijohn, 1980), the superhelical tension presumably being alleviated by wrapping the DNA

around the nucleosome. In this study, however, torsional stress in a small fraction of the genome would not be detected, and subsequent studies have suggested that the active portion is indeed under torsional stress.

Studies with SV40 have shown that a small fraction of minichromosomes (2-5%), whose properties correlate with the transcriptionally active fraction, are under torsional stress (Luchnik, Bakayev, Zbarsky & Georgiev, 1982). Worcel and colleagues have analysed chromatin assembly and transcription on *Xenopus* 5S RNA gene-containing plasmids injected into *Xenopus* oocytes. Although nucleosomes are formed within 10-30 min of injection, transcription increases only gradually over the first 2 h, and correlates with an increase in superhelical tension (Ryoji & Worcel, 1984). Assembly of torsionally stressed chromatin and its transcription are inhibited by novobiocin, a topo II inhibitor, both *in vitro* (Glikin, Ruberti & Worcel, 1984; Kmiec & Worcel, 1985; Kmiec, Ryoji & Worcel, 1986) and *in vivo* (Ryoji & Worcel, 1984, 1985), implying that torsional stress is maintained by topo II and is required for transcription.

Studies on the effect of novobiocin on host cellular chromatin also suggest that DNA torsional stress is involved in active chromatin structure. Novobiocin blocks the heat-induced transcription of the *Drosophila* HSP genes (Han, Udvardy & Schedl, 1985), and reverses the preferential DNase I sensitivity of the active β -globin gene domain in chicken erythrocytes (Villegonteau, Lundell & Martinson, 1984), implying that topo II-mediated torsional stress is required for the DNase I sensitive "open" structure of active chromatin. It has been suggested, however, that novobiocin may act by a mechanism distinct from topo

II inhibition (Cotton, Bresnahan, Thompson, Sealy & Chalkley, 1986; Gottesfeld, 1986; Villeponteau, Pribyl, Grant & Martinson, 1986). Nevertheless, Villeponteau & Martinson (1987) have shown that the DNase I sensitivity of the β -globin gene domain is also reversed by γ -rays and by bleomycin, agents which remove torsional stress by introducing nicks into the DNA. Therefore, the DNase I sensitive conformation of active chromatin appears to require torsionally stressed DNA, but whether this is maintained by topo II is still unclear.

In order to maintain torsional stress and DNase I sensitivity, the integrity of the DNA must be maintained throughout the entire domain. Therefore, these properties will be lost when a single nick is introduced into the domain. Villeponteau & Martinson (1987) found that the DNase I sensitivity of the β -globin domain is reversed at around one nick per 150 kb of DNA, implying that the β -globin gene is surrounded by a DNase I sensitive domain of length ~ 150 kb.

The mechanism of how torsional stress is related to active chromatin structure is not understood, but it provides an attractive model correlating the DNase I sensitive domains with the independently constrained supercoiled loops attached to the nuclear matrix. Increasing the torsional stress in a loop would translate into a structural alteration in chromatin spread uniformly throughout the domain. Torsionally stressed DNA may have an altered binding affinity for transcription factors, HMG proteins, histones, *etc.* Topo II has been shown to be a major component of the mitotic chromosome scaffold and interphase nuclear matrix, and topo II recognition sites have been mapped to DNA sequences at the base of chromosomal loops (see section 1.2.3), suggesting that topo II may act at

the base of the loop to regulate torsional stress, and therefore chromatin structure, throughout the entire loop/domain.

1.1.6. DNase I hypersensitive sites

Nuclease digestion of chromatin reveals not only the large DNase I sensitive domains, but also relatively short regions of chromatin (100-500 bp) that are extremely sensitive to double-strand DNA cleavage by DNase I and other nucleases. These hypersensitive (HS) sites are frequently, but not exclusively, located in the 5'-flanking sequences of active and potentially active genes, often at important *cis*-acting regulatory sequences such as transcription promoters, enhancers, and hormone-responsive elements (reviewed in Elgin, 1984; Yaniv & Cereghini, 1986). HS sites are thought to represent local regions of altered chromatin structure in which the DNA is exposed in order to allow access of these *cis*-acting regulatory sequences to *trans*-acting transcription factors.

In developmentally regulated genes the appearance of HS sites is tissue- and stage-specific. For example, an HS site is present close to the 5' end of the active embryonic β -globin gene in chicken embryonic erythroblasts, but absent in adult erythroblasts and brain cells, which do not express this gene. Conversely, new HS sites appear in adult erythroblast chromatin at 2 kb and 6 kb upstream from an expressed adult β -globin gene, whereas these are absent in embryonic erythroblasts and brain cells, (Stalder, Larsen, Engel, Dolan, Groudine & Weintraub, 1980b). Also, an HS site of \sim 300 bp is present immediately upstream from the active preproinsulin gene in rat pancreatic cells, but absent in tissues that do not express this gene (Wu & Gilbert, 1981).

The location and tissue-specificity of HS sites suggests that they are related to gene expression. However, they are not merely a consequence of the transcription process *per se*, since HS sites can be detected before the onset of transcription, *e.g.* in the α - and β -globin gene domains in chicken erythroid precursor cells (Weintraub, Beug, Groudine & Graf, 1982). They can also be maintained after transcription has ceased. Three HS sites are induced in the 5'-flanking region of the vitellogenin II gene in chicken liver by estrogen. On withdrawal of the hormone two of these sites persist, indicating that they can be maintained in the absence of transcription and hormone (Burch & Weintraub, 1983). Groudine & Weintraub (1982) analysed the HS sites induced in the α - and β -globin gene domains of chicken embryo fibroblasts by transformation with a temperature sensitive Rous sarcoma virus (RSV). At the permissive temperature (36°C) the active RSV *v-src* gene product induces the formation of DNase I HS sites in the globin genes and transcription of these genes. At the non-permissive temperature (41°C) the *v-src* gene product is inactive and globin gene transcription ceases. The HS sites persist, however, even after 20 generations, indicating that once induced, they can be stably propagated to progeny cells in the absence of transcription and the original inducing agent. Therefore, HS sites appear to be necessary, but not sufficient, for transcription, and may signify the commitment of a differentiated cell lineage to express a specific gene.

Studies on SV40 minichromosomes suggest that the increased nuclease sensitivity at HS sites may result from the absence of a nucleosome. During late SV40 infection, a ~350 bp HS site is present at a region containing the origin of

replication, the early and late promoters, and the transcriptional enhancer (Scott & Wigmore, 1978; Varshavsky, Sundin & Bohn, 1979; Saragosti, Moyne & Yaniv, 1980). In the EM, this region appears as a "gap" in the beaded nucleosomal structure, indicating that the HS site corresponds to a nucleosome-free region of the minichromosome (Jakobovits, Bratosin & Aloni, 1980; Saragosti *et al.* 1980). Furthermore, when the enhancer element is moved to another position on the SV40 genome, a nucleosome-free HS site is generated at the new position, independent of the orientation of the enhancer (Jongstra, Reudelhuber, Oudet, Benoist, Chae, Jeltsch, Mathis & Chambon, 1984). Also, mutational analysis has shown that sequences within the enhancer element are essential for generating the HS chromatin structure (Jongstra *et al.* 1984; Gerard, Montelone, Walter, Innis & Scott, 1985).

Similar observations have been made in cellular chromatin. A tissue-specific HS site occurs in the 5'-flanking sequences of the rat elastase I gene, at a 134 bp enhancer element responsible for tissue-specific transcription of this gene. When this enhancer is linked to a heterologous promoter and introduced into the germ line of mice, a tissue-specific HS site is generated at the enhancer, whether it is positioned upstream or downstream from the promoter (Hammer, Swift, Ornitz, Quaife, Palmiter, Brinster & MacDonald, 1987). Mutations within the 134 bp enhancer abolish the HS site, indicating that specific sequences are required for formation of the HS chromatin structure.

While HS sites in chromatin may be nucleosome-free, these regions do not appear to be devoid of protein. Higher resolution mapping of the nuclease

sensitivity pattern within HS sites reveals alternating regions of enhanced sensitivity and relative protection, suggesting that proteins are bound at the protected sequences. For example, in chicken erythrocyte chromatin, a 200 bp HS region at the 5' end of an active adult β -globin gene is accessible to digestion with *MspI*, which excises a 115 bp restriction fragment with the properties of nucleosome-free DNA (McGhee, Wood, Dolan, Engel & Felsenfeld, 1981). Within this fragment, however, two discrete regions of relative protection from DNase I digestion (DNase I "footprints") are detected (Jackson & Felsenfeld, 1985). The HS site can be reconstructed *in vitro* on DNA plasmids containing these sequences in the presence of histones and a partially purified protein extract from adult erythrocytes, but not from embryonic erythrocytes (Emerson & Felsenfeld, 1984), and DNase I footprinting of this *in vitro*-reconstructed site detects the same two protected regions as in chromatin (Emerson, Lewis & Felsenfeld, 1985). These results indicate that protein factors bind to specific sequences within the HS region in cells that express or have a history of expressing the adult β -globin gene. In cells that do not express this gene, these factors are either absent or modified, as they do not bind the HS region in chromatin or DNA.

Wu (1984) developed another technique for detecting protein-binding sequences within HS regions of chromatin, the exonuclease III (Exo III) protection assay. Chromatin is digested with a restriction enzyme followed by Exo III, which "nibbles" in from the ends of the restriction fragment until it encounters a barrier to further digestion, indicating the presence of a bound protein. An HS site of ~200 bp is present at the 5' end of the *Drosophila HSP70* gene in heat shocked

and control cells (Wu, 1980). Within this region, an Exo III resistant site (the TATA box site) is detected between positions -40 bp and -12 bp relative to the transcription initiation site. On heat shock, additional upstream sequences (up to position -108 bp) become Exo III resistant (Wu, 1984). This heat-inducible binding site contains a heat shock control element (HSE), present upstream of all heat shock genes and required for heat-induced transcription (Pelham 1982). *Trans*-acting protein factors that bind specifically to the TATA box and HSE sequences have been purified from *Drosophila* (Parker & Topol, 1984a,b; Wu, 1985; Weiderrecht, Shuey, Kibbe & Parker, 1987; Wu, Wilson, Walker, Dawid, Paisley, Zimarino & Ueda, 1987).

Deletion of the HSE has no effect on formation of the HS site, whereas deletion of sequences in the vicinity of the TATA box region abolishes this site (Costlow, Simon & Lis, 1985). This suggests that binding of the TATA box factor is required to organize the local chromatin structure into an HS site in which ~200 bp of DNA is exposed, possibly by displacing a nucleosome. In this model, therefore, binding of the *trans*-acting factor induces the HS chromatin structure.

An alternative model is suggested from the observation that specific sequences can adopt an altered DNA conformation which may exclude nucleosomes. Larsen & Weintraub (1982) showed that specific sequences within the 200 bp HS site of the adult β -globin gene (discussed above) are preferentially sensitive to S1 nuclease digestion. The same sequences are also S1 sensitive when in the form of pure DNA in supercoiled, but not relaxed, recombinant plasmids, indicating that the information for the altered DNA secondary structure

recognized by S1 resides in the DNA sequence itself, and that torsional stress is required to maintain this conformation. When chromatin is reconstituted on these supercoiled plasmids *in vitro*, the HS region remains S1 sensitive and has a lower affinity for nucleosomes, suggesting that the altered DNA secondary structure in this region does not favour nucleosome formation (Weintraub, 1983). In addition, the HS site of SV40 minichromosomes is abolished by topo I, which relaxes supercoiled DNA, indicating that torsional stress is required to maintain the nucleosome-free HS site (Barsoum & Berg, 1985; Luchnik, Bakayev, Yugai, Zbarsky & Georgiev, 1985). Therefore torsional stress, possibly induced by unfolding of higher-order chromatin structures, may induce specific sequences to adopt an altered DNA conformation, resulting in displacement of one or more nucleosomes. Sequences within the HS region would then be accessible to *trans*-acting regulatory factors. In this model, therefore, *trans*-acting factor binding is the result of the HS chromatin structure.

1.2. The nuclear matrix

1.2.1. Introduction

The spatial organization of chromatin within the interphase nucleus is thought to be maintained by a nuclear substructure or framework. Ultrastructural and biochemical studies of a wide variety of eukaryotic cell types have identified nuclear structural components referred to as the nuclear cage, scaffold, skeleton, ghost, *etc.*, but most commonly as the nuclear matrix (reviewed in Berezney, 1984; Nelson *et al.* 1986b). The nuclear matrix is defined as the residual proteinaceous structure after nuclei are treated with non-ionic detergent,

high ionic strength buffer, and nucleases. The resulting structure comprises ~10% of the original nuclear proteins, and consists of a peripheral nuclear lamina, including residual nuclear pores, an internal fibrillar protein matrix, and a residual nucleolus. The nuclear matrix retains the shape and size of the original nucleus, suggesting that it plays a role in maintaining the structure of the nucleus.

When the DNase digestion step is omitted from the isolation procedure, the DNA remains attached to the residual nuclear matrix in the form of large supercoiled loops, anchored at their bases to the matrix (section 1.1.2). Therefore, the matrix appears to play a role in organizing the distribution of chromatin within the nucleus. In addition to this structural role, it has been proposed that nuclear functions such as DNA replication, transcription, RNA processing and transport take place in association with the matrix, rather than free in the nucleoplasm. However, the evidence for this has not been unequivocal, and even the existence of the nuclear matrix *in vivo* has been questioned. One reason for the conflicting data stems from the fact that the "nuclear matrix" is an operational definition, and different workers have used a variety of different protocols and conditions to isolate nuclear substructures.

1.2.2. Structure and composition

The term "nuclear protein matrix" was introduced by Berezney & Coffey (1974) to describe the residual structure isolated from rat liver nuclei after a series of extractions that removes most of the components of the nucleus, but does not destroy its shape or size (Berezney & Coffey, 1974, 1977). Similar skeletal substructures have been isolated from a wide variety of eukaryotic cell types,

from protozoan to human (reviewed in Berezney, 1984). Generally, the nuclear matrix is isolated by purifying nuclei, solubilizing the lipids of the nuclear envelope with non-ionic detergent, extracting the histones and most of the non-histone proteins with high ionic strength buffers [2 M NaCl or 0.4 M $(\text{NH}_4)_2\text{SO}_4$], and digesting the DNA and RNA with nucleases. The resulting structure resembles the nucleus in size and shape, and consists of three distinct components, a) the lamina-pore complex, a peripheral meshwork of fibres derived from the inner surface of the nuclear envelope, and containing embedded residual nuclear pores, b) a residual nucleolus, and c) an internal network of fibres extending throughout the nuclear interior. However, the residual nuclear structures isolated by some investigators do not contain all of these components, and the structure and composition of the nuclear matrix is a matter of some controversy. This appears to be due to differences in the isolation conditions used, which can greatly affect the nature of the residual nuclear structures obtained. Also, the use of relatively harsh conditions to extract chromatin (e.g. 2 M NaCl) raises the possibility that the residual insoluble structures obtained may be artifacts due to high salt-induced aggregation or precipitation of nuclear components that are soluble *in vivo*.

If the ribonuclease (RNase) digestion step is omitted from the isolation procedure, the resulting nuclear structures retain 60-80% of the heterogeneous nuclear RNA (hnRNA) and a dense internal network of RNP fibres (Herman, Weymouth & Penman, 1978; Miller, Huang & Pogo, 1978; Ciejek, Nordstrom, Tsai & O'Malley, 1982). Subsequent RNase digestion has no significant effect on

the morphology or protein composition of these structures, suggesting that RNA is not a structural component of the matrix. However, several groups have found that if RNase digestion precedes the high salt extraction, only the peripheral lamina is isolated (Herman *et al.* 1978; Kaufmann, Coffey & Shaper, 1981; Bouvier, Hubert, Seve & Bouteille, 1982). This has led to the suggestion that the internal matrix is an artifact formed by aggregation of the RNPs in high ionic strength buffers. Once formed, the protein-protein interactions between the RNP particles are resistant to subsequent RNase digestion, whereas RNase digestion before high salt extraction disrupts the integrity of the RNP particles, rendering their proteins soluble in high ionic strength buffers. However, some workers have isolated all three components of the nuclear matrix, even when the RNase digestion precedes high-salt extraction (Fisher, Berrios & Blobel, 1982; van Eekelen, Salden, Habets, van de Putte & van Venrooij, 1982).

On the other hand, others argue that the RNP network exists *in situ*, and that RNase digestion artificially renders it soluble in high ionic strength buffers. Antibodies recognizing two RNP proteins, p107 and p28, bind to macromolecular assemblies localized in discrete interchromatin domains in human and rat nuclei *in situ* (Smith, Spector, Woodcock, Ochs & Bhorjee, 1985). The morphology and distribution of these domains is unaltered in nuclear matrices extracted with high salt in the absence of RNase digestion, suggesting that an RNP network is present both before and after high salt extraction. RNase digestion of nuclei *in situ*, however, induces alterations in nuclear morphology and distribution of the RNP domains, suggesting that degradation of RNA *in situ* artificially disrupts the

RNP network, thus rendering it soluble in high ionic strength buffers (Smith, Ochs, Fernandez & Spector, 1986).

Another factor that can affect the morphology and composition of the nuclear matrix is the extent of disulphide bond formation between nuclear proteins during the isolation procedure. Nuclei are exposed to oxidizing conditions during the various *in vitro* manipulations involved in isolating the nuclear matrix, through exposure to atmospheric oxygen, and heavy metals that may contaminate buffers and glassware. Since these conditions vary among laboratories, the different types of residual structures isolated by different investigators may reflect the extent of oxidative crosslinking that has occurred between protein sulphhydryl groups during the isolation procedure.

When rat liver nuclear matrices are isolated in the presence of sulphhydryl-blocking agents such as iodoacetamide (IAA) or *N*-ethylmaleimide (NEM), digested with DNase and RNase, and extracted with 1.6 M NaCl, the resulting residual structures contain the peripheral lamina but lack the internal matrix components (Kaufmann *et al.* 1981; Kaufmann & Shaper, 1984). These agents irreversibly block free sulphhydryl groups, but do not reduce existing disulphide bonds, suggesting that the internal matrix network observed in their absence depends on disulphide crosslinks formed *in vitro*, rather than crosslinks present *in vivo*. In the presence of sulphhydryl crosslinking agents such as sodium tetrathionate (NaTT) or disulphiram, the same isolation procedure yields residual structures containing the peripheral lamina, plus an extensive network of internal fibres and prominent residual nucleoli (Kaufmann *et al.* 1981; Kaufmann &

Shaper, 1984). Subsequent treatment of these crosslinked structures with reducing agents such as dithiothreitol (DTT) or β -mercaptoethanol renders the internal matrix components soluble in 1.6 M NaCl, whereas the lamina remains insoluble (Kaufmann & Shaper, 1984). Similar observations have been made in 3T3 and HeLa cells (Staufenbiel & Deppert, 1984).

One interpretation of these results is that the internal matrix observed in the absence of sulphhydryl-blocking agents is an artifact due to disulphide crosslinking *in vitro* between proteins that do not interact in the intact nucleus, but do so during matrix isolation as a result of rearrangements induced by 1.6 M NaCl. Alternatively, the internal matrix may exist *in vivo*, but the protein-protein interactions maintaining its integrity may simply be disrupted by high ionic strength buffers unless they are stabilized by disulphide crosslinking, either fortuitously or deliberately. In this case, the disulphide bonds merely stabilize protein-protein interactions which exist in the intact nucleus. Consistent with this interpretation is the observation that NaTT does not result in indiscriminate crosslinking of nuclear proteins - only a specific sub-set of non-chromatin, non-lamina proteins are stabilized (Kaufmann & Shaper, 1984; Kaufmann, Fields & Shaper, 1986). In contrast to these results, however, others have found that the internal matrix components are isolated regardless of whether IAA or NEM is present during isolation of residual nuclear structures from HeLa, 3T3 (Capco, Wan & Penman, 1982; van Eekelen *et al.* 1982) and *Drosophila* embryo cells (Fisher *et al.* 1982).

Clearly, resolution of these contradictory results and interpretations requires

demonstration of an internal nuclear matrix *in vivo*, or at least in nuclei isolated under conditions of physiological ionic strength. This has proved difficult, since under these conditions putative internal matrix elements are obscured by chromatin and other diffuse nucleoplasmic components. Generally, therefore, the chromatin must be extracted in order to observe these elements. Under certain conditions, however, internal nuclear matrix fibres have been observed both *in vivo* and in nuclei extracted at physiological ionic strength. Brasch (1982) treated chicken liver cells with the transcription inhibitor α -amanitin, which "clears" the diffuse nucleoplasmic background by inducing chromatin condensation, RNP aggregation and nuclear swelling. This reveals an *in situ* nuclear matrix, visible in the EM as an interchromatin network of fibres, 10-15 nm in diameter, contiguous with the chromatin and the nuclear envelope. These fibres are also visible when poliovirus-infected human fibroblasts are extracted with non-ionic detergent at physiological ionic strength (Capco *et al.* 1982). In this case, the virus induces chromatin clumping, revealing the interchromatin fibre network. The same extraction procedure also reveals internal matrix fibres in cells entering prophase, as chromatin starts to condense for mitosis (Capco & Penman, 1983).

Penman and co-workers have used relatively moderate ionic strength conditions [0.25 M $(\text{NH}_4)_2\text{SO}_4$] to remove chromatin after DNase and RNase digestion of detergent-extracted cells. When the resulting structures are viewed as whole cell mounts by transmission electron microscopy, a dense network of fibres can be seen throughout the nuclear interior (Capco *et al.* 1982; Fey, Wan & Penman, 1984). When residual structures prepared in the same way are viewed

by conventional thin section electron microscopy, the peripheral lamina is detected, but the nuclear interior appears empty (Capco *et al.* 1982), as reported by others (discussed above). Penman and colleagues suggest that the failure to detect the internal matrix network in sectioned material may be due to contrast-matching between these fibres and the embedding resin used in conventional thin sectioning. These workers have used a resinless section technique to demonstrate clearly the presence of an internal network of nuclear matrix fibres in HeLa nuclei extracted with non-ionic detergent at physiological ionic strength, and in residual nuclear structures after nuclease digestion and extraction of chromatin at 0.25 M $(\text{NH}_4)_2\text{SO}_4$ (Fey, Krochmalnic & Penman, 1986).

Jackson & Cook (1985a) developed a technique for extracting chromatin under physiological ionic strength conditions. Living cells are encapsulated in 0.5% agarose mini-beads, which prevents cell clumping and chromatin aggregation during the subsequent manipulations, while the cells remain accessible to detergents and enzymes through the pores in the agarose. After lysis of the encapsulated cells with non-ionic detergent, the solubilized components are free to diffuse out of the beads. The residual structures are then digested with restriction enzymes, and the chromatin removed by electrophoresis. In HeLa cells, this procedure has uncovered a "nucleoskeleton", a three-dimensional network of nuclear filaments extending from the lamina throughout the nuclear interior (Jackson & Cook, 1988). The dimensions of these filaments are similar to those of the cytoplasmic intermediate filaments (IFs), *i.e.* ~10 nm diameter with 23 nm axial repeat, suggesting that IFs may form the skeleton of both the cytoplasm and the nucleus (see below).

The proteins of the nuclear matrix comprise ~10% of the original nuclear proteins, corresponding to a specific subset of non-histone structural proteins. These proteins have a complex electrophoretic pattern, with species in the *Mr* range ~50,000-70,000 predominating (Berezney & Coffey, 1974, 1977; Hodge, Mancini, Davis & Heywood, 1977; Peters, Okada & Comings, 1982). Much effort has been directed towards characterizing these proteins, along with their interactions and organization within the nucleus. However, with the exception of the lamina proteins, the proteins of the nuclear matrix remain poorly defined. Monoclonal antibodies against nuclear matrix proteins have recently become available, and should provide extremely useful tools for analyzing the distribution of the nuclear matrix proteins, their fate at mitosis, and possible artificial rearrangements during the various extraction steps involved in nuclear matrix isolation.

The three major proteins of the mammalian nuclear matrix are derived exclusively from the lamina, and are designated lamins A, B, and C (*Mr* 70,000, 68,000, and 62,000, respectively) (Gerace, Blum & Blobel, 1978; Gerace & Blobel, 1980). Related lamin proteins have been identified in many other vertebrate and invertebrate species (reviewed in Krohne & Benavente, 1986). The amino acid sequence of the human lamins A and C have been deduced from their complementary DNA (cDNA) clones, revealing that these two proteins are identical except for the lengths of their carboxy termini, and arise by differential splicing from the same gene (Fisher, Chaudhury & Blobel, 1986; McKeon, Kirschner & Caput, 1986). The sequence data also reveal structural homologies

between lamins A and C and the cytoskeletal IF proteins. In the EM, the isolated lamina appears as a dense meshwork of long filaments of diameter ~ 10 nm, *i.e.* the diameter of cytoskeletal IFs, and isolated lamins A and C will assemble *in vitro* into long, ~ 10 nm diameter filaments similar in structure to *in vitro*-assembled cytoskeletal IFs (Aebi, Cohne, Buhle & Gerace, 1986). In biochemical fractionation studies, lamins A and C are soluble, whereas lamin B remains membrane-bound, suggesting that lamin B may be responsible for anchoring the lamina meshwork to the inner surface of the nuclear envelope (Gerace & Blobel, 1980; Burke & Gerace, 1986). Furthermore, recent *in vitro* studies suggest that lamin B may serve as the nuclear envelope attachment site for the vimentin-containing cytoskeletal IFs, thus forming a continuous IF network between the nucleus and the cytoplasm (Georgatos & Blobel, 1987).

The nuclear envelope is disassembled at mitosis, and the lamins are transiently depolymerized and dispersed throughout the cytoplasm, lamins A and C in a soluble form, and lamin B associated with cytoplasmic vesicles corresponding to remnants of the nuclear envelope (Gerace & Blobel, 1980; Burke & Gerace, 1986). At prophase, disassembly of the nuclear envelope is accompanied by lamin hyperphosphorylation, which is reversed at telophase as the nuclear envelope reassembles (Gerace & Blobel, 1980; Ottaviano & Gerace, 1985). Therefore, phosphorylation of the lamins may play a role in regulating their reversible depolymerization and nuclear envelope disassembly at mitosis.

Nuclear pore complexes are the sites of exchange of macromolecules between the nucleus and the cytoplasm. They are large protein complexes ($M_r \sim 10^8$)

consisting of eight globular subunits arranged in a ring, creating a channel across the nuclear envelope (reviewed in Newport & Forbes, 1987). After extraction of nuclei with non-ionic detergents, 2 M NaCl, and nucleases, the residual pore complexes remain embedded in the lamina meshwork and retain their characteristic organization. They appear to consist of a small number of proteins, but these have not been well characterized. Anti-lamin antibodies do not recognize the nuclear pores of rat lamina-pore complexes, indicating that lamins are not part of the pore complex (Gerace, Ottaviano & Kondor-Koch, 1982). These workers identified a glycoprotein of *Mr* 190,000 (gp190) as a component of rat liver nuclear pores by immunoferritin electron microscopy. In addition, monoclonal antibodies raised against detergent-extracted rat liver nuclear envelopes have been used to identify a glycoprotein of *Mr* 62,000 (p62) (Davis & Blobel, 1986), and a series of eight distinct glycoproteins, *Mr* 54,000-210,000 (Snow, Senior & Gerace, 1987), as nuclear pore components. However, each of these proteins is extracted by high ionic strength buffers, and so does not appear to be a component of the residual nuclear matrix.

The major proteins of the internal nuclear matrix are in the *Mr* range 60,000-70,000, although these are distinct from the lamins (Kaufmann & Shaper, 1984; Noaillac-Depeyre, Azum, Geraud, Mathieu & Gas, 1987). Nucleolar proteins C23 (nucleolin) (Long & Ochs, 1983) and B23 (numatrin) (Fields, Kaufmann & Shaper, 1986; Feuerstein & Mond, 1987; Feuerstein, Chan & Mond, 1988) have been identified as nuclear matrix proteins and localized to the residual nucleolus using antisera specific for these proteins.

A series of monoclonal antibodies raised against mouse and bovine nuclear matrix preparations have been used to analyse the distribution of matrix proteins in 3T3 cells during the cell cycle and at each of the matrix isolation steps (Chaly, Bladon, Setterfield, Little, Kaplan & Brown, 1984; Chaly, Little & Brown, 1985). One of these antibodies, P1, recognizes three proteins in the *Mr* range 27,000-31,000, located exclusively at the nuclear periphery during interphase. Unlike the lamins, these antigens become associated with the surface of the condensed chromosomes during mitosis, suggesting that they may be components of the metaphase chromosome scaffold (Chaly *et al.* 1984). The distribution of these antigens is markedly altered during the nuclear matrix isolation procedure, whereas that of the lamins remains unchanged. The P1 staining pattern remains unaffected after non-ionic detergent extraction and DNase I digestion. After extraction with 2 M NaCl, however, P1 no longer stains the nuclear periphery, but an internal meshwork of threads and patches (Chaly *et al.* 1985).

A second monoclonal antibody, II, recognizes an antigen with an exclusively internal distribution, staining non-heterochromatin and non-nucleolar regions of interphase nuclei. At mitosis, II stains both the surface and the interior of the condensed chromosomes (Chaly *et al.* 1984). After detergent extraction, DNase I digestion, and 2 M NaCl extraction of interphase nuclei, the II staining pattern becomes exclusively nucleolar, indicating that the antigen becomes associated with the residual nucleolus after extraction of chromatin at high ionic strength (Chaly *et al.* 1985). Therefore, the proteins recognized by P1 and II appear to undergo artificial redistribution during the nuclear matrix isolation procedure.

Another two monoclonal antibodies, P11 and P12, recognizing proteins of *Mr* 60,000 (P11), and *Mr* 35,000, 70,000, and 140,000 (P12), stain interphase cells at the nuclear periphery, and at interchromatin and non-nucleolar regions of the nuclear interior. During mitosis, these antigens are dispersed in the cytoplasm (Chaly *et al.* 1984). Unlike P1 and P2, the characteristic staining patterns of P11 and P12 are not altered by the nuclear matrix isolation procedure, suggesting that these antibodies recognize components of an interchromatin protein network present in interphase nuclei *in vivo*, and retained in residual nuclear matrices (Chaly *et al.* 1985). Other internal nuclear matrix proteins identified by monoclonal antibodies, and whose *in situ* distribution remains unaltered by the nuclear matrix isolation procedure, include a protein of *Mr* 52,000 in canine kidney cells (Fey *et al.* 1984), and proteins of *Mr* 40,000 and 36,000 in chick embryo fibroblasts (Lehner, Eppenberger, Fakan & Nigg, 1986).

In summary, these immunological studies provide evidence for the existence of an internal network of nuclear matrix proteins *in vivo*, whose distribution is unaltered by the nuclear matrix isolation procedure. This suggests that their presence and distribution in the isolated nuclear matrix are not due to structural rearrangements or artificial associations induced by the isolation procedure. However, there is also evidence that some proteins, although operationally defined as nuclear matrix proteins, are not associated with this network *in vivo*, but may become so during the isolation procedure as a result of aggregation or fortuitous co-precipitation with nuclear matrix components.

1.2.3. Organization of DNA relative to the nuclear matrix

When cells are lysed in non-ionic detergent and extracted with 2 M NaCl to remove histones and other chromosomal proteins, the resulting structures (nucleoids) contain all of the chromosomal DNA in the form of supercoiled loops (~20-200 kb) attached at their bases to the nuclear matrix (section 1.1.2). After staining with ethidium bromide, the DNA loops can be observed by fluorescence microscopy as a "halo" surrounding the residual nuclear matrix. *Uv*-irradiation in the presence of ethidium causes a gradual increase in the radius of the halos, as the introduction of single-strand nicks into the DNA relaxes the supercoils (Cook *et al.* 1976; Vogelstein *et al.* 1980). DNase I digestion of the matrix-halo structures results in gradual disappearance of the halos, as the loops of DNA are progressively removed (Vogelstein *et al.* 1980). However, even after extensive DNase I digestion, 0.1-1.0% of the DNA remains associated with the nuclear matrix, representing those sequences located at the base of the loops anchored to the matrix (Berezney & Coffey, 1975; Pardoll, Vogelstein & Coffey, 1980). Alternatively, the DNA loops can be cleaved with restriction enzymes. After centrifugation, the matrix associated restriction fragments are recovered from the matrix pellet, whereas those fragments detached by restriction enzyme cleavage, representing sequences in the distal regions of the DNA loops, remain in the supernatant (Cook & Brazell, 1980).

The fraction of DNA that remains associated with the nuclear matrix after DNase I or restriction enzyme digestion has been analysed extensively to determine if specific DNA sequences are involved in matrix-DNA interactions.

Studies using *in vivo* incorporation of radiolabelled DNA precursors have shown that this fraction is greatly enriched in newly replicated DNA, suggesting that the nuclear matrix is the site of DNA synthesis (Berezney & Coffey, 1975; Dijkwel, Mullenders & Wanka, 1979; Pardoll *et al.* 1980; Berezney & Buchholtz, 1981). The degree of enrichment decreases with longer labelling times, implying that once replicated, the nascent DNA moves out into the distal portion of the loops. This interpretation is supported by autoradiographic analyses, which show that in nucleoids prepared after a short pulse of label, the replicated DNA is confined within the diameter of the nuclear matrix, whereas after longer periods of labelling the replicated DNA is found progressively further out in the DNA halo region (McCready, Goodwin, Mason, Brazell & Cook, 1980; Vogelstein *et al.* 1980). Based on these results, a model for DNA replication has been proposed in which the DNA loops are reeled through fixed replication complexes associated with the nuclear matrix (Pardoll *et al.* 1980). Each DNA loop, therefore, is equivalent to a replicon, the individual unit of DNA replication (Huberman & Riggs, 1968). Origins of replication appear to be matrix associated throughout the cell cycle, whereas the growing replication forks are associated only transiently during the DNA synthetic (S) phase (Aelen, Opstelten & Wanka, 1983; Carri, Micheli, Graziano, Pace & Buongiorno-Nardelli, 1986; Dijkwel, Wenink & Poddighe, 1986).

The proposed model for a fixed site of DNA replication on the nuclear matrix requires that the enzymes involved in DNA synthesis also be matrix associated. Accordingly, a cell cycle- and replicative-dependent association has

been demonstrated between DNA polymerase α (the replicative or S phase eukaryotic DNA polymerase) and the nuclear matrix of regenerating rat liver cells (Smith & Berezney, 1980, 1982). In addition, the nuclear matrix has been shown to contain significant levels of DNA primase (Wood & Collins, 1986; Tubo & Berezney, 1987c), DNA topoisomerases (Nishizawa, Tanabe & Takahashi, 1984; Berrios, Osheroff & Fisher, 1985), and DNA methylase (Burdon, Qureshi & Adams, 1985). Recently, a multienzyme DNA replication complex, or "replisome", containing DNA polymerase α , DNA primase, DNA methylase, 3'-5' exonuclease, and ribonuclease H, has been shown to associate with the nuclear matrix prior to S phase, and dissociate after DNA replication is completed (Tubo & Berezney, 1987a,b).

The fact that nuclear matrices are exposed to 2 M NaCl during isolation raises the possibility that the association between DNA replication and the nuclear matrix is artificially induced by the high ionic strength conditions. For example, a component of the DNA replication complex may fortuitously coprecipitate with the nuclear matrix proteins during isolation, resulting in attachment to the matrix of the entire replication complex and its associated DNA. However, HeLa nucleoskeletons prepared from agarose-encapsulated cells under physiological ionic strength conditions (Jackson & Cook 1985a, described above) also retain the newly replicated DNA (Jackson & Cook, 1986a) and active DNA polymerase α (Jackson & Cook, 1986b). Moreover, exposure of these nucleoskeletons to 2 M NaCl results in detachment of some of the nascent DNA, rather than artificial attachment (Jackson & Cook, 1986a).

The nuclear matrix has also been proposed as the site of gene transcription. Nascent hnRNA (Herman *et al.* 1978; Miller *et al.* 1978; Jackson, McCready & Cook, 1981) and nuclear proteins involved in regulation of transcription, *e.g.* steroid hormone-receptor complexes (Barrack & Coffey, 1982), and the viral T antigens of SV40 (Deppert, 1979; Staufenberg & Deppert, 1983) and polyomavirus (Buckler-White, Humphrey & Pigiet, 1983) have been shown to be associated with the nuclear matrix. In most cases studied (although not all), transcriptionally active genes have been shown to be located at the base of the DNA loops, at or near their point of attachment to the nuclear matrix (reviewed in Nelson *et al.* 1986b; Razin, 1987). In these experiments, the matrix associated DNA fraction is assessed for its content of a specific gene by quantitative filter or solution hybridization. If the gene is located at the base of the DNA loop, it will not be detached from the matrix by nuclease digestion, and so will be enriched in the matrix associated DNA fraction relative to an equal amount of total unfractionated DNA. If the gene is located in the matrix-distal portion of the loop, it will be detached by nuclease digestion and therefore depleted in the matrix associated DNA fraction. No enrichment or depletion relative to total DNA implies that the gene is randomly located relative to the nuclear matrix. [Note that in these experiments, the chromatin components responsible for the differential nuclease sensitivity of transcriptionally active and inactive sequences, *i.e.* histones and HMG proteins (section 1.1.5), have been extracted with 2 M NaCl. The DNA loops are therefore assumed to be uniformly sensitive to DNase I and restriction enzymes, and cleaved randomly by these nucleases.]

Pardoll & Vogelstein (1980) first demonstrated that the rRNA genes of rat liver cells are associated with the nuclear matrix, and subsequent studies by many investigators have shown that specific genes are associated with the nuclear matrix in cells in which they are transcribed. In the oviduct cells of adult laying hens, the transcriptionally active ovalbumin gene is associated with the nuclear matrix, but this gene is not associated in tissues where it is transcriptionally inactive (Robinson, Nelkin & Vogelstein, 1982). The ovalbumin gene is also matrix associated in the oviduct cells of estrogen-stimulated immature chicks, but this association is reversed on hormone withdrawal as transcription ceases, indicating that association of specific sequences with the nuclear matrix is related to transcriptional activity (Ciejek, Tsai & O'Malley, 1983; Robinson, Small, Idzerda, McKnight & Vogelstein, 1983).

This raises the possibility that the association of active genes with the nuclear matrix may be artificially induced by co-precipitation of RNA polymerase II or an associated transcription factor with the nuclear matrix in 2 M NaCl, or by aggregation of nascent RNP particles. However, a non-transcribed restriction fragment 3.8 kb downstream from the 3' end of the ovalbumin gene is independently associated with the nuclear matrix, indicating that matrix association does not require the presence of transcription complexes or RNP particles (Robinson *et al.* 1983). This conclusion is further supported by studies on the chicken vitellogenin II gene. This gene is transcribed in the liver of adult laying hens and estrogen-stimulated immature chicks, and is associated with the nuclear matrix in these cells, but not in tissues where it is transcriptionally

inactive (Jost & Seldran, 1984). After primary estrogen stimulation of immature chicks, there is a lag period before vitellogenin mRNA is synthesized. However, association of the vitellogenin II gene with the nuclear matrix precedes the onset of transcription, indicating that transcription *per se* is not responsible for association with the nuclear matrix.

In the case of the chicken ovalbumin and vitellogenin II genes, the entire transcription unit plus 2-4 kb of 5'- and 3'-flanking non-transcribed sequences were found to be independently attached to the nuclear matrix (Ciejek *et al.* 1983; Robinson *et al.* 1983; Jost & Seldran, 1984). However, in the case of the *Drosophila HSP70* and β -actin genes (Small, Nelkin & Vogelstein, 1985), and the chicken histone H5 gene (Dalton, Younghusband & Wells, 1986), the matrix associated sequences are restricted to the 5'-flanking sequences and/or the 5' end of the gene. In addition, these attachment sites are independent of transcription, since the same sequences are attached to the matrix in heat shocked and non-heat shocked *Drosophila* cells (Small *et al.* 1985). The finding that transcribed sequences downstream from these attachment sites are not matrix associated provides further evidence that attachment to the nuclear matrix is not merely due to precipitation or aggregation of transcription complexes in 2 M NaCl. Studies on nucleoskeletons prepared from agarose-encapsulated HeLa cells under physiological ionic strength conditions also support this conclusion. After the bulk of the chromatin is removed by restriction enzyme or DNase I digestion followed by electrophoresis, most of the nascent RNA and active RNA polymerase II remains associated with the residual nucleoskeleton (Jackson & Cook, 1985b).

Also, sequences hybridizing to cytoplasmic poly(A⁺)RNA, *i.e.* transcribing genes, are enriched in the fraction of DNA remaining associated with the nucleoskeleton. Therefore, these interactions exist under physiological ionic strength conditions, and do not require 2 M NaCl.

Small & Vogelstein (1985) analysed the DNA loop organization in a region of the *Drosophila* 7F locus devoid of known active genes. Of 52 contiguous *Eco*RI restriction fragments spanning 163 kb, five are attached to the nuclear matrix, organizing this region into four loops of 75, 52, 12, and 14 kb. All five attached fragments were found to contain previously unknown transcribed sequences, suggesting that attachment to the nuclear matrix may require transcription of a sequence at or near the base of the loop. Of 16 non-attached fragments analysed, one is transcriptionally active, suggesting that whereas transcription may be required for attachment to the nuclear matrix, matrix attachment is not required for transcription.

While most workers have found active genes to be preferentially associated with the nuclear matrix, others have found no such association. For example, a cDNA probe synthesized from poly(A)⁺RNA, and so representing active genes, hybridized to a similar extent with the matrix associated DNA fraction and total unfractionated DNA from rat liver cells (Basler, Hastie, Pietras, Matsui, Sandberg & Berezney, 1981). Similarly, the globin genes of chicken erythroblasts were found to be neither enriched nor depleted in the matrix associated DNA fraction (Ross, Yen & Chae, 1982). Hancock & Hughes (1982) analysed the distribution of active transcription sites relative to the nuclear matrix in mouse tissue culture

cells by electron microscopy, and found these to be located primarily in the matrix-distal regions of the DNA loops.

Studies by Razin and colleagues indicate that these findings may be due to the conditions used to isolate nuclear matrices. These workers showed that the transcribed IgM C μ sequences of mouse hybridoma cells are attached to the nuclear matrix after DNase I or MNase digestion of isolated nuclei, followed by extraction with 2 M NaCl (Razin, Yarovaya & Georgiev, 1985). However, extraction of the nuclease digested nuclei with a low ionic strength buffer (2 mM EDTA, 1 mM Tris-HCl) prior to 2 M NaCl results in detachment of the C μ sequences from the matrix. In the studies described above, in which transcribed genes and transcription complexes were found not to be associated with the nuclear matrix, the methods used to prepare nuclear matrices include at least one extraction with a low ionic strength buffer (0.2-2.0 mM EDTA, in the absence of monovalent cations), suggesting that exposure of nuclei to low ionic strength conditions destroys the attachment of active genes to the nuclear matrix. The residual nuclear structures obtained by Hancock & Hughes (1982) using low ionic strength conditions followed by 2 M NaCl extraction contain no internal structural elements. Therefore, depolymerization of the internal matrix fibres under these conditions may account for the detachment of the transcribed sequences. Indeed, the ionic strength conditions used in these experiments are similar to those used to prepare Miller spreads (section 1.1.3), in which structural elements are not detected.

The results obtained by another group suggest that the association of active

genes with the nuclear matrix depends on the order of the DNase I digestion and 2 M NaCl extraction (Kirov, Djondjurov & Tsanev, 1984). These workers found that in Friend erythroleukemia cells, the matrix associated DNA fraction prepared by extracting nuclei with 2 M NaCl followed by DNase I digestion is enriched in the active α -globin genes. However, if the DNase I digestion precedes the 2 M NaCl extraction, the matrix associated DNA fraction is not enriched in these genes. The reason for this is not clear. It does not appear to be due to the preferential sensitivity of active sequences to DNase I digestion of chromatin, since the extent of DNase I digestion in these studies (<1% acid soluble DNA) does not result in loss of α -globin sequences (Kirov *et al.* 1984). Also, others have shown that active genes remain associated with the matrix when the DNase I digestion precedes extraction with 2 M NaCl (*e.g.* Pardoll & Vogelstein, 1980; Razin *et al.* 1985).

Laemmli and colleagues developed a low salt extraction procedure in which histones are extracted with an ionic detergent, lithium diiodosalicylate (LIS, 25 mM), instead of 2 M NaCl. The resulting nuclear matrix (referred to as the nuclear scaffold by Laemmli and colleagues) contains both the peripheral lamina and the internal matrix networks (Mirkovitch, Mirault & Laemmli, 1984). These workers have identified specific sequences involved in attachment to the nuclear matrix in the *Drosophila* histone and *HSP70* genes. The histone gene cluster is organized into ~ 100 repeated units of 5 kb, each containing the five histone genes. There is one matrix attached region [MAR, referred to as scaffold attached region (SAR) by Laemmli and colleagues] per repeat unit, which maps to

a 657 bp restriction fragment in the non-transcribed spacer between the histone H1 and H3 genes, whereas all other sequences, including the transcribed regions, are detached (Mirkovitch *et al.* 1984). This implies that the histone gene cluster is organized into a series of 5 kb loops, with the histone genes in the loop regions. Within the 657 bp attached fragment, Exo III nuclease protection assays have identified two nuclease resistant domains of ~ 200 bp each, separated by a central accessible region of ~ 100 bp (Gasser & Laemmli, 1986a). The protected sequences presumably represent sites of interaction between the DNA and nuclear matrix proteins.

The *MARs* of the *Drosophila HSP70* genes are located in the non-transcribed 5'-flanking sequences, whereas the transcribed regions are detached (Mirkovitch *et al.* 1984). The same sequences are attached in heat shocked and non-heat shocked cells, indicating that the matrix-DNA interactions are not altered by transcription. These results are similar to those obtained by Small *et al.* (1985) with *Drosophila* nuclear matrices prepared in 2 M NaCl (discussed above). Others have obtained identical results using both the LIS and 2 M NaCl methods to map the attachment sites in *e.g.* the human rRNA genes (Keppel, 1986) and the chicken histone H5 gene (Dalton *et al.* 1986). Generally, however, the minimum size fragment that remains attached after LIS extraction is smaller than that after 2 M NaCl extraction, allowing higher resolution mapping of *MARs* with the former. In addition, the matrix associated sequences after 2 M NaCl extraction often include the entire transcription unit, and although these interactions are not due to transcription *per se*, they are related to transcriptional

activity. It is possible, therefore, that different DNA-protein interactions are detected with these two methods.

Whereas all the *Drosophila* MARs identified to date occur in non-transcribed regions (Mirkovitch *et al.* 1984; Gasser & Laemmli, 1986b; Mirkovitch, Spierer & Laemmli, 1986), they have been identified in both non-transcribed and transcribed regions of vertebrate genes. For example, a MAR has been mapped to the transcribed region of the mouse κ IgL gene, both in the highly transcribed rearranged gene in B-cells, and in the inactive germline sequence in non-B-cells (Cockerill & Garrard, 1986). Therefore, these attachments do not appear to be cell type-specific, nor disrupted by transcription through the MAR. Intragenic MARs have also been identified in the mouse immunoglobulin heavy chain (IgH) gene (Cockerill, Yuen & Garrard, 1987), the hamster dihydrofolate reductase gene (Kas & Chasin, 1987), and the human hypoxanthine-guanine phosphoribosyltransferase gene (Sykes, Lin, Hwang, Framson & Chinault, 1988).

Cockerill & Garrard (1986) also developed an *in vitro* matrix-binding assay for mapping MARs. Nuclei are digested extensively with DNase I and extracted with 2 M NaCl. (Identical results are obtained with LIS.) The matrices are incubated with purified DNA restriction fragments from the region of interest, and fragments binding specifically to the matrix in an excess of non-specific competitor DNA are defined as *in vitro* MARs. The MARs identified in this way have been found to be identical to the endogenous MARs (Cockerill & Garrard, 1986; Cockerill *et al.* 1987; Kas & Chasin, 1987). The *Drosophila* histone gene MAR binds specifically to mouse nuclear matrices, and competes efficiently with

the mouse κ IgL *MAR* for the same matrix binding sites, indicating that these sites are evolutionarily conserved (Cockerill & Garrard, 1986).

Comparison of the *MARs* identified to date reveals that they do not share extensive sequence homology, and a specific matrix attachment sequence has not been identified. They do, however, have a number of features in common: they are generally a few hundred base pairs in length (at least 200 bp), contain clusters of A/T-rich sequences, are rich in sequences homologous to the 15 bp consensus sequence for topo II (DNA topoisomerase II) cleavage (Sander & Hsieh, 1985), and are often located adjacent to transcriptional enhancer elements (reviewed in Gasser & Laemmli, 1987). The presence of topo II consensus sequences in *MARs* is significant, since topo II is a major component of the interphase nuclear matrix (Berrios *et al.* 1985) and the metaphase chromosome scaffold, where it is located at the bases of the DNA loops (section 1.1.2). Therefore, the chromosomal DNA loop organization may be mediated by LIS-stable interactions between *MARs* and topo II in the nuclear matrix. Topo II may act at the base of each loop to regulate the degree of supercoiling, which in turn may result in an altered (DNase I sensitive) chromatin structure throughout the entire loop/domain, and the appearance of HS sites to expose important regulatory elements such as enhancers. The proximity of enhancer elements to *MARs* implies that the enhancers are also located at the base of the DNA loops. This may explain why enhancer elements can exert their influence over many kilobases, and are independent of distance and orientation relative to promoters. DNA looping may bring enhancers close to promoters, RNA polymerases, and transcriptional

regulatory factors to form functional transcription complexes on the nuclear matrix.

A prediction of this model is that the boundaries of a DNase I sensitive chromatin domain should be defined by the *MARs* anchoring the corresponding DNA loop to the nuclear matrix. The 5' and 3' boundaries have been determined for the DNase I sensitive domains surrounding the chicken ovalbumin, glyceraldehyde-3-phosphate dehydrogenase, and lysozyme genes (section 1.1.4). Within the 100 kb chromatin domain surrounding the ovalbumin gene family, the ovalbumin gene, the related X and Y genes, and sequences flanking these genes are associated with the nuclear matrix prepared by extraction with 2 M NaCl (Ciejek *et al.* 1983; Robinson *et al.* 1983). However, other sequences within the DNase I sensitive domain are not matrix associated, indicating that there is no correlation between the DNase I sensitive chromatin domain and sequences associated with the nuclear matrix in 2 M NaCl (Ciejek *et al.* 1983). LIS-stable *MARs* have been mapped to 9-11.5 kb upstream and 1-5 kb downstream from the chicken lysozyme gene (Phi-Van & Stratling, 1988), whereas the boundaries of the 24 kb DNase I sensitive chromatin domain map to ~14 kb upstream and ~6 kb downstream from this gene (Jantzen *et al.* 1986). While these *MARs* do not define the boundaries of the DNase I sensitive domain, they may correspond to the boundaries of the 19 kb chromatin domain defined by MNase sensitivity (Stratling, Dolle & Sippel, 1986). Furthermore, in all three cases, the transition from the DNase I sensitive to the DNase I resistant conformation occurs gradually over 5-10 kb, whereas a sharper transition would be expected if a *MAR* formed

the boundary between the DNase I sensitive and resistant chromatin structures of adjacent loops. Therefore, the relationship between DNase I sensitive chromatin domains and the DNA loops anchored to the nuclear matrix remains to be demonstrated.

1.3. Adenovirus transformation

1.3.1. Introduction

The human adenoviruses are a family of viruses responsible for relatively mild respiratory infections, mostly in infants and children. (For a review see Tooze, 1980). To date around 40 different serotypes have been isolated, and these have been classified into five subgenera on the basis of a) agglutination of rhesus monkey and rat erythrocytes, b) oncogenicity in newborn hamsters, and c) DNA sequence homology (Wigand, Bartha, Dreizin, Esche, Ginsberg, Green, Heirholzer, Kalter, McFerran, Petterson, Russell & Wadell, 1982). The virus particle consists of a non-enveloped, icosahedral protein capsid of diameter 70-80 nm (Horne, Brenner, Waterson & Wildy, 1959), and an inner nucleoprotein core. This contains the viral genome, which is a linear, double-stranded DNA molecule of $20\text{-}25 \times 10^6$ daltons ($\sim 36,000$ bp) (Green, Pina, Kimes, MacHattie & Thomas, 1967).

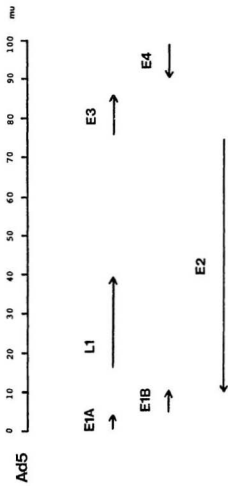
The infectious cycle of adenovirus consists of two phases, early and late, separated by the onset of viral DNA replication. During the early phase, 0-6 h post-infection (p.i.), six regions are expressed, E1A, E1B, E2, E3, E4, and L1 (Fig. 1-1), with different kinetics (reviewed by Flint, 1986). The first of these to be

expressed, early region 1A (E1A), encodes functions required for efficient transcription of the other early regions (Berk, Lee, Harrison, Williams & Sharp, 1979; Jones & Shenk, 1979a; Nevins, 1981). After the onset of viral DNA replication (~6-9 h p.i.), transcription from the early regions is reduced, and there is a dramatic increase in transcription from the major late promoter (MLP) at 16.4 map units (μ ; 1 μ = 1% of the genome). During the late phase, the structural proteins of the viral capsid are synthesized and mature virus particles assembled, and the cycle ends with cell lysis and release of new infectious virus particles. The regulation of viral genes during infection has provided an ideal model system in which to study gene regulation in mammalian cells, since viral transcripts are synthesized in the nucleus by cellular RNA polymerases, and undergo the same processing as cellular transcripts, *i.e.* capping, polyadenylation and splicing.

A second reason for the interest shown in the adenoviruses is their oncogenic potential. When injected into newborn hamsters, subgenus A viruses, *e.g.* adenovirus types 12 and 18 (Ads12 and 18), are highly oncogenic, inducing tumours rapidly and at high frequency (Trentin, Yabe & Taylor, 1962), whereas subgenus B viruses, *e.g.* Ads3 and 7, are defined as weakly oncogenic, inducing tumours after a longer latent period and with a lower frequency (Huebner, Casey, Chanock & Schell, 1965). Subgenus C viruses, *e.g.* Ads2 and 5, are non-oncogenic in newborn hamsters, but they share with subgenera A and B the ability to transform rodent cells in culture (Freeman, Black, Vanderpool, Henry, Austin & Huebner, 1967).

Figure 1-1 Ad5 early transcription units.

The Ad5 genome is represented as a straight line, and is divided into 100 map units (mu; 1 mu = 1% of the Ad5 genome = ~360 bp). The positions of the viral early transcription units and the direction of transcription are shown.



Adenovirus-transformed cells have typical morphology and growth properties of transformed cells in culture. They are less susceptible to contact inhibition of movement, and will overgrow the surrounding layer of untransformed cells to form dense foci. Cell lines derived from such foci are immortal, can grow in low serum concentrations, and are anchorage-independent for growth. They have an epithelioid, rather than fibroblastic morphology, are smaller and less flattened than their untransformed counterparts, and express virus-specific T antigens. In addition, many cell lines transformed by subgenus C adenoviruses are tumorigenic when inoculated into nude mice (Williams, 1973).

1.3.2. Integration of viral DNA

Adenovirus transformation involves the integration of viral DNA into the cellular genome and expression of the integrated viral sequences. However, infection of cells permissive for viral DNA replication, *e.g.* human or hamster fibroblasts, with either virus particles or intact viral DNA molecules, results in a productive infection ending in cell lysis. Therefore, transformed cells survive only under conditions that preclude viral DNA replication. Examples of such conditions are: a) infection of non-permissive cells, *e.g.* rat fibroblasts, b) infection with mutant viruses defective for DNA replication, or c) transformation with viral DNA rendered non-infectious by enzymatic cleavage or mechanical shearing.

The mechanism of recombination between viral and cellular DNA is presently unknown. The integration patterns of viral DNA in many adenovirus-transformed cells have been analysed by Southern hybridization. Most adenovirus type C-transformed cells have simple integration patterns with low copy numbers

of viral sequences integrated as colinear fragments (reviewed in Doerfler, 1982). The integration pattern is unique for each cell line, suggesting random or accidental insertion. The integration sites have also been analysed by cloning and sequencing viral-cell junction fragments (Deuring, Winterhoff, Tamanoi, Stabel & Doerfler, 1981; Gahlmann, Leister, Vardimon & Doerfler, 1982; Visser, Reemst, van Mansfeld & Rozijn, 1982; Westin, Visser, Zabielski, van Mansfeld, Pettersson & Rozijn, 1982), and reveal no specific cell or viral sequences to be involved at the sites of integration. Computer analyses of the junction sequences have detected short "patch" homologies (8-12 bp) between cellular and viral DNA, which may play a role in stabilizing recombination complexes (Gahlmann *et al.* 1982; Schellner, Stuber & Doerfler, 1986). These short sequences are common throughout the cell genome and are therefore consistent with random integration. However, patch homologies are not present in all adenovirus-transformed cell lines, so their role, if any, in the integration process remains unclear.

Chromatin structure may be an important feature of the cellular integration site. Doerfler and colleagues have detected low molecular weight RNA molecules (~300 nucleotides) homologous to the cellular DNA at the viral-cell junction sites of several Ad2- and Ad12-transformed cell lines (Gahlmann, Schulz & Doerfler, 1984; Schulz, Freisem-Rabien, Jessberger & Doerfler, 1987). These RNA molecules are also present in the untransformed counterparts, indicating that the viral DNA has integrated at a site previously active in transcription. The structure of active chromatin may provide a more accessible target for insertion of viral DNA, or the selection process for transformed cells may select for those cells

in which viral sequences have integrated into an active site, thereby allowing their expression.

Once integrated, the viral sequences become complexed with cellular histones to form nucleosomes. MNase digestion of integrated viral sequences generates a nucleosome repeat pattern typical of cellular chromatin (Flint & Weintraub, 1977; Dery, Toth, Brown, Horvath, Allaire & Weber, 1985).

1.3.3. The transforming region

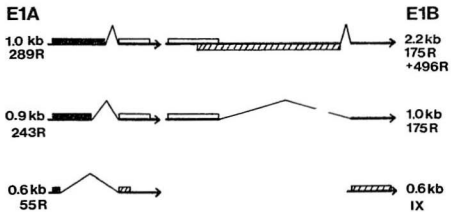
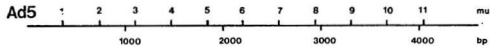
Two methods have shown that the E1 region contains the viral sequences responsible for transformation. First, analysis of the viral DNA sequences retained in several Ad2- and Ad5-transformed cell lines showed that although the DNA content varies among cell lines, all retain the left-end 12-14% of the viral genome and express sequences from this region (Gallimore, Sharp & Sambrook, 1974; Sharp, Petterson & Sambrook, 1974; Sambrook, Botchan, Gallimore, Orzanne, Pettersson, Williams & Sharp, 1975; Flint, Sambrook, Williams & Sharp, 1976). Second, it was shown that rodent cells can be transformed in culture by transfection with purified adenovirus DNA, and a restriction fragment corresponding to the left-end 15% of the viral genome is sufficient for transformation (Graham, Abrahams, Mulder, Heijneker, Warnaar, de Vries, Fiers & van der Eb, 1975). The phenotype of cells transformed by this fragment is indistinguishable from that of cells transformed by intact DNA or virus particles, indicating that all functions necessary for the induction and maintenance of the transformed phenotype reside in this region of the viral genome.

Region E1 has been sequenced in Ad2 (Gingeras, Sciaky, Bing-Dong, Yen, Kelly, Bullock, Parsons, O'Neill & Roberts, 1982) and Ad5 (van Ormondt, Maat & van Bevern, 1980) and the promoters, transcription units and mRNAs well characterized (reviewed in Pettersson, Virtanen, Perricaudet & Akusjarvi, 1983). (The organization of the E1 region is similar in all adenovirus serotypes. Unless otherwise stated, reference is made only to the closely related Ad2 and 5.) The E1 mRNAs present in the cytoplasm of transformed cells correspond to those transcribed during the early phase of infection, indicating that the viral early promoters are recognized when integrated into the host cell genome in the form of cellular chromatin. Where present, the other viral early genes are usually expressed, whereas the late genes are not, possibly due to the fact that their expression is dependent on viral DNA synthesis.

Region E1 actually consists of two separate transcription units, E1A (1.3-4.5 mu) and E1B (4.6-11.2 mu) (Fig. 1-2), each with its own promoter (Wilson, Fraser & Darnell, 1979). Early in infection, two E1A mRNAs are produced, of length 1.0 kb (18S) and 0.9 kb (12S), and these are also present in the cytoplasm of transformed cells (Lewis & Mathews, 1981). They are generated by differential splicing of a common primary transcript initiated from the E1A promoter at 1.3 mu, and share common 5'- and 3'-termini, but differ in the size of the internal segment removed by splicing (Perricaudet, Akusjarvi, Virtanen & Pettersson, 1979). The products of the 1.0 kb and 0.9 kb mRNAs, proteins of 289 and 243 residues (289R and 243R), respectively, are translated in the same reading frame, and so are identical except for 46 additional internal amino acids encoded by the

Figure 1-2 E1A and E1B transcription units and gene products.

The sizes of the E1 mRNAs are indicated in kb. Exons are represented by straight lines, introns by carets. The sizes of the E1 proteins are indicated in amino acid residues (R). Solid, hatched, and open areas represent the three different reading frames.



1.0 kb mRNA (Perricaudet *et al.* 1979). In infected cells, a third mRNA of 0.6 kb (9S) is produced from the E1A primary transcript during the late phase, but this species is not present in transformed cells (Spector, McGrogan & Raskas, 1978; van den Elsen, Klein, Dekker, van Ormondt & van der Eb, 1983c).

Region E1B also produces two major mRNA species early in infection, of 2.2 kb (22S) and 1.0 kb (13S), generated by differential splicing of a primary transcript initiated from the E1B promoter at 4.6 mu. They also share common 5'- and 3'-termini, and differ in the size of the intron removed during splicing (Perricaudet, Le Moullec & Pettersson, 1980). A third mRNA of 0.6 kb (9S), coding for the structural protein IX, is transcribed during the late phase from a separate promoter at 9.8 mu (Alestrom, Akusjarvi, Perricaudet, Mathews, Klessig & Pettersson, 1980). Only the 2.2 kb mRNA is present in transformed cells (van den Elsen *et al.* 1983c), and this codes for proteins of 496R and 175R, initiated at different *AUG* codons (Bos, Polder, Bernards, Schrier, van den Elsen, van der Eb & van Ormondt, 1981). These are translated in different reading frames and so share no common amino acid sequences.

1.3.4. The E1 proteins

The predicted *Mr* values for the E1A 289R and 243R proteins are 32,000 (32K) and 27,000 (27K), respectively. However, several species in the 35-60K range are detected after SDS-polyacrylamide gel electrophoresis of the *in vitro* translation products of E1A mRNA (Halbert, Spector & Raskas, 1979; Jochemsen, Hertoghs, Lupker, Davis & van der Eb, 1981; Smart, Lewis, Mathews, Harter & Anderson, 1981), and multiple species are detected on two-dimensional gels (Harter

& Lewis, 1978; Harlow, Franza Schley, 1985). Monoclonal antibodies raised against E1A synthetic peptides detect major species of 52K and 48.5K from the 1.0 kb mRNA, and 50K and 45K from the 0.9 kb mRNA, as well as several minor species (Rowe, Yee, Otis, Graham & Branton, 1983b; Yee, Rowe, Tremblay, McDermott & Branton, 1983; Yee & Branton, 1985). The higher than expected M_r values and the heterogeneity are probably due to post-translational modifications, and all major E1A proteins have been shown to be phosphorylated (Rowe *et al.* 1983b; Yee *et al.* 1983; Yee & Branton, 1985).

The E1B 496R and 175R proteins have predicted M_r values of 55,000 and 20,500 respectively, and proteins corresponding to these are present in infected and transformed cells. The *in vitro* translation products of the E1B 2.2 kb mRNA migrate on SDS-polyacrylamide gels at \sim 58K and \sim 21K (Halbert *et al.* 1979; Schrier, van den Elsen, Hertoghs & van der Eb, 1979; Jochemsen *et al.* 1981), and proteins of these sizes are also immunoprecipitated from extracts of infected and transformed cells with antisera and monoclonal antibodies directed against E1B synthetic peptides (Yee *et al.* 1983; Zantema, Franssen, Davis-Olivier, Ramaekers, Vooijs, deLeys & van der Eb, 1985). The 496R protein has been shown to be phosphorylated at serine and threonine residues (Levinson & Levine, 1977a; Malette, Yee & Branton, 1983). The 496R and 175R proteins are the viral T antigens commonly detected with antisera from animals bearing adenovirus-induced tumours (Gilead, Jeng, Wold, Sugawara, Rho, Harter & Green, 1976; Levinson & Levine, 1977b).

The intracellular localization of the E1 proteins has been studied mostly in

infected cells, where they are more abundant and more easily detected than in transformed cells. In immunofluorescence studies in infected cells, the E1A proteins have been found predominantly in the nucleus, and in diffuse areas of the cytoplasm (Feldman & Nevins, 1983; Yee *et al.* 1983). In cell fractionation studies, they have been found in the nucleus and cytoplasm, with the cytoplasmic forms associated with the cytoskeleton (Rowe, Graham & Branton, 1983a; Chatterjee & Flint, 1986), and a fraction of the nuclear forms associated with the nuclear matrix (Feldman & Nevins, 1983; Chatterjee & Flint, 1986; Schmitt, Fahnestock & Lewis, 1987). By infecting cells with mutant viruses producing one or the other of the E1A proteins, Schmitt *et al.* (1987) showed that only the 289R protein is matrix associated. In transformed cells, the E1A proteins are detected by immunofluorescence primarily in the nucleus, (A. Zantema, unpublished results cited in van der Eb & Bernards, 1984), and cell fractionation studies have shown the distribution of the E1A proteins to be similar to that in infected cells (Chatterjee & Flint, 1986; Schmitt *et al.* 1987).

The nuclear localization of the E1A proteins is consistent with their role in transcriptional activation of the other early viral genes during infection. Indeed, purified E1A proteins synthesized in *Escherichia coli* from plasmid expression vectors and injected into the cytoplasm of mammalian cells localize rapidly to the nucleus, where they are functional in activating viral early gene expression (Krippel, Ferguson, Rosenberg & Westphal, 1984; Ferguson, Krippel, Andrisani, Jones, Westphal & Rosenberg, 1985). A nuclear localization in transformed cells is also consistent with their role as transcriptional regulators of host cell genes (see section 1.3.6).

The E1B 496R protein is found in soluble nuclear and cytoplasmic fractions of infected cells during the early phase, accumulates in the nucleus during the late phase (Rowe *et al.* 1983a), and is detected by immunofluorescence predominantly in the nucleus and perinuclear area of the cytoplasm (Sarnow, Sullivan & Levine, 1982b; Yee *et al.* 1983). In infected cells, the 496R protein is physically associated with an E4-encoded 25K protein (Sarnow, Hearing, Anderson, Halbert, Shenk & Levine, 1984). The localization of the 496R protein in transformed cells is different from that seen in infected cells. In immunofluorescence studies the protein is detected not in the nucleus, but in a discrete cytoplasmic body close to the nucleus, as well as at cell-cell contacts and weakly in the cytoplasm (Zantema *et al.* 1985). The 496R protein is complexed with the cellular protein *p53* in transformed cells (Sarnow, Ho, Williams & Levine, 1982a), and this complex is present in the cytoplasmic body, but not at the cell-cell contacts. The cytoplasmic body also contains clusters of 8 nm diameter filaments, but these do not correspond to any of the known IFs (Zantema *et al.* 1985). The function of the 496R protein and the cytoplasmic body in transformed cells is not clear.

In both infected and transformed cells, the E1B 175R protein co-purifies with the membrane fraction (Persson, Katze & Phillipson, 1982; Rowe *et al.* 1983a), and to a lesser extent with the nucleoplasm (Green, Brackman, Cartas & Matsuo, 1982). It is detected by immunofluorescence associated with the nuclear envelope and lamina, and possibly the endoplasmic reticulum (White, Blose & Stillman, 1984; Zantema *et al.* 1985). The 175R protein has or induces an anti-nuclease activity, since infection with mutant viruses in which this protein is

The contributions of the E1A and E1B regions in DNA-mediated transformation have been analysed by van der Eb and colleagues by comparing the transformation properties of plasmids containing either the E1A or E1B region alone, with those containing the complete E1 region. Transfection of primary BRK cells with E1-containing plasmids, or a combination of E1A- and E1B-containing plasmids, induces the fully transformed phenotype, whereas E1A-containing plasmids induce partial transformation, and at much lower frequencies than E1 (van den Elsen, de Pater, Houweling, van der Veer & van der Eb, 1982; van den Elsen, Houweling & van der Eb, 1983a). E1B alone has no transforming activity, even when efficiently expressed from the SV40 promoter (van den Elsen *et al.* 1982, 1983a). Therefore, the lack of transforming activity of the E1B region in the absence of E1A is not merely due to the E1A gene products being required for expression of the E1B gene. If the contribution of the E1A region is restricted to immortalization, then E1B should be able to morphologically transform an established, *i.e.* previously immortalized, cell line. However, neither the E1B plasmid nor the E1B-SV40 construct induces morphological transformation in the established rat cell line 3Y1 (van den Elsen *et al.* 1983a), indicating that an E1A function(s) has a direct role in morphological transformation.

Although the E1B region has no transforming activity in the absence of E1A, E1B clearly plays a role in morphological transformation in co-operation with E1A, since cells transformed by E1A alone exhibit a partially transformed phenotype compared to those transformed by the complete E1 region. Also, E1B mutant viruses have been shown to be transformation-defective in primary and

established rat cells (Graham, Harrison & Williams, 1978; Jones & Shenk, 1979b; Chinnadurai, 1983; Mak & Mak, 1983; Babiss, Fisher & Ginsberg, 1984; Bernards, deLeeuw, Houweling & van der Eb, 1986; Barker & Berk, 1987). The observation that E1-transformed cells contain higher levels of E1A mRNA than those transformed by E1A alone led to the suggestion that at least one of the roles of the E1B region in transformation is to regulate expression of the E1A gene (van den Elsen, Houweling & van der Eb, 1983b). The E1B region has subsequently been shown to stimulate E1A expression at the level of transcription initiation (Natarajan, 1986; Jochemsen, Peltenburg, te Pas, de Wit, Bos & van der Eb, 1987) through *trans*-activation of the E1A enhancer by the E1B 175R protein (Natarajan, 1986; Yoshida, Venkatesh, Kuppuswamy & Chinnadurai, 1987). In fact, full morphological transformation of established NIH-3T3 cells is induced in the absence of E1B when the E1A gene is expressed at high levels from the metallothionein gene promoter, whereas the E1A gene expressed from its own promoter induces only partial transformation (Senear & Lewis, 1986). Therefore, the E1A proteins are capable of inducing full morphological transformation when expressed at high levels, and the role of E1B in this process appears to be indirect, through increasing the level of expression of E1A gene products. Attempts to isolate primary cells transformed by E1A expressed at high levels have so far failed, and it has been suggested that high levels of E1A proteins in the absence of E1B may be toxic to primary cells (Jochemsen, de Wit, Bos & van der Eb, 1986; Jochemsen *et al.* 1987).

In summary, these studies show that the E1A region plays a major role in

immortalization and morphological transformation. The E1B region has no transforming activity in the absence of E1A, but in co-operation with E1A increases the efficiency of transformation and induces full transformation. At least some of the properties of the fully transformed phenotype appear to be due to the higher levels of E1A proteins induced by E1B.

1.3.6. The E1A proteins and transformation

The role of the E1A proteins in transformation was initially investigated using E1A mutant viruses. These viruses are either unable to transform primary rat cells, or can induce only partial transformation (Graham *et al.* 1978; Ruben, Bacchetti & Graham, 1982). However, assigning functions to the individual E1A 243R and 289R proteins using these mutants is complicated due to the overlapping nature of their coding regions. More recently, site-directed mutagenesis has been used to mutate specific sites in the E1A gene, resulting in mutant viruses expressing only one of the E1A proteins. A small deletion at the splice site unique to the 0.9 kb mRNA prevents splicing of this molecule, resulting in no 243R protein synthesis, while synthesis of the 289R protein is unaffected (Montell, Fisher, Caruthers & Berk, 1982). Similarly, a deletion at the 1.0 kb mRNA-unique splice site results in synthesis of the 243R protein only (Montell, Courtois, Eng & Berk, 1984). In another approach, viruses expressing either the 243R or 289R protein have been reconstructed by replacing the wild-type E1A region with a cDNA copy of the 0.9 kb or 1.0 kb mRNA (Winberg & Shenk, 1984; Moran, Grodzicker, Roberts, Mathews & Zerler, 1986a).

Viruses expressing only the 243R protein can transform primary and

established rat cells, but the transformants have a partially transformed phenotype *i.e.* they remain fibroblastic and are anchorage-dependent for growth (Haley, Overhauser, Babiss, Ginsberg & Jones, 1984; Winberg & Shenk, 1984; Moran *et al.* 1986a). Therefore, in the absence of the 289R protein, the 243R protein can induce foci of partially transformed cells, but morphological transformation and anchorage-independent growth require the expression of the 289R protein. Foci of primary cells transformed by these mutants are extremely difficult to establish as permanent cell lines, indicating that the 289R protein is important for this process also.

Viruses expressing only the 289R protein can transform primary and established rat cells, although the transformation frequency is reduced compared to wild-type virus, and only a partially transformed phenotype is induced (Montell *et al.* 1984; Winberg & Shenk, 1984; Hurwitz & Chinnadurai, 1985a, 1985b). The transformants express both E1B proteins and are readily established as permanent cell lines, but are anchorage-dependent for growth. These cells are more defective for growth in semi-solid medium than those expressing only the 243R protein, suggesting that for anchorage-independent growth, the requirement for the 243R protein is more critical than for the 289R protein (Montell *et al.* 1984). The morphology of transformed primary rat embryo cells expressing only the 289R protein has been reported by one group to be epithelioid (Winberg & Shenk, 1984), but by another to be more fibroblastic than wild-type transformants (Hurwitz & Chinnadurai, 1985b), suggesting that the 243R protein may also be important for this process.

In summary, each of the E1A proteins on its own can immortalize primary cells and induce a partially transformed phenotype, but efficient transformation and expression of the fully transformed phenotype requires the expression of both E1A proteins. The 289R protein appears to play an important role in morphology and establishment of permanent cell lines, whereas the 243R protein appears to be more important for anchorage-independent growth.

While it has become clear that many of the changes in morphology and growth properties associated with adenovirus transformation are mediated by the E1A proteins, the mechanism of E1A's transforming activity remains unknown. Given the variety of phenotypic changes brought about by E1A, it is unlikely that each is due directly to the E1A proteins: rather, they are likely the result of E1A-induced changes in cellular gene expression. The E1A proteins not only regulate adenovirus gene expression, but they also have the ability to stimulate or repress the transcription of several cellular genes. It is likely, therefore, that the transforming activity of E1A involves regulation of the expression of cellular genes involved in growth control.

The E1A gene products have been shown to be required in *trans* for efficient transcription of the other viral early genes (reviewed by Flint, 1986). In the absence of the E1A proteins, activation of the viral early promoters occurs slowly, through a *cis*-acting mechanism. The E1A proteins are thought to *trans*-activate these genes by catalysing the formation of stable transcription complexes at their promoters (Gaynor & Berk, 1983; Kovessi, Reichel & Nevins, 1986b; Richter, Hurst & Jones, 1987). However, the E1A proteins are not

sequence-specific DNA binding proteins (Ferguson *et al.* 1985), implying that they do not interact directly with the viral early promoters. Also, mutational analysis of the viral early promoters have failed, with the exception of the E4 promoter, to detect sequences required specifically for E1A-induced transcription, suggesting that E1A stimulation of transcription is mediated indirectly, through other regulatory factors (reviewed by Berk, 1986). Several such protein factors have been detected in extracts from uninfected HeLa cells using the gel retardation technique, and their binding sites on the viral early promoters mapped by DNase I footprinting and Exo III protection. One of these, activating transcription factor (ATF), was identified independently by two groups and originally named E2A-EF (SivaRaman, Subramanian & Thimmappaya, 1986) and E4F1 (Lee & Green, 1987). ATF has been shown to bind to regulatory sequences in the E1A, E2A, E3 and E4 promoters, but the binding activity of ATF is similar in the absence and presence of E1A proteins (SivaRaman *et al.* 1986; Lee & Green, 1987; Lee, Hai, SivaRaman, Thimmappaya, Hurst, Jones & Green, 1987; Yee, Reichel, Kovesdi & Nevins, 1987). A second cellular factor, E2F, binds to the E2A and E1A promoters, and the amount of E2F, or its binding activity, is increased in the presence of E1A proteins (Kovesdi, Reichel & Nevins, 1986a, 1987). ATF and E2F bind simultaneously to adjacent but distinct sites on the E2A promoter (SivaRaman & Thimmappaya, 1987; Yee *et al.* 1987). Thus, E1A-induced transcription of the viral early genes appears to involve changes in the interactions of cellular transcription factors with their binding sites on the early promoters.

Studies with E1A-mutant viruses and plasmids expressing one or other of the E1A proteins have established that the 280R protein is responsible for efficient *trans*-activation of early viral gene transcription (Montell *et al.* 1984; Winberg & Shenk, 1984; Roberts, Miller, Kimelman, Cepko, Lemischka & Mulligan, 1985; Moran *et al.* 1986a). However, the ability of the 243R protein to *trans*-activate is less clear. Several groups have reported that the 243R protein has no *trans*-activating activity (Haley *et al.* 1984; Montell *et al.* 1984; Svensson & Akusjarvi, 1984; Glenn & Ricciardi, 1985; Moran *et al.* 1986a), whereas others have reported that the 243R protein can *trans*-activate, although inefficiently compared to the 280R protein (Leff, Elkaim, Goding, Jalinot, Sassone-Corsi, Perricaudet, Kedinger & Chambon, 1984; Winberg & Shenk, 1984; Ferguson *et al.* 1985; Roberts *et al.* 1985).

The E1A proteins can *trans*-activate not only the adenovirus early genes, but also several cellular genes when introduced into cells on transfected plasmids. The human β -globin (Green, Treisman & Maniatis, 1983), human ϵ -globin (Allan, Zhu, Montague & Paul, 1984) and rat preproinsulin (Gaynor, Hillman & Berk, 1984; Svensson & Akusjarvi, 1984) promoters are *trans*-activated by E1A gene products in transient expression assays. However, transcription of the corresponding endogenous genes remains unaffected, suggesting that E1A's *trans*-activating activity may be directed towards exogenously introduced DNA. This rather non-specific activity may contribute to the stimulation of adenovirus genes during infection, since they are also on newly-introduced DNA molecules. However, adenovirus early genes stably integrated into cellular chromatin are also

stimulated by E1A (Courtois & Berk, 1984; Kingston, Kaufman & Sharp, 1984), indicating that stimulation of these genes is specific and independent of chromatin structure. In addition, certain endogenous cellular genes are stimulated by E1A, although this is not a general effect, as the overall rate of cellular transcription does not increase during adenovirus infection (Beltz & Flint, 1979). The human *HSP70* gene is activated by E1A at the level of transcription, both in Ad5-infected HeLa cells and in 293 cells, an Ad5-transformed cell line (Nevins, 1982; Kao & Nevins, 1983). Also, transcription of the β -tubulin gene is stimulated by E1A in Ad5-infected HeLa cells (Stein & Ziff, 1984). These cellular genes may be stimulated by E1A by a mechanism similar to the *trans*-activation of viral early genes, involving changes in the interactions between cellular transcriptional regulatory factors and their promoter binding sequences. In contrast to the activation of the viral early genes, however, both the 243R and 289R proteins can efficiently activate the *HSP70* gene (Simon, Kitchener, Kao, Hickey, Weber, Voellmy, Heintz & Nevins, 1987).

In addition to its role as an activator of gene expression, E1A can also repress transcription of genes linked to several viral and cellular enhancer elements. The E1A proteins can repress the enhancer activity of the SV40, polyoma, and adenovirus E1A enhancers (Borrelli, Hen & Chambon, 1984; Velcich & Ziff, 1985; Velcich, Kern, Basilico & Ziff, 1986), and the endogenous cellular enhancers of the mouse IgH gene (Hen, Borrelli & Chambon, 1985) and the human insulin gene (Stein & Ziff, 1987). E1A regulation of enhancer activity, like *trans*-activation, appears to be mediated through cellular regulatory factors, since

the IgH enhancer is repressed by E1A in lymphoid cells (Hen *et al.* 1985), but stimulated by E1A in fibroblasts (Borrelli, Hen, Wasylyk, Wasylyk & Chambon, 1986). Unlike *trans*-activation, however, the 243R and 289R proteins have been shown to be equally efficient in enhancer repression (Borrelli *et al.* 1984; Velcich & Ziff, 1985).

The E1A proteins induce cellular DNA synthesis and cell cycle progression in growth-arrested cells (Rossini, Jonak & Baserga, 1981; Braithwaite, Cheetham, Li, Parish, Waldon-Stevens & Bellet, 1983; Stabel, Argos & Philipson, 1985; Kaczmarek, Ferguson, Rosenberg & Baserga, 1986; Nakajima, Masuda-Murata, Hara & Oda, 1987), and an increase in the expression of several host cell enzymes involved in these processes, *e.g.* thymidine kinase (Braithwaite *et al.* 1983; Lui, Baserga & Mercer, 1985), dihydrofolate reductase (Yoder, Robberson, Leys, Hook, Al-Ubaidi, Yeung, Kellems & Berget, 1983), thymidylate synthetase and proliferating cell nuclear antigen (PCNA) (Zerler, Roberts, Mathews & Moran, 1987). It is likely that during productive infection, induction of the host cell DNA synthesis machinery by E1A facilitates efficient viral DNA replication. In transformed cells, the ability to induce cellular DNA synthesis and release cells from growth arrest may also be an important aspect of E1A's immortalizing function. In this respect, it is significant that both the 243R and 289R proteins, which can each immortalize primary cells, can also stimulate host cell DNA synthesis and cell cycle progression (Stabel *et al.* 1985; Kaczmarek *et al.* 1986; Nakajima *et al.* 1987; Zerler *et al.* 1987). Recent studies indicate that the E1A proteins may accomplish this by antagonizing a cellular function that normally

suppresses cell growth. In the nucleus of adenovirus-infected and -transformed human cells, the E1A proteins form stable complexes with several host cell proteins, one of which, a phosphoprotein of Mr 105,000, has been shown to be the product of the *retinoblastoma (Rb)* gene (Whyte, Buchkovitch, Horowitz, Friend, Raybuck, Weinberg & Harlow, 1988). The *Rb* gene has been termed an "anti-oncogene", since inactivation of both copies results in the development of tumors such as retinoblastomas and osteosarcomas. The E1A proteins may therefore inactivate the *Rb* gene product, relieving the suppression of cell proliferation.

The E1A proteins are therefore multi-functional, capable of *trans*-activating viral and cellular genes, repressing viral and cellular enhancers, inducing cell cycle changes and transforming primary cells. Recent studies have shown that separate functional domains of the E1A proteins are involved in each of these functions (reviewed by Moran & Mathews, 1987). The E1A gene contains three conserved regions (CR), identified by comparison of the E1A sequences of several adenovirus serotypes (Kimelman, Miller, Porter & Roberts, 1985). Two of these, CR1 and CR2, are common to both E1A proteins, while CR3 corresponds essentially to the region unique to the 289R protein (Fig. 1-3). The fact that these regions are conserved implies that they code for important functional domains, and this has been confirmed by mutational analysis. As discussed above, CR3-mutants, and those expressing only the 243R protein (which lacks CR3), have little or no *trans*-activating activity, suggesting that CR3 is important for this function. In fact, a synthetic peptide consisting of the 49 amino acids of CR3 *trans*-activates the E2 promoter as efficiently as the 289R protein, indicating that CR3 is an

autonomously-functioning *trans*-activating domain (Lillie, Loewenstein, Green & Green, 1987). However, these mutants transform primary cells as efficiently as wild-type virus, suggesting that the CR3 *trans*-activating activity is not required for transformation. Consistent with this, an E1A-mutant plasmid encoding a truncated product comprising only CR1 and CR2 can immortalize primary cells (Zerler, Moran, Marayuma, Moomaw, Grodzicker & Ruley, 1986). Furthermore, mutations in CR1 and CR2 do not affect E1A's *trans*-activating activity, but severely impair its transforming activity, suggesting that CR1 and CR2 functions are important for transformation (Lillie, Green & Green, 1986; Moran, Zerler, Harrison & Mathews, 1986b; Kuppuswamy & Chinnadurai, 1987; Lillie *et al.* 1987; Schneider, Fisher, Goding & Jones, 1987).

Whereas the transforming and *trans*-activating functions of E1A can be separated, the transforming and enhancer-repressing activities appear to be more closely linked. Both the 243R and 289R proteins can transform cells and repress enhancer activity, and mutations in CR1 and CR2 abolish transforming activity and impair enhancer repression (Lillie *et al.* 1986, 1987; Kuppuswamy & Chinnadurai, 1987; Schneider *et al.* 1987). No mutants have been isolated that are transformation-positive and enhancer repression-negative, or *vice versa*, suggesting that E1A's transforming activity may involve repression of an enhancer-linked cellular gene(s) normally required for negative regulation of cell growth. However, a role for positive regulation cannot be ruled out, as the 243R protein has been reported to have some *trans*-activating activity. Although *trans*-activation of the viral early genes by the 243R protein is relatively

Figure 1-3 E1A protein conserved regions.

E1A 289R and 243R proteins, showing conserved regions (CRs) 1-3 (hatched areas), and their positions (in amino acid residue number).



CR1 CR2 CR3



inefficient compared to the 289R protein, this may be sufficient to stimulate cellular genes involved in transformation. This is supported by the observation that the 243R and 289R proteins stimulate transcription of the *HSP70* gene with equal efficiency (Simon *et al.* 1987). In addition, the enhancer-repression activity encoded by CR1 and CR2 can also stimulate enhancer-linked genes, depending on the enhancer and the cell type, since E1A represses the IgH enhancer in lymphoid cells (Hen *et al.* 1985), but stimulates it in fibroblasts (Borrelli *et al.* 1986). Therefore, in the cell types transformed by adenovirus, the E1A CR1 and CR2 functions may positively regulate cellular genes involved in growth control.

The E1A CR1 and CR2 functions are also required for the induction of cellular DNA synthesis and cell cycle progression. As discussed above, the 243R and 289R proteins can both induce cellular DNA synthesis and cell cycle progression, implying that CR3 is not required for this. Mutational analysis has determined that both CR1 and CR2 are required for the induction of cellular DNA synthesis in serum-starved primary cells (Lillie *et al.* 1987), whereas only CR1 is required in non-starved cells (Zerler *et al.* 1987). CR2 has been shown to be required for the induction of mitosis and cell proliferation in primary cells (Zerler *et al.* 1987), and for binding the *Rb* gene product (Whyte *et al.* 1988).

In summary, the transforming activity of the E1A proteins resides in regions CR1 and CR2, common to both E1A proteins, and appears to be closely linked to the E1A functions involved in repression of enhancer activity and induction of cellular DNA synthesis and cell cycle progression. This suggests that E1A transformation may involve repression of an enhancer-linked cellular gene

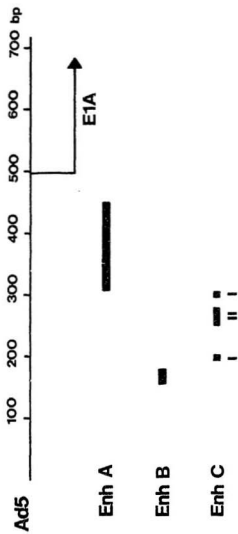
involved in negative regulation of cell growth, although activation of a cellular gene involved in positive regulation of cell growth cannot be ruled out.

1.3.7. The E1A enhancers

Transcription of the E1A gene is regulated by sequences in the region upstream from the E1A transcription start site, and several groups have identified sequences with enhancer activity within this region. A fragment containing Ad5 sequences from 0-2.4 mu linked to the herpes simplex virus thymidine kinase (HSV *tk*) promoter and structural gene results in an increase in the transformation frequency of human 143 TK⁻ cells to a TK⁺ phenotype, implying that this fragment contains a *cis*-acting element which stimulates transcription of the HSV *tk* gene (Weeks & Jones, 1983). Within this region, however, different enhancer elements have been identified in different assays. In transient expression assays in mouse L cells, insertion of an Ad5 fragment from 310-453 bp into a plasmid containing the E2 gene results in a 10- to 15-fold increase in E2 expression (Imperiale, Feldman & Nevins, 1983). This effect is seen when the fragment is inserted 5' or 3' to the E2 gene, and in either orientation, indicating that this fragment has enhancer-like properties (Fig. 1-4, Enh A). A different enhancer element has been identified by Chambon and colleagues, who inserted E1A upstream fragments into plasmids containing the Ad *MLP* and assayed transcription in HeLa cells. They found that a fragment from 0-270 bp has all the properties of an enhancer except the ability to function in the reverse orientation, and mapped the key sequences of this element by deletion analysis to between 155 and 178 bp (Fig. 1-4, Enh B) (Hen, Borrelli, Sassone-Corsi & Chambon, 1983).

Figure 1-4 E1A enhancers.

Upstream region of the E1A transcription unit, showing enhancers A, B, and C (solid lines), and the E1A transcription initiation site at position 499 bp.



Hearing & Shenk (1983, 1986) have mapped the enhancer elements important for EIA gene expression during infection of HeLa cells by deletion analysis of the EIA upstream region. Deletion of sequences between 193 and 357 bp results in a dramatic decrease in EIA transcription, and this fragment has enhancer activity when inserted 3' to the EIA gene, and in either orientation. Within this fragment they identified an 11 bp sequence repeated at ~200 bp and ~300 bp as being an important component of the enhancer (Fig. 1-4, Enh C, element I) (Hearing & Shenk, 1983). They also identified a second enhancer element at 248-282 bp (Enh C, element II), and showed that elements I and II can function independently as enhancers of EIA transcription, and that element II (but not element I) enhances transcription of the other viral early genes in *cis* (Hearing & Shenk, 1986).

The reason why different enhancer elements have been identified by these assays is not clear. The fact that enhancer A was identified in mouse L cells and enhancer B in HeLa cells may account for this, as enhancers do possess tissue specificity. Also, enhancer C was identified in viral DNA during infection, whereas enhancers A and B were identified on plasmids in transient expression assays. However, enhancer C functions in a plasmid containing the HSV *tk* gene, increasing transformation from TK⁻ to TK⁺ in both human 143 and mouse L cells (Hearing & Shenk, 1983), suggesting that the differences in the enhancers identified are not due to differences in cell type or to differences between plasmid and viral DNA molecules.

A cellular protein that interacts with the EIA enhancer region has been

detected in extracts from uninfected HeLa cells by the gel retardation technique (Barret, Clark & Hay, 1987). The binding site for this factor has been mapped by DNase I footprinting to 157-163 bp, corresponding to enhancer B (155-178 bp) identified by Hen *et al.* (1983). Also, sequences between 0-310 bp were shown to bind the cellular factor E2F (Kovesdi *et al.* 1987). The binding sites for E2F have been mapped by DNase I footprinting to 207-220 bp and 270-284 bp, which correspond closely to enhancer C elements I (~200 bp) and II (248-282 bp) identified by Hearing & Shenk (1983, 1986).

1.4. Summary and statement of objectives

Chromatin structure is related to gene activity, and the transition from an inactive to an active chromatin structure is an important aspect of eukaryotic gene regulation. Active and potentially active chromatin regions are preferentially sensitive to DNase I digestion, reflecting a more open conformation compared to bulk inactive chromatin. The active conformation extends well beyond the boundaries of the transcription unit, forming a chromatin structural domain. Also associated with active and potentially active genes are DNase I HS sites, thought to represent nucleosome-free regions of DNA in which regulatory sequences are exposed to allow access to sequence-specific transcription factors. The molecular basis for these structural alterations is not known, but may involve DNA supercoiling. Chromosomal DNA is organized into independently constrained supercoiled loops anchored at their bases to the nuclear matrix, and it has been proposed that each DNA loop defines a chromatin domain. Topo II in the nuclear matrix may regulate the degree of supercoiling in each DNA loop, which in turn may regulate the chromatin structure throughout the loop/domain.

Active genes have also been shown to be associated with the nuclear matrix, and it has been proposed that transcription occurs on the matrix. However, it is not clear how these interactions are related to the chromatin structural domains. According to the proposed model, the sequences anchoring a DNA loop to the nuclear matrix should define the boundaries of the corresponding DNase I sensitive chromatin domain. Few studies have examined these two properties in the same gene, and the results have not provided evidence to support this model. Therefore, the nature of the relationship between the chromosomal DNA loops and the chromatin structural domains remains to be demonstrated.

The objective of these studies was to examine these two properties, *i.e.* chromatin structure as determined by DNase I sensitivity and organization relative to the nuclear matrix, in the integrated viral sequences of Ad5-transformed cells. These sequences are integrated into the host cell genome in the form of cellular chromatin. Since maintenance of the transformed phenotype requires constitutive expression of the E1 genes, corresponding to the left-end 12 mu (~ 4 kb) of the Ad5 genome, these can be considered as "model" active eukaryotic genes. Viral sequences other than E1 may be integrated, but these are usually not expressed. One advantage offered by this system is that the Ad5 E1 region has been sequenced, and the transforming genes and their regulatory sequences have been well characterized. Another advantage is that non-transcribed viral sequences flanking the E1 genes can be analysed using viral DNA as hybridization probes. One of the cell lines examined contains the entire Ad5 genome (~ 36 kb), allowing analysis of ~ 30 kb of non-transcribed sequences

downstream from the active E1 region. Analysis of such an extensive region flanking a cellular gene usually requires extensive "chromosome walking" to obtain genomic DNA probes.

Chapter 2

Materials and Methods (General)

The materials and methods used throughout these studies are described here. Materials and methods used specifically in the chromatin structure and nuclear matrix experiments are described in Chapters 4 and 5, respectively.

2.1. Cells

The Ad5-transformed cell lines used were hamster lines 14b (Williams, 1973) and 945-C1 (Rowe, Branton, Yee, Bacchetti & Graham, 1984), the rat line 637-4 (Graham *et al.* 1978) and the human line 203 (Graham *et al.* 1975). These cell lines, plus HeLa cells, were obtained from Dr Frank Graham, McMaster University, Hamilton, Ontario.

Ad5-transformed cell lines were grown as monolayer cultures in Joklik's modification of Minimal Essential Medium (MEM), (Flow Laboratories) supplemented with 10% fetal calf serum. HeLa cells were grown as monolayers in Dulbecco's modification of MEM (Flow Laboratories) supplemented with 10% calf serum, penicillin (50 units/ml) and streptomycin (50 μ g/ml) (Flow Laboratories).

Cells were grown in a humidified incubator at 37°C in an atmosphere of 95% air and 5% CO₂.

2.2. Plasmids

Plasmids pXC1, pHE and pHF were obtained from Dr Frank Graham. pXC1 contains the Ad5 *Xho*I-C fragment (0-15.5 mu) inserted between the *Bam*HI and *Sa*II sites of pBR322 (McKinnon, Bacchetti & Graham, 1982). pHE and pHF contain the Ad5 *Hind*III-E (7.7-17.1 mu) and -F (89.1-97.2 mu) fragments, respectively, inserted into the *Hind*III site of pBR322. pE1A was obtained from Dr Hiroshi Hamada, Faculty of Medicine, MUN, and consists of the Ad5 *Sac*I-I fragment (0-4.8 mu) from pXC1 inserted into the *Sma*I site of pUC12 (Swift, Bhat, Youngusband & Hamada, 1987). pSH5 was constructed in our laboratory by Dr H. Banfield Youngusband, and consists of the Ad5 *Sma*I (2.8 mu)-*Hpa*I (4.3 mu) fragment inserted into the *Sma*I site of pUC12. pMHS 243, obtained from Dr Larry Moran, University of Toronto, Toronto, Ontario, contains a cDNA complementary to the HSP70-coding mRNA derived from mouse L-cells, inserted into pDPL13 (Lowe & Moran, 1986). pJH, obtained from Dr W. Marshall, Faculty of Medicine, MUN, contains the joining (J) region of the human immunoglobulin heavy chain gene.

2.3. Purification of DNA

DNA was purified by the method of Gross-Bellard, Oudet & Chambon (1973). Cells were incubated with 1 mg/ml protease (Sigma, type XIV) and 0.5% sodium dodecyl sulphate (SDS) at 55°C for 2 h, followed by phenol extraction and ethanol precipitation at -20°C. Precipitated nucleic acids were redissolved in 10 mM Tris-HCl (pH 7.4), 1 mM EDTA (TE), digested with 50 µg/ml RNase A (Sigma, type III-A) and 100 units/ml RNase T1 (Boehringer-Mannheim) at 37°C

for 30 min, followed by protease digestion, phenol extraction and ethanol precipitation as above. DNA was redissolved in TE, and the concentration measured by absorbance at 260 nm (path length = 1 cm), using a Pye Unicam SP6-550 spectrophotometer.

2.4. Analysis of DNA

DNA was digested with restriction endonuclease in the digestion buffer recommended by the suppliers (Bethesda Research Laboratories and Boehringer-Mannheim). Digestion products were separated by electrophoresis through 0.8% agarose gels (Sigma and Biorad) in Tris-acetate-EDTA (TAE) buffer [40 mM Tris-HCl (pH 7.9), 5 mM Na acetate, 1 mM EDTA] containing 0.5 $\mu\text{g/ml}$ ethidium bromide. Electrophoresis was for 12-16 h at 30-40 V (Sharp, Sugden & Sambrook, 1973). Gels were photographed under short wavelength uv light on a transilluminator.

DNA was transferred to nylon filters (NYTRAN, Schleicher and Schuell) by the blotting method of Southern (1975). First, the DNA was partially dephosphorylated by soaking gels in 0.25 N HCl for 10-15 min, then denatured by soaking in 0.5 M NaOH, 1.5 M NaCl twice for 15 min each. DNA was blotted onto filters in 10 x SSC (1 x SSC = 0.15 M NaCl, 0.015 M Na citrate) for 12-16 h, and fixed by baking for 2 h at 80°C in a vacuum oven.

Filters were pre-hybridized with 0.25 ml/cm² of 6 x SSC, 5 x Denhardt's solution (1 x Denhardt's solution = 0.02% BSA, 0.02% ficoll, 0.02% polyvinylpyrrolidone), 1% SDS, 100 $\mu\text{g/ml}$ low molecular weight (LMW) denatured

herring sperm DNA (Boehringer-Mannheim) and 10 $\mu\text{g}/\text{ml}$ poly-A (Calbiochem) at 42°C for 24 h. Filters were then hybridized with 0.1 ml/cm² of 50% formamide (pH 7.4), 6 x SSC, 1% SDS, 100 $\mu\text{g}/\text{ml}$ LMW denatured herring sperm DNA and denatured ³²P-labelled probe DNA (2-4 x 10⁶ cpm/ml), at 42°C for 24-48 h.

Probe DNA was labelled to a specific activity of 1-4 x 10⁸ cpm/ μg DNA with [α -³²P]dCTP by nick-translation (Rigby, Dieckmann, Rhodes & Berg, 1977) using a kit (Amersham, Ltd) and following the manufacturer's instructions. Unincorporated nucleotides were removed by spin-column chromatography through Sephadex G-50 (Pharmacia) as described in Maniatis, Fritsch & Sambrook (1982).

Filters were washed in 6 x SSC, 0.1% SDS twice for 15 min at room temperature, in 1 x SSC, 0.5% SDS twice for 15 min at 37°C, and in 0.1 x SSC, 1% SDS twice for 30 min at 60°C. Filters were then wrapped in Saran wrap and exposed to X-ray film (Kodak X-OmatRP) at -70°C with intensifying screens.

2.5. Isolation of RNA

Cells monolayers were rinsed three times with ice-cold phosphate-buffered saline [PBS = 0.14 M NaCl, 8 mM Na₂HPO₄, 1.5 mM KH₂PO₄, 2.7 mM KCl (pH 7.4)] containing cycloheximide (50 $\mu\text{g}/\text{ml}$), and harvested by scraping with a rubber policeman. After centrifugation at 250g for 5 min in a Sorvall HB4 rotor at 4°C, cells were resuspended in lysis buffer [0.1 M NaCl, 10 mM Tris-HCl (pH 7.5), 2.5 mM MgCl₂, 0.5% Nonidet P-40 (NP-40, Sigma), 200 $\mu\text{g}/\text{ml}$ heparin (Sigma), 10 mM vanadyl ribonucleosides] at 2 x 10⁷ cells/ml, and incubated at

0°C for 5 min with occasional vortexing. Lysis was monitored by phase-contrast microscopy. After centrifugation at 16,000g for 10 min in an HB4 rotor at 4°C, the supernatant was collected and adjusted to 0.1 M Tris-HCl (pH 7.5), 0.2 M NaCl, 12.5 mM EDTA, 1% SDS, 10 mM vanadyl ribonucleosides, and 200 µg/ml proteinase K (Boehringer-Mannheim), and incubated at 37°C for 30 min. The RNA was extracted with phenol, after which Na acetate (pH 4.5) was added to a final concentration of 0.3 M, and the RNA precipitated with 2.5 volumes of ethanol at -20°C.

Poly(A)⁺RNA was prepared by affinity chromatography using oligo(dT)-cellulose as described in Maniatis *et al.* (1982). Briefly, 150 µg of oligo(dT)-cellulose, type 3 (Collaborative Research, Inc.) was suspended in 1 M NaOH and packed in a column of length 1 cm. The column was washed with 2 volumes of 1 M NaOH followed by 2 volumes of distilled H₂O, and equilibrated with binding buffer [0.5 M NaCl, 20 mM Tris-HCl (pH 7.5), 1 mM EDTA, 0.1% SDS]. Total cytoplasmic RNA was dissolved in binding buffer, heated to 65°C for 5 min, chilled, and run through the column. The effluent was heated to 65°C for 5 min, chilled and run through the column again. The column was washed with binding buffer until the optical density at 260 nm of the effluent became zero. Poly(A)⁺RNA was then eluted with distilled H₂O, adjusted to 0.3 M Na acetate, and precipitated with 2.5 volumes of ethanol at -20°C.

2.6. Analysis of RNA

Poly(A)⁺RNA (~1 μg) was dissolved in 11 μl distilled H₂O and the following added; 2 μl of 10 x running buffer (1 x running buffer = 40 mM MOPS [3-(N-Morpholino)propane-sulphonic acid] (pH 7.0), 10 mM Na acetate, 1mM EDTA (pH 8.0)), 7 μl formaldehyde, and 20 μl formamide (pH 7.0), to give a final volume of 40 μl . After incubation at 60°C for 15 min, 4 μl of sample buffer (50% glycerol, 1 mM EDTA, 0.4% bromophenol blue) was added. RNA was fractionated by electrophoresis through 1.0% or 1.1% agarose gels containing 1 x running buffer and 2.2 M formaldehyde. Gels were run at 30 V for 16-18 h in 1 x running buffer. After rinsing gels briefly in distilled H₂O, RNA was blotted onto nylon filters in 20 x SSPE [1 x SSPE = 0.18 M NaCl, 10 mM Na phosphate buff. (pH 7.7), 1 mM EDTA] for 12-16 h. RNA was fixed to the filters by baking for 2 h at 80°C in a vacuum oven.

Filters were pre-hybridized with 0.25 ml/cm² of 50% formamide (pH 7.4), 5 x Denhardt's solution, 5 x SSPE, 0.1% SDS, and denatured LMW herring sperm DNA (100 $\mu\text{g}/\text{ml}$) at 42°C for 24 h. Filters were hybridized with 0.1 ml/cm² of 50% formamide (pH 7.4), 1 x Denhardt's solution, 5 x SSPE, 0.1% SDS, denatured LMW herring sperm DNA (100 $\mu\text{g}/\text{ml}$) plus denatured ³²P-labelled probe DNA (2-4 x 10⁶ cpm/ml), at 42°C for 24 or 48 h.

Filters were washed and exposed to X-ray film as for DNA blots.

Chapter 3

Viral DNA and RNA in transformed cells

3.1. Introduction

Transformation of cells by adenoviruses involves integration of viral DNA into the host cell chromosome and expression of sequences from the viral E1 region (section 1.3). In addition to the E1 region, other viral sequences may be integrated, but their expression is not required for transformation. The four Ad5-transformed cell lines examined in this study were established several years ago, and the viral DNA sequences integrated and expressed in these cells are summarized here briefly.

Cell line 14b was established by Williams (1973) from hamster embryo fibroblasts (HEF) transformed with a temperature sensitive mutant of Ad5, H5ts14, at the non-permissive temperature. Mutant virus was used, as HEF cells are permissive for Ad5 DNA replication, and infection with wild-type virus results in cell lysis. H5ts14 grows as efficiently as wild-type Ad5 on HEF cells at 31°C, but is defective for DNA replication at 38.5°C. Cultures of HEF cells were infected with H5ts14 at 38.5°C and maintained at this temperature for several weeks. Cell line 14b was established from one of the resulting foci of transformed cells, and maintained at 37°C. 14b cells have morphological and growth

properties typical of adenovirus-transformed cells in culture. They are smaller and less flattened than their untransformed counterparts, and tend to grow in clumps and pile up on each other (Goldman, Chang & Williams, 1975). They are tumorigenic in newborn hamsters (Williams, 1973), and serum from animals bearing 14b-induced tumours immunoprecipitates the E1B 496R protein (Rowe *et al.* 1984).

The viral DNA sequences present in 14b cells have been determined by measuring renaturation kinetics in solution hybridization studies. The rate of reannealing of a viral restriction fragment homologous to sequences present in 14b DNA is accelerated in the presence of 14b DNA relative to the rate in the presence of untransformed hamster cell DNA. It has been estimated from these studies that 14b contains ~5.5 copies of the left-hand ~40 mu of the Ad5 genome per diploid quantity of cell DNA (Sambrook *et al.* 1975; Flint *et al.* 1976). The viral mRNAs present in the cytoplasm of 14b cells have been identified by solution hybridization between cytoplasmic RNA and the separated strands of specific viral DNA restriction fragments. The only viral mRNAs detected are those complementary to the E1 transcription unit (Flint *et al.* 1976; Binger, Flint & Rekosh, 1982).

Cell line 945-C1 was established from primary baby hamster kidney (BHK) cells transformed with a total *Hind*III digest of wild-type Ad5 DNA (Rowe *et al.* 1984). Since BHK cells are permissive for Ad5 DNA replication, the restriction enzyme digestion was required to render the viral DNA non-infectious. The resulting transformed cells have morphological and growth properties typical of adenovirus-transformed cells in culture.

The integrated viral DNA sequences present in 945-C1 cells have been analysed by Southern blotting of 945-C1 DNA and hybridization with virus-specific DNA probes. The results indicate that 945-C1 DNA contains viral sequences hybridizing to Ad5 *HindIII*-G (0-7.7 mu), -E (7.7-17.1 mu), -F (89.1-97.1 mu), and -I (97.1-100 mu) fragments (see Fig. 3-1), at one copy per diploid amount of cell DNA (Downey, Rowe, Bacchetti, Graham & Bayley, 1983; Rowe *et al.* 1984). However, viral and host cell sequences are often lost during integration, and it has not been demonstrated which sequences within each of these fragments are present in 945-C1 DNA, nor their organization relative to one another. 945-C1 cells express the E1A proteins, the E1B 175R protein, and an E4-encoded protein of *Mr* 14,000 (14K), but do not express the E1B 496R protein (Downey *et al.* 1983; Rowe *et al.* 1984).

Cell line 637-4 was established after infection of primary baby rat kidney (BRK) cells with H5*hr1*, an *hr* group I mutant of Ad5 (Graham *et al.* 1978). *Hr1* contains a single base pair deletion in the region unique to the E1A 1.0 kb mRNA, resulting in production of a truncated form of the 289R protein, and an unaltered 243R protein (Ricciardi, Jones, Cepco, Sharp & Roberts, 1981). The transformed foci induced by *hr1* could not be established as clonal lines, but cell line 637-4 was established by passaging entire cultures containing 20 or more colonies. Unlike wild-type Ad5-transformants, 637-4 cells have a fibroblastic morphology, do not form colonies in soft agar and are non-tumorigenic in nude mice (Ruben *et al.* 1982).

637-4 cell DNA has been analysed by Southern blotting and hybridization

with virus-specific DNA probes, and shown to contain one complete copy of the viral genome colinearly integrated at a single site in the host cell DNA (Ruben *et al.* 1982). The E1B 496R and 175R proteins are detected in 637-4 cell extracts by immunoprecipitation with an antiserum specific for E1 proteins (Ruben *et al.* 1982). The E1A proteins cannot be precipitated with this antiserum. However, these proteins are usually expressed at very low levels in transformed cells and do not precipitate efficiently with polyclonal antisera. An antiserum which recognizes the E2A-encoded 72K DNA binding protein (72K DBP) in infected cells fails to precipitate this protein in 637-4 cell extracts (Ruben *et al.* 1982).

Cell line 293 is a line of human embryonic kidney (HEK) cells transformed by Ad5 DNA (Graham *et al.* 1975). Since HEK cells are permissive for Ad5, the DNA was first rendered non-infectious by mechanical shearing. 293 cells have an epithelioid morphology and growth properties typical of Ad5-transformed cells. They express the E1A and E1B proteins (Rowe *et al.* 1984), and are weakly tumorigenic in nude mice (Graham, Smiley, Russell & Nairn, 1977).

The DNA of 293 cells has been shown by renaturation kinetics and Southern blotting analyses to contain ~5 copies of the left-end 12-15 mu of the Ad5 genome per diploid amount of cell DNA, integrated at a unique site in the host cell DNA (Aeillo, Guilfoyle, Huebner & Weimann, 1979; Spector, 1983). The cytoplasm of 293 cells has been shown to contain E1A and E1B mRNAs by RNA (Northern) blotting and hybridization with E1A- and E1B-specific DNA probes (Kao, Capasso, Heintz & Nevins, 1985).

I analysed the DNA of each of these cell lines by Southern blotting and hybridization with viral DNA-specific probes to confirm the organization of the integrated viral sequences, and to ensure that viral sequences had not been lost or rearranged during passaging or subcloning since they were first characterized. As the properties that I have examined in this study, *i.e.* chromatin structure and nuclear matrix association, are related to gene activity, it was important to determine the transcriptional status of the integrated viral sequences. Therefore, I analysed the viral mRNAs transcribed in these cells by RNA (Northern) blotting and hybridization with viral DNA-specific probes.

3.2. Results and Discussion

3.2.1. Viral DNA in adenovirus-transformed cells

The Ad5 DNA sequences present in cell lines 637-4, 14b, 293 and 945-C1 were analysed by Southern blotting of transformed cell DNA cleaved with restriction enzymes, and hybridization with Ad5 DNA probes. Restriction maps of Ad5 are shown in Figure 3-1, along with the Ad5 DNA probes used throughout these studies.

Figure 3-2 shows the virus-specific *Hind*III fragments present in cell lines 637-4, 14b and 293. 637-4 DNA contained *Hind*III fragments corresponding to each of the Ad5 *Hind*III internal fragments, *i.e.* *Hind*III-A, -B, -C, -D, -E, -F, and -H (lane 2). The left-terminal -G and right-terminal -I fragments were missing, but at least two non-native size fragments were present. A plasmid containing the Ad5 left-end terminal *Sac*I fragment (pE1A) hybridized to the 4.3 kb non-

Figure 3-1 Ad5 restriction maps and DNA probes.

The Ad5 genome is divided into 100 mu (1 mu = ~360 bp). *HindIII*, *SmaI*, and *SacI* restriction maps are shown, with restriction site positions given in mu. The positions of the E1A, E1B, and E4 transcription units, and the probes used in these studies are shown below the corresponding region of the Ad5 genome.

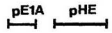
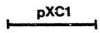
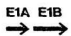
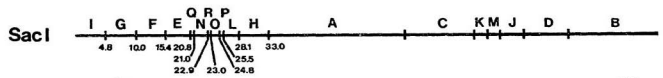
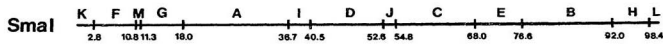
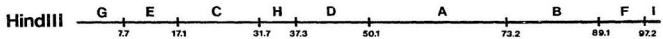
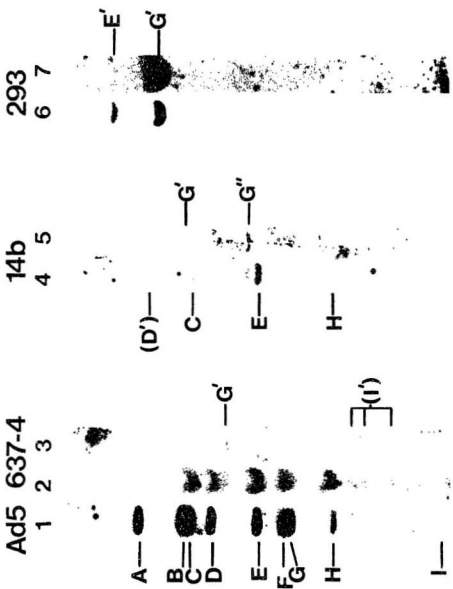


Figure 3-2 Analysis of Ad5 DNA in 637-4, 14b, and 293 cells.

Transformed cell DNA (~10 $\mu\text{g}/\text{lane}$) was digested with *Hind*III. Digestion products were separated by agarose gel electrophoresis and transferred to filters by Southern blotting. Lane 1, Ad5 DNA; lanes 2 and 3, 637-4 DNA; lanes 4 and 5, 14b DNA; lanes 6 and 7, 293 DNA. Filters were hybridized with α -³²P-labelled Ad5 DNA (lanes 1, 2 and 4), pE1A (lanes 3, 5 and 7), or pXC1 (lane 6).



native λ fragment (lane 3, G'), indicating that this fragment contains sequences from the left-terminal Ad5 *Hind*III fragment joined to cell DNA. Identification of the right-end virus-cell junction was less clear. Fragments of length 1.85 kb, 1.6 kb and 1.45 kb were faintly visible (lane 2), but which of these, if any, corresponds to the right-end virus-cell junction fragment could not be determined from these data. During integration, sequences may have been lost from the right-end terminus of the viral genome, leaving insufficient *Hind*III-I fragment sequences to be detected under these hybridization conditions. The most likely integration pattern for the Ad5 sequences in 637-4 DNA is presented in Figure 3-7. This integration pattern is identical to that suggested by Graham and co-workers, and is consistent with their conclusion that 637-4 DNA contains all of the Ad5 genome colinearly integrated at a single integration site (Ruben *et al.* 1982).

14b DNA contained *Hind*III fragments corresponding to the Ad5 *Hind*III-C, -E, and -H fragments, plus three non-native size fragments (Fig. 3-2, lane 4). The left-terminal-specific probe (pE1A) hybridized to the 5.8 kb and 3.7 kb non-native size fragments (lane 5, G' and G*, respectively), indicating that these two fragments contain sequences from the Ad5 *Hind*III-G fragment joined to cell DNA. The third non-native size fragment of 7.8 kb (lane 4, D') did not hybridize with *Hind*III-G, -E, or -H probes (results not shown), and most likely represents a joint fragment containing Ad5 *Hind*III-D sequences and cell DNA. The fact that two left-end junction fragments were detected implies that there are at least two viral DNA integration sites. However, only one (possible) right-end junction

fragment was detected. A possible explanation for this is that the second right-end viral junction site lies to the right of, but very close to, the viral *Hind*III site at 37.3 mu. Consequently, the virus-cell junction fragment generated by *Hind*III digestion may not be long enough to be detected with viral DNA probes under these hybridization conditions.

The presence of sequences hybridizing to Ad5 *Hind*III-G, -E, -C and -H is consistent with the results of Sambrook *et al.* (1975) and Flint *et al.* (1976) showing that 14b DNA contains the left-end ~40 mu of the Ad5 genome. The most likely integration pattern is shown in Figure 3-7.

293 DNA could not be probed with Ad5 DNA, as the source of the viral DNA was virus particles grown in HeLa cells. The viral DNA preparation contained trace amounts of contaminating human DNA which hybridized to 293 DNA, resulting in an extremely high background signal. Instead, 293 DNA was probed with pXC1, a plasmid containing the Ad5 *Xho*I-C fragment (0-15.5 mu). This probe hybridized to two fragments in *Hind*III-digested 293 DNA, of 11.8 kb (E') and 6.8 kb (G')(Fig. 3-2, lane 6). The left-terminal-specific probe (pE1A) hybridized to the 6.8 kb fragment (lane 7), indicating that this fragment contains Ad5 *Hind*III-G sequences joined to cell DNA. The 11.8 kb fragment, therefore, contains Ad5 *Hind*III-E sequences joined to cell DNA. These results are consistent with previous reports demonstrating that 293 DNA contains the left-end ~12 mu of the Ad5 genome integrated at a unique site in the host cell chromosome (Aeillo *et al.* 1979; Spector, 1983), as shown in Figure 3-7.

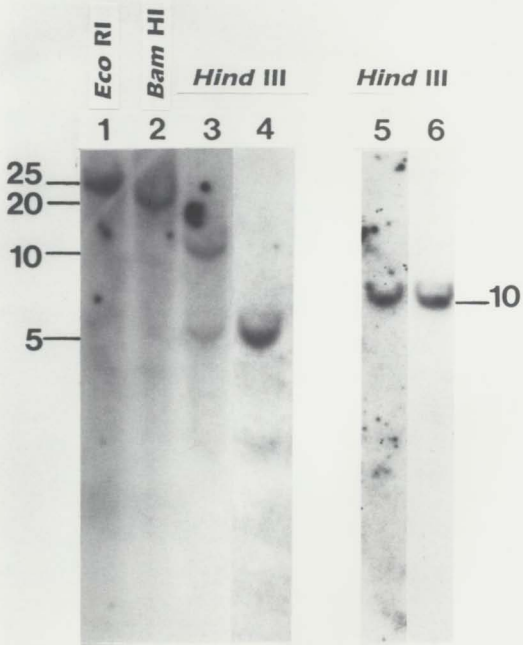
945-C1 DNA contains sequences from the Ad5 *HindIII*-G (0-7.7 mu), -E (7.7-17.1 mu), -F (89.1-97.2 mu), and -I (97.2-100 mu) fragments (Downey *et al.* 1983; Rowe *et al.* 1984), although it has not been shown which sequences within each of these restriction fragments are present, nor their organization relative to one another. In order to determine the viral DNA integration pattern, 945-C1 DNA was digested with several different restriction enzymes, and analysed by Southern blotting and hybridization with plasmids containing Ad5 sequences from different regions of the viral genome.

945-C1 DNA was first cleaved with *EcoRI* or *BamHI* and probed with total Ad5 DNA. Neither of these enzymes cleaves within any of the viral *HindIII* restriction fragments present in 945-C1 DNA, and so they should cleave only host cell DNA. Accordingly, *EcoRI* and *BamHI* each generated one viral DNA-containing fragment, an *EcoRI* fragment of ~25 kb (Fig. 3-3, lane 1) and a *BamHI* fragment of ~20 kb (lane 2), indicating that all the integrated viral sequences are located within one region of the host cell genome no more than 20 kb in length.

945-C1 DNA was digested with *HindIII* and probed with total Ad5 DNA, which hybridized to fragments of ~10 kb and ~5 kb (Fig. 3-3, lane 3). Plasmids pE1A (Ad5 *SacI*-I) and pHF (Ad5 *HindIII*-F), hybridized to the 10 kb fragment (lanes 5 and 6, respectively), whereas pHE (Ad5 *HindIII*-E), hybridized to the 5 kb fragment (lane 4). (For maps of the Ad5 DNA probes refer to Figure 3-1.) Therefore, the Ad5 E1A and E4 (*HindIII*-F) sequences are contained in a 10 kb *HindIII* fragment, and the Ad5 *HindIII*-E sequences are contained in a 5 kb *HindIII* fragment.

Figure 3-3 Analysis of Ad5 DNA in 945-C1 cells.

945-C1 cell DNA ($\sim 10 \mu\text{g}/\text{lane}$) was digested with *EcoRI* (lane 1), *BamHI* (lane 2), or *HindIII* (lanes 3-6), and analysed by Southern blotting as described in Figure 3-2. Filters were hybridized with Ad5 DNA (lanes 1-3), pHE (lane 4), pHF (lane 5), or pE1A (lane 6). Restriction fragment lengths are given in kb.

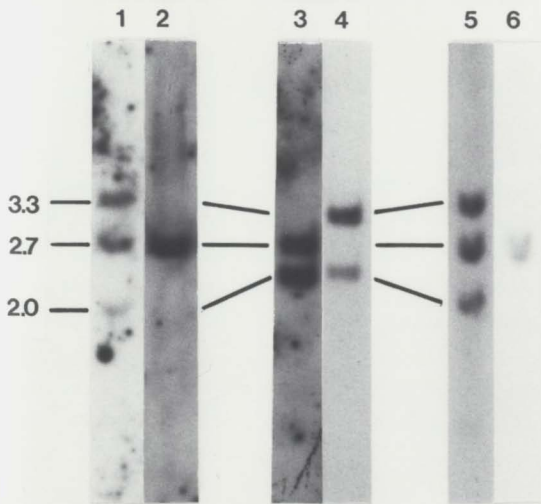


In order to analyse the integrated viral sequences in 945-C1 cells further, 945-C1 DNA was digested with *Sma*I and probed with total Ad5 DNA. *Sma*I generated three viral DNA-containing fragments of 3.3 kb, 2.7 kb and 2.0 kb (Fig. 3-4, lanes 1 and 5). The Ad5 *Hind*III fragments detected in 945-C1 DNA contain *Sma*I sites at position 1,008 bp (2.8 mu), 3,933 bp (10.8 mu), 4,133 bp (11.3 mu), 33,094 bp (92.0 mu), and 35,363 bp (98.4 mu) on the viral genome (Fig. 3-1). There is no reason *a priori* to suggest that any of these viral *Sma*I sites are present in 945-C1 DNA, as they may have been lost during integration. Therefore, the three viral DNA-containing fragments could be generated by four host cell DNA *Sma*I sites. However, the Ad5 *Sma*I site at 1,008 bp is located in the middle of the E1A transcription unit, in the region coding for the CR3 portion of the 289R protein. Since the CR3 region is required for the epithelioid morphology and anchorage-independent growth properties of fully-transformed cells, and since 945-C1 cells possess both of these properties, it was reasonable to assume that the CR3-coding sequences, including the *Sma*I site at 1,008 bp, are present in 945-C1 DNA.

In order to determine which two of these three *Sma*I fragments are separated by the site at 1,008 bp, *Sma*I-digested 945-C1 DNA was probed with pE1A (0-1,771 bp). This probe hybridized to the 2.7 kb and 2.0 kb fragments (Fig. 3-4, lane 3), indicating that these two fragments flank the 1,008 bp *Sma*I site. The plasmid pSH5, which contains Ad5 sequences from the *Sma*I site at 1,008 bp to the *Hpa*I site at 1,571 bp (4.3 mu), hybridized to the 2.7 kb fragment only (lane 2), indicating that this fragment lies to the immediate right of the 1,008

Figure 3-4 Analysis of Ad5 DNA in *Sma*I-digested 945-C1 cell DNA.

945-C1 cell DNA ($\sim 10 \mu\text{g}/\text{lane}$) was digested with *Sma*I and analysed by Southern blotting as described in Figure 3-2. Filters were hybridized with Ad5 DNA (lanes 1 and 5), pSH5 (lane 2), pE1A (lane 3), pHF (lane 4), or pHE (lane 6). Restriction fragment lengths are given in kb.



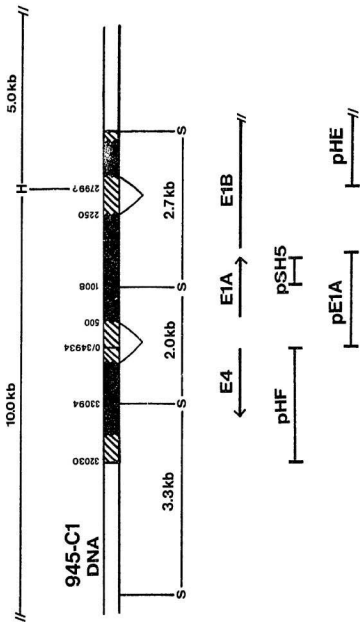
bp *Sma*I site, and the 2.0 kb fragment lies to the immediate left of this site. (See Fig. 3-5 for diagram.) The plasmid pHF, containing the Ad5 *Hind*III-F fragment (32,030-34,934 bp), hybridized to the 3.3 kb and 2.0 kb fragments (Fig. 3-4, lane 4), indicating that the order of the three fragments is, from left to right, 3.3 kb - 2.0 kb - 2.7 kb, and that the Ad5 *Hind*III-F-hybridizing sequences lie to the left of the E1A sequences.

In summary, the 945-C1 *Sma*I 3.3 kb fragment contains Ad5 *Hind*III-F sequences, the 2.0 kb fragment contains *Hind*III-F sequences also, plus those *Hind*III-G sequences to the left of position 1,008 bp, and the 2.7 kb fragment contains *Hind*III-G sequences to the right of position 1,008 kb. Plasmid pHE, containing the Ad5 *Hind*III-E fragment (2,798-6,232 bp), hybridized to the 2.7 kb *Sma*I fragment (Fig. 3-4, lane 6), indicating that this fragment also contains those *Hind*III-E-hybridizing sequences present in 945-C1 DNA. The Ad5 *Hind*III-G fragment contains ~1.8 kb of DNA from the *Sma*I site at 1,008 bp to its right-end boundary at 2,799 bp, and the *Hind*III-E fragment contains a total of ~3.4 kb of DNA. It is obvious, therefore, that not all of these viral sequences are present in 945-C1 DNA, since the integrated sequences were contained within a 2.7 kb-long fragment. It has been shown that the E1A region (~500-1,600 bp) and the E1B 175R protein-coding region (~1,700-2,250 bp) are expressed in 945-C1 cells (Downey *et al.* 1983; Rowe *et al.* 1984), implying that viral sequences between position 500 bp and ~2,250 bp, *i.e.* most of the *Hind*III-G sequences, are integrated.

945-C1 cells also express a 14K protein encoded by the E4 region (~99-91

Figure 3-5 Integrated Ad5 sequences in 945-C1 cell DNA.

Solid areas, viral sequences present in 945-C1 cell DNA; hatched areas, viral sequences that may be present; open areas, flanking cellular DNA sequences. Carets indicate viral sequences that may be contiguous or separated by cellular sequences. The corresponding positions on the Ad5 genome (in bp) are shown above the DNA. The orientation of the pHF-hybridizing region may be reversed. The positions of the E1A, E1B, and E4 transcription units, and the probes used in these studies are shown below the DNA. S, *Sma*I restriction sites; H, *Hind*III restriction sites.



mu), and sequences from this region have been detected in 945-C1 DNA with probes containing the Ad5 *HindIII*-F and -I fragments (Downey *et al.* 1983; Rowe *et al.* 1984). The fact that the Ad5 *HindIII*-F-hybridizing sequences in 945-C1 DNA were divided between two *SmaI* fragments (Fig. 3-4, lane 4) suggested that the *SmaI* site between them was viral. The Ad5 *HindIII*-F fragment contains one *SmaI* site, at position 33,094 bp (92.0 mu). It seemed likely, therefore, that this site separates the 3.3 kb and 2.0 kb *SmaI* fragments in 945-C1 DNA. However, the orientation of the E4 sequences relative to the adjacent E1A region could not be determined from these data. Also, an Ad5 *HindIII*-I fragment probe was not available.

The 945-C1 10 kb *HindIII* fragment contains the Ad5 E1A and E4 sequences, and the 5 kb *HindIII* fragment contains the *HindIII*-E-hybridizing sequences. Since the order of these sequences relative to one another is E4 - E1A - *HindIII*-E, then the *HindIII* site separating the 10 kb and 5 kb fragments must be located between the E1A and *HindIII*-E sequences. This site may be cellular, implying that the Ad5 *HindIII*-E sequences had integrated at a different site from the other viral sequences, and were separated from them by cell DNA sequences containing a *HindIII* site. Alternatively, this *HindIII* site may correspond to the site at position 2,799 bp (7.7 mu) on the viral genome. This may have arisen by incomplete digestion at this site in the *HindIII*-digested Ad5 DNA used to transform these cells, or by religation of the Ad5 *HindIII*-G and -E fragments before or during the integration event. If the viral 2,799 bp site is present, the *SmaI* 2.7 kb fragment must contain all of the Ad5 *HindIII*-G sequences from

1,008 bp to 2,799 bp (~1.8 kb), leaving room for at most 0.9 kb of Ad5 *Hind*III-E sequences, from position 2,799 bp to ~3,700 bp.

The most likely integration pattern of Ad5 sequences in 945-C1 DNA is presented in Figure 3-5. Unequivocal determination of the integration pattern will require cloning and sequencing of the integrated viral and flanking cellular DNA.

3.2.2. Viral RNA in adenovirus-transformed cells

The virus-specific mRNAs in Ad5-transformed cells were analysed by Northern blotting and hybridization with Ad5 DNA probes. Cytoplasmic poly(A)⁺ RNA was size-fractionated on agarose gels, blotted onto filters, and hybridized with plasmid DNA probes specific for different regions of the viral genome.

The E1A-specific probe, pSH5, hybridized to RNA species of ~1 kb, corresponding to the E1A 0.9 kb and 1.0 kb mRNAs, in all the Ad5-transformed cell lines (Fig. 3-6A, lanes 1-4), but did not hybridize to HeLa RNA (lane 5). The relative intensity of the hybridization signals indicated that 14b cells contained the highest steady-state level of cytoplasmic E1A mRNA, followed by 945-C1, 293, and 637-4. The low level of cytoplasmic E1A mRNA in 637-4 cells is likely due to the *hrI* mutation in the E1A gene of these cells, which results in a truncated E1A 289R product (Ricciardi *et al.* 1981). This protein is responsible for efficient *trans*-activation of the viral early regions, including E1A (section 1.3.6). Therefore, the E1A gene is likely to be transcribed less efficiently in 637-4 cells than in the other cell lines containing wild-type E1A gene products.

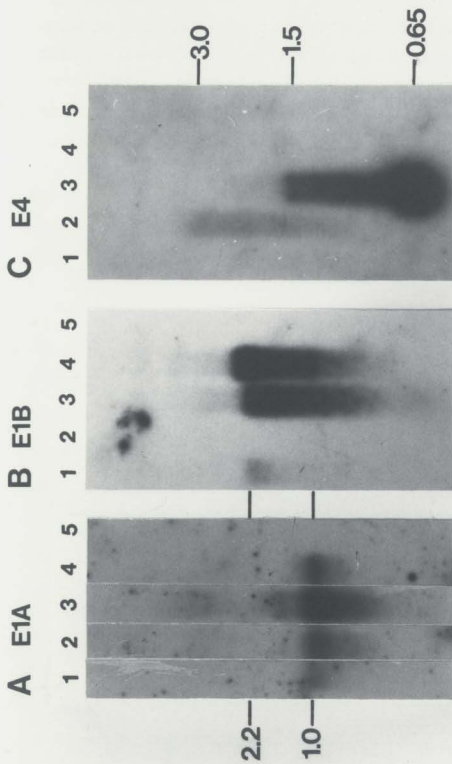
The E1B mRNAs were detected by probing with pHE (7.7-17.1 mu). This probe hybridized to RNA from 637-4, 14b, and 293 cells (Fig. 3-6B, lanes 1, 3 and 4, respectively), but not from 945-C1 or HeLa cells (lanes 2 and 5, respectively). The major RNA species detected corresponds to the E1B 2.2 kb mRNA. Previous studies have shown that this is the only E1B mRNA present in transformed cells (van den Elsen *et al.* 1983c). 637-4 cells contained low steady-state levels of the E1B 2.2 kb mRNA (lane 1), again possibly due to the effect of the *hri* mutation on E1A *trans*-activation of the E1B gene.

945-C1 cells did not contain detectable levels of cytoplasmic RNA complementary to pHE (Fig. 3-6B, lane 2). Therefore, although 945-C1 DNA contains pHE-hybridizing sequences (Fig. 3-3, lane 4; Fig. 3-4, lane 6), these appear not to be expressed as cytoplasmic mRNA. The E1B 175R protein is expressed in 945-C1 cells, but the coding sequences for this protein (~1,700-2,250 bp) are contained within the Ad5 *HindIII*-G fragment. Since pHE did not detect mRNA in 945-C1 cells, the E1B 175R protein must be translated from a mRNA that is truncated at or before the 2,799 bp *HindIII* site. This suggests that the Ad5 *HindIII*-G and -E sequences in 945-C1 DNA are not contiguous, and that the *HindIII* site dividing the 945-C1 10 kb and 5 kb fragments does not correspond to the viral site at 2,799 bp (see Fig. 3-5).

The E4 mRNAs were detected by hybridization with pHF, which hybridized to RNA from 945-C1 and 14b cells (Fig. 3-6C, lanes 2 and 3, respectively), but not from 637-4, 293, or HeLa cells (lanes 1, 4 and 5, respectively). The mRNA species detected in 945-C1 cells were of length 3.0 kb and 1.5 kb (lane 2). 945-C1 cells

Figure 3-8 Analysis of viral RNA in Ad5-transformed cells.

Cytoplasmic poly(A)⁺RNA (~1 μg/lane) from each cell line was size-fractionated by agarose gel electrophoresis, transferred to filters, and hybridized with pSH5 (panel A), pHE (panel B), or pHF (panel C). Lane 1, 637-4 cells; lane 2, 945-C1 cells; lane 3, 14b cells; lane 4, 203 cells; lane 5, HeLa cells. Lengths are given in kb.



have been shown to express an E4-encoded 14K protein (Downey *et al.* 1983; Rowe *et al.* 1984). However, the Ad5 E4 primary transcript is 2.8 kb in length, and is processed to form a series of mRNAs ranging from 2.4 kb to 0.6 kb, which suggests that the 3.0 kb mRNA detected in 045-C1 is a viral-cell hybrid. The Ad5 E4 transcription initiation site (~99 mu) may have been lost during integration, and the 3.0 kb mRNA may be transcribed from a cellular promoter in the upstream flanking DNA. Alternatively, the E4 transcription termination site may be lost, and transcription initiated at the viral E4 promoter may read through to the first termination site in the downstream flanking cellular sequences.

Ad5 E4 sequences are not integrated in 293 or 14b DNA, and so pHF should not hybridize to RNA from these cells. Accordingly, no E4 mRNA was detected in 293 cells (Fig. 3-6C, lane 4). However, pHF hybridized strongly to 14b mRNA at ~1.5 kb, and in a smear from ~1.5 kb ending in an intense signal at ~650 bp (lane 3). I have confirmed that pHF does not hybridize to 14b DNA (results not shown), so the presence of RNA hybridizing to this plasmid is puzzling. The intense signal at ~650 bp may represent degraded RNA. However, the filter shown in Figure 3-6C had been hybridized previously with a plasmid containing a mouse *HSP70* cDNA. The 14b RNA detected by this probe did not appear to be degraded (see Fig. 5-1, lane 3).

637-4 DNA contains the entire Ad5 *HindIII-F* fragment (Ruben *et al.* 1982; Fig. 3-2, lane 2). However, pHF did not hybridize to 637-4 RNA (Fig. 3-6C, lane 1), suggesting that the E4 region is transcriptionally inactive in these cells. This

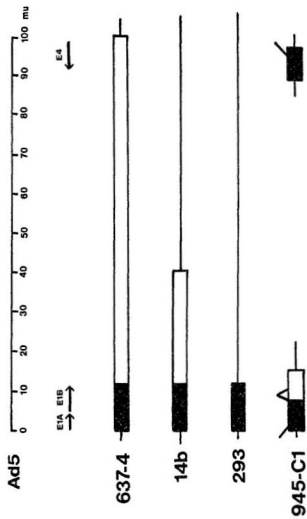
could be due to loss of the E4 promoter (~ 99 mu) during integration, or lack of *trans*-activation of the E4 promoter as a result of the *hr1* mutation.

3.2.3. Conclusions

I have analysed the viral DNA and RNA sequences present in the four adenovirus-transformed cell lines used in this study. I confirmed the pattern of the integrated viral DNA sequences shown previously for 637-4 cells, and demonstrated the *Hind*III digestion pattern of the viral sequences in 14b and 293 cells. I have also extended previous studies on 945-C1 DNA by more detailed restriction mapping of the viral DNA sequences present and their organization relative to one another. I confirmed that the E1 region of 14b, 293 and 637-4 cells and the E1A region of 945-C1 cells are expressed as cytoplasmic mRNA, and demonstrated that the E1B region of 945-C1 cells corresponding to the Ad5 *Hind*III-E fragment is not. I have also shown that the E4 sequences are expressed as cytoplasmic mRNA in 945-C1 cells, but are not expressed in 637-4 cells. A summary of these results is presented in Figure 3-7.

Figure 3-7 Viral sequences present in Ad5-transformed cells.

The top line represents the Ad5 genome, divided into 100 mu. Transcription units E1A, E1B, and E4 are shown. Boxes represent integrated viral DNA sequences, and lines represent the flanking cellular DNA sequences. Transcriptionally active regions are shown as solid areas. Carets indicate viral sequences that may either be contiguous or separated by cellular sequences.



Chapter 4

Chromatin Structure

4.1. Introduction

The chromatin structure of active genes has been shown to be preferentially sensitive to digestion with DNase I compared to inactive chromatin (section 1.1.4). The DNase I sensitive region is not confined to the transcription unit itself, but extends into the non-transcribed 5'- and 3'-flanking sequences. Thus, the boundaries of the DNase I sensitive region define a domain with a more "open" chromatin structure than inactive chromatin.

Transformation of cells by adenovirus involves integration of viral DNA into the host cell genome, and expression of the Ad E1 region. Sequences from other regions of the viral genome may be integrated, but their expression is not required for transformation (section 1.3). The integrated viral sequences are complexed with cellular histones and packaged into regularly repeating nucleosome particles typical of cellular chromatin (Flint & Weintraub, 1977; Dery *et al.* 1985). Since maintenance of the transformed phenotype requires transcription of the E1 sequences, this region can be considered a "model" active eukaryotic gene.

I have determined the DNase I sensitivities of the integrated Ad5 E1 genes

in the transformed cell lines 14b, 945-C1, 637-4 and 203. DNA from DNase I digested nuclei was digested with restriction enzymes and analysed by Southern blotting and hybridization with viral DNA probes. Sensitivity to DNase I was monitored by the disappearance of viral DNA-specific restriction fragments. I have also examined the DNase I sensitivities of additional viral sequences colinearly integrated with the E1 region, in order to determine if the DNase I sensitive conformation extends beyond E1 into the adjacent viral sequences. The DNase I sensitivity of the inactive human immunoglobulin heavy chain (IgH) gene joining (J) region provided a reference for inactive chromatin.

In addition to the overall DNase I sensitivity of the E1 region, I have also detected DNase I HS (hypersensitive) sites. These are relatively short regions of chromatin (~100-400 bp) in which the DNA is highly sensitive to cleavage by DNase I, and which are commonly found in the 5' regulatory regions of active and potentially active genes (section 1.1.6). Using the indirect end-labelling technique (Nedespasov & Georgiev, 1980; Wu, 1980), I have mapped these HS sites to the 5' regulatory region of the integrated E1A genes.

4.2. Materials and Methods

4.2.1. Preparation of DNase I digested chromatin

Cell monolayers were rinsed twice with ice-cold PBS, harvested by scraping with a rubber policeman, and washed twice in PBS. Cells were resuspended in reticulocyte standard buffer [RSB = 10 mM NaCl, 10 mM Tris-HCl (pH 7.4), 5 mM MgCl₂] containing 0.25 M sucrose, 0.5% NP-40, and 0.5 mM

phenylmethylsulphonyl fluoride (PMSF), and incubated at 0°C for 10 min with occasional vortexing. Lysis was monitored by phase contrast microscopy. Nuclei were pelleted by centrifugation at 200g for 5 min in an HB4 rotor at 4°C, and washed in RSBs (RSB containing 0.25 M sucrose). Nuclei were resuspended in RSBs at a concentration of 1 mg DNA/ml (1.2×10^8 nuclei/ml) and digested with DNase I (15 µg/ml) (Worthington) at 37°C for 1-10 min. DNase I digestion was terminated by the addition of EDTA to 25 mM, and DNA purified as in section 2.3.

4.2.2. DNase I digestion of DNA

Purified high molecular weight DNA (1 mg/ml) was digested with DNase I (150 ng/ml) in RSB at 37°C for 1-10 min. Digestion was terminated by the addition of EDTA to 25 mM, and DNA purified as in section 2.3.

4.2.3. Determination of extent of DNase I digestion

The extent of DNase I digestion was determined by calculating the mass average molecular weight (M_w) (Tanford, 1961). Purified DNA from DNase I digested chromatin and DNase I digested DNA was digested with *Hind*III, run on 0.8% agarose gels in ethidium bromide (0.5 µg/ml), and photographed under uv light. An example is shown in Figure 4-1. The photographic negatives were scanned using a Corning Model 750 scanning densitometer, and the scans divided into molecular weight intervals, as shown in Figure 4-2A. Molecular weight intervals were calculated from DNA molecular weight markers (not shown). M_w was calculated from the size distribution as described in Kunnath & Locker (1982). $M_w = \sum W_i M_i$, where W_i = mass fraction for interval i (mass of interval

i /total mass), and M_i = average molecular weight of interval i (molecular weight at mid-point of interval i).

Mass was measured by cutting out and weighing the area under the curve. The linear range of the photographic film was determined from standard plots of known amounts of DNA *versus* scan area, and only those scans within the linear range were used to calculate Mw .

4.2.4. Quantitation of DNase I sensitivity

DNA purified from DNase I digested chromatin was cleaved with restriction enzyme and analysed by Southern blotting and hybridization. DNase I sensitivity was monitored by the disappearance of specific restriction fragments with increasing DNase I digestion. Autoradiograms were scanned (at least twice), and for each fragment the area under the curve was measured to give intensity of hybridization (I). An example is shown in Figure 4-2B. For each fragment, the fraction of DNA remaining after DNase I digestion was expressed as I/I_0 , where I_0 = I (intensity of hybridization) for undigested DNA.

Standard plots of known amounts of DNA *versus* scan area showed that the response of the X-ray film was non-linear at low signal intensities. Therefore, the fraction of DNA remaining could not be obtained directly from the ratio of the scan areas. Instead, the standard plots of known amounts of DNA *versus* scan area were used to relate measured scan area to a known amount of DNA, and the fraction I/I_0 calculated from the amount of DNA corresponding to I divided by the amount of DNA corresponding to I_0 .

Figure 4-1 DNase I digested chromatin.

Nuclei were digested with DNase I at 37°C for the times indicated. DNA was purified, cleaved with *Hind*III, run on a 0.8% agarose gel containing ethidium bromide, and photographed under *uv* light.

DNase I

0 3 5 10 min

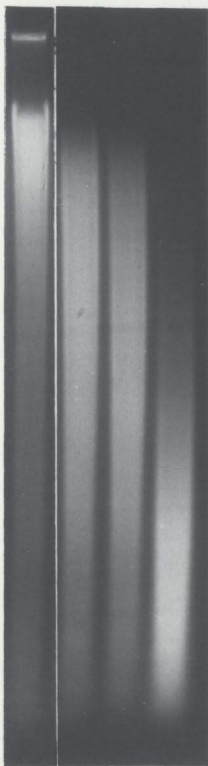
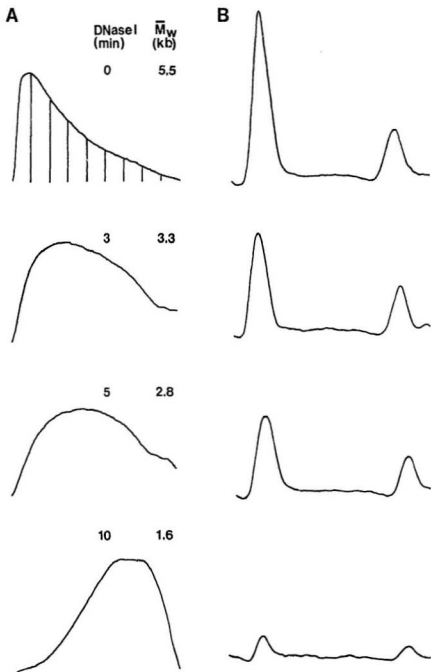


Figure 4-2 Quantitation of DNase I sensitivity.

A. The lanes shown in Figure 4-1 were scanned and divided into molecular weight intervals (as shown in top scan) to calculate Mw (kb), as described in section 4.2.3.

B. Scans of autoradiograms after Southern blotting and hybridization analysis of the DNA samples shown in **A.** The area under the curve was measured for each restriction fragment to give I.



I/I_0 was corrected for the amount of DNA in each lane. Gels were photographed before blotting, and the amount of DNA per lane determined by densitometric scanning.

For each restriction fragment I/I_0 was plotted against Mw and fitted to a straight line by linear regression analysis. A rate constant, k , for the rate of DNase I digestion, was defined as the slope of this line (Kunnath & Locker, 1985). The rate constant for a restriction fragment of the same length in naked DNA, k_d , was calculated in the same way. The sensitivity factor, S , was given by the ratio k/k_d (Kunnath & Locker, 1985).

4.3. Results

4.3.1. Rationale of the experiment

The structure of specific regions of chromatin has been analysed by sensitivity to DNase I. The rate of digestion of the DNA reflects the degree of chromatin condensation, with more "open" chromatin being digested faster than highly condensed chromatin.

Nuclei were isolated and digested with DNase I for various lengths of time. The DNA was purified and the Mw (mass average molecular weight) determined for each digest. Mw was used as a measure of the extent of DNase I digestion as this corresponds to the observed effect of DNase I digestion on the DNA, whereas DNase I digestion time corresponds to the expected effect.

The DNA was digested with restriction enzymes and analysed by Southern

blotting and hybridization with virus-specific probes. The DNase I sensitivity of the integrated viral sequences was monitored by the disappearance of virus-specific restriction fragments with increasing DNase I digestion, *i.e.* with decreasing *Mw*. The intensity of hybridization (*I*) was determined for each restriction fragment by densitometric scanning of the autoradiograms. The fraction of a particular restriction fragment remaining after DNase I digestion was obtained from the ratio I/I_0 , where $I_0 = I$ for undigested DNA. For each restriction fragment, I/I_0 was plotted against *Mw* to give a rate constant, *k*, defined as the slope of this plot (Kunnath & Locker, 1985).

Another factor that contributes to DNase I sensitivity is restriction fragment length: longer DNA molecules represent a larger target size and so are statistically more likely to be cleaved than shorter fragments. Therefore, the DNase I sensitivities of restriction fragments of different length cannot be compared unless this factor is taken into account. Purified cellular DNA was digested with DNase I for various lengths of time, and a rate constant for restriction fragments in naked DNA, k_d , determined as above. The ratio k/k_d was used to obtain a sensitivity factor, *S*, for each restriction fragment in chromatin independent of fragment length (Kunnath & Locker, 1985). Note that to obtain *Mw* values similar to those obtained for chromatin, purified DNA was digested with a 100-fold lower concentration of DNase I, *i.e.* 150 ng/ml instead of 15 μ g/ml (sections 4.2.1 and 4.2.2). Therefore, an *S* value of 1.0 does not imply that the chromatin is as sensitive to DNase I digestion as naked DNA.

4.3.2. DNase I sensitivity of naked DNA

The DNase I sensitivity of naked DNA was determined for several restriction fragments of different lengths. Purified DNA from 14b cells was digested with DNase I, cleaved with *Hind*III, and analysed by Southern blotting and hybridization with Ad5 DNA. This probe hybridized to fragments of length 7.8 kb (D'), 5.8 kb (G'), 5.3 kb (C), 3.7 kb (G*), 3.4 kb (E), and 2.1 kb (H) (Fig. 4-3). The k_d values were calculated for each of these fragments (Fig. 4-4). Fragments G' and C migrated too close together for their scan areas to be measured separately. Instead, their combined area was measured, and the length taken as 5.6 kb. The k_d values decreased with decreasing fragment length, from $k_d = 0.23$ for fragment D', to $k_d = 0.19$ for fragment H. The k_d values were plotted against fragment length, and a straight line fitted by linear regression analysis (Fig. 4-5). This graph was used as a standard to obtain k_d values for the other restriction fragments analysed.

4.3.3. DNase I sensitivity of chromatin

4.3.3.1. 293 cells

The DNase I sensitivity of the integrated Ad5 sequences in 293 cells was determined. This cell line contains ~5 copies of the left-end ~12 mu of the Ad5 genome per diploid amount of cell DNA, integrated at a unique site in the host cell genome (Aiello *et al.* 1979; Spector, 1983; section 3.2.1, Fig. 3-7). 293 cell nuclei were digested with DNase I for various lengths of time, and the purified DNA cleaved with *Sac*I. *Sac*I cleaves Ad5 E1 sequences at 4.8 mu and 10.0 mu, allowing the E1A and E1B transcription units to be analysed separately. (For

Figure 4-3 DNase I digested 14b cell DNA.

A. Purified DNA from 14b cells was digested with DNase I for various lengths of time, cleaved with *Hind*III, and run on a 0.8% agarose gel. The extent of DNase I digestion is expressed as *Mw*, which was calculated as described in section 4.2.3.

B. The DNA shown in **A** was transferred to a filter by Southern blotting and probed with Ad5 DNA.

14b DNA/HindIII

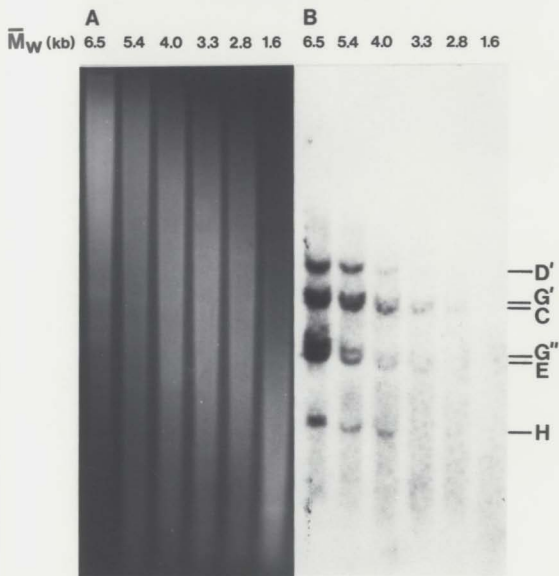
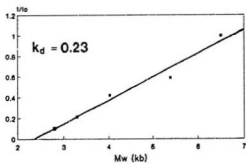


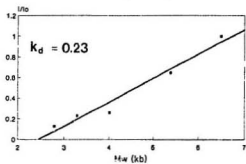
Figure 4-4 DNase I sensitivity of Ad5 sequences in 14b cell DNA.

I/I_0 was calculated for each of the Ad5-specific *Hind*III fragments in 14b cell DNA by densitometric scanning of the autoradiogram shown in Figure 4-3B as described in section 4.2.4. I/I_0 was plotted against Mw , a straight line fitted by linear regression analysis, and the slope calculated to give k_d .

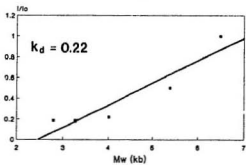
14b DNA/HindIII
D' (7.8 kb)



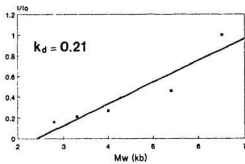
G'/C (5.6 kb)



G'' (3.7 kb)



14b DNA/HindIII E (3.4 kb)



H (2.1 kb)

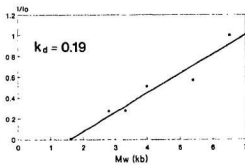
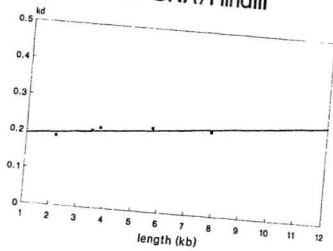


Figure 4-5 DNase I sensitivity of different length DNA fragments.

The k_d values of the 14b cell Ad5-specific restriction fragments were plotted against fragment length. A straight line was fitted by linear regression analysis.

14b DNA/HindIII



maps of the Ad5 genome and the probes used in these studies refer to Figure 3-1.) The DNA was run on an agarose gel, transferred to a filter and hybridized with pXC1 (0-15.5 mu). This probe hybridized to three *SacI* fragments, of 7.0 kb (A), 4.5 kb (B), and 1.9 kb (C) (Fig. 4-6A). To determine the origin of these fragments, they were hybridized with the left-end-specific probe pSH5. This probe hybridized to fragment A (lane M), indicating that this fragment contains sequences from the left-end terminal Ad5 *SacI*-I fragment (0-4.8 mu), i.e. the E1A transcription unit, joined to cell DNA. Based on its molecular weight, fragment C corresponds to the Ad5 *SacI*-G fragment (4.8-10.0 mu), which contains most of the E1B transcription unit. Fragment B, therefore, contains sequences from the Ad5 *SacI*-F fragment (10.0-15.4 mu), containing the 3'-terminal ~400 bp of the E1B transcription unit, joined to cell DNA.

The DNase I sensitivity of each of these fragments in chromatin was determined from plots of I/I_0 versus Mw (Fig. 4-7). The k values for fragments A, B, and C = 0.20, 0.19, and 0.14, respectively. From the standard plot of k_d versus fragment length (Fig. 4-5), for fragments of length 7.0 kb, 4.5 kb, and 1.9 kb, k_d = 0.23, 0.22, and 0.20, respectively. Therefore, the sensitivity factor, S , for A = 0.9, for B = 0.9, and for C = 0.7.

The transcriptionally inactive Igh gene J region was analysed to compare the DNase I sensitivity of inactive chromatin. The filter shown in Figure 4-6A was washed to remove pXC1, and re-probed with pJH. This probe hybridized to two *SacI* fragments, of 12 kb (A) and 3.9 kb (B) (Fig. 4-6B). For fragment A, k = 0.09 and k_d = 0.26, giving S = 0.3, and for fragment B, k = 0.09 and k_d =

Figure 4-6 DNase I digested 293 chromatin.

A. 293 cell nuclei were digested with DNase I for various lengths of time to give $Mw = 6.1$ kb, 3.7 kb, *etc.* DNA was purified, cleaved with *SacI*, and analysed by Southern blotting and hybridization with pXC1. Lane M (marker), 293 cell DNA probed with pSH5.

B. The filter shown in A was washed to remove pXC1, and re-probed with pJH.

293 chromatin/SacI

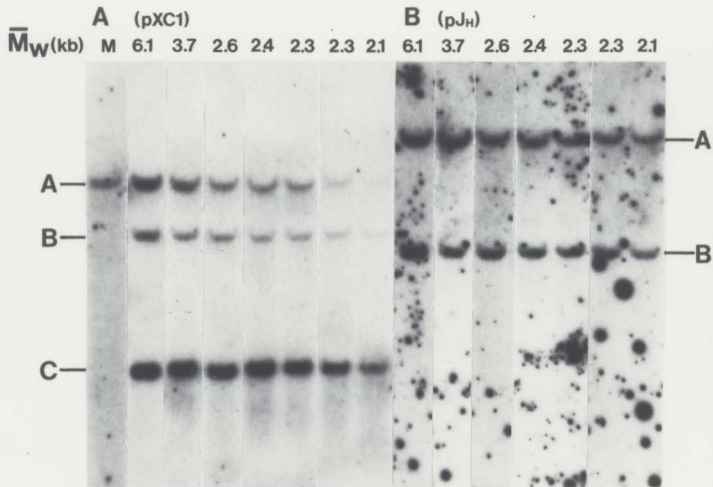
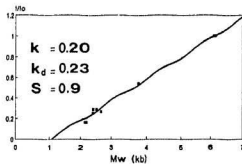


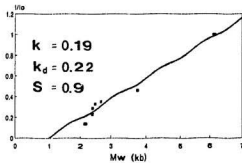
Figure 4-7 DNase I sensitivity of Ad5 E1 sequences in 293 chromatin.

I/I_0 was calculated for each of the Ad5-specific *SacI* fragments in 293 cells by densitometric scanning of the autoradiogram shown in Figure 4-6 as described in section 4.2.4. I/I_0 was plotted against Mw , and k calculated from the slope of the best-fit straight line. k_d values were obtained from Figure 4-5. $S = k/k_d$.

293 chromatin/Sacl (pXC1)
A (7.0 kb)



B (4.5 kb)



C (1.9 kb)

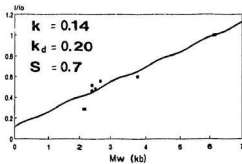
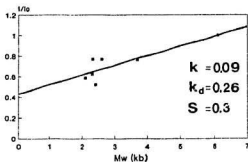


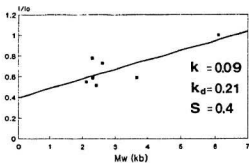
Figure 4-8 DNase I sensitivity of the IgH gene J region in 293 chromatin.

Analysis of Figure 4-6 gave k , k_d , and S values for the J-specific *SacI* fragments in 293 cells as described for Figure 4-7.

293 chromatin/SacI (pJH)
A (12 kb)



B (3.9 kb)



0.21, giving $S = 0.4$ (Fig. 4-8). In 293 cells, therefore, $S = 0.7$ or greater for the transcriptionally active E1A and E1B genes, whereas $S = 0.4$ or less for the inactive IgH gene J region. A summary of these results is presented in Figure 4-18.

4.3.3.2. 14b cells

Cell line 14b contains ~ 5.5 copies of the left-end ~ 40 mu of the Ad5 genome per diploid amount of DNA (Sambrook *et al.* 1975; Flint *et al.* 1976), probably at two distinct integration sites in the host cell genome (section 3.2.1). 14b cell nuclei were digested with DNase I, the DNA purified and cleaved with *Hind*III or *Sac*I, and the sensitivity of the virus-specific restriction fragments determined.

*Hind*III generated six virus-specific restriction fragments (Fig. 4-9A). The DNase I sensitivity of the 5.8 kb (G') and 5.3 kb (C) could not be analysed, as these fragments migrated too close together to allow their scan areas to be measured separately. Therefore, the DNase I sensitivities of the two left-end junction fragments, G' and G*, could not be compared. The k values for the remaining four *Hind*III fragments were determined (Fig. 4-10), and their k_d values obtained from Figure 4-5, to give $S = 0.9$ for fragment D' and $S = 1.1$ for fragments G*, E, and H. Therefore, the transcriptionally active E1 region, *i.e.* fragments G* and E, exhibits a DNase I sensitivity typical of transcriptionally active chromatin ($S = >0.7$). In addition, the *Hind*III-H (31.7-37.3 mu) and -D' (37.5-cell DNA) fragments, which are transcriptionally inactive (Flint *et al.* 1976; Binger *et al.* 1982), exhibit a DNase I sensitivity similar to that of the expressed

E1 region ($S = 1.1$ and 0.9 , respectively). This suggests that the DNase I sensitive conformation of the active E1 region extends into the adjacent non-transcribed viral sequences. (Summarized in Fig. 4-18.)

The E1A and E1B genes in 14b were analysed separately by digestion with *SacI* and hybridization with pXC1. This probe hybridized to three *SacI* fragments of 4.3 kb (A), 2.0 kb (B), and 1.9 kb (C) (Fig. 4-9B). The left-end-specific probe pSH5 hybridized to fragments A and B (see Fig. 4-21), indicating that these two fragments correspond to the different integration sites of the E1A-containing left-end terminal Ad5 *SacI*-I (0-4.8 mu) fragment joined to cell DNA. Unfortunately, the smaller of these co-migrated with the Ad5 *SacI*-F fragment (10.0-15.4 mu), containing the 3'-terminal ~400 bp of the E1B gene. Once again, therefore, the DNase I sensitivity of the two E1A-cell DNA junction fragments could not be directly compared. As in 293 cells, fragment C corresponds to the Ad5 *SacI*-G fragment (4.8-10.0 mu), containing most of the E1B gene.

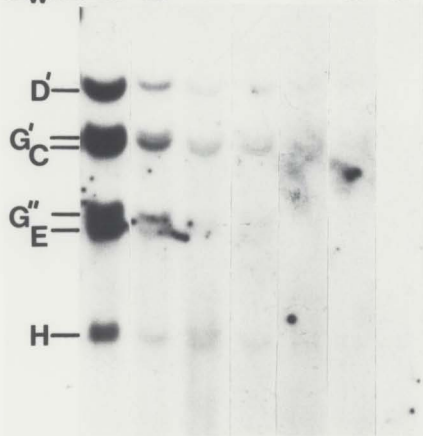
The k values for these fragments were determined and their DNase I sensitivities calculated (Fig. 4-11). For fragment A, containing the larger of the left-end Ad5 *SacI*-I-cell DNA junction fragments, $S = 1.6$. For fragment B, containing the smaller of the left-end junction fragments and the Ad5 *SacI*-F fragment, and for fragment C, containing the Ad5 *SacI*-G fragment, $S = 1.2$. These results are in agreement with the sensitivities of the *HindIII* fragments from this region ($S = 1.1$ for *HindIII*-G* and -E).

Figure 4-9 DNase I digested 14b chromatin.

14b cell nuclei were digested with DNase I for various lengths of time. DNA was purified, cleaved with *Hind*III, and probed with Ad5 DNA (A), or cleaved with *Sac*I and probed with pXC1 (B).

A 14b chromatin/HindIII

\bar{M}_W (kb) 5.5 2.9 1.8 1.4 1.4 1.3 1.2



B 14b chromatin/SacI

5.5 4.4 4.0 3.3 2.9 1.4

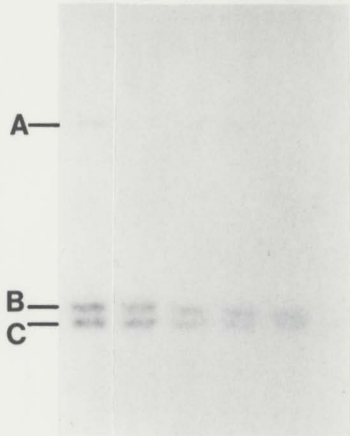
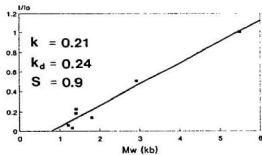


Figure 4-10 DNase I sensitivity of Ad5 sequences in 14b chromatin.

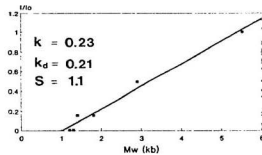
Analysis of Figure 4-9A gave k , k_d , and S values as described for Figure 4-7.

14b chromatin/HindIII

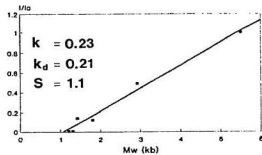
D' (7.8 kb)



E (3.4 kb)



G'' (3.7 kb)



H (2.1 kb)

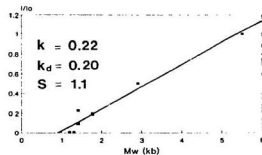
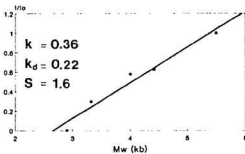


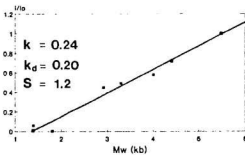
Figure 4-11 DNase I sensitivity of Ad5 E1 sequences in 14b chromatin.

Analysis of Figure 4-9B gave k , k_d , and S values as described for Figure 4-7.

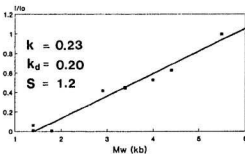
14b chromatin/SacI
A (4.3 kb)



B (2.0 kb)



C (1.9 kb)



4.3.3.3. 637-4 cells

Cell line 637-4 contains one copy of the entire Ad5 genome colinearly integrated at a unique site in the host cell genome (Ruben *et al.* 1982; section 3.2.1). The DNase I sensitivity of the integrated *HindIII*-A (8.3 kb), -D (4.6 kb), -E (3.4 kb), and -F (2.9 kb) fragments were analysed (Fig. 4-12A and B). The filter shown in panel B was re-probed with pSH5 in order to analyse the DNase I sensitivity of the left-end virus-cell junction fragment G' (4.3 kb) (panel C).

For the G' fragment, the k value of the best-fit straight line drawn through the plot of I/I_0 versus Mw was 0.43, giving $S = 2.0$ (Fig. 4-13a). However, this plot described a curve rather than a straight line, and for the initial part of this curve $k = 0.93$, giving $S = 4.2$ (Fig. 4-13b). The shape of this plot may be explained by the presence of a DNase I HS site in the G' fragment. As this fragment disappeared with increasing DNase I digestion, a new ~ 2.35 kb sub-band appeared (Fig. 4-12, G'1), suggesting the presence of an HS site in G'. (I have confirmed that G'1 is derived from the G' fragment, see section 4.3.4.3, Fig. 4-20.) The kinetics of DNase I digestion at this site may result in a curve, whereas digestion of chromatin domains which lack HS sites results in a straight line.

The amounts of DNA remaining in fragments G' and G'1 were added together, and I/I_0 plotted against Mw (Fig. 4-13c). In this case $k = 0.34$ and $S = 1.5$. This plot also described a curve, with $k = 0.84$ and $S = 3.8$ for the initial part of the curve (Fig. 4-13d).

Figure 4-12 DNase I digested 637-4 chromatin (*Hind*III).

637-4 cell nuclei were digested with DNase I for various lengths of time. DNA was purified, cleaved with *Hind*III, and probed with Ad5 DNA (**A** and **B**). The filter shown in **B** was washed and re-probed with pSI15 (**C**). [Note: in panel **A**, the *Mw* 6.3 kb lane contained more DNA than the *Mw* 4.4 kb, 3.3 kb, and 3.1 kb lanes. $1/I_0$ (Fig. 4-13) was corrected for the amount of DNA per lane.]

637-4 chromatin/HindIII

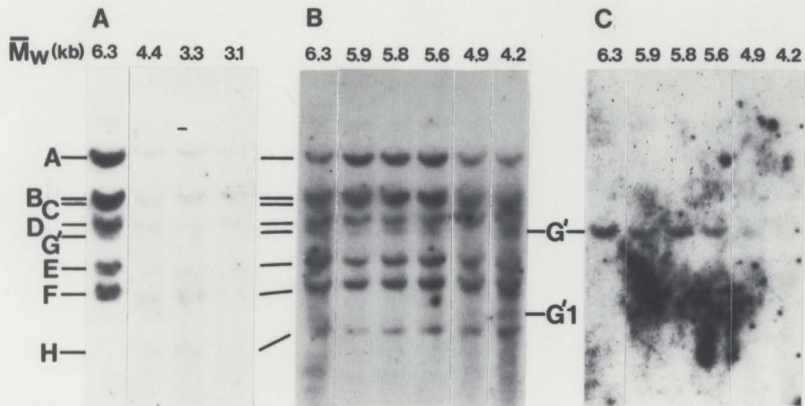
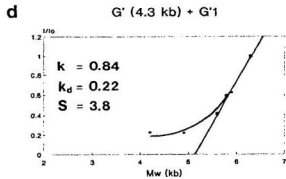
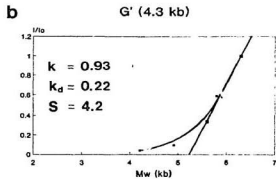
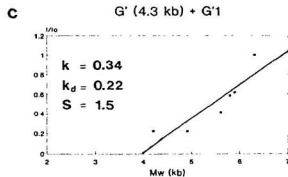
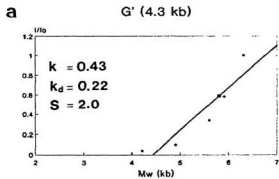


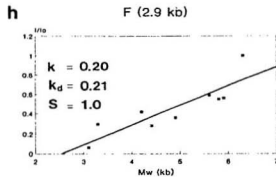
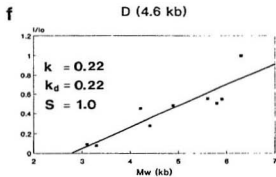
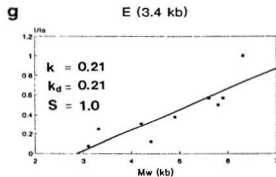
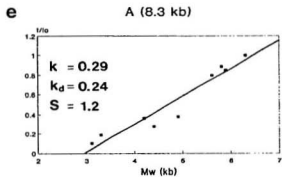
Figure 4-13 DNase I sensitivity of Ad5 sequences in 637-4 chromatin.

Analysis of Figure 4-12 gave k , k_d , and S values as described for Figure 4-7. For fragments G' (a) and G' + G'1 (c), the plots were re-drawn as best-fit curves, and k calculated for the initial part of the curve (b and d, respectively).

637-4 chromatin/HindIII



637-4 chromatin/HindIII



As shown in Figure 4-13e-h, $S = 1.2$ for the *Hind*III-A fragment, and $S = 1.0$ for the *Hind*III-D, -E, and -F fragments. Therefore, DNase I sensitivities typical of active chromatin were displayed not only by the *Hind*III-E fragment (7.7-17.1 mu), which contains the 3'-terminal half of the transcribed E1B gene, but also by the transcriptionally inactive *Hind*III-D (37.5-50.1 mu), -A (50.1-73.2 mu), and -F (89.1-97.1 mu) fragments. These results suggest that the DNase I sensitive conformation extends the entire length of the integrated Ad5 genome, *i.e.* ~ 36 kb. (Summarized in Fig. 4-18.)

The E1A and E1B genes in 637-4 were analysed separately by digestion with *Sac*I and hybridization with pXC1. This probe hybridized to three *Sac*I fragments of 2.7 kb (A), 2.0 kb (B), and 1.9 kb (C) (Fig. 4-14). The left-end-specific probe pSH5 hybridized to fragment A (lane M), indicating that this fragment corresponds to the E1A-containing left-end terminal Ad5 *Sac*I fragment (0-4.8 mu) joined to cell DNA. Based on their molecular weights, fragment C corresponds to the Ad5 *Sac*I-G fragment (4.8-10.0 mu), containing most of the E1B gene, and fragment B corresponds to the Ad5 *Sac*I-F fragment (10.0-15.4 mu), containing the 3'-terminal ~ 400 bp of the E1B gene.

For the *Sac*I-A fragment, the k value for the best-fit straight line through the plot of I/I_0 versus Mw was 0.36, giving $S = 1.8$ (Fig. 4-15a). However, as for the *Hind*III-G' fragment, this plot described a curve rather than a straight line, with $k = 1.29$ and $S = 6.5$ for the initial part of the curve (Fig. 4-15b). As the *Sac*I-A fragment disappeared with increasing DNase I digestion, new sub-bands appeared at 1.5 kb (A1), 1.3 kb (A2), and 1.1 kb (A3) (Fig. 4-14), suggesting the

Figure 4-14 DNase I digested 637-4 chromatin (*SacI*).

637-4 cell nuclei were digested with DNase I for various lengths of time. DNA was purified, cleaved with *SacI*, and probed with pXC1. Lane M, 637-4 cell DNA probed with pSH5.

637-4 chromatin/SacI

\bar{M}_W (kb) M 6.3 5.9 5.8 5.6 4.9 4.2 6.3 4.4 3.3 3.1

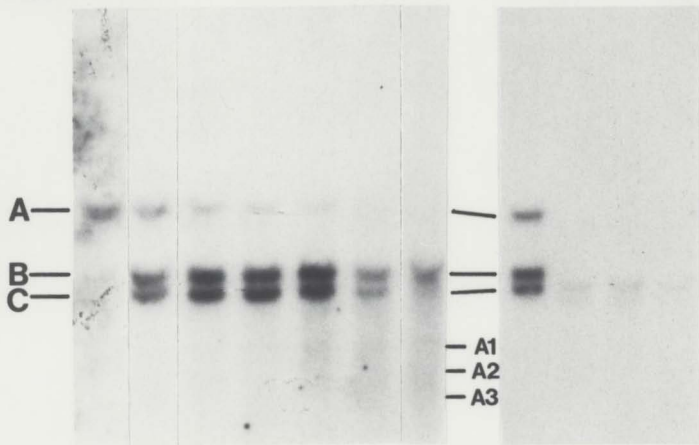
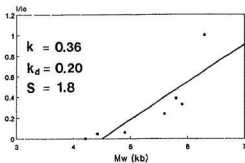


Figure 4-15 DNase I sensitivity of Ad5 E1 sequences in 637-4 chromatin.

Analysis of Figure 4-14 gave k , k_d , and S values as described for Figure 4-7. For fragments A (a) and A + A1, A2 & A3 (c), the plots were re-drawn as best-fit curves, and k calculated for the initial part of the curve (b and d, respectively).

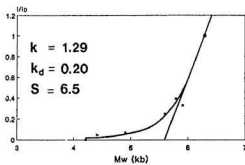
637-4 chromatin/SacI
A (2.7 kb)

a



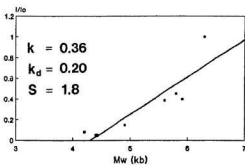
b

A (2.7 kb)

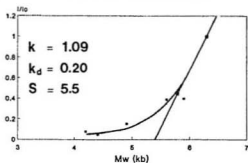


c

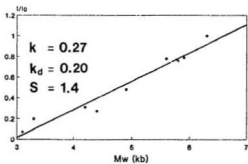
A (2.7 kb) + A1, A2 & A3



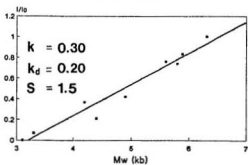
d 637-4 chromatin/SacI
A (2.7 kb) + A1, A2 & A3



e B (2.0 kb)



f C (1.9 kb)



presence of DNase I HS sites in this fragment. (I have confirmed that these subbands are derived from fragment A, see section 4.3.4.3, Fig. 4-20). The amounts of DNA remaining in fragments A, A1, A2, and A3 were added together and I/I_0 plotted against Mw (Fig. 4-15c). The slope of the best-fit straight line drawn through this plot remained the same as before ($k = 0.36$, $S = 1.8$). This plot also described a curve, with $k = 1.09$ and $S = 5.5$ for the initial part of the curve (Fig. 4-15d).

For fragment B, containing the Ad5 *SacI*-F fragment, $S = 1.4$, and for fragment C, containing the Ad5 *SacI*-G fragment, $S = 1.5$, (Fig. 4-15e and f, respectively), indicating that the DNase I sensitivity of the E1B region is typical for active chromatin. These results are in agreement with the DNase I sensitivity of the *HindIII* fragment in this region ($S = 1.0$ for *HindIII*-E, Fig. 4-13g).

4.3.3.4. 945-C1 cells

Cell line 945-C1 contains sequences from the Ad5 *HindIII*-G (0-7.7 mu), -E (7.7-17.1 mu), -F (89.1-97.1 mu), and -I (97.1-100 mu) fragments, at one copy per diploid amount of cell DNA (Downey *et al.* 1983; Rowe *et al.* 1984). Ad5 DNA hybridized to two 945-C1 *HindIII* fragments of 10 kb (A) and 5.0 kb (B) (Fig. 4-16). Fragment A contains sequences from the Ad5 *HindIII*-G and -F fragments, and so contains the E1A gene, the 5'-terminal half of the E1B gene, and the E4 gene, whereas fragment B contains sequences from the Ad5 *HindIII*-E fragment, and so contains the 3'-terminal half of the E1B gene (section 3.2.1, Fig. 3-5).

For fragment A, the slope of the best-fit straight line through the plot of I/I_0 versus Mw was 0.46, giving $S = 1.8$ (Fig. 4-17a). However, this plot

Figure 4-16 DNase I digested 945-C1 chromatin.

945-C1 cell nuclei were digested with DNase I for various lengths of time. DNA was purified, cleaved with *Hind*III, and probed with Ad5 DNA.

945-C1 chromatin/HindIII

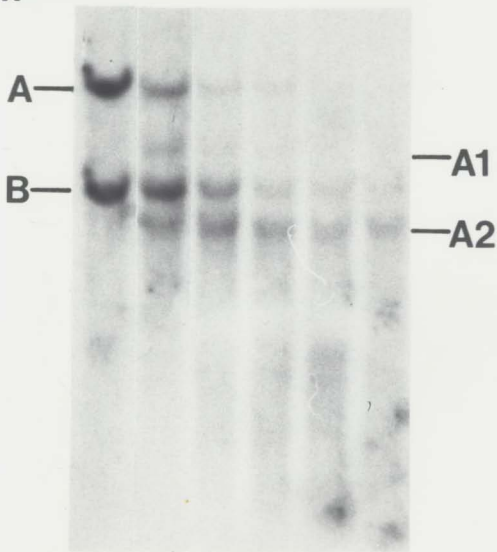
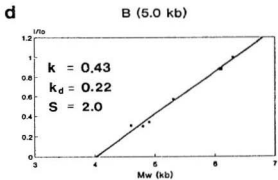
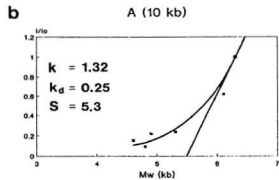
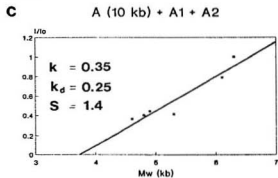
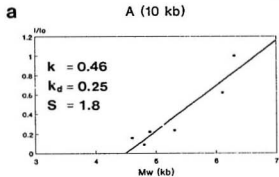
 \bar{M}_W (kb) 6.3 6.1 5.3 4.9 4.8 4.6

Figure 4-17 DNase I sensitivity of Ad5 sequences in 945-C1 chromatin.

Analysis of Figure 4-16 gave k , k_d , and S values as described for Figure 4-7. For fragment A (a), the plot was re-drawn as a best-fit curve, and k calculated for the initial part of the curve (b).

945-C1 chromatin/HindIII



described a curve rather than a straight line, with $k = 1.32$ and $S = 5.3$ for the initial part of the curve (Fig. 4-17b). DNase I digestion generated new sub-bands at 6.5 kb (A1) and 4.1 kb (A2) (Fig. 4-16), suggesting the presence of DNase I HS sites in fragment A. (I have confirmed that these sub-bands are derived from fragment A, see section 4.3.4.5, Fig. 4-22).

The DNA remaining in fragments A, A1, and A2 were added together, and I/I_0 plotted against Mw . In contrast to that for fragment A alone, this plot was linear, with $k = 0.35$ and $S = 1.4$ (Fig. 4-17c).

For fragment B, $k = 0.43$ and $S = 2.0$ (Fig. 4-17d). This fragment contains sequences from the Ad5 *HindIII*-E fragment, which are not expressed as mRNA in 945-C1 cells (section 3.2.2, Fig. 3-6B, lane 2). However, the DNase I sensitivity of this fragment is similar to that of the transcribed fragment A. (Summarized in Fig. 4-18.)

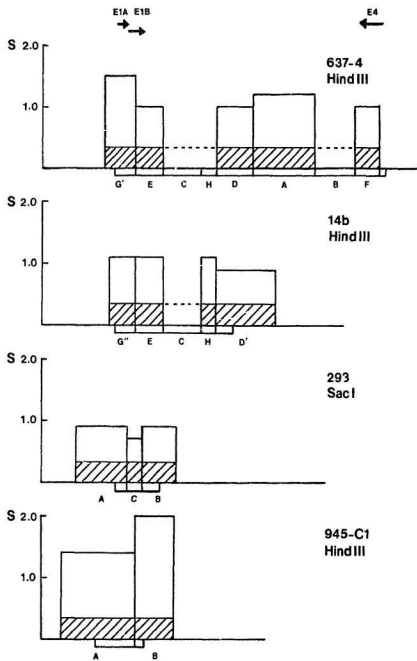
4.3.4. DNase I hypersensitive sites

4.3.4.1. Rationale of the experiment

In several of the experiments described above, DNase I digestion of chromatin generated discrete sub-bands, *e.g.* in 637-4 cells (Figs. 4-12 and 4-14) and 945-C1 cells (Fig. 4-16). The increase in intensity of these new sub-bands appeared to parallel the decrease in that of the E1A-containing left-end terminal restriction fragments, suggesting the presence of DNase I HS sites in this region. In order to confirm that the sub-bands were in fact derived from the left-end terminal fragments, they were hybridized with the left-end-specific probe pSH5.

Figure 4-18 DNase I sensitivity of the integrated viral sequences in Ad5-transformed cell lines.

S values are plotted on the y-axis, and the virus-specific restriction fragments positioned along the x-axis, so that the corresponding regions of the Ad5 genome are in register. Open areas, integrated Ad5 DNA sequences; straight lines, flanking cellular DNA sequences. The positions of the E1A, E1B, and E4 transcription units are indicated. For inactive chromatin, $S = 0.35$ (dotted lines and hatched areas), the mean of the S values for the IgH gene J region *Hind*III fragments.



Hybridization with this probe also allowed the HS sites to be mapped by the indirect end-labelling technique (Nedespasov & Georgiev, 1980; Wu, 1980) as follows. The Ad5 fragment in pSH5 (2.8-4.3 mu) hybridizes to the right end of the Ad5 *SacI*-I fragment (0-4.8 mu, Fig. 3-1), and so "end-labels" the viral *SacI*-I-cell DNA junction fragment (*e.g.* see Fig. 4-10B). This probe also detects sub-fragments bounded on the right by the *SacI* site at 4.8 mu (1771 bp), and on the left by a DNase I HS site. The length of the sub-fragment, therefore, defines the position of the HS site relative to the 1771 bp *SacI* site. These sites were also mapped relative to the *HindIII* site at 7.7 mu (2790 bp) using pSH5. Although not strictly end-labelling, this was done to confirm the position of HS sites mapped relative to the *SacI* site.

4.3.4.2. 293 cells

When 293 chromatin was digested with DNase I and analysed by *SacI* digestion and hybridization with pXC1, discrete sub-bands with faster mobility than fragment C were faintly visible (Fig. 4-6). In order to map the position of the HS sites giving rise to these sub-bands, they were hybridized with pSH5. This probe detected the native-sized junction fragment of 7.0 kb (A), plus six discrete sub-bands ranging in length from 4.4-1.3 kb (Fig. 4-19A, lanes 2 and 3, sub-bands 1-6). No sub-bands were detected in purified 293 DNA digested with DNase I to a similar extent, *i.e.* similar *Mw* (lane 1), indicating that cleavage was not due to specific recognition by DNase I of the DNA sequence at the HS sites. [Note that although purified DNA was digested to a similar *Mw* as chromatin, this required a 100-fold lower concentration of DNase I (sections 4.2.1 and 4.2.2). Therefore, the absence of cleavage at these sites in purified DNA does not imply that these

sequences are more resistant to DNase I in naked DNA compared to the same sequences in chromatin.]

The positions of the DNase I HS sites in chromatin giving rise to these sub-bands were mapped relative to the *SacI* site at 4.8 mu (1771 bp) on the Ad5 genome. For example, the 4.4 kb sub-band (Fig. 4-19A, lane 3, sub-band 1) was generated by DNase I cleavage at an HS site 4.4 kb to the left of the 1771 bp *SacI* site, *i.e.* in the flanking cellular DNA, ~ 2.63 kb (4.4 - 1.77 kb) from the left-end viral DNA integration site (Fig. 4-19B, *SacI* site 1). The 3.25 kb and 3.0 kb sub-bands (lane 2, sub-bands 2 and 3, respectively) were generated by DNase I cleavage at cellular HS sites ~ 1.48 kb (3.25 - 1.77 kb) and ~ 1.23 kb (3.0 - 1.77 kb) from the left-end integration site (*SacI* sites 2 and 3, respectively). However, these sub-bands were relatively faint, and sub-band 1 was not seen in lane 2, while sub-bands 2 and 3 were not seen in lane 3. Lanes 2 and 3 contain DNA from two independent DNase I digests of 293 chromatin (see below).

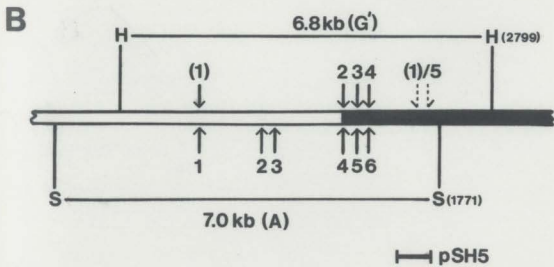
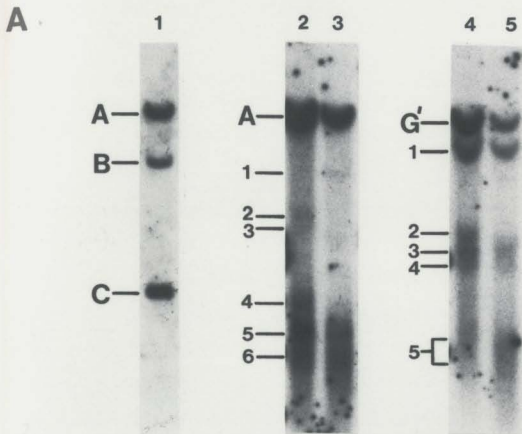
More intense sub-bands of length 1.5 kb and 1.3 kb (Fig. 4-19A, sub-bands 5 and 6, respectively) were detected in lanes 2 and 3, and a sub-band of length 1.77 kb (sub-band 4) was detected in lane 2, but not in lane 3. Sub-band 6 (1.3 kb), for example, was generated by DNase I cleavage at an HS site 1.3 kb to the left of the 1771 bp *SacI* site, *i.e.* at position 470 bp (1.77 - 1.3 kb) on the Ad5 genome (Fig. 4-19B, *SacI* site 6). Similarly, sub-bands 4 and 5 were generated by DNase I cleavage at positions ~ 1 bp (1.77 - 1.77 kb) and 270 bp (1.77 - 1.5 kb) on the Ad5 genome (*SacI* sites 4 and 5, respectively). The sample in lane 3 was digested with DNase I for a longer time than that in lane 2. Therefore, DNase I cleavage

Figure 4-10 DNase I HS sites in 293 E1A 5' region.

A. DNase I digested chromatin from 293 cells was cleaved with *SacI* (lanes 2 and 3) or *HindIII* (lanes 4 and 5) and probed with pSH5. Lane 1, DNase I digested DNA cleaved with *SacI* and probed with pXC1.

B. Position of DNase I HS sites (arrows) generating sub-bands detected in A. HS sites mapped relative to the 1771 bp *SacI* site are shown below the DNA (*SacI* sites 1-6), and HS sites mapped relative to the 2799 bp *HindIII* site are shown above the DNA (*HindIII* sites 1-5). The two possible positions of the *HindIII* site 1 are shown in parentheses. Solid region, integrated Ad5 sequences; open region, flanking cellular sequences; H, *HindIII* sites; S, *SacI* sites. The positions of the viral restriction sites are given in bp.

293



may occur initially at site 4, but with increasing DNase I digestion, cleavage at sites 5 and 6 may process sub-band 4 to sub-bands 5 and 6. A summary of these HS sites and their positions relative to the E1A transcription initiation site is given in Figure 4-23.

In order to confirm the position of the HS sites, these were also mapped relative to the Ad5 *HindIII* site at 7.7 mu (2799 bp). A portion of the DNase I digested chromatin samples shown in Figure 4-19A, lanes 2 and 3 were digested with *HindIII* instead of *SacI*, and hybridized with pSH5 (lanes 4 and 5, respectively). This probe hybridized to the native-sized junction fragment of 6.8 kb (G'), plus five sub-bands ranging in length from 5.4-1.4 kb (sub-bands 1-5). The 5.4 kb sub-band (lanes 4 and 5, sub-band 1) may have been generated by DNase I cleavage at an HS site 5.4 kb to the left of the 2799 bp *HindIII* site, *i.e.* in the flanking cellular DNA, ~2.6 kb (5.4 - 2.8 kb) from the left-end viral DNA integration site, suggesting that this site corresponds to that generating the *SacI* sub-band 1 [Fig. 4-19B, *HindIII* site (1)]. However, the *HindIII* sub-band 1 was very intense in both lanes 4 and 5, whereas the *SacI* sub-band 1 was not visible in lane 2 and was relatively weak in lane 3. Alternatively, the *HindIII* sub-band 1 may have been generated by DNase I cleavage at an HS site 5.4 kb to the right of the left-end *HindIII* site, *i.e.* at position 1,400 bp on the Ad5 genome (5.4 - 4.0 kb flanking cellular DNA) [*HindIII* site (1)/5]. In this case, pSH5 should also hybridize to the reciprocal 1.4 kb fragment. This may correspond to sub-band 5, a rather diffuse sub-band of ~1.4-1.2 kb, suggesting DNase I cleavage at HS sites around 1,400-1,600 bp on the Ad5 genome [*HindIII* site (1)/5].

The three sub-bands of length 2.8 kb, 2.52 kb, and 2.33 kb (Fig. 4-19A, lanes 4 and 5, sub-bands 2, 3, and 4, respectively) were generated by DNase I cleavage at positions ~ 1 bp (2.8 - 2.8 kb), 280 bp (2.8 - 2.52 kb), and 470 bp (2.8 - 2.33 kb) on the Ad5 genome (Fig. 4-19B, *HindIII* sites 2, 3, and 4, respectively). These sites correspond closely to sites 4, 5 and 6 mapped relative to the *SacI* site. As in lanes 2 and 3, the sample in lane 5 was digested with DNase I for a longer time than that in lane 4. Accordingly, the *HindIII* sub-band 2 was not visible in lane 5, similar to the corresponding *SacI* sub-band 4 in lane 3.

4.3.4.3. 637-4 cells

When 637-4 chromatin was digested with DNase I and analysed by *HindIII* digestion and hybridization with Ad5 DNA, a discrete sub-band of ~ 2.35 kb (G'1) was detected (Fig. 4-12). When this chromatin was analysed by *SacI* digestion and hybridization with pXC1, three sub-bands were detected (Fig. 4-14, A1, A2, and A3). In order to map the position of the DNase I HS sites giving rise to these sub-bands, they were analysed further by digestion with *SacI* or *HindIII* and hybridization with pSH5.

In the *SacI* digest, pSH5 hybridized with the native-sized junction fragment of 2.7 kb (A), plus three discrete sub-bands of 1.5 kb, 1.3 kb, and 1.1 kb (Fig. 4-20A, lanes 2 and 3, sub-bands 1, 2, and 3, respectively). These are equivalent to A1, A2, and A3 in Fig. 4-12). No sub-bands were detected when purified 637-4 DNA was digested with DNase I to a similar extent (lane 1). Sub-bands 1-3 were generated by DNase I cleavage at positions 270 bp (1.77 - 1.5 kb), 470 bp (1.77 - 1.3 kb), and 670 bp (1.77 - 1.1 kb) on the Ad5 genome (Fig. 4-20B, *SacI* sites 1, 2,

and 3, respectively). Sub-band 2 was the most intense in both lanes 2 and 3, implying that site 2 (470 bp) is the most sensitive of the three. In the sample digested with DNase I for the shorter time (lane 2), sub-band 1 was more intense than sub-band 3, whereas the reverse was true in the more digested sample (lane 3). This suggests that site 1 is initially digested faster than site 3, but with increasing DNase I digestion, cleavage at site 3 processes sub-bands 1 and 2 to sub-band 3.

In the *HindIII* digest, pSH5 hybridized to the native-sized junction fragment of 4.3 kb (G'), plus two discrete sub-bands of length 3.1 kb and 2.33 kb (Fig. 4-20A, lane 4, sub-bands 1 and 2, respectively). Sub-band 1 may have been generated by DNase I cleavage at an HS site 3.1 kb to the left of the 2799 bp *HindIII* site, *i.e.* in the flanking cellular DNA, ~ 300 bp (3.1 - 2.8 kb) from the left-end viral DNA integration site (Fig. 4-20B, site not shown). However, in the *SacI* digest, DNase I cleavage at this site should have generated a sub-band of length 2.0-2.1 kb ($1.77 + 0.3$ kb), while no such band was detected in the *SacI* digest of the same sample (lane 2). Therefore, sub-band 1 was more likely generated by DNase I cleavage at an HS site 3.1 kb to the right of the left-end *HindIII* site, *i.e.* at position 1,600 bp on the Ad5 genome (3.1 - 1.5 kb flanking cellular DNA), as in 293 cells (Fig. 4-20B, *HindIII* site 1). Unlike 293 cells, however, the reciprocal sub-band of ~ 1.2 kb that would be generated by DNase I cleavage at this site was not detected by pSH5 (Fig. 4-20A, lane 4).

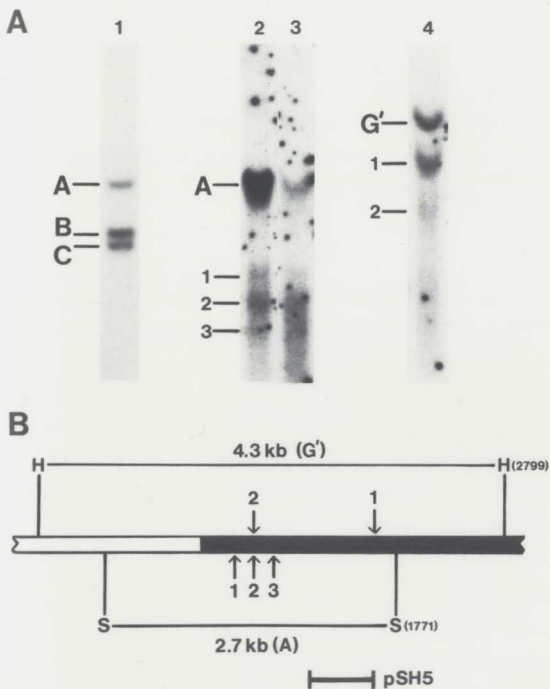
The *HindIII* sub-band 2 was generated by DNase I cleavage at position 470 bp (2.8 - 2.33 kb) on the Ad5 genome (Fig. 4-20B, *HindIII* site 2). This

Figure 4-20 DNase I HS sites in 637-4 E1A 5' region.

A. DNase I digested chromatin from 637-4 cells was cleaved with *SacI* (lanes 2 and 3) or *HindIII* (lane 4), and probed with pSH5. Lane 1, DNase I digested DNA cleaved with *SacI* and probed with pXC1.

B. Position of DNase I HS sites (arrows) generating sub-bands detected in **A**. HS sites mapped relative to the 1771 bp *SacI* site are shown below the DNA (*SacI* sites 1-3), and HS sites mapped relative to the 2799 bp *HindIII* site are shown below the DNA (*HindIII* sites 1 and 2). Solid region, integrated Ad5 sequences; open region, flanking cellular sequences; H, *HindIII* sites; S, *SacI* sites. The positions of the viral restriction sites are given in bp.

637-4



corresponds to site 2 mapped relative to the *SacI* site, confirming the presence of this site in the chromatin of the integrated viral DNA. A summary of these sites and their positions relative to the E1A transcription initiation site is given in Figure 4-23.

4.3.4.4. 14b cells

DNase I digested 14b chromatin was analysed by *HindIII* digestion and hybridization with pSH5. This probe detected the two native-sized junction fragments of 5.8 kb (G') and 3.7 kb (G*), plus two faint sub-bands at ~2.5 kb and ~2.35 kb (Fig. 4-21A, lanes 1 and 2, sub-bands 1 and 2, respectively). No sub-bands were detected when purified 14b DNA was digested to various extents with DNase I and analysed by *HindIII* digestion and hybridization with Ad5 DNA (Fig. 4-3). The HS sites giving rise to these sub-bands likely correspond to those mapped to position 270/280 bp and 470 bp in 293 and 637-4 cells (Fig. 4-21B, *HindIII* sites 1 and 2, respectively).

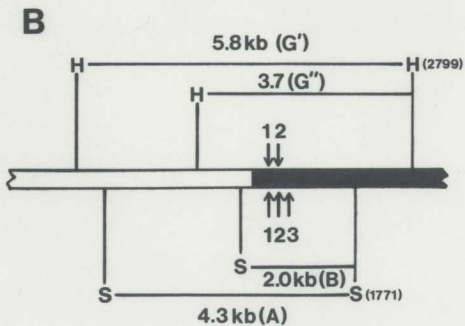
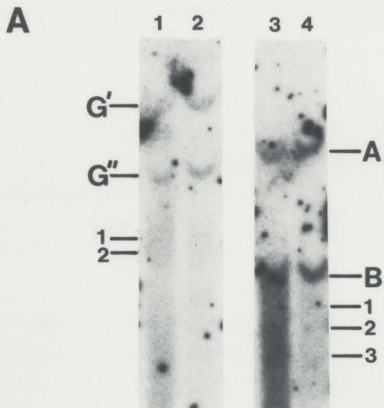
In the *SacI* digest, pSH5 hybridized to the native-sized junction fragments of 4.3 kb (A) and 2.0 kb (B) (Fig. 4-21A, lanes 3 and 4), plus faint sub-bands of 1.3 kb and 1.1 kb (sub-bands 2 and 3, respectively), and a very faint sub-band of 1.5 kb (sub-band 1). These were generated by DNase I cleavage at positions 270 bp (1.77 - 1.5 kb), 470 bp (1.77 - 1.3 kb), and 670 bp (1.77 - 1.1 kb) on the Ad5 genome (Fig. 4-21B, *SacI* sites 1, 2, and 3, respectively), confirming the presence of the 270 bp and 470 bp HS sites mapped relative to the *HindIII* site. A summary of these sites and their positions relative to the E1A transcription initiation site is given in Figure 4-23.

Figure 4-21 DNase I HS sites in 14b E1A 5' region.

A. DNase I digested chromatin from 14b cells was cleaved with *Hind*III (lanes 1 and 2) or *Sac*I (lanes 3 and 4) and probed with pSH5.

B. Position of DNase I HS sites (arrows) generating sub-bands detected in **A**. HS sites mapped relative to the 1771 bp *Sac*I site are shown below the DNA (*Sac*I sites 1-3), and HS sites mapped relative to the 2799 bp site are shown above the DNA (*Hind*III sites 1 and 2). Solid region, integrated Ad5 sequences; open region, flanking cellular sequences; H, *Hind*III sites; S, *Sac*I sites. The positions of the viral restriction sites are given in bp. In each restriction enzyme digest, the two left-end restriction fragments represent the two viral DNA integration sites (*i.e.* *Hind*III-G' and -G", and *Sac*I-A and -B).

14b



4.3.4.5. 945-C1 cells

When 945-C1 chromatin was digested with DNase I and analysed by *Hind*III digestion and hybridization with Ad5 DNA, this probe hybridized strongly to discrete sub-bands of 6.5 kb and 4.1 kb (Fig. 4-22A, lanes 2 and 3, sub-bands A1 and A2, respectively). When this filter was re-probed with pSH5, the native-sized A fragment plus sub-bands A1 and A2 were detected (lanes 4 and 5). No sub-bands were detected when purified 945-C1 DNA was digested with DNase I to a similar extent (Fig. 4-22A, lane 1).

Sub-bands A1 and A2 were generated by DNase I cleavage at HS sites 6.5 kb and 4.1 kb to the left of the *Hind*III site separating the *Hind*III-A (10 kb) and -B (5.0 kb) fragments (Fig. 4-22B, sites A1 and A2). The exact position of these sites could not be determined since the integration pattern of the Ad5 sequences in 945-C1 DNA is not known in sufficient detail. However, from the length of A1 and A2, it is unlikely that they were generated by HS sites in the E1A 5' regulatory region. These sites were estimated to be within the *Sma*I 3.3 kb fragment, with A2 possibly within or near the integrated E4 region.

4.4. Discussion

4.4.1. General level of DNase I sensitivity

I have analysed the chromatin structure of the integrated viral sequences in four Ad5-transformed cell lines by measuring the sensitivity of these sequences to DNase I digestion. The viral sequences are stably integrated into the chromosomal DNA and complexed with cellular histones to form the characteristic

Figure 4-22 DNase I HS sites in 945-C1 Ad5 sequences.

A. DNase I digested chromatin from 945-C1 cells was cleaved with *Hind*III and probed with Ad5 DNA (lanes 2 and 3) or pSH5 (lanes 4 and 5). Lane 1, DNase I digested DNA cleaved with *Hind*III and probed with Ad5 DNA.

B. Position of the DNase I HS sites (arrows) generating sub-bands detected in **A**. Solid region, integrated Ad5 sequences; hatched region, Ad5 sequences possibly present; open region, flanking cellular sequences; H, *Hind*III sites; S, *Sma*I sites. The positions of the viral restriction sites are given in bp.

945-C1

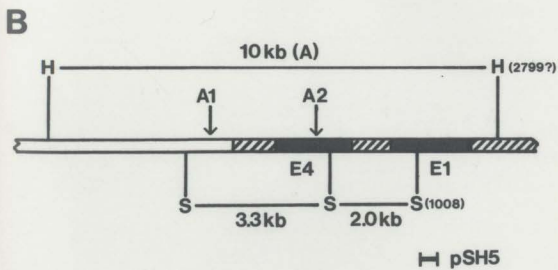
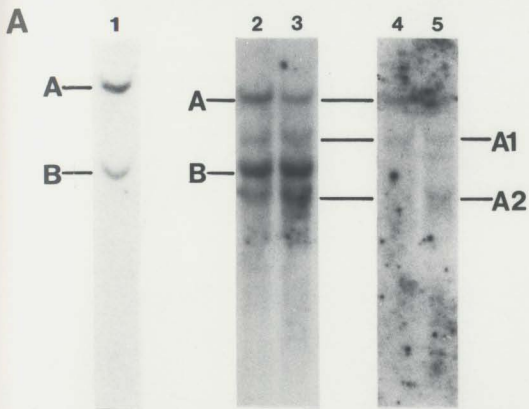
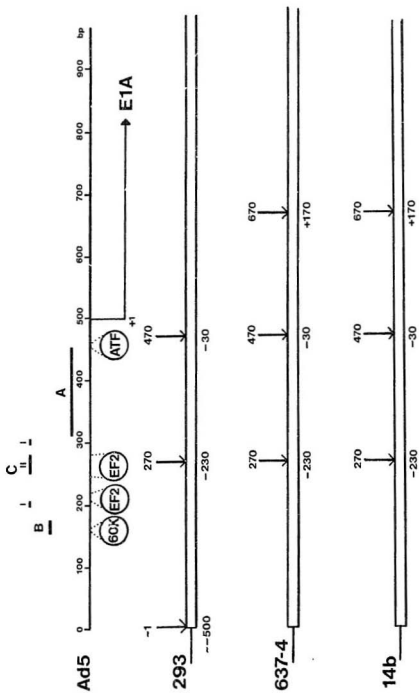


Figure 4-23 DNase I HS sites in 5' region of integrated E1A genes in Ad5-transformed cells.

Left end of Ad5 genome, showing the E1A transcription initiation site (at position 499 bp), and the E1A enhancers A, B, and C (discussed in section 1.3.7, and shown in Figure 1-4). Sequences protected by protein factors (60K, EF2 and ATF) in DNase I footprinting studies are indicated by dotted lines. Open regions, integrated Ad5 sequences, showing positions of DNase I HS sites (arrows). Numbers above the line refer to position on the Ad5 genome (in bp), those below the line, position relative to the E1A transcription initiation site (+ 1 bp).



nucleosomal structure of eukaryotic cellular chromatin (Flint & Weintraub, 1977; Dery *et al.* 1985). In each of the Ad5-transformed cell lines, these sequences were found to have a chromatin structure typical of transcriptionally active chromatin, *i.e.* they were preferentially sensitive to DNase I digestion compared to inactive chromatin.

DNase I sensitivity was monitored by the disappearance of virus-specific restriction fragments after increasing DNase I digestion of chromatin, and quantitated as described in Kunnath & Locker (1985). A rate constant, k , defined as the rate of DNase I digestion of chromatin, was obtained for each restriction fragment. Larger restriction fragments are intrinsically more sensitive to digestion than shorter fragments, therefore, the DNase I digestion rate for a purified DNA fragment of the same length, k_d , was determined. The ratio k/k_d gave a sensitivity factor, S , which is independent of fragment length, allowing comparison of the DNase I sensitivities of different restriction fragments.

The k_d values obtained by Kunnath & Locker (1985) vary with DNA fragment length to a greater extent than those obtained in this study, *i.e.* the slope of the plot of k_d versus fragment length is steeper than that shown in Figure 4-5. In addition, these workers found a considerable scatter around the linear relationship, presumably due to DNase I sequence specificity. In contrast, Figure 4-5 shows very little scatter around the linear plot, suggesting little or no DNase I sequence specificity. While DNase I does show some preference for cleavage at certain bases, this appears to be due to sequence-dependent variations in DNA structure rather than sequence-specific recognition *per se* (Drew &

Travers, 1984). These effects are relatively short-range and average out with increasing fragment length. Indeed, Kunnath & Locker (1985) found more scatter for shorter restriction fragments than for longer fragments. Therefore the difference in the amount of scatter detected in these two studies may be due to the fact that Kunnath & Locker (1985) analysed DNA restriction fragments of length 1.0-3.0 kb, whereas I have analysed fragments of length 2.1-7.8 kb. (The restriction fragments I analysed include both integrated Ad5 sequences and flanking cellular sequences, and so are representative of bulk DNA.) These observations are consistent with the conclusion that DNase I sequence specificity is not a significant factor within the range of fragment lengths used in this study.

Few authors actually quantitate the DNase I sensitivity of chromatin, and of those who have, most have used different methods (*e.g.* Felber, Gerber-Huber, Meier, May, Westley, Weber & Ryffel, 1981; Hoyle & Doering, 1987). Therefore, a direct comparison cannot be made between the values obtained by these authors and those obtained here. However, a direct comparison can be made with the values obtained by Kunnath & Locker (1985). These workers analysed the rat albumin and α -fetoprotein genes in various tissues, and obtained S values of 0.9-2.0 for active genes, and 0.6 or less for inactive genes. The S values obtained here for the integrated Ad5 sequences ranged from 0.7 for the *SacI*-C fragment in 293 cells (Fig. 4-7) to 2.0 for the *HindIII*-B fragment in 945-C1 cells (Fig. 4-17), compared to $S = 0.3$ and 0.4 for the transcriptionally inactive IgH gene J region in 293 cells (Fig. 4-8). Therefore, the S values obtained here are in excellent agreement with those obtained by Kunnath & Locker (1985).

Determining the S values of restriction fragments containing a DNase I HS site presented a problem, as the plot of I/I_0 versus Mw described a curve rather than a straight line. The curve may reflect biphasic DNase I digestion kinetics for these fragments. The initial part of the curve is very steep, indicating rapid digestion at the HS site. I have calculated the S values for this part of the curve, although the actual values are rather meaningless, since the range of the "initial" part of the curve was arbitrarily chosen. I have included these only to indicate that fragments containing HS sites were extremely sensitive to DNase I digestion.

It has been suggested that the DNase I sensitive conformation of chromatin requires torsionally stressed DNA, and that DNA nicking agents such as γ -rays and bleomycin reverse DNase I sensitivity by removing torsional stress (Villeponteau & Martinson, 1987). This implies that single-strand nicks introduced into the DNA by DNase I at an HS site should also result in loss of torsional stress, with subsequent loss of DNase I sensitivity in the remainder of the fragment. [Single-strand nicks in the remainder of the fragment, which is organized into nucleosome arrays, should result in loss of torsional stress only when introduced into the linker DNA: when introduced into nucleosomal DNA the topological conformation will be maintained by nucleosome core-DNA interactions. Since DNase I cleaves nucleosomal DNA as efficiently as linker DNA, the probability of digestion at linker DNA is $\sim 20\%$ (i.e. ~ 40 bp linker DNA/ ~ 200 bp nucleosomal repeat). Since HS sites lack nucleosomes (section 1.1.6), a single nick will result in loss of torsional stress with 100% probability.] Therefore, the first part of the curve may represent rapid DNase I digestion at the

HS site, whereas the second part may reflect the digestion kinetics of relaxed DNA, characteristic of inactive chromatin.

I also included the amount of DNA remaining in the sub-bands generated by HS sites in the calculation of the S values for these fragments. This might be expected to reflect more closely the DNase I sensitivity of the entire fragment rather than just the HS site. In the case of the 945-C1 *HindIII*-A fragment, this resulted in a plot that was closer to linearity (Fig. 4-17). In the case of the 637-4 left-end fragments (*HindIII*-G' and *SacI*-A), however, the plots remained curved (Figs. 4-13 and 4-15, respectively). This may be due to the fact that the reciprocal part of the fragment, *i.e.* to the left of the HS site, is not detected, and therefore its contribution to the amount of DNA remaining is not included in the calculation of the S value. In the summary shown in Figure 4-18, the S values shown for restriction fragments containing HS sites included the contributions of the sub-bands detected, and were calculated from the best-fit straight line through these plots, even where a curve was obtained, since the straight line more closely represented the "average" DNase I digestion rate over the time course of the incubation.

The integrated viral sequences analysed in this study included the transcriptionally active E1 transforming region, plus transcriptionally active and inactive sequences from other regions of the viral genome. All of the viral sequences analysed were preferentially sensitive to DNase I digestion, indicating that the DNase I sensitive chromatin conformation extended beyond the boundaries of the E1 transcription unit into the adjacent viral sequences. In 637-4

chromatin, this conformation extended from the E1 region to the transcriptionally inactive E4 region, over 30 kb away. This is in agreement with previous studies, which have shown that the DNase I sensitive conformation of active genes extends well beyond the boundaries of the transcribed region. For example, the DNase I sensitive chromatin domain surrounding the ovalbumin gene cluster in hen oviduct cells spans ~100 kb (Lawson *et al.* 1932).

Cell lines 14b and 293 contain 5-6 copies of the integrated viral sequences per diploid amount of DNA. The DNase I sensitivities of each of these copies cannot be determined separately, and the *S* value for a particular restriction fragment represents the average sensitivity of all copies of that fragment. In 14b cells there appear to be two separate integration sites, resulting in two left-end junction fragments. Unfortunately, the DNase I sensitivities of these two fragments could not be compared, as the *Hind*III-G' junction fragment migrated too close to the Ad5 *Hind*III-C fragment to be analysed, and the *Sac*I-B fragment co-migrated with the Ad5 *Sac*I-F fragment. In both cases, therefore, the left-end junction fragment representing only one of the integration sites could be analysed, *i.e.* *Hind*III-G* and *Sac*I-A. Whether these represent the same or different integration sites is not known. I attempted to analyse the left-end junction fragments by washing the Ad5 DNA probe from the filters and re-probing with a left-end-specific probe. However, the washing procedure did not always completely remove the probe DNA and/or other components of the hybridization mixture, resulting in an extremely high background signal when these filters were re-probed. This was the case when the filters shown in Figure 4-9 were washed and re-probed with pSH5.

Flint & Weintraub (1977) analysed the DNase I sensitivity of the integrated Ad5 sequences in 14b cells, using solution hybridization and reannealing kinetics to measure the amount of viral sequences remaining after DNase I digestion. Their studies suggest that only half of the integrated copies have a DNase I sensitive chromatin structure. It would have been interesting, therefore, to determine whether the two integration sites correspond to the sensitive and resistant copies. These workers found the DNase I sensitive region to be limited to the transcribed E1 sequences. The adjacent viral sequences flanking the 3' end (11.3~40 mu) and the 5' end (0-2.8 mu) were found to be resistant to DNase I digestion. In contrast, I have found the DNase I sensitive domain to extend to the *HindIII*-H (31.7-37.3 mu) and -D sequences (37.3~40 mu). These apparently contradictory results do not appear to be due to the use of solution *versus* filter hybridization assays, since Weintraub and colleagues have confirmed their results using filter hybridization (unpublished results cited in Stalder *et al.* 1980b).

Weintraub and colleagues demonstrated that in chicken erythrocytes, the α - and β -globin genes and their non-transcribed flanking sequences are in a DNase I sensitive conformation relative to the inactive ovalbumin gene, as assayed by both solution and filter hybridization (Stalder *et al.* 1980b). They were also able to distinguish between a very sensitive chromatin structure for the transcribed regions of the globin genes, and a moderately sensitive structure for the non-transcribed flanking regions. In 14b cells, therefore, the non-transcribed flanking viral sequences may correspond to a region of moderate sensitivity, since these workers did not analyse a known inactive gene in 14b cells to compare the DNase

I sensitivity of inactive chromatin (discussed in Stalder *et al.* 1980b). Nevertheless, it is surprising that sequences between 0 and 2.8 μ (1,008 bp) were found to be more resistant to DNase I digestion than E1 (Flint & Weintraub, 1977), since this region has been shown here to contain DNase I HS sites, albeit relatively weak ones.

The viral DNA in the Ad5-transformed cell lines may either have integrated into a chromatin domain that was already in a DNase I sensitive conformation, or into a resistant domain which subsequently became DNase I sensitive as a result of integration. In order to distinguish between these two possibilities, the left-end (or right-end) viral-cell DNA junction fragment could be cloned and used as a hybridization probe to determine the DNase I sensitivity of the pre-integration site in the untransformed counterparts of these cell lines. Doerfler and colleagues have reported that the pre-integration sites in several Ad2- and Ad12-transformed cell lines are transcriptionally active (Gahlmann *et al.* 1984; Shulz *et al.* 1987), although these workers did not examine the chromatin structure at these sites.

4.4.2. DNase I hypersensitive sites

In addition to the general level of DNase I sensitivity, I have also detected a number of DNase I HS sites in the vicinity of the integrated E1A genes. I have mapped several of these sites to the E1A 5'-flanking region, at positions \sim 1 bp, 270 bp, and 470 bp in 293 cells, and 270 bp, 470 bp, and 670 bp in 637-4 and 14b cells. These sites and their positions relative to the E1A transcription initiation site are summarized in Figure 4-23.

DNase I HS sites often occur in the 5'-flanking sequences of transcriptionally active and potentially active genes. They have been shown to contain enhancer elements and DNA binding sites for *trans*-acting factors involved in the regulation of transcription, and are thought to represent nucleosome-free regions of chromatin which allow access for these factors to their specific DNA binding sequences (section 1.1.6). The 5'-flanking region of the E1A gene has been shown to contain enhancer elements required for efficient E1A transcription. Within this region, different enhancers have been identified under different assay conditions (Hearing & Shenk, 1983, 1986; Hen *et al.* 1983; Imperiale *et al.* 1983), but they all map within the region ~150-500 bp on the Ad5 genome (section 1.3.7, Fig. 1-4, and Fig. 4-23). This region has also been shown by DNase I footprinting analyses to contain sequence-specific binding sites for cellular transcription factors (Fig. 4-23). A protein of Mr 60,000 from HeLa cells binds to enhancer B (Barret *et al.* 1987). This enhancer contains the SV40 enhancer "core" consensus sequence, and the SV40, polyomavirus, and Rous sarcoma virus enhancers also bind this protein (Jones, Rigby & Ziff, 1988). The transcription factor E2F binds enhancer C element II, and sequences adjacent to element I (Kovesdi *et al.* 1987). E1A 5'-flanking sequences compete with E2 and E4 promoters for binding of the transcription factor ATF, and ATF consensus binding sequences occur at positions 245-249 bp, 371-377 bp, and 454-460 bp (SivaRaman *et al.* 1986; Lee & Green, 1987). ATF binding to the last of these sites has recently been reported (Jones *et al.* 1988).

The DNase I HS sites in the chromatin of the integrated E1A genes have

therefore been mapped to a region containing enhancer elements and *trans*-acting transcription factor binding sites. The enhancer elements were identified in transient transcription assays with cloned plasmid DNA (Hen *et al.* 1983; Imperiale *et al.* 1983) and in Ad DNA molecules during viral infection (Hearing & Shenk, 1983, 1986). The transcription factor binding sites have been identified by *in vitro* DNase I footprinting on purified DNA fragments. The results presented here indicate that these same sequences adopt an altered chromatin structure when stably integrated into eukaryotic cell chromosomes in the form of cellular chromatin. This altered structure likely reflects a nucleosome-free chromatin region in which the enhancer sequences important for regulation of E1A transcription are exposed to facilitate binding of the *trans*-acting transcription factors.

Similar results have been reported for other DNA tumour viruses. The integrated SV40 DNA in the mouse transformed cell line SV101 contains a DNase I HS region at the same site as in lytic SV40 minichromosomes (Blanck, Chen & Pollack, 1984). This region contains the origin of replication, the early and late promoters, and the 72 bp repeat enhancer element. Lazo (1987) identified a DNase I HS site in the integrated human papilloma virus (HPV)-18 DNA in HeLa cells, in the viral E6/E7 region. The HS region contains several copies of the SV40 enhancer "core" consensus sequence. Similarly, the integrated proviral DNA of retroviruses has been shown to contain DNase I HS sites. Avian sarcoma virus-transformed rat cells contain HS sites at the 5'-end of the proviral DNA (Chiswell, Gillespie & Wyke, 1982). These sites appear to be related to

transcriptional activity, as revertant subclones that are morphologically normal and synthesize no detectable viral RNA lack these HS sites. The integrated proviral DNA in mouse mammary tumour virus-transformed L cells contains both constitutive HS sites, and those induced in the presence of dexamethasone (Zaret & Yamamoto, 1984). The inducible sites map to the glucocorticoid responsive element (GRE), an enhancer element that has been shown to bind the glucocorticoid hormone-receptor complex.

The probe used to map the EIA 5'-flanking HS sites (pSH5) labelled the right end of the *SacI* restriction fragment, and so mapped the right-end boundaries of the HS sites. Mapping the left-end boundaries would require a probe homologous to the left end of a viral-cell DNA junction fragment. Neither Ad5 nor pXC1 probes detected additional sub-bands other than those detected by pSH5, indicating that the reciprocal left-end sub-fragments do not contain sufficient viral sequences to hybridize to these probes. Therefore, the left-end boundary of the DNase I HS region appears to be located either close to the left-end viral DNA integration site or in the flanking cellular sequences. This implies that the DNase I HS region extends at least ~500 bp in 293 cells (~0-500 bp) and ~700 bp in 637-4 and 14b cells (~0-700 bp). Within this region, however, the DNA was not uniformly sensitive to DNase I digestion, as specific sites of enhanced cleavage were detected at positions ~1 bp, 270 bp, 470 bp, and 670 bp, with relatively resistant regions between these sites. The 200 bp repeat pattern of these sites is reminiscent of the typical nucleosomal repeat pattern generated by MNase (micrococcal nuclease) digestion. However, DNase I cleaves nucleosomal

DNA as efficiently as linker DNA, and so does not generate a nucleosomal ladder (Noll, 1974).

The relatively resistant regions between the HS sites may represent sequences associated with protein factors, and so protected from DNase I cleavage. As discussed above, such factors have been identified and their binding sites mapped by DNase I footprinting. In this technique, purified DNA fragments are allowed to bind protein factors *in vitro*, digested with DNase I, and the protected sequences mapped to within one or two nucleotides on sequencing gels. The method used here, *i.e.* DNase I digestion of chromatin *in vivo* and indirect end-labelling, did not permit such high resolution mapping of the sensitive and resistant sequences. The position given for each HS site corresponds to the centre of the region of enhanced cleavage, as defined by the fragment length at the mid-point of a sub-band. Although the sub-bands generated by DNase I cleavage at the HS sites were fairly discrete, the width of these sub-bands indicated that each contained a range of fragment lengths around ± 50 bp relative to the length at its mid-point. Therefore, the region of enhanced cleavage appears to extend ~ 50 bp on either side of these positions. Given this limit of resolution, it was difficult to correlate the pattern of DNase I sensitive and resistant regions with the protein factor binding sites mapped by DNase I footprinting. However, this pattern does indicate an altered chromatin structure in the regions of E2F binding to enhancer C element II, at 248-282 bp, and adjacent to element I, at 207-220 bp, and ATF binding within enhancer A, at 454-460 bp (Fig. 4-23).

Cell lines 293 and 14b contain 5-6 copies of the integrated viral sequences

per diploid amount of cell DNA, all or some of which may contain DNase I HS sites. In 293 cells, the sub-bands generated by DNase I digestion were very intense, suggesting that most, if not all, of the integrated copies contain HS sites. In contrast, the sub-bands generated in 14b cells were very faint, suggesting that only one or a few of the integrated copies contain HS sites. This is consistent with the suggestion that only about half of these copies are in a DNase I sensitive conformation (Flint & Weintraub, 1977).

In addition to the E1A 5'-flanking HS sites, I also detected other HS sites. One of these was tentatively mapped to position 1,400-1,600 bp in 293 and 637-4 cells (Figs. 4-19 and 4-20, respectively). This region contains the E1A transcription termination site (~1,600 bp) and the 5'-flanking sequences upstream from the E1B transcription initiation site (~1,700 bp) (Fig. 1-2). Therefore, an altered chromatin structure in this region may be related to termination of E1A transcription and/or regulation of E1B transcription initiation.

In 293 cells, three HS sites were detected in the left-end-flanking cellular DNA sequences, and one at the viral-cell DNA junction site (Fig. 4-19). Also, one or both of the HS sites detected in 945-C1 cells may be in the flanking cellular DNA (Fig. 4-22). These sites may be related to the integration process. The proviral DNA of retroviruses has been shown to integrate into the host cell genome preferentially at or near DNase I HS sites (Breindl, Harbers & Jaenisch, 1984; Schubach & Groudine, 1984; Vijaya, Steffen & Robinson, 1986; Rohdewohld, Weiher, Reik, Jaenisch & Breindl, 1987). Proviral DNA integration is catalysed by a retrovirus-encoded "integrase", which has an endonuclease

activity that cleaves host cell DNA as the first step in integration (Pangiban, 1985). This endonuclease, like DNase I, may act preferentially at HS sites due to their more accessible chromatin structure. Although no DNA virus- or cell-encoded integrase has been identified, recombination between Ig gene regions (Storb, Arp & Wilson, 1981) and between T-cell receptor gene regions (Yancopoulos, Blackwell, Suh, Hood & Alt, 1986) also occurs at or near DNase I HS sites. This suggests the presence of a cell-encoded integrase with a similar endonuclease activity, which may catalyse the integration of adenovirus DNA at or near DNase I HS sites.

Chapter 5

Nuclear Matrix

5.1. Introduction

The nuclear matrix is the residual proteinaceous structure after nuclei are treated with non-ionic detergent, high ionic strength buffer, and nucleases. The resulting structure consists of a three-dimensional network of protein filaments, and is the major structural component of the nucleus (section 1.2.2). In the nucleus, DNA is organized into supercoiled loops of ~ 100 kb, anchored at their bases to the nuclear matrix (sections 1.1.2 and 1.2.3). Thus, the nuclear matrix appears to be involved in the organization of DNA within the nucleus.

In many cases, transcriptionally active genes have been mapped to the base of the loops, in close association with the nuclear matrix, and it has been proposed that transcription occurs in association with the matrix (reviewed in Nelson *et al.* 1986b; Razin, 1987). However, not all workers have found active genes to be associated with the nuclear matrix, and the relationship between active genes, transcription, and the nuclear matrix remains unclear.

I have attempted to map the position relative to the nuclear matrix of the integrated viral sequences in the four Ad5-transformed cell lines. The viral

transforming region (E1) is transcribed in these cells, and can be considered a "model" active eukaryotic gene. Matrix associated and non-associated DNA fractions were prepared, and the amount of viral sequences present in each of these fractions analysed by Southern blotting and hybridization with Ad5 DNA probes. I have also examined the *HSP70* gene in Ad5-transformed cells. Transcription of this gene is induced by the E1A gene products (Nevins, 1982; Kao & Nevins, 1983), and *HSP70* mRNA is present in the cytoplasm of the cell lines used in this study (Fig. 5-1). I have also analysed the *HSP70* gene in heat shocked HeLa and 945-C1 cells.

5.2. Materials and Methods

5.2.1. Heat shock

Cells were heat shocked by placing culture dishes in a 43°C water bath for 15 min. They were then incubated at 37°C for 45 min, and harvested in PBS for preparation of nuclear matrix DNA fractions.

5.2.2. Preparation of nuclear matrix DNA fractions

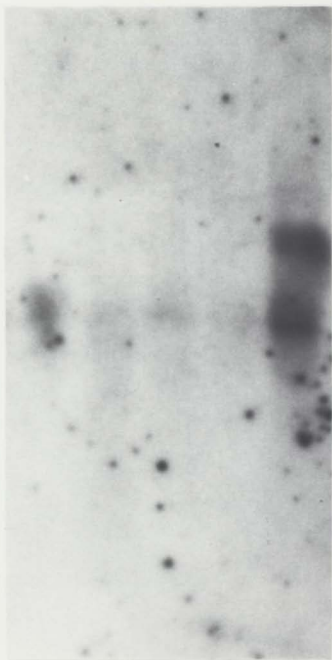
Cells were grown in the presence of (methyl-³H) thymidine (Amersham and ICN Radiobiochemicals) (0.3 µCi/ml) for 24-48 h to label DNA uniformly. Cell monolayers were rinsed twice in ice-cold PBS, and harvested by scraping with a rubber policeman. Cells were washed twice in PBS, and nuclear matrix DNA fractions prepared by one of the following methods.

Figure 5-1 *HSP70* RNA in Ad5-transformed cells and HeLa cells.

Cytoplasmic poly(A)⁺RNA (~1 μg/lane) from each cell line was size-fractionated by agarose gel electrophoresis, transferred to a filter, and hybridized to pMHS 243, a mouse *HSP70*-specific cDNA. Lane 1, 637-4 cells; lane 2, 945-C1 cells; lane 3, 14b cells; lane 4, 293 cells; lane 5, HeLa cells.

HSP70

1 2 3 4 5



— 2.1 kb

— 1.4 kb

5.2.2.1. Method 1

This is essentially the "detachment mapping" method of Cook and colleagues (Cook & Brazell, 1980; Cook, Lang, Hayday, Lania, Fried, Chiswell & Wyke, 1982). Cells were resuspended in PBS at a concentration of $1-2 \times 10^7$ cells/ml, lysed by the addition of 3 volumes of 1.33 x lysis buffer [1 x lysis buffer = 2.0 M NaCl, 100 mM EDTA, 10 mM Tris-HCl (pH 8.0), 0.5% Triton X-100 (Sigma)], and incubated at 0°C for 10 min. Cell lysis was monitored by phase contrast microscopy. The cell lysate was centrifuged through 7.5% sucrose in 2 M NaCl, 10 mM Tris-HCl (pH 8.0), 1 mM EDTA onto a cushion of 30% sucrose in the same buffer. Centrifugation was at 32,000g for 30 min in a Beckman SW 27.1 rotor at 4°C. Nucleoids (nuclear matrices with all the DNA attached) were removed from the surface of the 30% sucrose layer in a volume of 0.25-0.5 ml using a pasteur pipette, and diluted x20-40 in restriction enzyme buffer minus NaCl, so that the final NaCl concentration was optimal for restriction enzyme digestion (50-100 mM). Nucleoids were digested with restriction enzyme (10-20 units/ml) at 37°C for various lengths of time, and the reaction stopped by the addition of EDTA to a final concentration of 25 mM.

Nuclear matrices and attached DNA were pelleted by centrifugation at 13,000g for 20 min in an HB4 rotor at 4°C. The pellet (P) was resuspended in TE plus protease (1 mg/ml) and SDS (0.5%) and incubated at 55°C for 2 h. The supernatant (S) was incubated with protease (0.1 mg/ml) and SDS (0.1%) at 55°C for 2 h.

The fraction of DNA detached from the matrices was monitored by

measuring the ^3H -labelled DNA in the P and S fractions. The fraction of DNA remaining associated with the matrix was expressed as $[\text{cpm(P)}/\text{cpm(P+S)}] \times 100\%$. DNA was purified from P and S fractions as in section 2.3.

5.2.2.2. Method 2a

Nuclei were prepared by incubating cells in RSB containing 0.25 M sucrose, 0.5% NP-40 and 0.5 mM PMSF for 10 min at 0°C for 10 min, with occasional vortexing. Lysis was monitored by phase contrast microscopy. Nuclei were pelleted by centrifugation at 200g for 5 min in an HB4 rotor at 4°C , washed twice in RSBs, and once in restriction enzyme digestion buffer. Nuclei were resuspended in restriction enzyme digestion buffer at a concentration of 1 mg DNA/ml ($1\text{-}2 \times 10^8$ nuclei/ml) and digested with restriction enzyme (1 unit/ μg DNA) for 1-2 h at 37°C . The reaction was terminated by the addition of an equal volume of 4M NaCl, 10 mM Tris-HCl (pH 7.4), 50 mM EDTA, and incubated at 0°C for 10 min.

Nuclear matrices and attached DNA were pelleted by centrifugation at 4,000g for 10 min in an HB4 rotor at 4°C . The pellet was washed once in RSB containing 2M NaCl and 0.1% NP-40, and once in restriction enzyme digestion buffer minus NaCl. The supernatants from each of these spins were combined to give fraction S1. The pellet was resuspended in restriction enzyme digestion buffer (1mg DNA/ml) and digested with restriction enzyme (1 unit/ μg DNA) at 37°C for 1-2 h. The reaction was again terminated by the addition of an equal volume of 4 M NaCl, 10 mM Tris-HCl (pH 7.4), 50 mM EDTA, and incubated at 0°C for 10 min.

Nuclear matrices and attached DNA were pelleted by centrifugation at 4,000*g* for 10 min in an HB4 rotor at 4°C, and the pellet washed twice in RSB containing 2 M NaCl and 0.1% NP-40. The supernatants from each of these spins were combined to give fraction S2. The pellet (P) was resuspended in TE plus protease (1 mg/ml) and SDS (0.5%) and incubated at 55°C for 2 h. The S1 and S2 fractions were each incubated with protease (0.1 mg/ml) and SDS (0.1%) at 55°C for 2 h.

The percentage of DNA present in the P, S1 and S2 fractions was calculated as in Method 1, and DNA purified from each of these fractions as in section 2.3.

5.2.2.3. Method 2b

This method differs from Method 2a in that the preliminary digestion of nuclei with restriction enzyme is omitted.

Nuclei were prepared as in Method 2a, washed twice in RSB containing 0.25 M sucrose, 0.5% NP-40 and 0.5% PMSF, and resuspended in this buffer. An equal volume of 4 M NaCl, 10 mM Tris-HCl (pH 7.4), 50 mM EDTA was added, and incubated at 4°C for 10 min. Nuclear matrices with attached DNA were pelleted by centrifugation at 4,000*g* for 10 min in an HB4 rotor at 4°C. The pellet was washed once in RSBs containing 2M NaCl and 0.1% NP-40, and once in restriction enzyme digestion buffer minus NaCl. The supernatants from these spins were combined to give fraction S1. The pellet was resuspended in restriction enzyme digestion buffer and digested with restriction enzyme as in Method 2a to give fractions P and S2.

The percentage of DNA present in fractions P, S1 and S2 was calculated as before, and DNA purified from fractions P and S2. S1 was not analysed further, and not included in the final calculation of the percentage of DNA in fractions P and S2.

5.2.3. Analysis of nuclear matrix DNA

Equal amounts of DNA from P, S1 and S2 fractions and total DNA were digested to completion with the same restriction enzyme used to prepare nuclear matrix DNA, and analysed by Southern blotting and hybridization as in section 2.3. The amount of DNA/lane was monitored by ethidium bromide staining of the agarose gels after electrophoresis.

5.3. Results

5.3.1. Rationale of the experiment

The objective of this study was to determine the position relative to the nuclear matrix of the integrated viral sequences in Ad5-transformed cells. In this procedure, nuclear DNA is first separated into matrix-proximal and matrix-distal fractions. Cells or nuclei are treated with non-ionic detergent and 2 M NaCl to extract histones and most other chromosomal proteins. The resulting structures contain the chromosomal DNA in the form of supercoiled loops attached at their bases to the nuclear matrix. The DNA loops are cleaved with a restriction enzyme, which detaches those restriction fragments in the matrix-distal portion of the loops, while those in the matrix-proximal portion anchoring the loops to the matrix remain attached. After centrifugation, the attached restriction fragments

are recovered from the matrix pellet (P), while the detached fragments remain in the supernatant (S). DNA is purified from each of these fractions and assessed for its content of viral sequences by Southern blotting and hybridization with Ad5 DNA probes. If the viral sequences are located at the base of the loops, there will be an enrichment of these sequences in the P fraction and a depletion in the S fraction, relative to an equal amount of total unfractionated DNA. Conversely, if the viral sequences are located in the matrix-distal portion of the loops, there will be an enrichment of these sequences in the S fraction and a depletion in the P fraction. If the viral sequences are positioned randomly with respect to the nuclear matrix, these sequences will be equally distributed between the matrix DNA fractions.

5.3.2. Nuclear matrix DNA fractions

5.3.2.1. Method 1

Whole cells in suspension were lysed in 0.5% Triton X-100 in the presence of 2M NaCl and 100 mM EDTA. The non-ionic detergent solubilizes the cell and nuclear membranes, and the high ionic strength buffer extracts the cytoskeleton and most chromosomal proteins, including histones. The resulting structures (termed nucleoids) retained the size and shape of the original nuclei, as determined by phase contrast microscopy (not shown). The nucleoids were isolated and the DNA cleaved with a restriction enzyme (in most cases *HindIII*). Sequences remaining attached to the nuclear matrices were separated from detached sequences by centrifugation, and the percentage of DNA in the pellet (P) and supernatant (S) fractions determined. The fraction of DNA detached from

the matrices varied from 50% to 95%, depending on the concentration of restriction enzyme and the length of digestion. In control experiments, ~97% of the total DNA remained matrix associated when the restriction enzyme digestion was omitted.

Two examples of the P and S fraction DNA prepared by Method I are shown in Figure 5-2. The P fractions (28%P and 7%P) consisted of a fairly high molecular weight smear, corresponding to the matrix associated restriction fragments. The 93%S fraction consisted of a similar smear, corresponding to the restriction fragments detached by *Hind*III cleavage. However, the 72%S fraction was degraded, consisting solely of low molecular weight DNA. This was the case in 25% (7/28) of the S fractions prepared by Method I, whereas none of the P fractions were degraded. The reason for this could not be determined. All cell lines, including HeLa, were equally susceptible to degradation of the S fraction DNA. Degradation was not related to the extent of restriction enzyme digestion, since the 7%P/93%S preparation was digested for longer than the 28%P/72%S preparation. Degradation did not correspond to which particular batch of restriction enzyme was used, and a single batch could generate a non-degraded S fraction after generating a degraded S fraction. Both P and S fractions would have been exposed equally to any DNA degrading agents present, yet only the S fractions were degraded. It is possible that the nuclear matrix provided protection from endogenous nucleases to the attached DNA through steric hinderance. However, other workers have shown that restriction sites within matrix associated regions are accessible to restriction enzyme cleavage (Robinson

et al. 1983; Small *et al.* 1985), indicating that association with the nuclear matrix does not protect these sequences from digestion.

5.3.2.2. Method 2

In view of this unexplained DNA degradation, I used a second method to prepare nuclear matrix DNA fractions. In this procedure, nuclei were first isolated in 0.5% NP-40. At the DNA concentrations used here (~1mg/ml), intact DNA formed a viscous gel on extraction of histones with 2 M NaCl, and was extremely difficult to pellet. In Method 2a, therefore, the isolated nuclei were first digested with restriction enzyme to cleave the DNA partially. Subsequent extraction of the restriction enzyme digested nuclei with 2 M NaCl resulted in structures that retained the size and shape of the isolated nuclei, as determined by phase contrast microscopy (not shown). These structures were pelleted, and the detached DNA purified from the supernatant (S1). An example of an S1 fraction prepared by this method is shown in Figure 5-2 (^{33}P -S1). This fraction consisted of high molecular weight DNA, similar to total undigested DNA (T). This was expected, as the DNA was digested in the form of chromatin, and so was relatively protected.

In initial control experiments, incubation of nuclei at 37°C in the absence of restriction enzyme and subsequent extraction with 2 M NaCl resulted in ~30% of the radioactive label being released into the S1 fraction. This was not due to unincorporated labelled DNA precursors, since ~95% of the label in this fraction was precipitable in 10% trichloroacetic acid (not shown). Therefore, extraction of isolated nuclei with non-ionic detergent and 2 M NaCl resulted in the release of

Figure 5-2 Nuclear matrix DNA fractions.

Nuclear matrix DNA fractions were prepared by Method 1 or 2 as described in section 5.2.2. 2 μg of DNA from each fraction and from total unfractionated DNA (T) were run on a 0.8% agarose gel containing ethidium bromide, and photographed under *uv* light. The numbers at the top of each lane indicate the percentage of nuclear DNA in the matrix associated (P) and non-associated (S) fractions.

Method 1

28% 72% 7% 93%
T P S P S

**Method 2**

14% 33% 53%
T P S1 S2



~30% of the total DNA into the S1 fraction. This may have been due to degradation of either the DNA or the nuclear matrix. The DNA of fraction S1 consisted solely of high molecular weight DNA, even when the initial *Hind*III digestion was included (Fig. 5-2, 33%S1), suggesting that DNA degradation was not responsible. Furthermore, when the concentration of the protease inhibitor (PMSF) in the nuclear isolation and extraction buffers was increased from 0.1 mM to 0.5 mM, the amount of DNA released into S1 was reduced from ~30% to ~15%. (0.5 mM PMSF was used in all subsequent preparations.) This suggested that proteolytic degradation of the nuclear matrix was responsible for the release of DNA from the matrix attachment sites. Since this results in the release of entire loops, S1 DNA can be considered as equivalent to total unfractionated DNA with respect to its distribution relative to the nuclear matrix.

After removal of S1, the remaining pellet fraction was digested with *Hind*III, extracted with 2 M NaCl, and centrifuged to give fractions P and S2. Each of these fractions consisted of a fairly high molecular weight smear, corresponding to matrix associated and non-associated restriction fragments (Fig. 5-2, 14%P and 53%S2, respectively).

In Method 2b, the initial restriction enzyme digestion was omitted. In order to alleviate the aforementioned problems associated with handling highly viscous DNA solutions, nuclei were extracted at low DNA concentrations. The P and S2 fractions were identical to those shown in Figure 5-2. The S1 fraction, usually ~15%, was not analysed.

5.3.3. Viral sequences in Ad5-transformed cells

5.3.3.1. Method 1

Nuclear matrix DNA fractions were prepared from Ad5-transformed cells by Method 1 using *HindIII*. Equal amounts of P, S, and total unfractionated DNA were digested to completion with *HindIII*, and analysed by Southern blotting and hybridization with Ad5 DNA to determine the amount of viral sequences in each fraction. There was no enrichment or depletion of any of the virus-specific restriction fragments in the P or S fractions relative to total unfractionated (T) DNA in 14b, 637-4 (Fig. 5-3), or 945-C1 cells (Fig. 5-4, Ad5). (See Chapter 3 for the origin of these restriction fragments.) I have consistently obtained this result in 11 preparations using Method 1 from all four Ad5-transformed cell lines. These results are consistent with a random organization for the integrated Ad5 sequences relative to the nuclear matrix in these cells. The 14b 72%S and 637-4 70%S fractions were degraded, and as expected, no signal was detected in these lanes (Fig. 5-3).

The following control studies (not shown) confirmed that the hybridization assay was quantitative. Known amounts of Ad5 DNA were mixed with 15 μ g of non-transformed rat cell DNA at ratios of 1, 5, and 10 copies of Ad5 DNA per diploid amount of cell DNA, digested with *HindIII*, and analysed by Southern blotting and hybridization with Ad5 DNA probes as above. The appropriate increase in hybridization signal intensity was detected on the autoradiogram, indicating that an enrichment or depletion of the viral sequences in the nuclear matrix DNA fractions would have been detected.

Figure 5-3 Ad5 sequences in nuclear matrix DNA fractions from 14b and 637-4 cells.

Nuclear matrix DNA fractions were prepared by Method 1 using *HindIII*. 15 μ g of DNA from each fraction was re-digested with *HindIII*, and probed with pXC1 (14b) or Ad5 DNA (637-4).

637-4

30% 70%

T P S

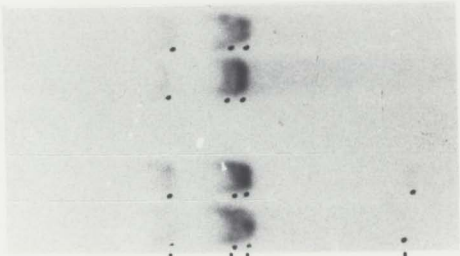


A —
B =
C =
D =
G' —
E —
F —
H —

14b

28% 72% 7% 93%

T P S P S

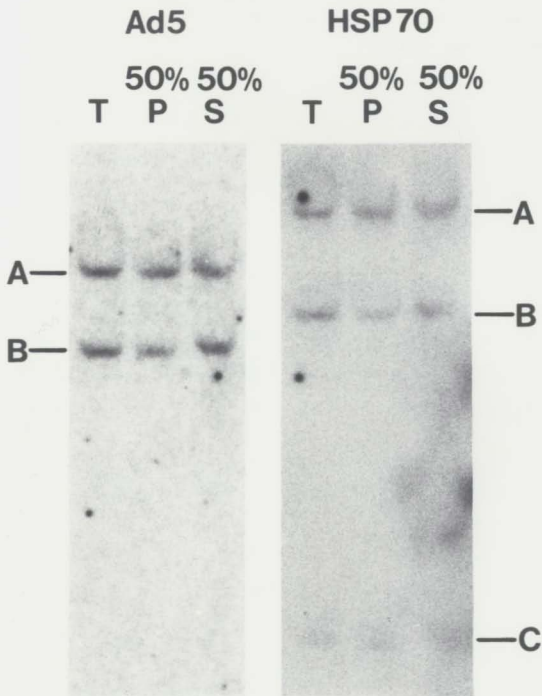


G' — .
G'' — .
E — .
H — .

Figure 5-4 Ad5 and *HSP70* sequences in nuclear matrix DNA fractions from 045-C1 cells.

Nuclear matrix DNA fractions were prepared by Method 1 using *HindIII*. 15 μ g of DNA from each fraction was re-digested with *HindIII*, and probed with Ad5 DNA (Ad5). The filter was washed and re-probed with the *HSP70* cDNA (HSP70).

945-C1



The filter containing the 945-C1 matrix DNA fractions was re-probed with a cDNA complementary to a mouse *HSP70* gene. This probe hybridized to three *Hind*III restriction fragments, of 17 kb (A), 6.5 kb (B), and 1.3 kb (C) (Fig. 5-4, HSP70). These sequences were transcriptionally active, since this probe detected *HSP70* mRNA in the cytoplasm of the Ad5-transformed cell lines (Fig. 5-1). Once again, however, there was no enrichment or depletion of the *HSP70* restriction fragments in the P or S fractions relative to total unfractionated DNA (Fig. 5-4, HSP70). I have consistently obtained this result in six preparations using Method 1, in 945-C1, 14b, and 637-4 cells, consistent with a random organization for the *HSP70* sequences relative to the nuclear matrix in these cells.

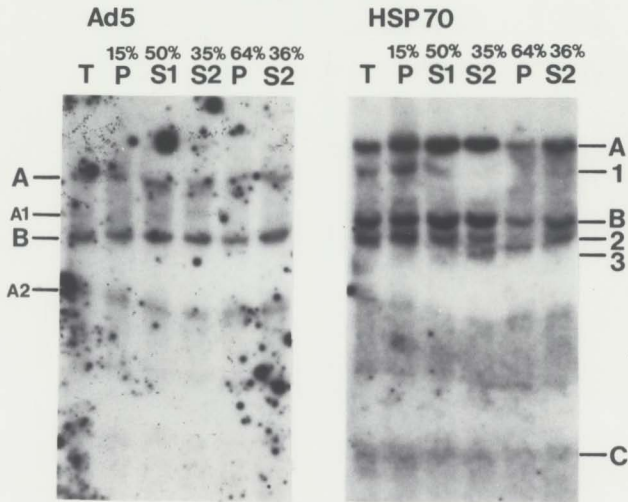
5.3.3.2. Method 2

Nuclear matrix DNA fractions were prepared from 945-C1 cells by Method 2 using *Hind*III, digested to completion with *Hind*III, and analysed by Southern blotting and hybridization with Ad5 DNA. There was no enrichment or depletion of the virus-specific restriction fragments in any of the nuclear matrix DNA fractions prepared by Method 2a ($15\%P/50\%S1/35\%S2$) or Method 2b ($64\%P/36\%S2$), relative to total unfractionated (T) DNA (Fig. 5-5, Ad5). (Slight differences in signal intensity could be accounted for by differences in the amount of DNA loaded per lane.) In some of the fractions, new bands of 6.5 kb (A1) and 4.1 kb (A2) were detected. These corresponded to the sub-bands generated by DNaseI cleavage at HS (hypersensitive) sites in 945-C1 chromatin (Figs. 4-16 and 4-22), and were likely generated by endogenous nucleases with DNase I-like activity. These nucleases would be active during the isolation of nuclei in non-ionic detergent, and during the initial restriction enzyme digestion of the detergent-extracted nuclei.

Figure 5-5 Ad5 and *HSP70* sequences in nuclear matrix DNA fractions from 045-C1 cells.

Nuclear matrix DNA fractions were prepared by Method 2 using *Hind*III. 15 µg of DNA from each fraction was re-digested with *Hind*III, and probed with Ad5 DNA (Ad5). The filter was washed and re-probed with the *HSP70* cDNA (*HSP70*).

945-C1



This filter was re-probed with the *HSP70* cDNA. Again, there was no enrichment or depletion of these sequences in any of the nuclear matrix DNA fractions (Fig. 5-5, *HSP70*). In addition to the *Hind*III-A, -B, and -C fragments, the *HSP70* probe also detected new bands at 11 kb (1), 5.6 kb (2), and 4.6 kb (3). These could be due to either HS sites in the *HSP70* chromatin, or related genes of the *HSP* family with partial homology to this probe. Filters containing DNase I digested 945-C1 and 637-4 chromatin (shown in Figs. 4-16 and 4-12B, respectively) were re-probed with the *HSP70* cDNA (Fig. 5-6). This probe detected the same sub-bands (1-3) in 945-C1 chromatin as in Figure 5-5. These sub-bands were not present in DNA from undigested chromatin (Fig. 5-6, 945-C1, left-end lane), but were generated only as a result of increasing DNase I digestion. These results confirmed that the *HSP70* sub-bands detected in Figure 5-5 were due to HS sites in the *HSP70* chromatin, which were likely cleaved by endogenous nucleases.

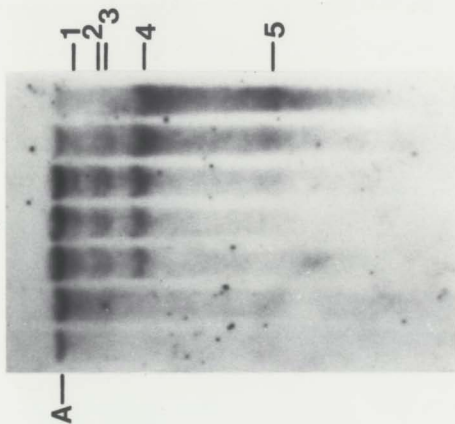
In 637-4 cell DNA, the *HSP70* probe hybridized to the *Hind*III-A (17 kb) fragment only (Fig. 5-6, 637-4, left-end lane). (637-4 is a rat cell line, whereas 945-C1 is a hamster cell line.) Increasing DNase I digestion of 637-4 chromatin generated five new sub-bands (1-5) due to cleavage at HS sites within this fragment.

In 14b cells, there was no enrichment or depletion of the Ad5- or *HSP70*-specific *Hind*III fragments in any of the nuclear matrix DNA fractions prepared by Method 2b (Fig. 5-7). The *HSP70* probe detected the same three sub-bands in 14b cells as in 945-C1 cells (both hamster cell lines). In 293 cells,

Figure 5-6 DNase I digested 945-C1 and 637-4 chromatin.

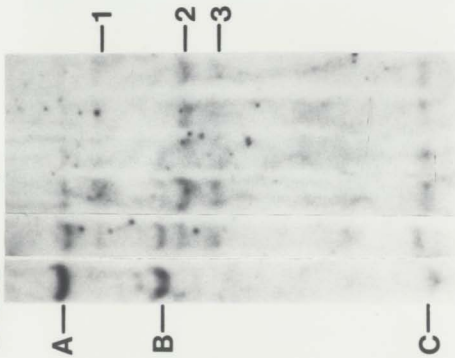
The filters shown in Figures 4-16 (945-C1) and 4-12B (637-4) were washed and re-probed with the *HSP70* cDNA. Arrows indicate increasing DNase I digestion.

637-4



945-C1

DNase I →



similar results were obtained with nuclear matrix DNA fractions prepared by Method 2a using *Hind*III (Fig. 5-8) or *Bam*HI (Fig. 5-9). (Less DNA was loaded in the 14%P and 53%S2 lanes in Figure 5-8, and in the 12%P lane in Figure 5-9.) In *Hind*III digested 293 cell DNA (human), the *HSP70* probe detected at least nine new bands (1-9) ranging from 11-2.1 kb (Fig. 5-8, *HSP70*). Some of these may correspond to related *HSP* genes (e.g. 3, 5, and 9) since they are also present in T DNA, whereas others are likely due to HS sites (e.g. 2 and 4).

The nuclear matrix fractions shown in Figure 5-9 were prepared from 293 cells using *Bam*HI instead of *Hind*III. *Bam*HI does not cleave the Ad5 sequences present in 293 cells, and so generated one virus-specific fragment, of 13 kb (A). The *HSP70* probe detected one major *Bam*III fragment of 7.0 kb (A), plus minor fragments of ~20 kb (1) and 5.6 kb (2), which likely correspond to related *HSP* genes. This probe also detected a 4.1 kb fragment (3), but only in the 12%P fraction. If this represented a related *HSP* gene, then it should have been detected in total unfractionated DNA. If it was generated by cleavage at a HS site, then it should have been detected in the S1 and S2 fractions. Therefore, it is not clear why this band was present only in the 12%P fraction. However, this result was not reproducible, as no extra bands were detected in the P fraction alone when prepared by *Hind*III (Fig. 5-8).

In summary, there was no enrichment or depletion of the integrated viral sequences or the *HSP70* sequences of Ad5-transformed cell lines in any of the nuclear matrix DNA fractions prepared by Method 2, relative to an equal amount of total unfractionated DNA. I have consistently obtained this result in 13

Figure 5-7 Ad5 and *HSP70* sequences in nuclear matrix DNA fractions from 14b cells.

Nuclear matrix DNA fractions were prepared by Method 2b using *HindIII*. 15 μ g of DNA from each fraction was re-digested with *HindIII*, and probed with Ad5 DNA (Ad5). The filter was washed and re-probed with the *HSP70* cDNA (HSP70).

14b

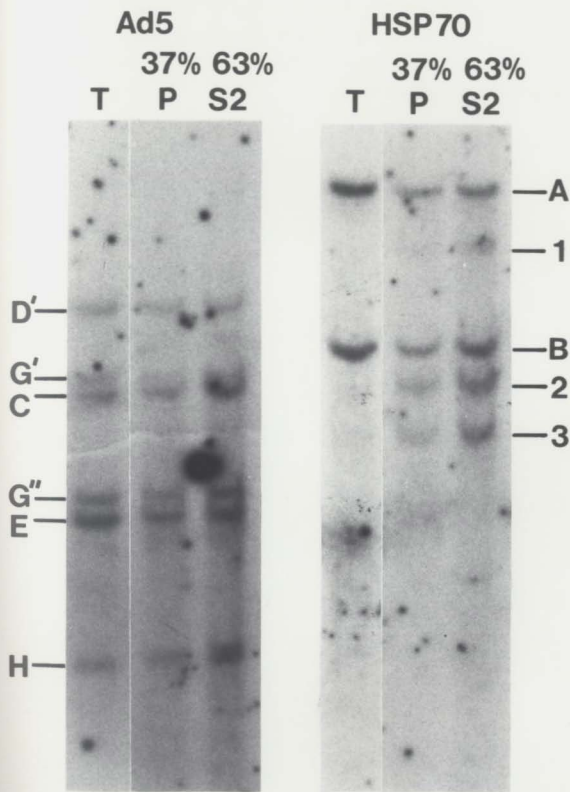


Figure 5-8 Ad5 and *HSP70* sequences in nuclear matrix DNA fractions from 293 cells.

Nuclear matrix DNA fractions were prepared by Method 2a using *Hind*III. ~10 µg of DNA from each fraction was re-digested with *Hind*III, and probed with pXC1 (Ad5). (Less DNA was loaded in the 14%P and 53%S2 lanes.) The filter was washed and re-probed with the *HSP70* cDNA (HSP70).

293

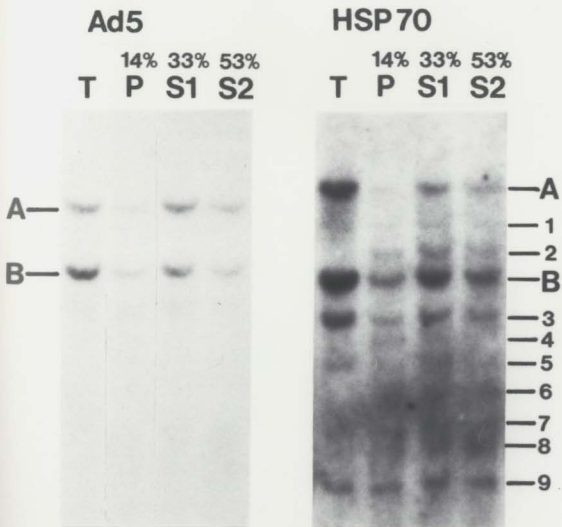
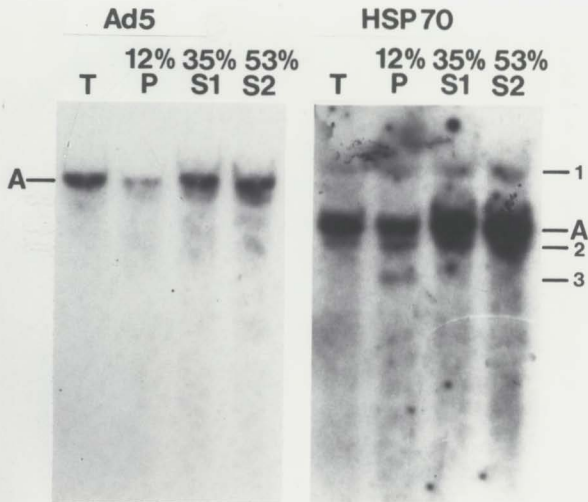


Figure 5-9 Ad5 and *HSP70* sequences in nuclear matrix DNA fractions from 293 cells.

Nuclear matrix DNA fractions were prepared by Method 2a using *Bam*HI. ~10 μ g of DNA from each fraction was re-digested with *Bam*HI, and probed with pXC1 (Ad5). (Less DNA was loaded in the 12%P lane.) The filter was washed and re-probed with the *HSP70* cDNA (*HSP70*).



preparations from all four Ad5-transformed cell lines. These results are consistent with a random organization for the integrated viral sequences and the *HSP70* sequences relative to the nuclear matrix in these cells.

5.3.4. *HSP70* sequences in heat shocked cells

The integrated viral genes and the *HSP70* gene appeared to be transcribed at relatively low levels in Ad5-transformed cells (Figs. 3-6 and 5-1, respectively). Even in non-heat shocked HeLa cells, *i.e.* in the absence of the E1A gene products, the steady-state level of cytoplasmic mRNA was higher than in Ad5-transformed cells (Fig. 5-1). In order to analyse the *HSP70* gene at a higher level of transcription, nuclear matrix DNA fractions were prepared from non-heat shocked and heat shocked HeLa cells, and from heat shocked 945-C1 cells. Cells were heat shocked (43°C) for 15 min, and allowed to recover at 37°C for 45 min. This procedure has been used previously in our laboratory, and results in a dramatic increase in *HSP70* transcription (S. Buch and H.B. Youngusband, unpublished results).

Nuclear matrix DNA fractions were prepared by Method 2a from heat shocked 945-C1 cells, and hybridized with the *HSP70* probe. Again, there was no enrichment or depletion of the *HSP70* sequences in any of the nuclear matrix DNA fractions relative to an equal amount of total unfractionated DNA (Fig. 5-10, 945-C1 HS). Similar results were obtained with heat shocked and non-heat shocked HeLa cells (HeLa HS and NHS, respectively), although comparison between the matrix DNA fractions and total unfractionated DNA (T) was complicated by the presence of HS sites in the *HSP70* chromatin. Therefore, a

total DNA fraction (T^*) was reconstituted by combining 10% of each matrix DNA fraction (taken immediately after fractionation), and DNA purified from T^* as from the other fractions. In both heat shocked and non-heat shocked cells, the higher molecular weight bands, e.g. A, B, 2, and 3, were slightly enriched in the P fractions and depleted in the S1 and S2 fractions relative to T^* . However, this was balanced by an enrichment of the lower molecular weight bands (7-10) in the S1 and S2 fractions. Therefore, the overall level of hybridization with the *HSP70* probe was not significantly increased or decreased in any of the nuclear matrix DNA fractions compared to T^* , in either heat shocked or non-heat shocked cells.

5.4. Discussion

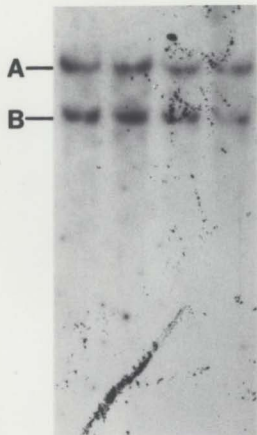
I have attempted to map the position relative to the nuclear matrix of the integrated viral sequences in Ad5-transformed cells. Cells or nuclei were extracted with non-ionic detergent and 2 M NaCl to remove histones and other chromosomal proteins, and the resulting matrix-halo structures digested with a restriction enzyme. The matrix associated and non-associated DNA fractions were separated by centrifugation, and assessed for their content of viral sequences by Southern blotting and hybridization with Ad5 DNA probes. In the four Ad5-transformed cell lines examined, the matrix associated and non-associated fractions were neither enriched nor depleted in Ad5 sequences relative to an equal amount of total unfractionated DNA, implying that these sequences are positioned randomly relative to the nuclear matrix. If the viral sequences were positioned mid-way between the matrix-proximal and matrix-distal ends of a DNA loop, there would be a slight enrichment of these sequences in the matrix associated

Figure 5-10 *HSP70* sequences in nuclear matrix DNA fractions from heat shocked and non-heat shocked cells.

Nuclear matrix DNA fractions were prepared from heat shocked 945 C1 cells (945 C1 HS) and from heat shocked and non-heat shocked HeLa cells (HeLa HS and NHS, respectively) by Method 2a using *HindIII*. T^{*} was reconstituted from 10% of each of fractions P, S1, and S2. 15 μ g of DNA from each fraction was re-digested with *HindIII*, and probed with the *HSP70* cDNA.

945-C1 HS

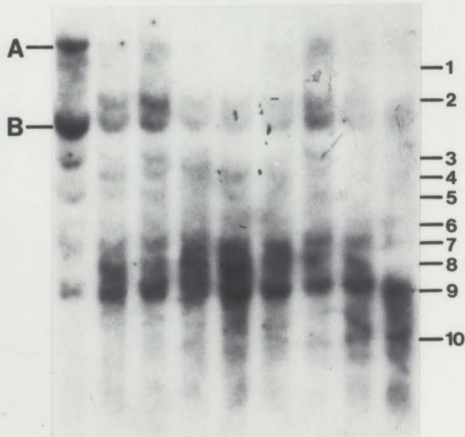
52% 24% 24%
T P S1 S2



HeLa HS

44% 18% 38%

T T* P S1 S2



NHS

34% 23% 43%

T* P S1 S2

DNA fraction when 0-50% of the DNA was detached, and a progressive depletion in this fraction as more DNA was removed (*i.e.* 50-100%). However, the Ad5 sequences were distributed equally between these fractions regardless of the percentage of DNA detached.

These results were unexpected, since the Ad5 E1 region is transcribed in transformed cells, and active genes are generally found to be associated with the nuclear matrix. Before it could be concluded that the viral sequences were actually organized randomly relative to the nuclear matrix, however, it was necessary to demonstrate an enrichment or depletion of another gene in the matrix DNA fractions prepared by these methods, *i.e.* a positive control. Ideally, this gene would have been shown previously to be associated with the nuclear matrix in these cell types. However, previous studies have focussed mainly on developmentally regulated and hormone-inducible genes, and the organization of these genes has not been examined in the cell types studied here. Instead, I analysed the heat- and E1A-inducible *HSP70* genes, which have been shown to be transcribed in HeLa and 293 cells (Kao & Nevins, 1983; Kao *et al.* 1985). In addition, the *HSP70* genes have been reported to be matrix associated in *Drosophila* cells (Mirkovitch *et al.* 1984; Small *et al.* 1985). However, in the Ad5-transformed cell lines, and in heat shocked and non-heat shocked HeLa cells, there was no enrichment or depletion of the *HSP70* sequences in the matrix DNA fractions. Therefore, in the absence of a positive control, it was not possible to conclude that the viral or *HSP70* sequences are positioned randomly relative to the nuclear matrix.

A number of possible explanations were considered for the lack of enrichment or depletion of these active genes in the matrix DNA fractions. If these genes were cell cycle regulated, then they may be associated with the nuclear matrix only during those stages of the cell cycle when they are transcribed. These dynamic matrix attachments would therefore not be detected in unsynchronized cell cultures. However, Kao *et al.* (1985) have shown that the transcription rates of the integrated E1A and E1B genes in 293 cells do not vary during the cell cycle, whereas the *HSP70* gene transcription rate fluctuates only slightly. Another possibility was that an association with the nuclear matrix may be detected only in highly transcribed genes, whereas the *Ad5* and *HSP70* genes appear to be transcribed at relatively low levels in the *Ad5*-transformed cell lines. However, the same result was obtained in non-heat shocked and heat shocked HeLa cells, where the *HSP70* gene is transcribed at higher levels.

In Method 2a, isolated nuclei were incubated with a restriction enzyme at 37°C to cleave the DNA partially before extraction with 2 M NaCl. During this incubation the DNA was in the form of chromatin, and so active sequences may have been preferentially susceptible to digestion by endogenous nucleases with DNase I-like activity. However, there was no preferential loss of the active viral or *HSP70* sequences relative to undigested DNA as determined by the overall levels of hybridization, indicating that the level of endogenous nuclease activity was not sufficient to degrade active sequences. In some cases, however, this activity was sufficient to generate discrete sub-bands by cleavage at the same HS sites as recognized by DNase I. In both heat shocked and non-heat shocked HeLa

cells, the matrix associated DNA fractions were slightly enriched in the higher molecular weight *HSP70* fragments, and the non-associated DNA fractions were slightly enriched in the lower molecular weight sub-bands generated by cleavage at the HS sites. However, these differences were relatively small, and may reflect differences in chromatin solubility related to fragment size, rather than specific matrix attachments. For example, Rose & Garrard (1984) found that increasing MNase digestion "processed" insoluble high molecular weight chromatin (higher oligonucleosomes) into soluble mono- and dinucleosomes (section 1.1.4).

Studies by Small & Vogelstein (1985) suggest that attachment to the nuclear matrix may not be required for transcription. These workers examined the organization of the *Drosophila* 7F locus relative to the nuclear matrix prepared by 2 M NaCl extraction, and found that one of the 16 non-associated *EcoRI* fragments analysed contains transcribed sequences. Also, the *MARs* detected by LIS extraction are in some cases located in the non-transcribed flanking sequences, while the transcribed sequences are detached. In the case of the integrated Ad5 sequences, therefore, the matrix attachment points may be located in the flanking cellular DNA, beyond the region analysed. The fact that the boundaries of the DNase I sensitive chromatin domain surrounding these sequences were also not detected within the analysed region (Chapter 4) supports this, since it has been proposed that these boundaries are defined by matrix attachment points. However, in the studies described above, the detached sequences are absent or significantly depleted in the matrix associated DNA fraction, whereas the integrated Ad5 sequences and *HSP70* sequences analysed here were neither

depleted nor enriched in this fraction, consistent with a random organization relative to the nuclear matrix.

Both methods used in this study to prepare nuclear matrix DNA fractions have been used previously to demonstrate an association between active sequences and the nuclear matrix. For example, the matrix associated DNA fraction prepared by Method 1 is enriched in the integrated viral sequences in polyoma- and avian sarcoma virus-transformed rat cells (Cook *et al.* 1982), and this fraction prepared by Method 2 is enriched in the chicken histone genes (Dalton *et al.* 1986). Studies in this laboratory have shown that in Ad5-infected HeLa cells, the viral DNA is associated with the nuclear matrix prepared by Method 1 (Younghusband & Maundrell, 1982) and Method 2 (Younghusband, 1985). However, others have obtained results similar to those obtained in this study, apparently due to differences in the nuclear matrix isolation conditions (*e.g.* see Kirov *et al.* 1984; Razin *et al.* 1985). Since minor differences in isolation conditions can result in different types of nuclear matrix structures, it is likely that these minor differences can also affect the interactions between the residual matrix and chromosomal DNA.

Although the results obtained in this study suggest that the integrated Ad5 sequences and the *HSP70* genes are organized randomly relative to the nuclear matrix, in the absence of a positive control it is not possible to make a firm conclusion regarding the organization of these sequences. Although the evidence for an association between active sequences and the nuclear matrix is less than conclusive, recent studies have provided more compelling evidence for a non-

random organization of the DNA loops relative to the nuclear matrix. In light of this evidence, it is possible that the results obtained in this study may be due to disruption of specific matrix-DNA interactions under the conditions used to prepare the nuclear matrix DNA fractions.

REFERENCES

- Adolph, K.W., Cheng, S.M. & Laemmli, U.K. (1977). Role of non-histone proteins in metaphase chromosome structure. *Cell* **12**, 805-816.
- Aebi, U., Cohn, J., Buhle, L. & Gerace, L. (1986). The nuclear lamina is a meshwork of intermediate-type filaments. *Nature* **323**, 560-564.
- Aelen, J.M.A., Opstelten, R.J.G. & Wanka, F. (1983). Organization of DNA replication in *Physarum polycephalum*. Attachment of origins of replicons and replication forks to the nuclear matrix. *Nucleic Acids Research* **11**, 1181-1195.
- Aiello, L., Guilfoyle, R., Huebner, K. & Weinmann, R. (1979). Adenovirus 5 DNA sequences present and RNA sequences transcribed in transformed human embryo kidney cells (HEK-Ad5 or 293). *Virology* **94**, 460-469.
- Albright, S.C., Wiseman, J.M., Lange, R.A. & Garrard, W.T. (1980). Subunit structures of different electrophoretic forms of nucleosomes. *Journal of Biological Chemistry* **255**, 3673-3684.
- Alestrom, P., Akusjarvi, G., Perricaudet, M., Mathews, M.B., Klessig, D.F. & Pettersson, U. (1980). The gene for polypeptide IX of adenovirus type 2 and its unspliced messenger RNA. *Cell* **19**, 671-681.
- Allan, M., Zhu, J., Montague, P. & Paul, J. (1984). Different response of multiple ϵ -globin cap sites to cis- and trans-acting controls. *Cell* **38**, 399-407.
- Alonso, W.R., Ferris, R.C., Zhang, D. & Nelson, D.A. (1987). Chicken erythrocyte β -globin chromatin: enhanced solubility is a direct consequence of induced histone hyperacetylation. *Nucleic Acids Research* **15**, 9325-9337.
- Alvey, M.C., Tsai, M. & O'Malley, B.W. (1984). DNase I sensitive domain of the gene coding for the glycolytic enzyme glyceraldehyde-3-phosphate dehydrogenase. *Biochemistry* **23**, 2309-2314.
- Anderson, J.N., Vanderbilt, J.N., Lawson, G.M., Tsai, M. & O'Malley, B.W. (1983). Chromatin structure of the ovalbumin gene family in the chicken oviduct. *Biochemistry* **22**, 21-30.

- Ashburner, M. (1972). Puffing patterns in *Drosophila melanogaster* and related species. In: *Results and Problems in Cell Differentiation* vol 4, ed. Beermann, W., pp. 102-151. Springer, Berlin.
- Babiss, L.E., Fisher, P.B. & Ginsberg, H.S. (1984). Effect on transformation of mutations in the early region 1b-encoded 21- and 55-kilodalton proteins of adenovirus 5. *Journal of Virology* **52**, 389-395.
- Ball, D.J., Gross, D.S. & Garrard, W.T. (1983). 5-methylcytosine is localized in nucleosomes that contain histone H1. *Proceedings of the National Academy of Sciences USA* **80**, 5490-5494.
- Barker, D.D. & Berk, A.J. (1987). Adenovirus proteins from both E1b reading frames are required for transformation of rodent cells by viral infection and DNA transfection. *Virology* **156**, 107-121.
- Barrack, E.R. & Coffey, D.S. (1982). Biological properties of the nuclear matrix: steroid hormone binding. *Recent Progress in Hormone Research* **38**, 133-195.
- Barret, P., Clark, L. & Hay, R.T. (1987). A cellular protein binds to a conserved sequence in the adenovirus type 2 enhancer. *Nucleic Acids Research* **15**, 2719-2735.
- Barsom, J. & Berg, P. (1985). Simian virus 40 minichromosomes contain torsionally strained DNA molecules. *Molecular and Cellular Biology* **5**, 3018-3057.
- Barsom, J. & Varshavsky, A. (1985). Preferential location of variant nucleosomes near the 5'-end of the mouse dihydrofolate reductase gene. *Journal of Biological Chemistry* **260**, 7688-7697.
- Basler, J., Hastie, N.D., Pietras, D., Matsui, S., Sandberg, A.A. & Berezney, R. (1981). Hybridization of nuclear matrix attached deoxyribonucleic acid fragments. *Biochemistry* **20**, 6921-6929.
- Beermann, W. (1952). Chromomerenkonstanz und spezifische Modifikationen der Chromosomenstruktur in der Entwicklung und Organdifferenzierung von *Chironomus tentans*. *Chromosoma* **5**, 130-198.
- Bellard, M., Dretzen, G., Bellard, F., Oudet, P. & Chambon, P. (1982). Disruption of the typical nucleosome structure in a 2500 base-pair region at

- the 5' end of the actively transcribed ovalbumin gene. *EMBO J.* **1**, 223-230.
- Bellard, M., Gannon, F. & Chambon, P. (1978). Nucleosome structure III: The structure and transcriptional activity of the chromatin containing the ovalbumin and globin genes in chicken oviduct nuclei. *Cold Spring Harbor Symposium* **42**, 779-791.
- Beltz, G.A. & Flint, S.J. (1979). Inhibition of HeLa cell protein synthesis during adenovirus infection: restriction of cellular messenger RNA sequences to the nucleus. *Journal of Molecular Biology* **131**, 353-373.
- Benyajati, C. & Worcel, A. (1976). Isolation, characterization, and structure of the folded interphase genome of *Drosophila melanogaster*. *Cell* **9**, 393-407.
- Berezney, R. (1984). Organization and function of the nuclear matrix. In: *Chromosomal Non-histone Proteins*, ed. Hnilica, L.S., Vol. **4**, pp 119-180. CRC Press, Boca Raton.
- Berezney, R. & Buchholtz, L.A. (1981). Dynamic association of replicating DNA fragments with the nuclear matrix of regenerating rat liver. *Experimental Cell Research* **132**, 1-13.
- Berezney, R. & Coffey, D.S. (1974). Identification of a nuclear protein matrix. *Biochemical and Biophysical Research Communications* **60**, 1410-1417.
- Berezney, R. & Coffey, D.S. (1975). Nuclear protein matrix: association with newly synthesized DNA. *Science* **189**, 291-293.
- Berezney, R. & Coffey, D.S. (1977). Nuclear matrix: isolation and characterization of a framework structure from rat liver nuclei. *Journal of Cell Biology* **73**, 616-637.
- Berk, A.J. (1986). Adenovirus promoters and E1a transactivation. *Annual Review of Genetics* **20**, 45-79.
- Berk, A.J., Lee, F., Harrison, T., Williams, J. & Sharp, P.A. (1979). Pre-early adenovirus 5 gene product regulates synthesis of early messenger RNAs. *Cell* **17**, 1935-1944.

- Bernards, R., de Leeuw, M.G.W., Houweling, A. & van der Eb, A.J. (1986). Role of the adenovirus early region 1b tumor antigens in transformation and lytic infection. *Virology* **150**, 126-139.
- Berros, M., Osheroff, N. & Fisher, P.A. (1985). *In situ* localization of DNA topoisomerase II, a major polypeptide component of the *Drosophila* nuclear matrix fraction. *Proceedings of the National Academy of Sciences USA* **82**, 4142-4146.
- Binger, M.H., Flint, S.J. & Rekosh, D.M. (1982). Expression of the gene encoding the adenovirus DNA terminal protein precursor in productively infected and transformed cells. *Journal of Virology* **42**, 488-501.
- Blank, G., Chen, S. & Pollack, R. (1984). DNase I sensitivity of integrated simian virus 40 DNA. *Molecular and Cellular Biology* **4**, 559-562.
- Bloom, K.S. & Anderson, J.N. (1978). Fractionation of hen oviduct chromatin into transcriptionally active and inactive regions after selective micrococcal nuclease digestion. *Cell* **15**, 141-150.
- Bloom, K.S. & Anderson, J.N. (1979). Conformation of ovalbumin and globin genes during differential gene expression. *Journal of Biological Chemistry* **254**, 10532-10539.
- Bloom, K.S. & Anderson, J.N. (1982). Hormonal regulation of the conformation of the ovalbumin gene in chicken oviduct chromatin. *Journal of Biological Chemistry* **257**, 13018-13027.
- Borrelli, E., Hen, R. & Chambon, P. (1984). Adenovirus-2 E1A products repress enhancer-induced stimulation of transcription. *Nature* **312**, 608-612.
- Borrelli, E., Hen, R., Wasylyk, C., Wasylyk, B. & Chambon, P. (1986). The immunoglobulin heavy chain enhancer is stimulated by the adenovirus type 2 E1A products in fibroblasts. *Proceedings of the National Academy of Sciences USA* **83**, 2846-2849.
- Bos, J.L., Polder, L.J., Bernards, R., Schrier, P.L., van den Elsen, P.J., van der Eb, A.J. & van Ormondt, H. (1981). The 2.2 kb E1b mRNA of human ad12 and ad5 codes for two tumor antigens starting at different AUG triplets. *Cell* **27**, 121-131.

- Bouvier, D., Hubert, J., Seve, A. & Bouteille, M. (1982). RNA is responsible for the three-dimensional organization of nuclear matrix proteins in HeLa cells. *Biology of the Cell* **43**, 143-146.
- Braithwaite, A.W., Cheetham, B.F., Li, P., Parish, C.R., Waldon-Stevens, L.K. & Bellet, A.J.D. (1983). Adenovirus-induced alterations of the cell growth cycle: A requirement for expression of E1A but not E1B. *Journal of Virology* **45**, 192-199.
- Brasch, K. (1982). Fine structure and localization of the nuclear matrix in situ. *Experimental Cell Research* **140**, 161-171.
- Breindl, M., Harbers, K. & Jaenisch, R. (1984). Retrovirus induced lethal mutation in collagen I gene of mice is associated with an altered chromatin structure. *Cell* **38**, 9-16.
- Brotherton, T.W. & Ginder, G.D. (1986). Preferential in vitro binding of high mobility group proteins 14 and 17 to nucleosomes containing active and DNase I sensitive single-copy genes. *Biochemistry* **25**, 3447-3454.
- Buckler-White, A.J., Humphrey, G.W. & Pigiet, V. (1980). Association of polyoma T antigen and DNA with the nuclear matrix from lytically infected 3T6 cells. *Cell* **22**, 37-46.
- Burch, J.B.E. & Weintraub, H. (1983). Temporal order of chromatin structural changes associated with activation of the major chicken vitellogenin gene. *Cell* **33**, 65-76.
- Bardon, R.H., Qureshi, M. & Adams, R.L.P. (1985). Nuclear matrix-associated DNA methylase. *Biochimica et Biophysica Acta* **825**, 70-79.
- Burke, B. & Gerace, L. (1986). A cell free system to study reassembly of the nuclear envelope at the end of mitosis. *Cell* **44**, 630-652.
- Callan, H.G. (1982). Lampbrush chromosomes. *Proceedings of the Royal Society of London* **B214**, 417-448.
- Capco D.G. & Penman, S. (1983). Mitotic architecture of the cell: the filament networks of the nucleus and cytoplasm. *Journal of Cell Biology* **96**, 806-906.
- Capco, D.G., Wan, K.M. & Penman, S. (1982). The nuclear matrix: three-

- dimensional architecture and protein composition. *Cell* **29**, 847-858.
- Caplan, A., Kimura, T., Gould, H. Allan, J. (1987). Perturbation of chromatin structure in the region of the adult beta-globin gene in chicken erythrocyte chromatin. *Journal of Molecular Biology* **193**, 57-70.
- Carri, M.T., Micheli, G., Graziano, E., Pace, T. & Buongiorno-Nardelli, M. (1986). The relationship between chromosomal origins of replication and the nuclear matrix during the cell cycle. *Experimental Cell Research* **164**, 426-436.
- Chaly, N., Bladon, T., Setterfield, G., Little, J.E., Kaplan, J.G. & Brown, D.L. (1984). Changes in distribution of nuclear matrix antigens during the mitotic cell cycle. *Journal of Cell Biology* **99**, 661-671.
- Chaly, N., Little, J.E. & Brown, D.L. (1985). Localization of nuclear antigens during preparation of nuclear matrices *in situ*. *Canadian Journal of Biochemistry and Cell Biology* **63**, 641-653.
- Chatterjee, P.K. & Flint, S.J. (1986). Partition of E1a proteins between soluble and structural fractions of adenovirus-infected and -transformed cells. *Journal of Virology* **60**, 1018-1026.
- Chinnadurai, G. (1983). Adenovirus lp^+ locus codes for the 19-kd tumor antigen that plays an essential role in cell transformation. *Cell* **33**, 759-766.
- Chiswell, D.J., Gillespie, D.A. & Wyke, J.A. (1982). The changes in proviral chromatin structure that accompany morphological variation in avian sarcoma virus-infected rat cells. *Nucleic Acids Research* **10**, 3967-3980.
- Ciejek, E.M., Nordstrom, J.L., Tsai, M. & O'Malley, B. (1982). Ribonucleic acid precursors are associated with the chick oviduct nuclear matrix. *Biochemistry* **21**, 4945-4953.
- Ciejek, E.M., Tsai, M. & O'Malley, B. (1983). Actively transcribed genes are associated with the nuclear matrix. *Nature* **306**, 607-609.
- Cockerill, P.N. & Garrard, W.T. (1986). Chromosomal loop anchorage of the kappa immunoglobulin gene occurs next to the enhancer in a region containing topoisomerase II sites. *Cell* **44**, 273-282.

- Cockerill, F.N., Yuen, M. & Garrard, W.T. (1987). The enhancer of the immunoglobulin heavy chain locus is flanked by presumptive chromosomal loop anchorage elements. *Journal of Biological Chemistry* **262**, 5394-5397.
- Cook, P.R. & Brazell, I.A. (1975). Supercoils in human DNA. *Journal of Cell Science* **10**, 261-279.
- Cook, P.R. & Brazell, I.A. (1976). Conformational constraints in nuclear DNA. *Journal of Cell Science* **22**, 287-302.
- Cook, P.R. & Brazell, I.A. (1980). Mapping sequences in loops of nuclear DNA by their progressive detachment from the nuclear cage. *Nucleic Acids Research* **8**, 2895-2906.
- Cook, P.R., Brazell, I.A. & Jost, E. (1976). Characterization of nuclear structures containing superhelical DNA. *Journal of Cell Science* **22**, 303-321.
- Cook, P.R., Lang, J., Hayday, A., Lania, L., Fried, M., Chiswell, D.J. & Wyke, J.A. (1982). Active viral genes in transformed cells lie close to the nuclear cage. *EMBO Journal* **1**, 417-452.
- Costlow, N.A., Simon, J.A. & Lis, J.T. (1985). A hypersensitive site in *hsp70* chromatin requires adjacent not internal DNA sequence. *Nature* **313**, 147-149.
- Cotten, M., Bresnahan, D., Thompson, S., Sealy, L. & Chalkley, R. (1986). Novobiocin precipitates histones at concentrations normally used to inhibit eukaryotic type II topoisomerase. *Nucleic Acids Research* **14**, 3671-3686.
- Courtois, G. & Berk, A. (1984). Adenovirus E1A protein activation of an integrated viral gene. *EMBO Journal* **3**, 1145-1149.
- Dalton, S., Younghusband, H.B. & Wells, J.R.E. (1986). Chicken histone genes retain nuclear matrix association throughout the cell cycle. *Nucleic Acids Research* **14**, 6507-6523.
- Davie, J.R. & Candido, E.P.M. (1978). Acetylated histone H4 is preferentially associated with template-active chromatin. *Proceedings of the National Academy of Sciences USA* **75**, 3574-3577.
- Davie, J.R. & Nickel, B.E. (1987). The ubiquitinated histone species are

- enriched in histone H1-depleted chromatin regions. *Biochimica et Biophysica Acta* **909**, 183-189.
- Davie, J.R. & Saunders, C.A. (1981). Chemical composition of nucleosomes among domains of calf thymus chromatin differing in micrococcal nuclease sensitivity and solubility properties. *Journal of Biological Chemistry* **256**, 12574-12580.
- Davies, H.G. & Haynes, M.E. (1976). Electron-microscope observations on cell nuclei in various tissues of a teleost fish: The nucleolus-associated monolayer of chromatin structural units. *Journal of Cell Science* **21**, 315-327.
- Davis, L.I. & Blobel, G. (1986). Identification and characterization of a nuclear pore complex protein. *Cell* **45**, 699-709.
- DeBernardin, W., Koller, T. & Sogo, J.M. (1986). Structure of *in vivo*-transcribing chromatin as studied in simian virus 40 minichromosomes. *Journal of Molecular Biology* **191**, 469-482.
- Deppert, W. (1979). Simian virus 40 T- and U- antigen: immunological characterization and localization in different nuclear subfractions of simian virus 40-transformed cells. *Journal of Virology* **29**, 576-586.
- Derenzini, M., Hernandez-Verdun, D. & Bouteille, M. (1981). Subunit configuration of rat hepatocyte chromatin fixed *in situ*, as visualized in thin sections selectively stained for DNA. *Biology of the Cell* **41**, 161-164.
- Derenzini, M., Hernandez-Verdun, D. & Bouteille, M. (1982). Visualization *in situ* of extended DNA filaments in nucleolar chromatin of rat hepatocytes. *Experimental Cell Research* **141**, 463-469.
- Derenzini, M., Hernandez-Verdun, D., Farabegoli, F., Pession, A. & Novello, F. (1987). Structure of ribosomal genes of mammalian cells *in situ*. *Chromosoma* **95**, 63-70.
- Derenzini, M., Pession, A., Licastro, F. & Novello, F. (1985). Electron-microscopical evidence that ribosomal chromatin of human circulating lymphocytes is devoid of histones. *Experimental Cell Research* **157**, 50-62.
- Dery, C.V., Toth, M., Brown, M., Horvath, J., Allaire, S. & Weber, J.M. (1985). The structure of adenovirus chromatin in infected cells. *Journal of*

general Virology **66**, 2671-2684.

- Deuring, R., Winterhoff, U., Tamanoi, F., Stabel, S. & Doerfler, W. (1981). Site of linkage between adenovirus type 12 and cell DNAs in hamster tumor line CLAC3. *Nature* **293**, 81-84.
- Dijkwel, P.A., Mullenders, L. & Wanka, F. (1979). Analysis of the attachment of replicating DNA to a nuclear matrix in mammalian interphase nuclei. *Nucleic Acids Research* **6**, 219-230.
- Dijkwel, P.A., Wenink, P.W. & Poddighe, J. (1986). Permanent attachment of replication origins to the nuclear matrix in BHK-cells. *Nucleic Acids Research* **14**, 3241-3249.
- Doerfler, W. (1982). Uptake, fixation and expression of foreign DNA in mammalian cells: The organization of integrated adenovirus sequences. *Current Topics in Microbiology and Immunology* **101**, 127-194.
- Doerfler, W. (1983). DNA methylation and gene activity. *Annual Review of Biochemistry* **52**, 93-124.
- Downey, J.F., Rowe, D.T., Bacchetti, S., Graham, F.L. & Bayley, S.T. (1983). Mapping of a 14,000-dalton antigen to early region 4 of the human adenovirus 5 genome. *Journal of Virology* **45**, 514-523.
- Drew, H.R. & Travers, A. (1984). DNA structural variations in the E.coli *tyrT* promoter. *Cell* **37**, 491-502.
- Earshaw, W.C., Halligan, B., Cooke, C.A., Heck, M.M.S. & Liu, L.F. (1985). Topoisomerase II is a structural component of mitotic chromosome scaffolds. *Journal of Cell Biology* **100**, 1706-1715.
- Earshaw, W.C. & Heck, M.M.S. (1985). Localization of topoisomerase II in mitotic chromosomes. *Journal of Cell Biology* **100**, 1716-1725.
- Earshaw, W.C. & Laemmli, U.K. (1983). Architecture of metaphase chromosomes and chromosome scaffolds. *Journal of Cell Biology* **96**, 84-93.
- Elgin, S.C.R. (1984). Anatomy of hypersensitive sites. *Nature* **309**, 213-214.
- Emerson, B.M. & Felsenfeld, G. (1984). Specific factor conferring nuclease

- hypersensitivity at the 5' end of the chicken adult β -globin gene. *Proceedings of the National Academy of Sciences USA* **81**, 95-99.
- Emerson, B.M., Lewis, C.D. & Felsenfeld, G. (1985). Interaction of specific nuclear factors with the nuclease-hypersensitive region of the chicken adult β -globin gene: nature of the binding domain. *Cell* **41**, 21-30.
- Ezoe, H., LaiFatt, R.B. & Mak, S. (1981). Degradation of intracellular DNA in KB cells infected with cyt mutants of human adenoviruses. *Journal of Virology* **40**, 20-27.
- Fakan, S. (1978). High resolution autoradiography studies on chromatin functions. In: *The Cell Nucleus* vol 5, ed. Busch, H., pp. 3-53. Academic Press, New York.
- Felber, B.K., Gerber-Huber, S., Meier, C., May, F.E.B., Westley, B., Weber, P. & Ryffel, G.U. (1981). Quantitation of DNase I sensitivity in *Xenopus* chromatin containing active and inactive globin, albumin and vitellogenin genes. *Nucleic Acids Research* **9**, 2455-2474.
- Feldman, L.T. & Nevins, J.R. (1983). Localization of the adenovirus E1a protein, a positive acting transcription factor, in infected cells. *Molecular and Cellular Biology* **3**, 829-838.
- Felsenfeld, G. & McGhee, J.D. (1986). Structure of the 30 nm chromatin fiber. *Cell* **44**, 375-377.
- Ferguson, B., Krippel, B., Andrisani, O., Jones, N., Westphal, H. & Rosenberg, M. (1985). The E1a 13S and 12S mRNA products made in *Escherichia coli* both function as nucleus-localized transcription activators but do not directly bind DNA. *Molecular and Cellular Biology* **5**, 2653-2661.
- Feuerstein, N., Chan, P.K. & Mond, J.J. (1988). Identification of numatrin, the nuclear matrix protein associated with induction of mitogenesis, as the nucleolar protein B23. *Journal of Biological Chemistry* **263**, 10608-10612.
- Feuerstein, N. & Mond, J.J. (1987). "Numatrin", a nuclear matrix protein associated with induction of proliferation in B lymphocytes. *Journal of Biological Chemistry* **262**, 11389-11397.
- Fey, E.G., Krochmalnic, G. & Penman, S. (1986). The nonchromatin

- sub-structures of the nucleus: the ribonucleoprotein (RNP)-containing and RNP-depleted matrices analysed by sequential fractionation and resinless section electron microscopy. *Journal of Cell Biology* **102**, 1654-1665.
- Fey, E.G., Wan, K.M. & Penman, S. (1984). Epithelial cytoskeletal framework and nuclear matrix-intermediate filament scaffold: three-dimensional organization and protein composition. *Journal of Cell Biology* **98**, 1973-1984.
- Fields, A.P., Kaufmann, S.H. & Shaper, J.H. (1986). Analysis of the internal nuclear matrix. Oligomers of a 38 kD nucleolar polypeptide stabilized by disulphide bonds. *Experimental Cell Research* **164**, 139-153.
- Finch, J.T. & Klug, A. (1976). Solenoidal model for superstructure in chromatin. *Proceedings of the National Academy of Sciences USA* **73**, 1897-1901.
- Fisher, D.Z., Chaudhury, N. & Blobel, G. (1986). cDNA sequencing of nuclear lamins A and C reveals primary and secondary structural homology to intermediate filament proteins. *Proceedings of the National Academy of Sciences USA* **83**, 6450-6454.
- Fisher, P.A., Berrios, M. & Blobel, G. (1982). Isolation and characterization of a proteinaceous subnuclear fraction composed of nuclear matrix, peripheral lamina, and nuclear pore complexes from embryos of *Drosophila melanogaster*. *Journal of Cell Biology* **92**, 674-686.
- Flint, S.J. (1986). Regulation of adenovirus mRNA formation. *Advances in Virus Research* **31**, 169-228.
- Flint, S.J., Sambrook, J., Williams, J.F. & Sharp, P.A. (1976). Viral nucleic acid sequences in transformed cells IV. A study of the sequences of adenovirus 5 DNA and RNA in four lines of adenovirus 5-transformed rodent cells using specific fragments of the viral genome. *Virology* **72**, 456-470.
- Flint, S.J. & Weintraub, H.M. (1977). An altered subunit configuration associated with the actively transcribed DNA of integrated adenovirus genes. *Cell* **12**, 783-794.
- Foe, V.E. (1978). Modulation of ribosomal RNA synthesis in *Oncopeltus*

- fasciatus*: an electron microscope study of the relationship between changes in chromatin structure and transcriptional activity. *Cold Spring Harbor Symposium* **42**, 723-740.
- Foe, V.E., Wilkinson, L.E. & Laird, C.D. (1976). Comparative organization of active transcription units in *Oncopeltus fasciatus*. *Cell* **9**, 131-146.
- Franke, W.W., Scheer, U., Trendelenburg, M.F., Spring, H. & Zentgraf, H. (1976). Absence of nucleosomes in transcriptionally active chromatin. *Cytobiologie* **13**, 401-434.
- Freeman, A.E., Black, P.H., Vanderpool, E.A., Henry, P.H., Austin, J.B. & Huebner, R.J. (1967). Transformation of primary rat embryo cells by adenovirus type 2. *Proceedings of the National Academy of Sciences USA* **58**, 1205-1212.
- Gahlmann, R., Leister, R., Vardimon, L. & Doerfler, W. (1982). Patch homologies in the integration of adenovirus DNA in mammalian cells. *EMBO Journal* **1**, 1101-1104.
- Gahlmann, R., Schulz, M. & Doerfler, W. (1984). Low molecular weight RNAs with homologies to cellular DNA at sites of adenovirus DNA insertion in hamster or mouse cells. *EMBO Journal* **3**, 3263-3269.
- Gallimore, P.H., Sharp, P.A. & Sambrook, J. (1974). Viral DNA in transformed cells: II. A study of the sequences of adenovirus 2 DNA in nine lines of transformed rat cells using specific fragments of the viral genome. *Journal of Molecular Biology* **89**, 49-72.
- Garel, A. & Axel, R. (1976). Selective digestion of transcriptionally active ovalbumin genes from oviduct nuclei. *Proceedings of the National Academy of Sciences USA* **73**, 3966-3970.
- Gariglio, P., Llopis, R., Oudet, P. & Chambon, P. (1979). The template of the isolated native simian virus 40 transcriptional complex is a minichromosome. *Journal of Molecular Biology* **131**, 75-105.
- Gasser, S.M. & Laemmli, U.K. (1986a). The organization of chromatin loops: characterization of a scaffold attachment site. *EMBO Journal* **5**, 511-518.
- Gasser, S.M. & Laemmli, U.K. (1986b). Cohabitation of scaffold binding

- regions with upstream/enhancer elements of three developmentally regulated genes of *D. melanogaster*. *Cell* **46**, 521-530.
- Gasser, S.M. & Laemmli, U.K. (1987). A glimpse at chromosomal order. *Trends in Genetics* **3**, 16-22.
- Gasser, S.M., Laroche, T., Falquet, J., Boy de la Tour, E. & Laemmli, U.K. (1986). Metaphase chromosome structure: involvement of topoisomerase II. *Journal of Molecular Biology* **188**, 613-629.
- Gaynor, R.B. & Berk, A.J. (1983). Cis-acting induction of adenovirus transcription. *Cell* **33**, 683-693.
- Gaynor, R.B., Hillman, D. & Berk, A.J. (1984). Adenovirus early region 1A protein activates transcription of a nonviral gene introduced into mammalian cells by infection or transfection. *Proceedings of the National Academy of Sciences USA* **81**, 1193-1197.
- Gazit, B., Panet, A. & Cedar, H. (1980). Reconstitution of a deoxyribonuclease I-sensitive structure on active genes. *Proceedings of the National Academy of Sciences USA* **77**, 1787-1790.
- Georgatos, S.D. & Blobel, G. (1987). Lamin B constitutes an intermediate filament attachment site at the nuclear envelope. *Journal of Cell Biology* **105**, 117-125.
- Gerace, L. & Blobel, G. (1980). The nuclear envelope lamina is reversibly depolymerized during mitosis. *Cell* **19**, 277-287.
- Gerace, L., Blum, A. & Blobel, G. (1978). Immunocytochemical localization of the major polypeptides of the nuclear pore complex-lamina fraction. *Journal of Cell Biology* **79**, 546-566.
- Gerace, L., Ottaviano, Y. & Kondor-Koch, C. (1982). Identification of a major polypeptide of the nuclear pore complex. *Journal of Cell Biology* **95**, 826-837.
- Gerard, R.D., Montelone, B.A., Walter, C.F., Innis, J.W. & Scott, W.A. (1985). Role of specific simian virus 40 sequences in the nuclease-sensitive structure in viral chromatin. *Molecular and Cellular Biology* **5**, 52-58.
- Gilead, Z., Jeng, Y., Wold, W.S.M., Sugawara, K., Rho, H.M., Harter, M.L.

- & Green, M. (1976). Immunological identification of two adenovirus 2-induced early proteins possibly involved in cell transformation. *Nature* **264**, 263-266.
- Gingeras, T.R., Sciaky, D., Gelinas, R.E., Bing-Dong, J., Yen, C.E., Kelly, M.M., Bullock, P.A., Parsons, B.L., O'Neill, K.E. & Roberts, R.J. (1982). Nucleotide sequences from the adenovirus-2 genome. *Journal of Biological Chemistry* **257**, 13475-13491.
- Glenn, G.M. & Ricciardi, R.P. (1985). Adenovirus 5 early region 1A host range mutants hr3, hr4, and hr5 contain point mutations which generate single amino acid substitutions. *Journal of Virology* **56**, 66-74.
- Glikin, G.C., Ruberti, I. & Worcel, A. (1984). Chromatin assembly in *Xenopus* oocytes: in vitro studies. *Cell* **37**, 33-41.
- Goldman, R.D., Chang, C. & Williams, J.F. (1975). Properties and behavior of hamster embryo cells transformed by human adenovirus type 5. *Cold Spring Harbor Symposium* **39**, 601-614.
- Gottesfeld, J.M. (1986). Novobiocin inhibits RNA polymerase III transcription *in vitro* by a mechanism distinct from DNA topoisomerase II. *Nucleic Acids Research* **14**, 2075-2088.
- Graham, F.L., Abrahams, P.J., Mulder, C., Heijneker, H.L., Warnaar, S.O., de Vries, F.A.J., Fiers, W. & van der Eb, A.J. (1975). Studies on in vitro transformation by DNA and DNA fragments of human adenoviruses and simian virus 40. *Cold Spring Harbor Symposium* **39**, 637-650.
- Graham, F.L., Harrison, T. & Williams, J. (1978). Defective transforming capacity of adenovirus type 5 host-range mutants. *Virology* **86**, 10-21.
- Graham, F.L., Smiley, J., Russell, W.C. & Nairn, R. (1977). Characterization of a human cell line transformed by DNA from human adenovirus type 5. *Journal of general Virology* **36**, 59-72.
- Green, M., Brackmann, H., Cartas, M.A. & Matsuo, T. (1982). Identification and purification of a protein encoded by the human adenovirus type 2 transforming region. *Journal of Virology* **42**, 30-41.
- Green, M., Mackey, J.K., Wold, W.S.H. & Rigden, P. (1979). Thirty-one human adenovirus serotypes (Ad1-Ad31) form five groups (A-E) based on

- DNA genome homologies. *Virology* **93**, 481-492.
- Green, M., Pinn, M., Kimes, R., Wensink, P.C., MacLattie, L.A. & Thomas, Jr., C.A. (1967). Adenovirus DNA, I. Molecular weight and conformation. *Proceedings of the National Academy of Sciences USA* **67**, 1302-1309.
- Green, M.R., Treisman, R. & Maniatis, T. (1983). Transcriptional activation of cloned human β -globin genes by viral immediate-early gene products. *Cell* **35**, 137-148.
- Griffith, J.D. (1975). Chromatin structure: deduced from a minichromosome. *Science* **187**, 1202-1203.
- Gross-Bellard, M., Oudet, P. & Chambon, P. (1973). Isolation of high-molecular-weight DNA from mammalian cells. *European Journal of Biochemistry* **38**, 32-36.
- Groudine, M. & Weintraub, H. (1982). Propagation of globin DNase I-hypersensitive sites in the absence of factors required for induction: a possible mechanism for determination. *Cell* **30**, 131-139.
- Halbert, D.N., Spector, D.J. & Raskas, H.J. (1979). In vitro translation products specified by the transforming region of adenovirus type 2. *Journal of Virology* **31**, 621-629.
- Haley, A.P., Overhauser, J., Babiss, L.E., Ginsberg, H.S. & Jones, N. (1984). Transformation properties of type 5 adenovirus mutants that differentially express the E1a gene products. *Proceedings of the National Academy of Sciences USA* **81**, 5731-5738.
- Hamkalo, B.A. & Miller, Jr., O.L. (1973). Electronmicroscopy of gene activity. *Annual Review of Biochemistry* **42**, 379-396.
- Hammer, R.E., Swift, G.H., Ornitz, D.M., Quaipe, C.J., Palmiter, R.D., Brinster, R.L. & MacDonald, R.J. (1987). The rat elastase I regulatory element is an enhancer that directs correct cell specificity and developmental onset of expression in transgenic mice. *Molecular and Cellular Biology* **7**, 2956-2967.
- Han, S., Udvardy, A. & Schedl, P. (1985). Novobiocin blocks the *Drosophila* heat shock response. *Journal of Molecular Biology* **183**, 13-29.

- Hancock, R. (1982). Topological organisation of interphase DNA: the nuclear matrix and other skeletal structures. *Biology of the Cell* **46**, 105-121.
- Hancock, R. & Hughes, M.E. (1982). Organisation of DNA in the interphase nucleus. *Biology of the Cell* **44**, 201-212.
- Hansson, L. & Lambertsson, A. (1983). The role of *su(f)* gene function and ecdysterone in transcription of glue polypeptide mRNAs in *Drosophila melanogaster*. *Molecular and General Genetics* **192**, 395-401.
- Hansson, L., Lineruth, K. & Lambertsson, A. (1981). Effect of the $l(1)su(f)^{ts67g}$ mutation of *Drosophila melanogaster* on glue protein synthesis. *Wilhelm Roux's Archives of Developmental Biology* **190**, 308-312.
- Harlow, E., Franza, B. & Schley, C. (1985). Monoclonal antibodies specific for adenovirus early region 1a proteins: extensive heterogeneity in early region 1a products. *Journal of Virology* **55**, 533-546.
- Harter, M.L. & Lewis, J.B. (1978). Adenovirus type 2 early proteins synthesized in vitro and in vivo: identification in infected cells of the 38 000- to 50 000-molecular-weight protein encoded by the left end of the adenovirus type 2 genome. *Journal of Virology* **26**, 736-746.
- Hearing P. & Shenk, T. (1983). The adenovirus type 5 E1A transcriptional control region contains a duplicated enhancer element. *Cell* **33**, 695-703.
- Hearing P. & Shenk, T. (1986). The adenovirus type 5 E1A enhancer contains two functionally distinct domains: one is specific for E1A and the other modulates all early transcription units in cis. *Cell* **45**, 229-236.
- Hen, R., Borrelli, E. & Chambon, P. (1985). Repression of the immunoglobulin heavy chain enhancer by the adenovirus-2 E1A products. *Science* **230**, 1391-1394.
- Hen, R., Borrelli, E., Sassone-Corsi, P. & Chambon, P. (1983). An enhancer element is located 340 base pairs upstream from the adenovirus-2 E1A cap site. *Nucleic Acids Research* **11**, 8747-8760.
- Herman, R., Weymouth, L. & Penman, S. (1978). Heterogeneous nuclear RNA-protein fibres in chromatin depleted nuclei. *Journal of Cell Biology*

- 78, 663-674.
- Heumann, H. (1974). Electron microscope observations of the organisation of chromatin fibers in isolated nuclei of rat liver. *Chromosoma* **47**, 133-146.
- Hodge, L.D., Mancini, P., Davis, F.M. & Heywood, P. (1977). Nuclear matrix of HeLa S3 cells: polypeptide composition during adenovirus infection and in phases of the cell cycle. *Journal of Cell Biology* **72**, 194-208.
- Horne, R.W., Brenner, S., Waterson, A.P. & Wildy, P. (1959). The icosahedral form of an adenovirus. *Journal of Molecular Biology* **1**, 84-86.
- Houweling, A., van den Elsen, P.J. & van der Eb, A.J. (1980). Partial transformation of primary rat cells by the leftmost 4.5% fragment of adenovirus 5 DNA. *Virology* **105**, 537-550.
- Hoyle, H.D. & Doering, J.L. (1987). DNase I sensitivities in chromatin of the *Xenopus laevis* somatic and oocyte 5S DNAs. *Biochimica et Biophysica Acta* **908**, 224-230.
- Huang, S., Barnard, M.B., Xu, M., Matsui, S., Rose, S.M. & Garrard, W.T. (1986). The active immunoglobulin κ chain gene is packaged by non-ubiquitin-conjugated nucleosomes. *Proceedings of the National Academy of Sciences USA* **83**, 3738-3742.
- Hubermann, J.A. & Riggs, A.D. (1968). On the mechanism of DNA replication in mammalian chromosomes. *Journal of Molecular Biology* **32**, 327-341.
- Huebner, R.J., Casey, M.J., Chanock, R.M. & Schell, K. (1965). Tumors induced in hamsters by a strain of adenovirus type 3: sharing of tumor antigens and "neoantigens" with those produced by adenovirus type 7 tumors. *Proceedings of the National Academy of Sciences USA* **54**, 281-388.
- Hurwitz D.R. & Chinnadurai, G. (1985a). Evidence that a second tumor antigen encoded by an adenovirus early gene region E1a is required for efficient cell transformation. *Proceedings of the National Academy of Sciences USA* **82**, 163-167.

- Hurwitz D.R. & Chinnadurai, G. (1985b). Immortalization of rat embryo fibroblasts by an adenovirus 2 mutant expressing a single functional E1a protein. *Journal of Virology* **54**, 358-363.
- Ide, T., Nakagami, M., Anzai, K. & Andoh, T. (1975). Supercoiled DNA folded by non-histone proteins in cultured mammalian cells. *Nature* **258**, 445-447.
- Igo-Kemenes, T., Horz, W. & Zachau, H.G. (1982). Chromatin. *Annual Review of Biochemistry* **51**, 82-121.
- Imai, B.S., Yan, P., Baldwin, J.P., Ibel, K., May, P.R. & Bradbury, E.M. (1986). Hyperacetylation of core histones does not cause unfolding of nucleosomes. *Journal of Biological Chemistry* **261**, 8784-8792.
- Imperiale, M.J., Feldman, L.T. & Nevins, J.R. (1983). Activation of gene expression by adenovirus and herpesvirus regulatory genes acting in *trans* and by a *cis*-acting adenovirus enhancer element. *Cell* **35**, 127-136.
- Jackson, D.A. & Cook, P.R. (1985a). A general method for preparing chromatin containing intact DNA. *EMBO Journal* **4**, 913-918.
- Jackson, D.A. & Cook, P.R. (1985b). Transcription occurs at a nucleoskeleton. *EMBO Journal* **4**, 919-925.
- Jackson, D.A. & Cook, P.R. (1986a). Replication occurs at a nucleoskeleton. *EMBO Journal* **5**, 1403-1410.
- Jackson, D.A. & Cook, P.R. (1986b). A cell cycle-dependent DNA polymerase activity that replicates intact DNA in chromatin. *Journal of Molecular Biology* **192**, 65-76.
- Jackson, D.A. & Cook, P.R. (1988). Visualization of a filamentous nucleoskeleton with a 23 nm axial repeat. *EMBO Journal* **7**, 3667-3677.
- Jackson, D.A., McCreedy, S.J. & Cook, P.R. (1981). RNA is synthesized at the nuclear cage. *Nature* **292**, 552-555.
- Jackson, P.D. & Felsenfeld, G. (1985). A method for mapping intranuclear protein-DNA interactions and its application to a nuclease hypersensitive site. *Proceedings of the National Academy of Sciences USA* **82**, 2296-2300.

- Jacobovits, E.B., Bratosin, S. & Aloni, Y. (1980). A nucleosome-free region in SV40 minichromosomes. *Nature* **285**, 263-265.
- Jantzen, K., Fritton, H.P. & Igo-Kemenes, T. (1986). The DNase I sensitive domain of the chicken lysozyme gene spans 24 kb. *Nucleic Acids Research* **14**, 6085-6090.
- Jochemsen, H. Hertoghs, J.J.L., Lupker, J.H., Davies, A. & van der Eb, A.J. (1981). In vitro synthesis of adenovirus type 5 T antigens. II. Translation of virus-specific RNA from cells transformed by fragments of adenovirus type 5 DNA. *Journal of Virology* **37**, 530-534.
- Jochemsen, A.G., de Wit, C.M., Bos, J.L. & van der Eb, A.J. (1986). Transforming properties of a 15-kDa truncated Ad12 E1A gene product. *Virology* **152**, 375-383.
- Jochemsen, A.G., Peltenburg, L.T.C., te Pas, M.F.W., de Wit, C.M., Bos, J.L. & van der Eb, A.J. (1987). Activation of adenovirus type 5 E1a transcription by region E1b in transformed primary rat cells. *EMBO Journal* **6**, 3399-3405.
- Jones, N.C., Rigby, P.W.J. & Ziff, E.B. (1988). Trans-acting protein factors and the regulation of eukaryotic transcription: lessons from studies on DNA tumor viruses. *Genes and Development* **2**, 267-281.
- Jones, N. & Shenk, T. (1979a). An adenovirus type 5 early gene function regulates expression of the other early viral genes. *Proceedings of the National Academy of Sciences USA* **76**, 3665-3669.
- Jones, N. & Shenk, T. (1979b). Isolation of adenovirus type 5 host range deletion mutants defective for transformation of rat embryo cells. *Cell* **17**, 683-689.
- Jongstra, J., Reudelhuber, T.L., Oudet, P., Benoist, C., Chae, C., Jeltsch, J., Mathis, D.J. & Chambon, P. (1984). Induction of altered chromatin structures by simian virus 40 enhancer and promoter elements. *Nature* **307**, 708-714.
- Jost, J. & Seldran, M. (1984). Association of transcriptionally active vitellogenin II gene with the nuclear matrix of chicken liver. *EMBO Journal* **3**, 2005-2008.

- Kaczmarek, L., Ferguson, B., Rosenberg, M., & Baserga, R. (1986). Induction of cellular DNA synthesis by purified adenovirus E1A proteins. *Virology* **152**, 1-10.
- Kao, H., Capasso, O., Heintz, N. & Nevins, J.R. (1985). Cell cycle control of the human HSP70 gene: Implications for the role of a cellular E1a-like function. *Molecular and Cellular Biology* **5**, 628-633.
- Kao, H. & Nevins, J.R. (1983). Transcriptional activation and subsequent control of the human *hprt* shock gene during adenovirus infection. *Molecular and Cellular Biology* **3**, 2058-2065.
- Kas, E. & Chasin, L.A. (1987). Anchorage of the Chinese hamster dihydrofolate reductase gene to the nuclear scaffold occurs in a intragenic region. *Journal of Molecular Biology* **198**, 677-692.
- Kaufmann, S.H., Coffey, D.S. & Shaper, J.H. (1981). Considerations in the isolation of rat liver nuclear matrix, nuclear envelope and pore complex lamina. *Experimental Cell Research* **132**, 105-132.
- Kaufmann, S.H., Fields, A.P. & Shaper, J.H. (1986). The nuclear matrix: current concepts and unanswered questions. *Methods and Achievements in Experimental Pathology* **12**, 141-171.
- Kaufmann, S.H. & Shaper, J.H. (1984). A subset of non-histone nuclear proteins reversibly stabilized by the sulfhydryl cross-linking reagent tetrathionate. *Experimental Cell Research* **155**, 477-495.
- Keppel, F. (1986). Transcribed human ribosomal RNA genes are attached to the nuclear matrix. *Journal of Molecular Biology* **187**, 15-21.
- Kimelman, D., Miller, J.S., Porter, D. & Roberts, B.E. (1985). E1a regions of the human adenoviruses and of the highly oncogenic simian adenovirus type 7 are closely related. *Journal of Virology* **53**, 390-409.
- Kingston, R.E., Kaufman, R.J. & Sharp, P.A. (1984). Regulation of transcription of the adenovirus E1 promoter by E1a gene products: absence of sequence specificity. *Molecular and Cellular Biology* **4**, 1970-1979.
- Kirov, N., Djondjurov, L. & Tsanev, R. (1984). Nuclear matrix and transcriptional activity of the mouse α -globin gene. *Journal of Molecular*

Biology **180**, 601-614.

- Kmiec, E.B., Ryoji, M. & Worcel, A. (1986). Gyration is required for 5S RNA transcription from a chromatin template. *Proceedings of the National Academy of Sciences* **83**, 1305-1309.
- Kmiec, E.B. & Worcel, A. (1985). The positive transcription factor of the 5S RNA gene induces a 5S DNA-specific gyration in *Xenopus* oocyte extracts. *Cell* **41**, 945-953.
- Korge, G. (1977). Larval saliva in *Drosophila melanogaster*: production, composition and relationship to chromosome puffs. *Developmental Biology* **58**, 339-355.
- Korge, G. (1987). Polytene chromosomes. In: *Results and Problems in Cell Differentiation* vol **14**, ed. Hennig, W., pp. 27-58. Springer, Berlin.
- Kornberg, R.D. (1974). Chromatin structure: a repeating unit of histones and DNA. *Science* **184**, 868-871.
- Kornberg, R.D. (1977). Structure of chromatin. *Annual Review of Biochemistry* **46**, 931-954.
- Kovesdi, I., Reichel, R. & Nevins, J.R. (1986a). Identification of a cellular transcription factor involved in E1A-trans-activation. *Cell* **45**, 219-228.
- Kovesdi, I., Reichel, R. & Nevins, J.R. (1986b). E1A transcription induction: enhanced binding of a factor to upstream promoter sequences. *Science* **231**, 719-722.
- Kovesdi, I., Reichel, R. & Nevins, J.R. (1987). Role of an adenovirus E2 promoter binding factor in E1A-mediated coordinate gene control. *Proceedings of the National Academy of Sciences USA* **84**, 2180-2184.
- Krippel, B., Ferguson, B., Rosenberg, M. & Westphal, H. (1984). Functions of purified E1A protein microinjected into mammalian cells. *Proceedings of the National Academy of Sciences USA* **81**, 6988-6992.
- Krohne, G. & Benavente, R. (1986). The nuclear lamins: a multigene family of proteins in evolution and differentiation. *Experimental Cell Research* **162**, 1-10.
- Kunnath, L. & Locker, J. (1982). Characterization of DNA methylation in

- the rat. *Biochimica et Biophysica Acta* **609**, 264-271.
- Kunnath, L. & Locker, J. (1985). DNase I sensitivity of the rat albumin and α -fetoprotein genes. *Nucleic Acids Research* **13**, 115-120.
- Kuppuswamy, M.N. & Chinnadurai, G. (1987). Relationship between the transforming and transcriptional regulatory functions of adenovirus 2 E1a oncogene. *Virology* **150**, 31-38.
- Labhart, P. & Koller, T. (1982). Structure of the active nucleolar chromatin of *Xenopus laevis* oocytes. *Cell* **28**, 279-292.
- Labhart, P., Ness, P., Banz, E., Parish, R. & Koller, T. (1983). Model for the structure of the active nucleolar chromatin. *Cold Spring Harbor Symposium* **47**, 557-564.
- Lacey, E. & Axel, R. (1975). Analysis of DNA of isolated chromatin subunits. *Proceedings of the National Academy of Sciences USA* **72**, 3078-3082.
- LaiFatt, R.B. & Mak, S. (1982). Mapping of an adenovirus function involved in the inhibition of DNA degradation. *Journal of Virology* **42**, 969-977.
- Laird, C.D., Wilkinson, L.E., Foe, V.E. & Chooi, W.Y. (1976). Analysis of chromatin-associated fiber arrays. *Chromosoma* **58**, 169-192.
- Loeb, M.M. & Danbolt, B. (1979). Characterization of active transcription units in Balbiani rings in *Chironomus tentans*. *Cell* **17**, 835-848.
- Langmore, J.P. & Paulson, J.R. (1983). Low angle x-ray diffraction studies of chromatin structure in vivo and in isolated nuclei and metaphase chromosomes. *Journal of Cell Biology* **96**, 1120-1131.
- Langmore, J.P. & Schutt, C. (1980). The higher-order structure of chicken erythrocyte chromosomes in vivo. *Nature* **288**, 620-622.
- Larsen, A. & Weintraub, H. (1982). An altered DNA conformation detected by S1 nuclease occurs at specific regions in active chick globin chromatin. *Cell* **29**, 609-622.
- Lawson, G.M., Knoll, B.J., March, C.J., Woo, S.L.C., Tsai, M. & O'Malley,

- B.W. (1982). Definition of 5' and 3' structural boundaries of the chromatin domain containing the ovalbumin multigene family. *Journal of Biological Chemistry* **267**, 1501-1507.
- Lazo, P.A. (1987). Structure, DNase I sensitivity and expression of integrated papilloma virus in the genome of HeLa cells. *European Journal of Biochemistry* **165**, 393-401.
- Lee, K.A.W. & Green, M.R. (1987). A cellular transcription factor E4F1 interacts with an E1a-inducible enhancer and mediates constitutive enhancer function in vitro. *EMBO Journal* **6**, 1345-1353.
- Lee, K.A.W., Hai, T., SivaRaman, L., Thimmappaya, B., Hurst, H.C., Jones, N.C. & Green, M.R. (1987). A cellular protein, activating transcription factor, activates transcription of multiple E1A-inducible adenovirus early promoters. *Proceedings of the National Academy of Sciences USA* **84**, 8355-8359.
- Leff, T., Elkaim, R., Goding, C.R., Jalinot, P., Sassone-Corsi, P., Perrieaudet, M., Keding, C. & Chambon, P. (1984). Individual products of the adenovirus 12S and 13S mRNAs stimulate viral E1a and E1b expression at the transcriptional level. *Proceedings of the National Academy of Sciences USA* **81**, 4381-4385.
- Lehner, C.F., Eppenberger, H.M., Fakan, S. & Nigg, E.A. (1986). Nuclear substructure antigens. *Experimental Cell Research* **162**, 205-219.
- Lennard, A.G. & Thomas, J.O. (1985). The arrangement of H5 molecules in extended and condensed chicken erythrocyte chromatin. *EMBO Journal* **4**, 3455-3462.
- Levinger, L., Barsoum, J. & Varshavsky, A. (1981). Two-dimensional hybridization mapping of nucleosomes: comparison of DNA and protein patterns. *Journal of Molecular Biology* **146**, 287-304.
- Levinger, L. & Varshavsky, A. (1982). Selective arrangement of ubiquitinated and D1 protein-containing nucleosomes within the *Drosophila* genome. *Cell* **28**, 375-385.
- Levinson, A. & Levine, A.J. (1977a). The isolation and identification of the adenovirus group C tumor antigens. *Virology* **76**, 1-11.

- Levinson, A.D. & Levine, A.J. (1977b). The group C adenovirus tumor antigens: identification in infected and transformed cells and a peptide map analysis. *Cell* **11**, 871-879.
- Levy, A. & Noll, M. (1981). Chromatin fine structure of active and repressed genes. *Nature* **289**, 198-203.
- Levy-Wilson, B., Connor, W. & Dixon, G.H. (1979). A subset of trout testis nucleosomes enriched in transcribed DNA sequences contains high mobility group proteins as major structural components. *Journal of Biological Chemistry* **254**, 600-620.
- Lewis, C.D. & Laemmli, U.K. (1982). Higher order metaphase chromosome structure: evidence for metalloprotein interactions. *Cell* **29**, 171-181.
- Lewis, J.B. & Mathews, M.B. (1981). Viral messenger RNAs in six lines of adenovirus-transformed cells. *Virology* **115**, 345-360.
- Lillie, J.W., Green, M. & Green, M.R. (1986). An adenovirus E1a protein region required for transformation and transcriptional repression. *Cell* **46**, 1043-1051.
- Lillie, J.W., Loewenstein, P.M., Green, M.R. & Green, M. (1987). Functional domains of adenovirus type 5 E1a proteins. *Cell* **50**, 1091-1100.
- Lin, H.T., Baserga, R. & Mercer, W.E. (1985). Adenovirus type 2 activates cell cycle-dependent genes that are a subset of those activated by serum. *Molecular and Cellular Biology* **5**, 2936-2942.
- Long, B.H. & Ors, R.L. (1983). Nuclear matrix, hnRNA, and snRNA in Friend erythroleukemia nuclei depleted of chromatin by low ionic strength EDTA. *Biology of the Cell* **48**, 89-98.
- Losa, R., Thoma, F. & Koller, T. (1984). Involvement of the globular domain of histone III in the higher order structures of chromatin. *Journal of Molecular Biology* **175**, 529-551.
- Lowe, D.G. & Moran, L.A. (1986). Molecular cloning and analysis of DNA complementary to three mouse $M_r = 68,000$ heat shock protein mRNAs. *Journal of Biological Chemistry* **261**, 2102-2112.
- Luchnik, A.N., Bakayev, V.V., Yugai, A.A., Zbarsky, I.B. & Georgiev, G.P.

- (1985). DNase I-hypersensitive minichromosomes of SV40 possess an elastic torsional strain in DNA. *Nucleic Acids Research* **13**, 1135-1149.
- Luchnik, A.N., Bakayev, V.V., Zbarsky, I.B. & Georgiev, G.P. (1982). Elastic torsional strain in DNA within a fraction of SV40 minichromosomes: relation to transcriptionally active chromatin. *EMBO Journal* **1**, 1353-1358.
- Mak, I. & Mak, S. (1983). Transformation of rat cells by cyt mutants of adenovirus type 12 and mutants of adenovirus type 5. *Journal of Virology* **45**, 1107-1117.
- Malette, P., Yee, S. & Branton, P.E. (1983). Studies on the phosphorylation of the 58 000 dalton early region 1b protein of human adenovirus type 5. *Journal of general Virology* **64**, 1069-1078.
- Maniatis, T., Fritsch, E.F. & Sambrook, J. (1982). *Molecular Cloning: A laboratory manual*. Cold Spring Harbor, New York.
- Marsden, M.P.F. & Laemmli, U.K. (1979). Metaphase chromosome structure: evidence for a radial loop model. *Cell* **17**, 849-858.
- McCready, S.J., Goodwin, J., Mason, D.W., Brazell, I.A. & Cook, P.R. (1980). DNA is replicated at the nuclear cage. *Journal of Cell Science* **46**, 365-386.
- McGhee, J.D., Nickol, J.M., Felsenfeld, G. & Rau, D.C. (1983). Higher order structure of chromatin: Orientation of nucleosomes within the 30 nm chromatin solenoid is independent of species and spacer length. *Cell* **33**, 831-841.
- McGhee, J.D., Rau, D.C., Charney, E. & Felsenfeld, G. (1980). Orientation of the nucleosome within the higher structure of chromatin. *Cell* **22**, 87-96.
- McGhee, J.D., Wood, W.L., Dolan, M., Engel, J.D. & Felsenfeld, G. (1981). A 200 bp region at the 5' end of the chicken adult β -globin gene is accessible to nuclease digestion. *Cell* **27**, 45-55.
- McKeon, F.D., Kirschner, M.W. & Caput, D. (1986). Homologies in both primary and secondary structure between nuclear envelope and intermediate filament proteins. *Nature* **319**, 463-468.

- McKeon, C., Ohkubo, H., Pastan, I. & deCrombrugge, B. (1982). Unusual methylation pattern of the $\alpha 2(I)$ collagen gene. *Cell* **29**, 203-210.
- McKinnon, R.D., Bacchetti, S. & Graham, F.L. (1982). Tn5 mutagenesis of the transforming genes of human adenovirus type 5. *Gene* **19**, 33-42.
- McKnight, S.L., Bustin, M. & Miller, Jr., O.L. (1978). Electron microscopic analysis of chromosome metabolism in the *Drosophila melanogaster* embryo. *Cold Spring Harbor Symposium* **42**, 741-754.
- Miller, Jr., O.L. & Beatty, B.R. (1969). Visualization of nucleolar genes. *Science* **164**, 955-957.
- Miller, Jr., O.L. & Hamkalo, B.A. (1972). Visualization of RNA synthesis on chromosomes. *International Review of Cytology* **33**, 1-25.
- Miller, T.E., Huang, C. & Pogo, A.O. (1978). Rat liver nuclear skeleton and ribonucleoprotein complexes containing hnRNA. *Journal of Cell Biology* **76**, 675-691.
- Mirkovitch, J., Mirault, M. & Laemmli, U.K. (1984). Organization of the higher-order chromatin loop: specific DNA attachment sites on nuclear scaffold. *Cell* **39**, 223-232.
- Mirkovitch, J., Spierer, P. & Laemmli, U.K. (1986). Genes and loops in 320,000 base-pairs of the *Drosophila melanogaster* chromosome. *Journal of Molecular Biology* **190**, 255-258.
- Montell, C., Courtois, G., Eng, C. & Berk, A.J. (1984). Complete transformation by adenovirus 2 requires both E1a proteins. *Cell* **36**, 951-961.
- Montell, C., Fisher, E.F., Caruthers, M.H. & Berk, A.J. (1982). Resolving the functions of overlapping viral genes by site-specific mutagenesis at a mRNA splice site. *Nature* **295**, 380-384.
- Moran, E., Grodzicker, T., Roberts, R.J., Mathews, M. & Zerler, B. (1986a). Lytic and transforming functions of individual products of the adenovirus E1A gene. *Journal of Virology* **57**, 765-775.
- Moran, E. & Mathews, M.B. (1987). Multiple functional domains in the adenovirus E1A gene. *Cell* **48**, 177-178.

- Moran, E., Zerler, B., Harrison, T.M. & Mathews, M.B. (1986b). Identification of separate domains in the adenovirus E1a gene for immortalization activity and the activation of virus early genes. *Molecular and Cellular Biology* **6**, 3470-3489.
- Nakajima, T., Masuda-Murata, M., Hara, E. & Oda, K. (1987). Induction of cell cycle progression by adenovirus E1A gene 13S- and 12S-mRNA products in quiescent rat cells. *Molecular and Cellular Biology* **7**, 3846-3852.
- Natarajan, V. (1986). Adenovirus 2 E1a and E1b gene products regulate enhancer mediated transcription. *Nucleic Acids Research* **14**, 9445-9456.
- Naveh-Manny, T. & Cedar, H. (1981). Active gene sequences are undermethylated. *Proceedings of the National Academy of Sciences USA* **78**, 4246-4250.
- Nedespasov, S.A. & Georgiev, G.P. (1980). Non-random cleavage of SV40 DNA in the compact minichromosome and free in solution by micrococcal nuclease. *Biochemical and Biophysical Research Communications* **92**, 532-539.
- Nelson, D.A., Ferris, R.C., Zhang, D. & Ferenz, C. (1986a). The β -globin domain in immature erythrocytes: enhanced solubility is coincident with histone hyperacetylation. *Nucleic Acids Research* **14**, 1667-1682.
- Nelson, W.G., Pienta, K.J., Barraek, E.R. & Coffey, D.S. (1986b). The role of the nuclear matrix in the organization and function of DNA. *Annual Review of Biophysics and Biophysical Chemistry* **15**, 457-475.
- Nevins, J.R. (1981). Mechanism of activation of early viral transcription by the adenovirus E1a gene products. *Cell* **26**, 213-220.
- Nevins, J.R. (1982). Induction of the synthesis of a 70,000 dalton mammalian heat shock protein by the adenovirus E1A gene product. *Cell* **29**, 913-919.
- Newport, J.W. & Forbes, D.J. (1987). The nucleus: structure, function, and dynamics. *Annual Review of Biochemistry* **56**, 535-565.
- Nicolas, R.H., Wright, C.A., Cockerill, P.N., Wyke, J.A. & Goodwin, G.H. (1983). The nuclease sensitivity of active genes. *Nucleic Acids Research*

11, 753-772.

- Nishizawa, M., Tanabe, K. & Takahashi, T. (1984). DNA polymerases and topoisomerases solubilized from the nuclear matrices of regenerating rat livers. *Biochemical and Biophysical Research Communications* **124**, 917-924.
- Noailles-Depeyre, J., Azum, M., Geraud, M., Mathieu, C. & Gas, N. (1987). Distribution of nuclear matrix proteins in interphase CHO cells and rearrangements during the cell cycle. An ultrastructural study. *Biology of the Cell* **61**, 23-32.
- Noll, M. (1974). Internal structure of the chromatin subunit. *Nucleic Acids Research* **1**, 1573-1578.
- Olins, A.L. & Olins, D.E. (1974). Spheroid chromatin units (ν bodies). *Science* **183**, 330-332.
- Olins, A.L. & Olins, D.E. (1979). Stereo electron microscopy of the 25-nm chromatin fibers in isolated nuclei. *Journal of Cell Biology* **81**, 260-255.
- Olins, D.E., Olins, A.L., Levy, H.A., Durfee, R.C., Margle, S.M., Tinnel, E.J. & Dover, S.D. (1983). Electron microscope tomography: transcription in three dimensions. *Science* **220**, 498-500.
- Ottaviano, Y. & Gerace, L. (1985). Phosphorylation of the nuclear lamina during interphase and mitosis. *Journal of Biological Chemistry* **260**, 621-632.
- Oudet, P., Gross-Bellard, M. & Chambon, P. (1975). Electron microscopic and biochemical evidence that chromatin structure is a repeating unit. *Cell* **4**, 281-300.
- Pangiban, A.T. (1985). Retroviral DNA integration. *Cell* **42**, 5-6.
- Pardoll, D.M. & Vogelstein, B. (1980). Sequence analysis of nuclear matrix associated DNA from rat liver. *Experimental Cell Research* **128**, 466-470.
- Pardoll, D.M., Vogelstein, B. & Coffey, D.S. (1980). A fixed site of DNA replication in eukaryotic cells. *Cell* **19**, 527-536.
- Parker, C.S. & Topol, J. (1984a). A Drosophila RNA polymerase II transcription factor contains a promoter-region-specific DNA-binding

- activity. *Cell* **36**, 357-369.
- Parker, C.S. & Topol, J. (1984b). A *Drosophila* RNA polymerase II transcription factor binds to the regulatory site of an hsp70 gene. *Cell* **37**, 273-283.
- Paulson, J.R. & Laemmli, U.K. (1977). The structure of histone-depleted metaphase chromosomes. *Cell* **12**, 817-828.
- Pederson, D.S., Thoma, F. & Simpson, R.T. (1986). Core particle, fiber, and transcriptionally active chromatin structure. *Annual Review of Cell Biology* **2**, 117-147.
- Pehrson, J. & Cole, R.D. (1980). Histone H1^o accumulates in growth-inhibited culture cells. *Nature* **285**, 43-44.
- Pelham, H.R.B. (1982). A regulatory upstream promoter element in the *Drosophila* hsp70 heat-shock gene. *Cell* **30**, 517-528.
- Pelling, C. (1964). Ribonukleinsäure-Synthese der Reisenchromosomen. Autoradiographische Untersuchungen an *Chironomus tentans*. *Chromosoma* **15**, 71-122.
- Perricaudet, M., Akusjarvi, G., Virtanen, A. & Pettersson, U. (1979). Structure of two spliced mRNAs from the transforming region of human β group C adenoviruses. *Nature* **281**, 694-696.
- Perricaudet, M., Le Moullec, J.P. & Pettersson, U. (1980). The predicted structure of two adenovirus T-antigens. *Proceedings of the National Academy of Sciences USA* **77**, 3778-3782.
- Perry, M. & Chalkley, R. (1982). Histone acetylation increases the solubility of chromatin and occurs sequentially over most of the chromatin. *Journal of Biological Chemistry* **257**, 7336-7347.
- Persson, H., Katze, M.G. & Phillipson, L. (1982). An adenovirus tumor antigen associated with membranes in vivo and in vitro. *Journal of Virology* **42**, 905-917.
- Peters, K.E., Okada, T.A. & Comings, D.E. (1982). Chinese hamster nuclear proteins: an electrophoretic analysis of interphase, metaphase and nuclear matrix preparations. *European Journal of Biochemistry* **129**,

221-232.

- Petterson, U., Virtanen, A., Perricaudet, M. & Akusjarvi, G. (1983). The messenger RNAs from the transforming region of human adenoviruses. *Current Topics in Microbiology and Immunology* **109**, 107-123.
- Phi-Van, L. & Stratling, W.H. (1988). The matrix attachment regions of the chicken lysozyme gene co-map with the boundaries of the chromatin domain. *EMBO Journal* **7**, 655-664.
- Rattner, J.B. & Lin, C.C. (1985). Radial loops and helical coils coexist in metaphase chromosomes. *Cell* **42**, 291-296.
- Razin, S.V. (1987). DNA interactions with the nuclear matrix and spatial organization of replication and transcription. *BioEssays* **6**, 19-23.
- Razin, S.V., Yarovaya, O.V. & Georgiev, G.P. (1985). Low ionic strength extraction of nuclease-treated nuclei destroys the attachment of transcriptionally active DNA to the nuclear skeleton. *Nucleic Acids Research* **13**, 7427-7444.
- Reeves, R. (1984). Transcriptionally active chromatin. *Biochimica et Biophysica Acta* **782**, 343-393.
- Reeves, R. & Chang, D. (1983). Investigations of the possible functions for glycosylation in the high mobility group proteins. *Journal of Biological Chemistry* **258**, 679-687.
- Renz, M., Nehls, P. & Hozier, J. (1977). Involvement of histone H1 in the organization of the chromatin fiber. *Proceedings of the National Academy of Sciences USA* **74**, 1879-1883.
- Ricciardi, R.P., Jones, R.L., Cepco, C.L., Sharp, P.A. & Roberts, B.E. (1981). Expression of early adenovirus genes requires a viral encoded acidic polypeptide. *Proceedings of the National Academy of Sciences USA* **78**, 6121-6125.
- Richmond, T.J., Finch, J.T., Rushton, B., Rhodes, D. & Klug, A. (1984). Structure of the nucleosome core particle at 7 Å resolution. *Nature* **311**, 532-537.
- Richter, J.D., Hurst, H.C. & Jones, N.C. (1987). Adenovirus E1A requires

- synthesis of a cellular protein to establish a stable trancription complex in injected *Xenopus laevis* oocytes. *Molecular and Cellular Biology* **7**, 3040-3056.
- Rigby, P.W.J., Dieckmann, M., Rhodes, C. & Berg, P. (1977). Labeling deoxyribonucleic acid to high specific activity *in vitro* by nick-translation with DNA polymerase I. *Journal of Molecular Biology* **113**, 237-251.
- Ring, D. & Cole, R.D. (1979). Chemical cross-linking of H1 histone to the nucleosomal histones. *Journal of Biological Chemistry* **254**, 11688-11695.
- Roberts, B.E., Miller, J.S., Kimelman, D., Cepco, C.L., Lemischka, I.R. & Mulligan, R.C. (1985). Individual adenovirus type 5 early region 1A gene products elicit distinct alterations of cellular morphology and gene expression. *Journal of Virology* **56**, 404-413.
- Robinson, S.L., Nelkin, B.D. & Vogelstein, B. (1982). The ovalbumin gene is associated with the nuclear matrix of chicken oviduct cells. *Cell* **38**, 99-106.
- Robinson, S.L., Small, D., Idzerda, R., McKnight, G.S. & Vogelstein, B. (1983). The association of transcriptionally active genes with the nuclear matrix of the chicken oviduct. *Nucleic Acids Research* **11**, 5113-5130.
- Rocha, F., Davie, J.R., van Holde, K.E. & Weintraub, H. (1984). Differential salt fractionation of active and inactive genomic domains in chicken erythrocyte. *Journal of Biological Chemistry* **259**, 8558-8563.
- Roche, J., Gorka, C., Goeltz, P. & Lawrence, J.J. (1985). Association of histone H1^o with a gene repressed during liver development. *Nature* **314**, 197-198.
- Rohdewohld, H., Weiher, H., Reik, W., Jaenisch, R. & Breindl, M. (1987). Retrovirus integration and chromatin structure: Moloney murine leukemia proviral integration sites map near DNase I-hypersensitive sites. *Journal of Virology* **61**, 336-343.
- Rose, S.M. & Garrard, W.T. (1984). Differentiation-dependent chromatin alterations precede and accompany transcription of immunoglobulin light chain genes. *Journal of Biological Chemistry* **259**, 8534-8544.
- Ross, D.A., Yen, R. & Chae, C. (1982). Association of globin ribonucleic

- acid and its precursors with the chicken erythroblast nuclear matrix. *Biochemistry* **21**, 764-771.
- Rossini, M., Jonak, G.J. & Baserga, R. (1981). Identification of adenovirus 2 early genes required for induction of cellular DNA synthesis in resting hamster cells. *Journal of Virology* **38**, 982-986.
- Rowe, D.T., Branton, P.E., Yee, S. Bacchetti, S. & Graham, F.L. (1984). Establishment and characterization of hamster cell lines transformed by restriction endonuclease fragments of adenovirus type 5. *Journal of Virology* **49**, 162-170.
- Rowe, D.T., Graham, F.L. & Branton, P.E. (1983a). Intracellular localization of adenovirus type 5 tumor antigens in productively infected cells. *Virology* **129**, 456-468.
- Rowe, D.T., Yee, S., Otis, J., Graham, F.L. & Branton, P.E. (1983b). Characterization of human adenovirus type 5 early region 1a polypeptides using antitumor sera and an antiserum specific for the carboxy terminus. *Virology* **127**, 253-271.
- Ruben, M., Bacchetti, S. & Graham, F.L. (1982). Integration and expression of viral DNA in cells transformed by host-range mutants of adenovirus type 5. *Journal of Virology* **41**, 671-685.
- Ryoji, M. & Worcel, A. (1984). Chromatin assembly in *Xenopus* oocytes: in vivo studies. *Cell* **37**, 21-32.
- Ryoji, M. & Worcel, A. (1985). Structure of two distinct types of minichromosomes that are assembled on DNA injected into *Xenopus* oocytes. *Cell* **40**, 923-932.
- Sambrook, J., Botchan, M., Gallimore, P., Orzanne, B., Pettersson, U., Williams, J. & Sharp, P.A. (1975). Viral DNA sequences in cells transformed by simian virus 40, adenovirus type 2 and adenovirus type 5. *Cold Spring Harbor Symposium* **39**, 615-632.
- Sandeen, G., Wood, W.I. & Felsenfeld, G. (1980). The interaction of high mobility proteins HMG 14 and 17 with nucleosomes. *Nucleic Acids Research* **8**, 3757-3778.
- Sander, M. & Hsieh, T.S. (1985). *Drosophila* topoisomerase II double-

- strand DNA cleavage: analysis of DNA sequence homology at the cleavage site. *Nucleic Acids Research* **13**, 1057-1072.
- Sanders, M.M. (1978). Fractionation of nucleosomes by salt elution from micrococcal nuclease-digested nuclei. *Journal of Cell Biology* **79**, 97-109.
- Saragosti, S., Moyné, G. & Yaniv, M. (1980). Absence of nucleosomes in a fraction of SV40 chromatin between the origin of replication and the region coding for the late leader RNA. *Cell* **20**, 65-73.
- Sarnow, P., Hearing, P., Anderson, C.W., Halbert, D.N., Shenk, T. & Levine, A.J. (1984). Adenovirus early region 1b 58,000 dalton tumor antigen is physically associated with an early region 4 25,000 dalton protein in productively infected cells. *Journal of Virology* **49**, 692-700.
- Sarnow, P., Ho, Y.S., Williams, J. & Levine, A.J. (1982a). Adenovirus E1b-55 kd tumor antigen and SV40 large tumor antigen are physically associated with the same 54 kd cellular protein in transformed cells. *Cell* **28**, 387-394.
- Sarnow, P., Sullivan, C.A. & Levine, A.J. (1982b). A monoclonal antibody detecting the adenovirus type 5 E1b-58K tumor antigen: Characterization of the E1b-58K tumor antigen in adenovirus-infected and -transformed cells. *Virology* **120**, 510-517.
- Scheer, U. (1978). Changes of nucleosome frequency in nucleolar and non-nucleolar chromatin as a function of transcription: an electro microscope study. *Cell* **13**, 535-549.
- Scheer, U. (1987). Contributions of electron microscopic spreading preparations (*Miller spreads*) to the analysis of chromatin structure. In: *Results and Problems in Cell Differentiation* vol **14**, ed. Hennig, W., pp. 147-171. Springer, Berlin.
- Scheer, U., Sommerville, J. & Bustin, M. (1979a). Injected histone antibodies interfere with transcription of lampbrush chromosome loops in oocytes of *Pleurodeles*. *Journal of Cell Science* **40**, 1-20.
- Scheer, U., Spring, H. & Trendelenburg, M.F. (1979b). Organization of transcriptionally active chromatin in lampbrush chromosome loops. In: *The Cell Nucleus* vol **7**, ed. Busch, H., pp 3-47. Academic Press, New

York.

- Schellner, J., Stuber, K. & Doerfler, W. (1986). Computer analyses on the structure of junction sites between adenovirus DNA and cellular DNA. *Biochimica et Biophysica Acta* **867**, 114-123.
- Schmitt, R.C., Fahnestock, M.L. & Lewis, J.B. (1987). Differential nuclear localization of the major adenovirus type 2 E1a proteins. *Journal of Virology* **61**, 247-255.
- Schneider, J.F., Fisher, F., Goding, C.R. & Jones, N.C. (1987). Mutational analysis of the adenovirus E1a gene: the role of transcriptional regulation in transformation. *EMBO Journal* **6**, 2053-2060.
- Schrier, P.I., van den Elsen, P.J., Hertoghs, J.J.L. & van der Eb, A.J. (1979). Characterization of tumor antigens in cells transformed by fragments of adenovirus type 5 DNA. *Virology* **99**, 372-385.
- Schubach, W. & Groudine, M. (1984). Alteration of *c-myc* chromatin structure by avian leukosis virus integration. *Nature* **307**, 702-708.
- Schulz, M., Freisem-Rabien, U., Jessberger, R. & Doerfler, W. (1987). Transcriptional activities of mammalian genomes at sites of recombination with foreign DNA. *Journal of Virology* **61**, 344-353.
- Scott, W.A. & Wigmore, D.J. (1978). Sites in simian virus 40 which are preferentially cleaved by endonucleases. *Cell* **15**, 1511-1518.
- Sedat, J. & Manuelidis, L. (1978). A direct approach to the structure of eukaryotic chromosomes. *Cold Spring Harbor Symposium* **42**, 331-349.
- Senear, A.W. & Lewis, J.B. (1986). Morphological transformation of established rodent cell lines by high-level expression of the adenovirus type 2 E1a gene. *Molecular and Cellular Biology* **6**, 1253-1260.
- Sharp, P.A., Pettersson, U. & Sambrook, J. (1974). Viral DNA in transformed cells. I. A study of the sequences of adenovirus 2 DNA in a line of transformed rat cells using specific fragments of the viral genome. *Journal of Molecular Biology* **86**, 709-726.
- Sharp, P.A., Sugden, B. & Sambrook, J. (1973). Detection of two restriction endonuclease activities in *Haemophilus para-influenzae* using

- analytical agarose-ethidium bromide electrophoresis. *Biochemistry* **12**, 3055-3063.
- Simon, M.C., Kitchener, K., Kao, H., Hickey, E., Weber, L., Voellmy, R., Heintz, N. & Nevins, J.R. (1987). Selective induction of human heat shock gene transcription by the adenovirus E1A gene products, including the 12S E1A product. *Molecular and Cellular Biology* **7**, 2884-2890.
- Simpson, R.T. (1978). Structure of the chromatosome, a chromatin particle containing 160 base pairs of DNA and all the histones. *Biochemistry* **17**, 5524-5531.
- Sinden, R.R., Carlson, J.O. & Pettijohn, D.E. (1980). Torsional tension in the DNA double helix measured by trimethylpsoralen in living *E. coli* cells: analogous measurements in insect and human cells. *Cell* **21**, 773-783.
- SivaRaman, L., Subramanian, S. & Thimmappaya, B. (1986). Identification of a factor in HeLa cells specific for an upstream transcriptional control sequence of an E1a-inducible adenovirus promoter and its relative abundance in infected and uninfected cells. *Proceedings of the National Academy of Sciences USA* **83**, 5914-5918.
- SivaRaman, L. & Thimmappaya, B. (1987). Two promoter-specific host factors interact with adjacent sequences in an E1a-inducible adenovirus promoter. *Proceedings of the National Academy of Sciences USA* **84**, 6112-6116.
- Small, D., Nelkin, B. & Vogelstein, B. (1985). The association of transcribed genes with the nuclear matrix of *Drosophila* cells during heat shock. *Nucleic Acids Research* **13**, 2413-2431.
- Small, D., & Vogelstein, B. (1985). The anatomy of supercoiled loops in the *Drosophila* 7F locus. *Nucleic Acids Research* **13**, 7703-7713.
- Smart, J.E., Lewis, J.B., Mathews, M.B., Harter, M.L. & Andersson, C.W. (1981). Adenovirus type 2 early proteins. Assignment of the early region 1a proteins synthesized in vivo and in vitro to specific mRNAs. *Virology* **112**, 703-713.
- Smith, G.R. (1981). DNA supercoiling: another level for regulating gene expression. *Cell* **24**, 599-600.

- Smith, H.C. & Berezney, R. (1980). DNA polymerase is tightly bound to the nuclear matrix of actively replicating liver. *Biochemical and Biophysical Research Communications* **104**, 548-556.
- Smith, H.C. & Berezney, R. (1982). Nuclear matrix-bound deoxyribonucleic acid synthesis: an in vitro system. *Biochemistry* **21**, 6751-6761.
- Smith, H.C., Ochs, R.L., Fernandez, E.A. & Spector, D.L. (1986). Macromolecular domains containing nuclear protein p107 and U-snRNP protein p28: further evidence for an *in situ* nuclear matrix. *Molecular and Cellular Biochemistry* **70**, 151-168.
- Smith, H.C., Spector, D.L., Woodcock, C.L.F., Ochs, R.L. & Bhorjee, J. (1985). Alterations in chromatin conformation are accompanied by reorganization of nonchromatin domains that contain U-snRNP protein p28 and nuclear protein p107. *Journal of Cell Biology* **101**, 560-567.
- Snow, C.M., Senior, A. & Gerace, L. (1987). Monoclonal antibodies identify a group of nuclear pore complex glycoproteins. *Journal of Cell Biology* **104**, 1143-1156.
- Southern, E.M. (1975). Detection of specific sequences among DNA fragments separated by gel electrophoresis. *Journal of Molecular Biology* **98**, 503-517.
- Spector, D.J. (1983). The pattern of integration of viral DNA sequences in the adenovirus 5-transformed human cell line 293. *Virology* **130**, 533-538.
- Spector, D.J., McGrogan, M. & Raskas, H.J. (1978). Regulation of the appearance of cytoplasmic RNAs from region 1 of the adenovirus genome. *Journal of Molecular Biology* **120**, 395-414.
- Stabel, S., Argos, P. & Phillipson, L. (1985). The release from growth arrest by microinjection of adenovirus E1A DNA. *EMBO Journal* **4**, 2329-2336.
- Stalder, J., Groudine, M., Dodgson, J.B., Engel, J.D. & Weintraub, H. (1980a). Hb switching in chickens. *Cell* **10**, 973-980.
- Stalder, J., Larsen, A., Engel, J.D., Dolan, M., Groudine, M. & Weintraub, H. (1980b). Tissue-specific DNA cleavages in the globin chromatin domain introduced by DNase I. *Cell* **20**, 451-460.

- Staufenbiel, M. & Deppert, W. (1983). Different structural systems of the nucleus are targets for SV-40 large T antigen. *Cell* **33**, 173-181.
- Staufenbiel, M. & Deppert, W. (1984). Preparation of nuclear matrices from cultured cells: subfractionation of nuclei in situ. *Journal of Cell Biology* **98**, 1886-1894.
- Stein, A. & Kunzler, P. (1983). Histone H5 can correctly align randomly arranged nucleosomes in a defined *in vitro* system. *Nature* **302**, 548-550.
- Stein, R. & Ziff, E.B. (1984). HeLa cell β -tubulin gene transcription is stimulated by adenovirus 5 in parallel with viral early genes by an Ela-dependent mechanism. *Molecular and Cellular Biology* **4**, 2792-2801.
- Stein, R.W. & Ziff, E.B. (1987). Repression of insulin gene expression by adenovirus type 5 Ela protein. *Molecular and Cellular Biology* **7**, 1164-1170.
- Storb U., Arp, B. & Wilson, R. (1981). The switch region associated with immunoglobulin C μ genes is DNase I hypersensitive in T lymphocytes. *Nature* **294**, 90-92.
- Stratling, W.H., Dolle, A. & Sippel, A.E. (1986). Chromatin structure of the chicken lysozyme gene domain as determined by chromatin fractionation and micrococcal nuclease digestion. *Biochemistry* **25**, 495-502.
- Suan, P., Bradbury, E.M. & Baldwin, J.P. (1979). Higher order structures of chromatin in solution. *European Journal of Biochemistry* **97**, 593-602.
- Svensson, C. & Akuskarvi, G. (1984). Adenovirus 2 early region 1A stimulates expression of both viral and cellular genes. *EMBO Journal* **3**, 789-794.
- Swift, F.V., Bhat, K., Youngusband, H.B. & Hamada, H. (1987). Characterization of a cell type-specific enhancer found in the human papilloma virus type 18 genome. *EMBO Journal* **6**, 1339-1344.
- Sykes, R.C., Lin, D., Hwang, S.J., Framson, P.E. & Chinault, A.C. (1988). Yeast ARS function and nuclear matrix association coincide in a short sequence from the human *HPRT* locus. *Molecular and General Genetics* **212**, 301-309.

- Takahashi, K. & Tashiro, Y. (1979). Binding of antibodies against histone H1 to unfolded and folded nucleofilaments. *European Journal of Biochemistry* **97**, 353-360.
- Takemori, N., Riggs, J.L. & Aldrich, C. (1968). Genetic studies with tumorigenic adenoviruses. I. Isolation of cytidal (cyt) mutants of adenovirus type 12. *Virology* **36**, 575-586.
- Tanford, C. (1961). *The Physical Chemistry of Macromolecules*, pp. 138-180. Wiley, New York.
- Thoma, F., Koller, T. & Klug, A. (1979). Involvement of histone H1 in the organization of the nucleosome and of the salt-dependent superstructures of chromatin. *Journal of Cell Biology* **83**, 403-427.
- Tooze, J. (1980). *The Molecular Biology of Tumor Viruses (2nd edition), Part Two, DNA Tumor Viruses*. Cold Spring Harbor, New York.
- Trentin, J.J., Yabe, Y. & Taylor, G. (1962). The quest for human cancer viruses. *Science* **137**, 835-841.
- Tube, R.A. & Berezney, R. (1987a). Pre-replicative association of multiple replicative enzyme activities with the nuclear matrix during rat liver regeneration. *Journal of Biological Chemistry* **262**, 1148-1154.
- Tube, R.A. & Berezney, R. (1987b). Identification of 100 and 150 S DNA polymerase α -primase megacomplexes solubilized from the nuclear matrix of regenerating rat liver. *Journal of Biological Chemistry* **262**, 5857-5865.
- Tube, R.A. & Berezney, R. (1987c). Nuclear matrix-bound DNA primase. *Journal of Biological Chemistry* **262**, 6637-6642.
- van den Elsen, P.J., de Pater, S., Houweling, A., van der Veer, J. & van der Eb, A.J. (1982). The relationship between region E1a and E1b of human adenoviruses in cell transformation. *Gene* **18**, 175-185.
- van den Elsen, P.J., Houweling, A. & van der Eb, A.J. (1983a). Expression of region E1b of human adenoviruses in the absence of region E1a is not sufficient for complete transformation. *Virology* **128**, 377-390.
- van den Elsen, P.J., Houweling, A. & van der Eb, A.J. (1983b). Morphological transformation of human adenoviruses is determined to a

- large extent by gene products of region E1a. *Virology* **131**, 242-246.
- van den Elsen, P.J., Klein, B., Dekker, B.M.M., van Ormondt, H. & van der Eb, A.J. (1983c). Analysis of virus-specific mRNAs present in cells transformed with restriction fragments of adenovirus type 5 DNA. *Journal of general Virology* **64**, 1079-1090.
- van der Eb, A.J. & Bernards, R. (1984). Transformation and oncogenicity by adenoviruses. *Current Topics in Microbiology and Immunology* **110**, 23-51.
- van der Eb, A.J., van Ormondt, H., Schrier, P.I., Lupker, J.H., Jochemsen, H., van den Elsen, P.J., deLeys, R.J., van Beveren, C.P., Dijkema, R. & de Waard, A. (1989). Structure and function of the transforming genes of human adenoviruses and SV40. *Cold Spring Harbor Symposium* **44**, 383-399.
- van der Ploeg, L.H.T. & Flavell, R.A. (1980). DNA methylation in the human γ ₂-globin locus in erythroid and nonerythroid tissues. *Cell* **19**, 917-958.
- van Eekelen, C.A.G., Salden, M.H.L., Habets, W.J.A., van de Putte, L.B.A. & van Venrooij, W.J. (1982). On the existence of an internal nuclear protein structure in HeLa cells. *Experimental Cell Research* **141**, 181-190.
- van Ormondt, H., Maat, J. & van Beveren, C.P. (1980). The nucleotide sequence of the transforming region E1 of adenovirus type 5 DNA. *Gene* **11**, 299-309.
- Varshavsky, A.J., Sundin, O. & Bohn, M. (1979). A stretch of the "late" SV40 viral DNA about 400 bp long which includes the origin of replication is specifically exposed in SV40 minichromosomes. *Cell* **16**, 453-466.
- Velich, A., Kern, F.G., Basilico, C. & Ziff, E.B. (1986). Adenovirus E1a proteins repress expression from polyomavirus early and late promoters. *Molecular and Cellular Biology* **6**, 4019-4025.
- Velich, A. & Ziff, E.B. (1985). Adenovirus E1a proteins repress transcription from the SV40 early promoter. *Cell* **40**, 705-716.
- Vidali, G., Boffa, L.C., Bradbury, E.M. & Allfrey, V.G. (1978). Butyrate suppression of histone deacetylation leads to accumulation of

- multiacetylated forms of histones H3 and H4 and increased DNase I sensitivity of the associated DNA sequences. *Proceedings of the National Academy of Sciences USA* **75**, 2230-2243.
- Villeponteau, B., Lundell, M. & Martinson, H. (1984). Torsional stress promotes the DNase I sensitivity of active genes. *Cell* **39**, 469-478.
- Villeponteau, B. & Martinson, H.G. (1987). Gamma rays and bleomycin nick DNA and reverse the DNase I sensitivity of β -globin gene chromatin in vivo. *Molecular and Cellular Biology* **7**, 1917-1924.
- Villeponteau, B., Pribyl, T.M., Grant, M.H. & Martinson, H.G. (1986). Novobiocin induces the *in vivo* cleavage of active gene sequences in intact cells. *Journal of Biological Chemistry* **261**, 10350-10365.
- Visser, L., Reemst, A.C.M.B., van Mansfeld, A.D.M. & Rozijn, T.H. (1982). Nucleotide sequence analysis of the linked left and right terminal regions of adenovirus type 5 DNA present in the transformed rat cell line 5RK20. *Nucleic Acids Research* **10**, 2189-2198.
- Vijaya, S., Steffen, D.L. & Robinson, H.L. (1986). Acceptor sites for retroviral integrations map near DNase I-hypersensitive sites in chromatin. *Journal of Virology* **60**, 683-692.
- Vogelstein, B., Pardoll, D.M. & Coffey, D.S. (1980). Supercoiled loops and eukaryotic DNA replication. *Cell* **22**, 79-85.
- Vosberg, H. (1985). DNA topoisomerases: enzymes that control DNA conformation. *Current Topics in Microbiology and Immunology* **114**, 19-102.
- Wang, J.C. (1985). DNA topoisomerases. *Annual Review of Biochemistry* **54**, 665-697.
- Weeks, D.L. & Jones, N.C. (1983). EIA control of gene expression is mediated by sequences 5' to the transcriptional starts of the early viral genes. *Molecular and Cellular Biology* **3**, 1222-1234.
- Weintraub, H. (1978). The nucleosome repeat length increases during erythropoiesis in the chick. *Nucleic Acids Research* **5**, 1179-1188.
- Weintraub, H. (1979). Assembly of an active chromatin structure during

- replication. *Nucleic Acids Research* **7**, 781-792.
- Weintraub, H. (1983). A dominant role for DNA secondary structure in forming hypersensitive structures in chromatin. *Cell* **32**, 1191-1203.
- Weintraub, H. (1984). Histone-III-dependent chromatin superstructures and the suppression of gene activity. *Cell* **38**, 17-27.
- Weintraub, H., Beug, H., Groudine, M. & Graf, T. (1982). Temperature-sensitive changes in the structure of globin chromatin in lines of red cell precursors transformed by ts-AEV. *Cell* **28**, 931-940.
- Weintraub, H. & Groudine, M. (1976). Chromosomal subunits have an altered conformation. *Science* **193**, 848-856.
- Weisbrod, S. (1982a). Active chromatin. *Nature* **297**, 289-295.
- Weisbrod, S. (1982b). Properties of active nucleosomes as revealed by HMG 14 and 17 chromatography. *Nucleic Acids Research* **10**, 2017-2042.
- Weisbrod, S., Groudine, M. & Weintraub, H. (1980). Interaction of HMG 14 and 17 with actively transcribing genes. *Cell* **19**, 289-301.
- Weisbrod, S. & Weintraub, H. (1979). Isolation of a subclass of nuclear proteins responsible for conferring a DNase I-sensitive structure on globin chromatin. *Proceedings of the National Academy of Sciences USA* **76**, 630-634.
- Weisbrod, S. & Weintraub, H. (1981). Isolation of actively transcribed nucleosomes using immobilized HMG 14 and 17 and analysis of α -globin chromatin. *Cell* **23**, 391-400.
- Westin, G., Visser, L., Zabielski, J., van Mansfeld, A.D.M., Pettersson, U. & Rozijn, T.H. (1982). Sequence organization of a viral DNA insertion present in the adenovirus type 5-transformed hamster line BHK268-C31. *Gene* **17**, 263-270.
- White, E., Blöse, S.H. & Stillman, B.W. (1984). Nuclear envelope localization of an adenovirus tumor antigen maintains the integrity of cellular DNA. *Molecular and Cellular Biology* **4**, 2865-2875.
- Whyte, P., Buchkovich, K.J., Horowitz, J.M., Friend, S.H., Raybuck, M., Weinberg, R.A. & Harlow, E. (1988). Association between an oncogene and

- an anti-oncogene: the adenovirus E1A proteins bind to the retinoblastoma gene product. *Nature* **334**, 124-129.
- Wiederrecht, G., Shuey, D.J., Kibbe, W.A. & Parker, C.S. (1987). The *Saccharomyces* and *Drosophila* heat shock transcription factors are identical in size and DNA binding properties. *Cell* **48**, 507-515.
- Wigand, R., Bartha, A., Dreizin, R.S., Esche, H., Ginsberg, H.S., Green, M., Hierholzer, J.C. Kalter, S.S., McFerran, J.B., Pettersson, U., Russell, W.C. & Wadell, G. (1982). Adenoviridae, second report. *Intervirology* **18**, 169-176.
- Williams, J. (1973). Oncogenic transformation of hamster embryo cells *in vitro* by adenovirus type 5. *Nature* **243**, 162-163.
- Williams, S.P., Athey, B.D., Muglia, L.J., Schappe, R.S., Gough, A.H. & Laugmore, J.P. (1986). Chromatin fibers are left-handed double helices with diameter and mass per unit length that depend on linker length. *Biophysics Journal* **49**, 233-248.
- Wilson, M., Fraser, N. & Darnell, J. (1979). Mapping of RNA initiation sites by high doses of UV irradiation. Evidence of three independent promoters within the left 11% of the Ad2 genome. *Virology* **94**, 175-184.
- Winberg, G. & Shenk, T. (1984). Dissection of overlapping functions within the adenovirus type 5 E1a gene. *EMBO Journal* **3**, 1907-1912.
- Wood, S.H. & Collins, J.M. (1986). Preferential binding of DNA primase to the nuclear matrix in HeLa cells. *Journal of Biological Chemistry* **261**, 7119-7122.
- Woodcock, C.L.F., Frado, L.Y. & Rattner, J.B. (1984). The higher order structure of chromatin: Evidence for a helical ribbon arrangement. *Journal of Cell Biology* **99**, 42-52.
- Worcel, A., Strogatz, S. & Riley, D. (1981). Structure of chromatin and the linking number of DNA. *Proceedings of the National Academy of Sciences USA* **78**, 1461-1465.
- Wu, C. (1980). The 5' ends of *Drosophila* heat shock genes in chromatin are hypersensitive to DNase I. *Nature* **286**, 854-860.

- Wu, C. (1984). Two protein-binding sites in chromatin implicated in the activation of heat-shock genes. *Nature* **309**, 229-234.
- Wu, C. (1985). An exonuclease protection assay reveals heat-shock element and TATA box DNA-containing proteins in crude nuclear extracts. *Nature* **317**, 84-87.
- Wu, R.S., Kohn, K.W. & Bonner, W.M. (1981). Metabolism of ubiquitinated histones. *Journal of Biological Chemistry* **256**, 5916-5920.
- Wu, C., Wilson, S., Walker, B., Dawid, I., Paisley, T., Zimarino, V. & Ueda, H. (1987). Purification and properties of *Drosophila* heat shock activator protein. *Science* **238**, 1247-1253.
- Wu, C., Wong, Y. & Elgin, S.C.R. (1979). The chromatin structure of specific genes: II. Disruption of chromatin structure during gene activity. *Cell* **16**, 807-814.
- Wurtz, T. & Fakan, S. (1983). Isolation and characterisation of a transcribing polynucleosomal chromatin fraction. *Biology of the Cell* **48**, 109-120.
- Xu, M., Barnard, M.B., Rose, S.M., Cockerill, P.N., Huang, S. & Garrard, W.T. (1986). Transcription termination and chromatin structure of the active immunoglobulin κ gene locus. *Journal of Biological Chemistry* **261**, 3838-3845.
- Yancopoulos, G., Blackwell, T.K., Suh, H., Hood, L. & Alt, F.W. (1986). Introduced T cell receptor variable region gene segments in pre-B cells: evidence that B and T cells use a common recombinase. *Cell* **44**, 251-259.
- Yaniv, M. & Cereghini, S. (1986). Structure of transcriptionally active chromatin. *CRC Critical Reviews in Biochemistry* **21**, 1-26.
- Yee, S. & Branton, P.E. (1985). Analysis of multiple forms of human adenovirus type 5 E1a polypeptides using an anti-peptide antiserum specific for the amino terminus. *Virology* **146**, 315-322.
- Yee, A.S., Reichel, R., Kovetski, I. & Nevins, J.R. (1987). Promoter interaction of the E1A-inducible factor E2F and its potential role in the formation of a multi-component complex. *EMBO Journal* **6**, 2061-2068.

- Yee, S., Rowe, D.T., Tremblay, M.L., McDermott, M. & Branton, P.E. (1983). Identification of human adenovirus early region 1 proteins using antisera against synthetic peptides corresponding to the predicted carboxy termini. *Journal of Virology* **46**, 1003-1013.
- Yoder, S.S., Robberson, B.L., Leys, E.J., Hook, A.G., Al-Ubaidi, M., Yeung, C.Y., Kellems, R.E. & Berget, S.M. (1983). Control of cellular gene expression during adenovirus infection: induction and shut-off of dihydrofolate reductase gene expression by adenovirus type 2. *Molecular and Cellular Biology* **3**, 819-828.
- Yoshida, K., Venkatesh, L., Kuppuswamy, M. & Chinnadurai, G. (1987). Adenovirus transforming 19-kD T antigen has an enhancer-dependent trans-activation function and relieves enhancer repression mediated by viral and cellular genes. *Genes and Development* **1**, 645-658.
- Younghusband, H.B. (1985). An association between replicating adenovirus DNA and the nuclear matrix of infected HeLa cells. *Canadian Journal of Biochemistry and Cell Biology* **63**, 651-660.
- Younghusband, H.B. & Maundrell, K. (1982). Adenovirus DNA is associated with the nuclear matrix of infected cells. *Journal of Virology* **43**, 705-713.
- Zantema, A., Fransen, J.A.M., Davis-Olivier, A., Ramaekers, F.C.S., Vooijs, G.P., deLeys, B. & van der Eb, A.J. (1985). Localization of the E1b proteins of adenovirus type 5 in transformed cells, as revealed by interaction with monoclonal antibodies. *Virology* **142**, 44-58.
- Zaret, K.S. & Yamamoto, K.R. (1984). Reversible and persistent changes in chromatin structure accompany activation of a glucocorticoid-dependent enhancer element. *Cell* **38**, 29-38.
- Zerler, B., Moran, B., Maruyama, K., Moomaw, J., Grodzicker, T. & Ruley, H.E. (1986). Adenovirus E1A coding sequences that enable *ras* and *pmt* oncogenes to transform cultured primary cells. *Molecular and Cellular Biology* **6**, 887-899.
- Zerler, B., Roberts, R.J., Mathews, M.B. & Moran, E. (1987). Different functional domains of the adenovirus E1A gene are involved in regulation

of host cell cycle gene products. *Molecular and Cellular Biology* **7**, 821-829.



